ISSN 0021-9673

VOL. 662 NO. 2 FEBRUARY 25, 1994

THIS ISSUE COMPLETES VOL. 662

JOURNAL OF CHROMATOGRAPHY A

INCLUDING ELECTROPHORESIS AND OTHER SEPARATION METHODS

ELSEVIER

JOURNAL OF CHROMATOGRAPHY A

INCLUDING ELECTROPHORESIS AND OTHER SEPARATION METHODS

Scope. The *Journal of Chromatography A* publishes papers on all aspects of **chromatography, electrophoresis** and related methods. Contributions consist mainly of research papers dealing with chromatographic theory, instrumental developments and their applications. In the *Symposium volumes*, which are under separate editorship, proceedings of symposia on chromatography, electrophoresis and related methods are published. *Journal of Chromatography B: Biomedical Applications* —This journal, which is under separate editorship, deals with the following aspects: developments in and applications of chromatographic and electrophoretic techniques related to clinical diagnosis or alterations during medical treatment; screening and profiling of body fluids or tissues related to the analysis of active substances and to metabolic disorders; drug level monitoring and pharmacokinetic studies; clinical toxicology; forensic medicine; veterinary medicine; occupational medicine; results from basic medical research with direct consequences in clinical practice.

Submission of Papers. The preferred medium of submission is on disk with accompanying manuscript (see *Electronic manuscripts* in the Instructions to Authors, which can be obtained from the publisher, Elsevier Science B.V., P.O. Box 330, 1000 AH Amsterdam, Netherlands). Manuscripts (in English; *four* copies are required) should be submitted to: Editorial Office of *Journal of Chromatography A*, P.O. Box 681, 1000 AR Amsterdam, Netherlands, Telefax (+31-20) 5862 304, or to: The Editor of *Journal of Chromatography B: Biomedical Applications*, P.O. Box 681, 1000 AR Amsterdam, Netherlands. Review articles are invited or proposed in writing to the Editors who welcome suggestions for subjects. An outline of the proposed review should first be forwarded to the Editors for preliminary discussion prior to preparation. Submission of an article is understood to imply that the article is original and unpublished and is not being considered for publication elsewhere. For copyright regulations, see below.

Publication information. *Journal of Chromatography A* (ISSN 0021-9673): for 1994 Vols. 652–682 are scheduled for publication. *Journal of Chromatography B: Biomedical Applications* (ISSN 0378-4347): for 1994 Vols. 652–662 are scheduled for publication. Subscription prices for *Journal of Chromatography A*, *Journal of Chromatography B: Biomedical Applications* or a combined subscription are available upon request from the publisher. Subscriptions are accepted on a prepaid basis only and are entered on a calendar year basis. Issues are sent by surface mail except to the following countries where air delivery via SAL is ensured: Argentina, Australia, Brazil, Canada, China, Hong Kong, India, Israel, Japan, Malaysia, Mexico, New Zealand, Pakistan, Singapore, South Africa, South Korea, Taiwan, Thailand, USA. For all other countries airmail rates are available upon request. Claims for missing issues must be made within six months of our publication (mailing) date. Please address all your requests regarding orders and subscription queries to: Elsevier Science B.V., Journal Department, P.O. Box 211, 1000 AE Amsterdam, Netherlands. Tel.: (+31-20) 5803 642; Fax: (+31-20) 5803 598. Customers in the USA and Canada wishing information on this and other Elsevier journals, please contact Journal Information Center, Elsevier Science Inc., 655 Avenue of the Americas, New York, NY 10010, USA, Tel. (+1-212) 633 3750, Telefax (+1-212) 633 3764.

Abstracts/Contents Lists published in Analytical Abstracts, Biochemical Abstracts, Biological Abstracts, Chemical Abstracts, Chemical Titles, Chromatography Abstracts, Current Awareness in Biological Sciences (CABS), Current Contents/Life Sciences, Current Contents/Physical, Chemical & Earth Sciences, Deep-Sea Research/Part B: Oceanographic Literature Review, Excerpta Medica, Index Medicus, Mass Spectrometry Bulletin, PASCAL-CNRS, Referativnyi Zhurnal, Research Alert and Science Citation Index.

US Mailing Notice. *Journal of Chromatography A* (ISSN 0021-9673) is published weekly (total 52 issues) by Elsevier Science B.V. (Sara Burgerhartstraat 25, P.O. Box 211, 1000 AE Amsterdam, Netherlands). Annual subscription price in the USA US$ 4994.00 (US$ price valid in North, Central and South America only) including air speed delivery. Second class postage paid at Jamaica, NY 11431. **USA POSTMASTERS**: Send address changes to *Journal of Chromatography A*, Publications Expediting, Inc., 200 Meacham Avenue, Elmont, NY 11003. Airfreight and mailing in the USA by Publications Expediting.

See inside back cover for Publication Schedule, Information for Authors and information on Advertisements.

0021-9673/94/$07.00

Printed in the Netherlands

VOL. 662, NO. 2 JOURNAL OF CHROMATOGRAPHY A FEBRUARY 25, 1994

CONTENTS

(Abstracts/Contents Lists published in Analytical Abstracts, Biochemical Abstracts, Biological Abstracts, Chemical Abstracts, Chemical Titles, Chromatography Abstracts, Current Awareness in Biological Sciences (CABS), Current Contents/Life Sciences, Current Contents/Physical, Chemical & Earth Sciences, Deep-Sea Research/Part B: Oceanographic Literature Review, Excerpta Medica, Index Medicus, Mass Spectrometry Bulletin, PASCAL-CNRS, Referativnyi Zhurnal, Research Alert and Science Citation Index)

REVIEW

REGULAR PAPERS

Column Liquid Chromatography

Gas Chromatography

Supercritical Fluid Chromatography

(Continued overleaf)

Contents (continued)

ELSEVIER

Journal of Chromatography A, 662 (1994) 203–218

JOURNAL OF CHROMATOGRAPHY A

Review

Application of crown ether compounds as gas chromatographic stationary phases

Xi-Chun Zhou, Cai-Ying Wu*, Xue-Ran Lu, Yuan-Ying Chen

Department of Chemistry, Wuhan University, Wuhan 430072, China

(First received April 15th, 1993; revised manuscript received September 14th, 1993)

Abstract

Crown ether compounds have a unique structure owing to the cavity structure and the strong electronegative effect of heteroatoms. In recent years, some groups have succeeded in applying these ligands in gas chromatography. Typically, crown ethers have been coated on supports, polymerized and covalently bonded to a polysiloxane backbone. The last technique resulted in a series of significant GC stationary phases which show excellent thermostability and provide unique separations of polar compounds and aromatic hydrocarbons, especially positional isomers. Work about the application of crown ethers as GC stationary phases is reviewed.

Contents

1. Introduction

Crown ether compounds have been studied for over two decades since the first synthesis by Perderson [41] and Lehn [42]. All crown ethers are characterized by a cyclic carbon structure, containing heteroatoms such as oxygen, nitrogen and sulphur, which provide an electron-rich environment for solutes, some of which may fit into the central cavity of the molecule forming

* Corresponding author.

0021-9673/94/$07.00
SSDI 0021-9673(93)E0991-3

stable complexes. Owing to these advantages, crown ethers have been found wide applications in chemistry. In particular their application in analytical chemistry, such as in extraction, electrochemical analyses and chromatographic separations, has been extensively developed. Numerous publications have appeared concerning the applications of crown ether compounds for separating both cations and anions and organic solutes by high-performance liquid chromatographic and other methods, and two important review papers on the use of crown ethers in liquid chromatographic separations have been published by Kimura and Shono [1] and Lamb and Smith [2].

Poly(ethylene glycol) ether phase (Carbowax 20M) is a widely used stationary phase in capillary gas chromatography (GC) because of its high coating efficiency and unique selectivity for polar compounds. However, its usefulness as a stationary phase is limited owing to its relatively low thermal stability (220–240°C), high minimum operating temperature (160°C) and poor chemical stability (susceptibility to oxidation, resulting in short column life times). Clearly, there is a great need for more stable polar and medium polarity phases offering new and different selectivities for the separation of high-boiling polar compounds in high-temperature capillary GC.

It is well known that good diffusion of solutes in the stationary phase is a necessary condition for optimum performance in chromatography, and polysiloxane phases possess the best diffusion properties of the known polymeric materials [3]. Moreover, polysiloxane phases have also historically provided the highest thermal stability. Therefore, almost all new phases developed for capillary chromatography are based on a polysiloxane backbone, which range from polar cyanophenyl-substituted to non-polar alkyl-substituted polysiloxanes.

In recent years, some workers have tried to use crown ether compounds as GC stationary phases. These include low-molecular-mass crown ethers, polymeric crown ethers and crown ether polysiloxanes. In some instances, excellent separations among polar compounds and polar positional isomers have been achieved on these phases. Attempts to substitute polysiloxanes with crown ethers have proved successful in extending the applicable temperature range and creating an "inert" surface on fused-silica capillary materials.

This review deals with the application of crown ethers in GC, chiefly the application of crown ether polysiloxanes as GC stationary phases. The purpose is to stimulate work on the application of crown ethers in this field, because there are still few examples concerning their practical use in GC, particularly the application of crown ether polysiloxanes as stationary phase.

2. Methods of application

Four types of crown ethers incorporated in GC stationary phases have been achieved: low-molecular-mass crown ethers; polymeric crown ethers; crown ethers cross-linked with silicone *in situ* in a capillary column; and crown ether-substituted polysiloxanes.

2.1. Low-molecular-mass crown ethers

The first example of the use of crown ethers as stationary phases was the use of 18-crown-6 reported by Vigalok and Bubachinkowa [4]. Early work on the application of crown ethers often involved coating them on different supports such as Gas Chrom Q, firebrick or white 101 support for packed column chromatography [5–10]. Carbochromes have been modified with dibenzo-18-crown-6 and dinitrobenzo-18-crown-6 and used as stationary phases for the separation of aromatic and chlorinated compounds [11]. This modification leads to decreases in the number of non-specific interaction sites and in the energy of interaction and thus to a shortening of the retention times with preservation of the original elution order. Decreased retention makes it possible to perform chromatographic analyses at lower temperatures and within shorter periods of time, which is important for the determination of thermally unstable solutes, such as chlorine-containing pesticides (Fig. 1).

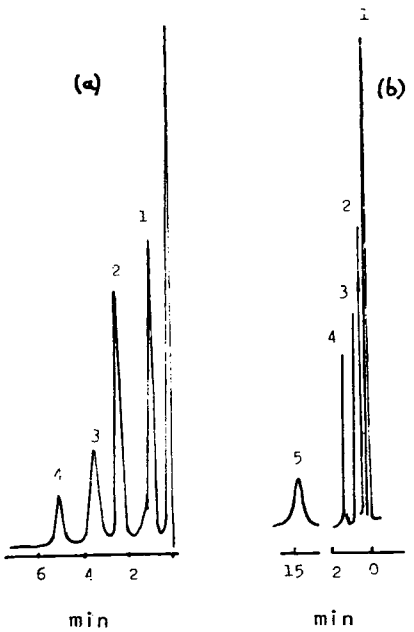

Fig. 1. Separations of chlorine-containing compounds (1 = α-HCL; 2 = γ-HCH; 3 = aldrin; 4 = heptachlor; 5 = DDE) (a) on Carbochrome at 260°C and (b) on Carbochrome modified with dibenzo-18-crown-6 at 200°C. Column, 100 cm × 1.2 mm I.D.; carrier gas (helium) flow-rate, 14 ml/min. From ref. 11.

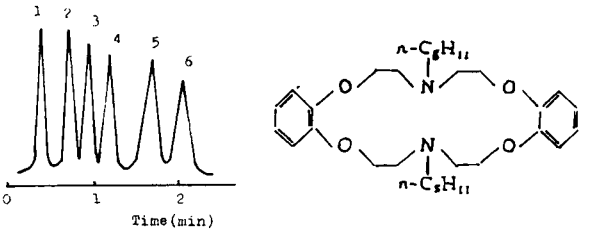

Fig. 2. Separation of nitrogen-containing compounds on a diaza-crown ether-packed column at 220°C. Carrier gas (hydrogen) flow-rate, 30 ml/min. Peaks: 1 = aniline: 2 = nitrobenzene; 3 = *o*-diaminobenzene: 4 = *m*-dinitrobenzene; 5 = N-hydroxyethenyl-N,N-ethylamine; 6 = *o*-aminophenol. From ref. 7.

Several types of crown ethers have been applied in coated column chromatography. Dibenzo-18-crown-6 or dicyclohexo-24-crown-8 (DCH-24C8) coated on Chromosorb W AW DMCS is useful for the direct determination of nitrophenol and nitroaniline isomers without any derivazation [8]. Tribenzopyridine-21-crown-7 [9] and biazo-crown ether [6,7] can separate amines (Fig. 2). The properties of (DCH-24C8) [8] and benzo-15-crown (B15C5) [10] were found to be similar to those of tricyresyl phosphate and di(2-methoxyethyl)adipate, respectively. All of these experiments using crown ethers as stationary phases achieved good separations of small numbers of homologous series of *n*-alkanes, alcohols and aromatic compounds.

Specifically, Jin *et al.* [12] coated two saturated urushiol crown ethers inside a glass or fused-silica capillary column. They gave excellent separations of alcohols without any tailing owing to the deactivation of the residual silanol groups on the surface of the column wall by crown ether rings. Andrews *et al.* [13] attempted to separate C_2-naphthalene isomers by the use of 24-crown-8 on a 60 m × 0.2 mm I.D. column (Supelco), but it was found to be unable to separate all of these isomers, presumably because the size of the crown ether cavity did not fit the isomers.

The poor film forming ability, poor column efficiency and column bleeding at high temperatures are problems with the use of low-molecular-mass crown ethers as coated column stationary phases.

2.2. Polymeric crown ether stationary phases

The only work dealing with crown ether polymers as stationary phases was reported by Fine *et al.* [14] in 1985. They used poly(vinylbezo-15-crown-5) (PVB-15C5) statically coated on the inside of a roughened, deactivated glass capillary, but no useful chromatographic characteristics were achieved. PVB-15C5 had a polarity similar to that of Carbowax 20M, but the maximum operating temperature was only 220°C. The poor efficiency of PVB-15C5 is probably due to the poor diffusion ability of polyethylene linkages. No other examples of the use of polymeric crown ethers as stationary phases have been reported since Fine *et al.*'s work, although the preparation of polymeric crown ethers is chemically easy.

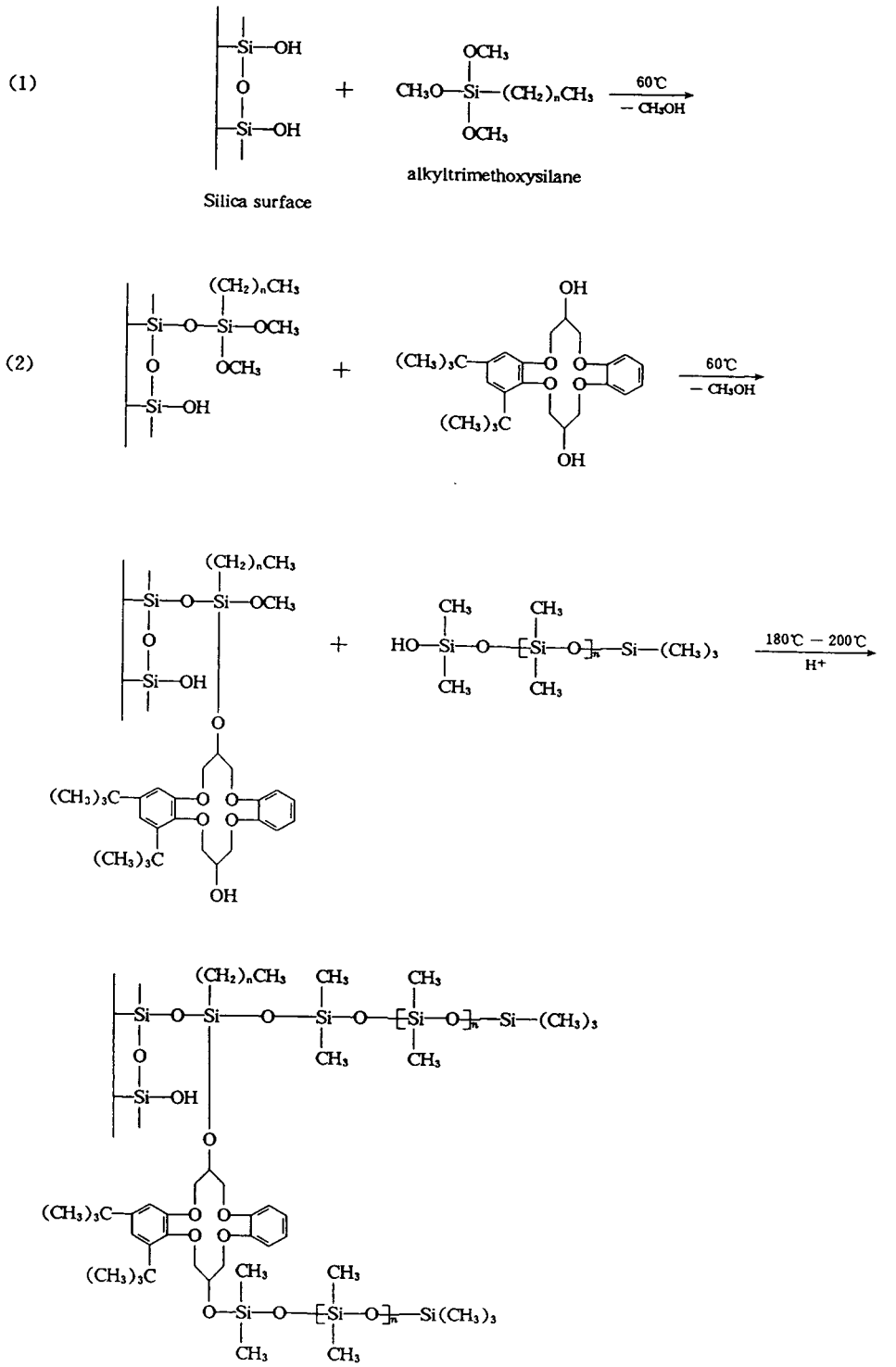

Fig. 3. Possible mechanism of the condensation reaction inside the glass capillary column. From ref. 17.

2.3. Crown ether cross-linking with silicone in situ inside a capillary column

In order to overcome the bleeding of low-molecular-mass crown ethers and the poor efficiency of polymeric crown ethers, some workers tried to incorporate crown ethers into polysiloxanes, and useful applications have been developed.

Fine *et al.* [14] pioneered the technique of preparing crown ether polysiloxanes by *in situ* cross-linking directly inside the column. Columns containing vinylmethylsila-17-crown-6(VMSi17C6) and vinylmethylsila-14-crown-5 (VMSi14C5) were prepared by polymerization of the crown ether inside the capillary. Before this *in situ* polymerization, the capillary was treated with γ-methacryloxypropyltrimethoxysilane (MAPTMS), which can provide methacryloxy groups that copolymerize with the vinylsilacrown ether, and hydrolysis of the methoxy groups provides silanols bonded to the glass surface. Although the separation of alcohols was achieved, the column efficiency was poor and the operating temperatures were only 70–100°C for VMSi17C6 and 58–154°C for VMSi14C4. A possible reason for the lower maximum allowable operating temperatures is incomplete polymerization of the vinyl groups in the silacrown ether.

Wu *et al.* [15] cross-linked used ω-undecyleneoxymethyl-15-crown-5 or -18-crown-6 with an SE-54 matrix by treatment with dicumyl peroxide (DCUP), which formed a crown ether polysiloxane film on the inner surface of a fused-silica capillary. No increase in polarity or activity was observed on cross-linking with DCUP. These two columns are convenient for separating apolar and polar compounds.

Zeng and co-workers [16–18] prepared some crown ether-containing polysiloxane columns by condensing dihydroxy-substituted saturated urushiol crown ethers or dicarboxyl-crown ether with OH-terminal silicone oil (Gy202) in different proportions on a glass capillary surface, using γ-chloropropltriethoxysiloxane or alkyltrimethoxysilane as coupling agent. The hydroxyl or carboxyl groups in the crown ether are convenient for condensation reactions. A possible mechanism of the condensation reaction is given in Fig. 3. These columns can provide high thermal stability and good inertness.

The above methods of preparing crown ether-containing polysiloxane columns are straightforward and free from the difficulties involved in the hydrosilylation technique discussed below. In this technique one or two active substituted groups in the crown ether such as terminal vinyl, hydroxyl or carboxyl groups are necessary for cross-linking or condensation.

Lack of reproducibility, a vague mechanism of reaction and an unknown composition of the final polysiloxane are still problems with this method.

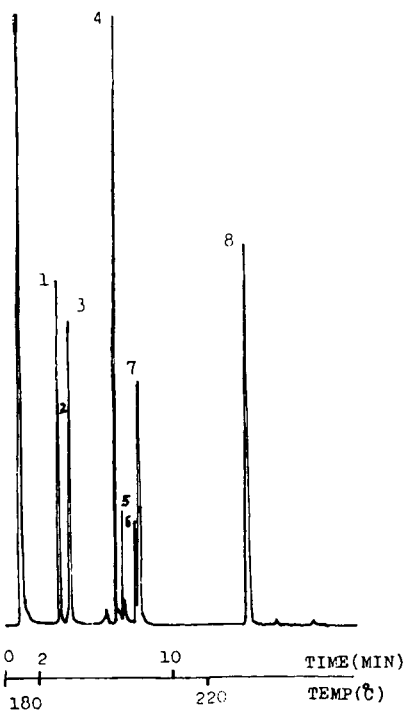

Fig. 4. Chromatogram of a series of secondary and tertiary nitrogen-containing polycyclic aromatic compounds on a crown ether stationary phase with cyanopropyl deactivation, coated on a 20 m × 200 μm I.D. fused-silica column with a film thickness of 0.25 μm. Peaks: 1 = indole: 2 = 3-methylindole; 3 = 2-methylindole; 4 = acridine; 5 = benzo[*h*]-quinoline; 6 = phenanthridine; 7 = benzo[*f*]quinoline; 8 = carbazole. From ref. 19.

2.4. Crown ether-anchored polysiloxanes

In 1988, Rouse *et al.* [19] first synthesized an 18-crown-6-modified poly(hydromethylsiloxane) by hydrosilylation with a propyloxymethyl spacer group, and used it as a capillary GC stationary phase. The crown–silica linkage was Si–CH_2– in this phase, which showed good thermostability and film forming ability. This phase exhibits excellent separations of polynitro-containing aromatic hydrocarbons (Fig. 4) [19,20]. Wu *et al.* [21] developed an 18-crown-6-substituted polysiloxane phase with an undecenyloxymethyl group as a spacer. The longer spacer of the polymeric phase facilitates immobilization on a fused-silica capillary with a coupling agent consisting of aza-*tert.*-butane (ATB) and DCUP [22,23]. The typical reaction scheme of this technique is illustrated in Fig. 5.

Several other types of crown ether compounds have also been used to prepare crown ether-anchored polysiloxane phases by Wu's group [24–26] and Fu's group [27,28], such as 2,3-benzo-9-[(propenyloxy)methyl]-15-crown-5, 2,3-benzo-9-[(propenyloxy)methyl]-18-crown-6 [24], di(*tert.*-butylbenzo)propenyl-15-crown-5, dibenzopropenyl-15-crown-5 [25], allylbenzo-15-crown-5 [27], dibenzo-14-crown-4 [28] and N-undecenylaza-15-crown-5 [26]. The use of substituted phenyl groups on the crown ring provides a π-electron and adds polarizability to the phases. All of these stationary phases had a selectivity similar to that of Carbowax 20M, but a much broader working temperature range and a unique selectivity for polar isomers.

As a special example, non-cyclic polyethers (*e.g.*, oligoethylene glycol) sometimes act as if they were crown ether derivative analogues [39,40]. Noncyclic polyethers are easily synthesized and have a high percentage yield compared with crown ethers. The attachment of end-capped polyethers to a well defined polymethylhydrosiloxane polymer has been reported. Rouse *et al.* [19] synthesized a polysiloxane phase containing a 3-[4-(2-methoxyethoxy)ethoxyphenyl]propyl substituent, which was found to be useful in the temperature range of 20–280°C and had a selectivity similar to that of Carbowax 20M. A series of similar phases have also been synthesized and studied by Tarbet *et al.* [29]. Among these materials, phases that have a phenyl unit in the side-chain were found to have higher thermal stability (260–270°C) than those without such a unit. The latter phases showed

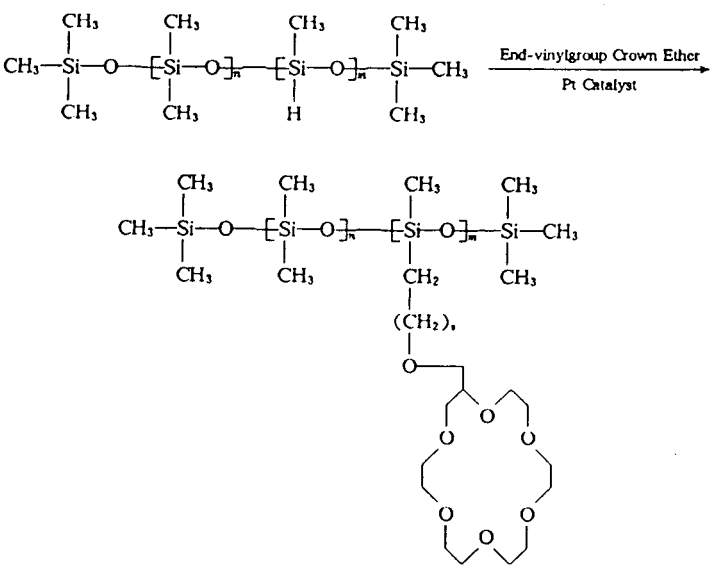

Fig. 5. Typical reaction scheme of hydrolylation ($s = 2$, ref. 13; $s = 10$, ref. 21).

serious degradation above 240°C. The higher stability of the former phases is possibly due to the phenyl group affording some steric protection to the polysiloxane backbone. Bradshaw *et al.* [30] prepared another series of polysiloxane phases containing polar or polarizable 4-cyanophenyl, 4-nitrophenyl, 2,4-dinitrophenyl or 8-quinolinyl units at the ends of diethylene oxide side-groups. These phases were found to possess both polar and polarizable characteristics, which facilitate the analysis of samples having components covering a broad polarity range, as shown in Fig. 6. Particularly, the 8-quinoline-substituted stationary phase satisfies the need for an efficient basic stationary phase for open-tubular columns. Recently, two α,ω-dialkenyl-substituted oligoethylene glyols were also attached to a polysiloxane backbone in our laboratory [31]. The maximum operating temperature of this phase is up to 300°C. The high thermal stability is due to various factors, but it is possible that it forms a net-like structure.

All of these crown ether polysiloxane phases were expected to be gums, which is required for efficient coating of capillary columns.

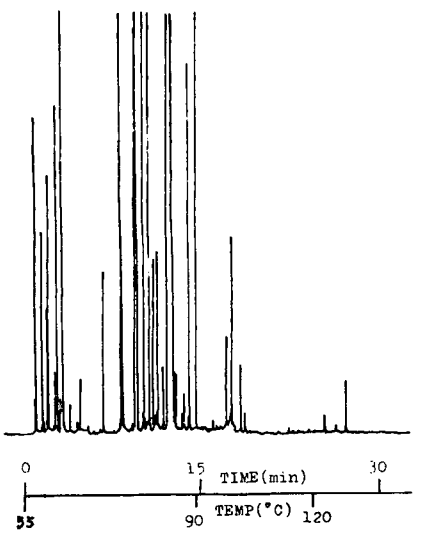

Fig. 6. Capillary gas chromatogram of peppermint essential oil. Column, 15 m × 20 μm I.D. fused silica, coated with a 0.15-μm film of 4-nitrophenyl-substituted poly(eugenol)-methylsiloxane as stationary phase; temperature, programmed from 55°C (2 min) to 150°C at 3°C min. From ref. 30.

The technique of attaching crown ethers or non-cyclic polyethers to polysiloxanes has been used for the preparation of polysiloxanes with complicated side-chains such as those containing liquid crystalline [32,33] and chiral carboxamide [34] units.

In these methods, a spacer of at least three carbons between the backbone of the polysiloxane and the crown ether ring or oligoethylene glycol is necessary to preserve the helical structure of the silicone backbone and high solute diffusivity. Moreover, for the objective to have a cross-linked phase, a measured amount of 1-octene in the hydrosilylation reaction along with a three-carbon-spacer crown ether or oligoetheylene oxide-containing alkene was essential, and it was shown that 2–5% octyl substitution can greatly enhance the cross-linkability of the phase [19,29,30].

It has been reported that phenyl substitution in the stationary phase hinders chemically induced cross-linking [35,36]. We failed to cross-link PSOB-3-15C5 phase (with a propyloxymethyl group as spacer) without octyl substitution in the phase using DCUP as a coupling agent. However, the experiments showed that cross-linking was effective with a much longer spacer group, such as undecyloxymethyl.

The method of preparing crown ether polysiloxanes by hydrosilylation provides some advantages. The yields in these hydrosilylation reactions are usually greater than 90%, and the molecular mass of the final polysiloxane phase and the percentage substitution can be fixed by using a starting polymethylhydrosiloxane of the appropriate molecular mass and SiH group content. Moreover, this procedure allows for the preparation of polysiloxane phases of known composition in a reproducible manner, which is helpful for elucidating the mechanism of selectivity.

On the other hand, we found that the beneficial effect of a crown ether substituent is optimum at a level of *ca.* 50% of the substituent for preserving good solute diffusity. The residual catalyst in the polymer which used in the re-

action may result in some acidity, and the residual catalyst should be carefully removed with methanol and water. Despite these constraints, the hydrosilylation technique is feasible, and much of the recent research into the application of crown ethers as GC stationary phase has been focused on the attachment of crown ethers to a polysiloxane backbone.

3. Characteristics of crown ether stationary phases in GC

The selectivity, polarity and thermostability of crown ether stationary phases have been reported by many workers. Each of these features is treated in detail below.

3.1. Selectivity of crown ether stationary phases

In GC, selectivity results from interactions between the solute and the stationary phase. These interactions are thought to be a complex combination of the following forces: charge transfer, hydrogen bonding, acid–base, dipole–dipole, dipole–induced dipole and dispersion. It is difficult to identify which forces are participating in any given separation as most stationary phase–solute interactions involve several of the forces listed above.

A crown ether stationary phase has a polar ring formed by the oxygen atoms or heteroatoms which are inside the crown. The polarity and electron cloud density of the crown ring vary with the type, number and placement of heteroatoms, the conformational flexibity and the shape(diameter) of the crown cavity and substituent group on the basic skeleton. Therefore, the selectivity of a crown ether stationary phase is assumed to be dominated mainly by hydrogen bonding, dipole–dipole and dispersion forces, and also the inclusion of the crown ring and the substituent functional group on the skeleton of the crown.

Hydrogen bonding plays an important role in the retention behaviour of alcohols and amines. For example, secondary amines that can form weaker hydrogen bonds with crown ether oxygen atoms than primary amines are eluted more rapidly; triethylamine, incapable of forming hydrogen bonds, is eluted most rapidly with a dibenzo-18-crown-6 or tribenzopyridine-21-crown-7 stationary phase [9]. Although the polarities of all crown ether phases are lower than that of Carbowax 20M, they show a higher selectivity for hydroxyl compounds than Carbowax 20M, especially for low-boiling alcohols, owing to the greater hydrogen bonding forces. A comparison of the resolution of alcohols on PEG and crown ether-substituted polysiloxane columns is shown in Fig. 7.

The heteroatoms or substituent group on the basic skeleton of the crown ether also affect the selectivity for some kinds of compounds. The slightly basic aza-crown ether-substituted polysiloxane phases have the ability to separate anilines and other basic compounds without derivatization (Fig. 8) [26]. Polarizable phenyl or

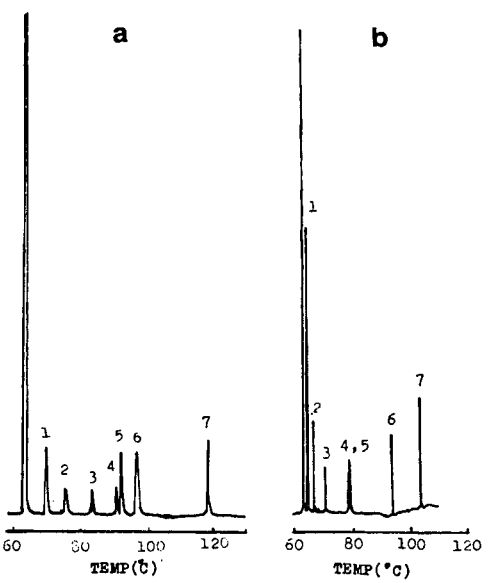

Fig. 7. Comparison of the resolution of *n*-alkanols on (a) a PSOB-3-15C5 column (15 m × 0.25 mm I.D.) and (b) a Carbowax 20M column (30 m × 0.24 mm I.D.). The column temperature was programmed from 60°C (1 min) to 130°C at 4°C min. Peaks: 1 = butanol; 2 = pentanol; 3 = hexanol; 4 = heptanol; 5 = octanol; 6 = nonanol; 7 = decanol. From ref. 24.

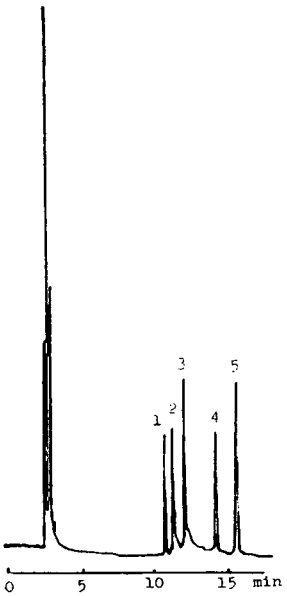

Fig. 8. Chromatogram of aniline compounds on a PUAC-18C6 column (15 m × 0.25 mm I.D.). Temperature, 120°C (isothermal). Peaks: 1 = *o*-methylaniline; 2 = *p*-methylaniline; 3 = *m*-methylaniline; 4 = N,N-diethyl-N-methylaniline; 5 = N-ethylmethylaniline. From ref. 26.

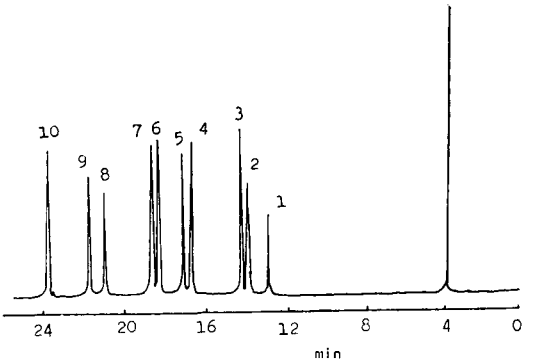

Fig. 9. Separation of a mixture of phenolic compounds on a 30 m × 0.28 mm I.D. PSOB-DB-14C4 column. Column temperature, programmed from 120 to 180°C at 2°C/min. Peaks: 1 = phenol; 2 = 2,6-dimethylphenol; 3 = *o*-cresol; 4 = *p*-cresol; 5 = *m*-cresol; 6 = 2,4-dimethylphenol; 7 = 2,5-dimethylphenol; 8 = 2,3-dimethylphenol; 9 = 3,5-dimethylphenol; 10 = 3,4-dimethylphenol. From ref. 28.

nitrophenyl substituents on the crown ether have been found to increase the selective separation of isomeric polar polyaromatic compounds and cresols. The resonating π-electrons in the phenyl ring add polarizability to the phases and introduce "soft" dipole–induced dipole interactions between the stationary phase and sample solute, which give excellent resolution of isomeric pairs without excessive retention of these isomers; such results are not usually possible using highly polar stationary phases. An excellent separation of phenolic compounds is shown in Fig. 9.

The cavity structure of the crown ether is another important factor with regard to the selectivity. Initially, the influence of the cavity was described as "the fitting ability with the crown ring" of solute moleculars by some workers.

There have been many investigations of the contribution of the crown ether cavity to the retention behaviour of solutes. For example, the *para* isomers of nitrophenol and nitroaniline fit well in the cavities of dibenzo-24-crown-8 and dicyclohexanol-24-crown-8, respectively, in contrast to the *ortho* and *meta* isomers, as is indicated by their long retention times [8]. In the separation of alcohols using DB-18C6 [8], the retention of methanol exhibits a significant increase because of the inclusion of the whole molecule in the crown cavity, and the retention decreases with increasing length of the *n*-alkanol chain, in agreement with decreasing stability of the complexes between DB-18C6 and *n*-alkanols [9].

According to the study of the thermodynamic properties at infinite dilution of several solutes in 18-crown-6 reported by Arancibia *et al.* [37], the more negative values of ΔH_E^{∞} (partial molar enthalpies of solutions) of methanol, chloroform and dichloromethane confirm that a complex is formed in the separation procedure.

Wu *et al.* [38] studied the dissolution entropies, $\Delta(\Delta S)$, of some isomers on five kinds of crown ether stationary phases (CSPS) and PEG-20M and OV-1701 stationary phases. The $\Delta(\Delta S)$ values, which reflect the effect of the configuration of the solute molecules on the stationary phase, are larger on CSPS than that on PEG-20M or OV-1701. This finding confirms the assumption that the cavity of the crown ether has an effect on the retention behaviour of solutes on CSPS. However, it cannot form inclusion

complexes with solutes as do the cyclodextrins, because the shape of many organic solutes is larger than the normal crown ether cavity; the unique selectivity of crown ether polymers for larger solutes is probably due to the fact that they are capable of forming sandwich-type 2:1 (crown ether ring:solute molecule) complexes.

The steric hindrance of solute molecules to the crown ether also adds some selectivity for CSPS. In the separation of nitrotoluene isomers on PSOB-15C-5, although the dipole–induced dipole force of 2,6-DNT is larger than that of 2,5-DNT and 2,4-DNT, it eluted first because of the steric hindrance effect. That is, the *ortho* substituent decreased the fitting ability of the solute molecule to the crown ether cavity (Fig. 10) [24].

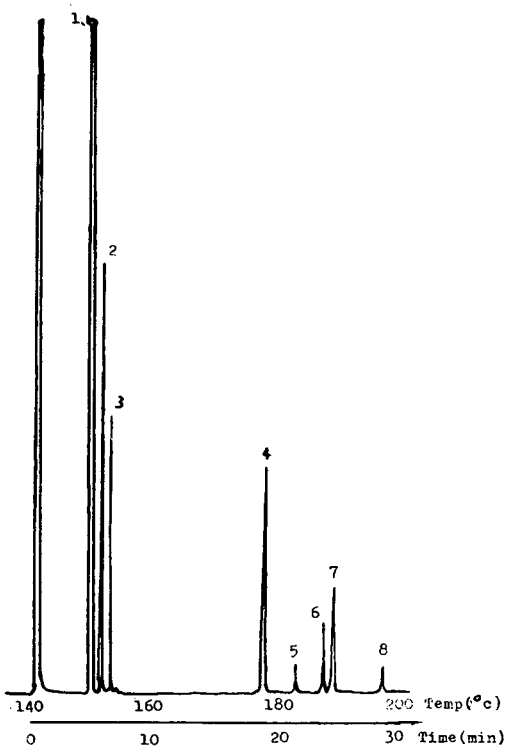

Fig. 10. Separation of mono-(MNT) and dinitrotoluene (DNT) isomers on a 15 m × 0.25 mm I.D. PSOB-3-15C5 column. Column temperature, programmed from 140 to 200°C at 2°C/min. Peaks: 1 = *o*-MNT; 2 = *m*-MNT; 3 = *p*-MNT; 4 = 2,6-DNT; 5 = 2,5-DNT; 6 = 2,4-DNT; 7 = 3,5-DNT; 8 = 3,4-DNT. From ref. 24.

3.2. Average polarity and thermostability of crown ether stationary phases

The polarity of low-molecular-mass crown ethers is mainly dominated by the crown ether structure. When the crown ether has a hydrophobic substituent such as a long apolar alkyl or cyclohexylene group, its polarity is low, whereas a polar or polarizable substituent such as phenyl or nitrophenyl may increase the polarity. All of the crown ether polysiloxane phases are of medium polarity, which is between 200 and 400 as represented by McReynolds constants. However, the polarity of crown ether-substituted polysiloxanes prepared by immoblization *in situ* inside the column is lower than that of the phases prepared by hydrosilylation, probably owing to the degree of polymerization of the crown ether in the former method being lower than that in the latter. Table 1 summarizes the chromatographic characteristics of some crown ether stationary phases.

The maximum allowable operating temperature (MAOT) of low-molecular-mass crown ether columns is relatively high, if the molecular masses are taken into account, because the crown ether compounds have intrinsically good chemical stability. The minimum allowable operating temperatures for these columns are dominated by the melting points of the crown ethers, because the column efficiency is low below the melting point owing to the increase in the mass-transfer resistance.

The MAOT of a polymeric crown ether which has a polyethylene backbone is higher than that of low-molecular-mass crown ether columns, but it is much lower than that of crown ether polysiloxanes. Crown ether polysiloxanes have been found to be stable up to 300°C, which is higher than for bondable PEG-20M (260°C). A phenyl ring included in a medium-polarity oligoethylene oxide or a crown ether can particularly increase the thermostability of a polysiloxane stationary phase. The minimum allowable temperature of a crown ether polysiloxane is determined by the glass transition temperature. However, because the changes in the thermodynamic and kinetic properties of many

Table 1
Characteristics of crown ether polymers used as GC stationary phases

Stationary phase[a]	Structure	Average polarity	Phase transition temperature (°C)	Min./max. operating temperature (°C)	Ref.
PVB-15C5	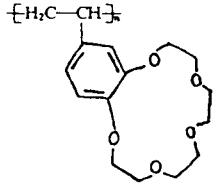	526	73, 155	55/220	14
VMSi17C6[b]	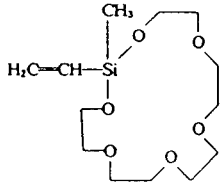	448	70	70/100	14
VMSi14C5[b]	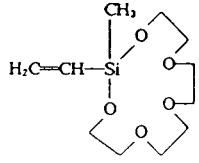	327	155	58/154	14
	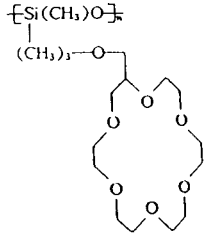	144		120/300	19
	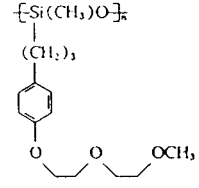			20/280	19

(Continued on p. 214)

Table 1 (*continued*)

Stationary phase[a]	Structure		Average polarity	Phase transition temperature (°C)	Min./max. operating temperature (°C)	Ref.
PSO-11-18C6 (a) PSO-11-15C5 (b)	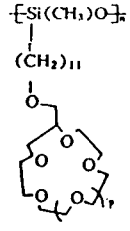	(a) $p = 2$; (b) $p = 1$	229 206	136 150	70/300 70/300	21 22
PSOB-3-15C5 (a) PSOB-3-18C6 (b)	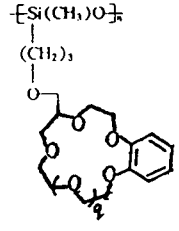	(a) $q = 1$ (b) $q = 2$	231 239	119 121	70/300 70/300	26
PSO-DTB-3-15C5	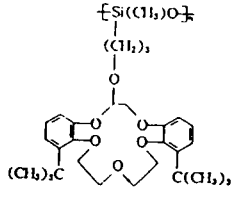		211	100	<310	25
PSO-DB-3-15C5	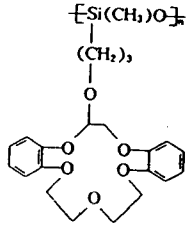		352	104	<310	25

PPADEG (a) PPATEG (b)	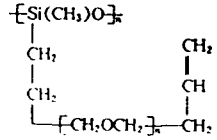	(a) $n = 3$; (b) $n = 5$	296 309	150 970	<300 <300	31
PUAC-11-18C6 (a) PUAC-11-15C5 (b)	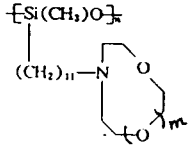	(a) $m = 4$ (b) $m = 3$	394 265	137 140	75/305 75/305	24
PAB-15C5	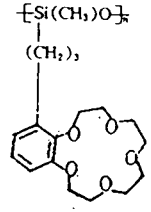		318	124	300	27
PSO-DB-14C4	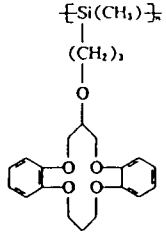		286	58, 156	280	28

(Continued on p. 216)

Table 1 (*continued*)

Stationary phase[a]	Structure	Average polarity	Phase transition temperature (°C)	Min./max. operating temperature (°C)	Ref.
	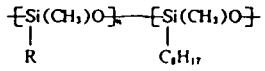				29
	R = 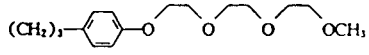				
	R = 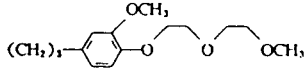			260–270	
	R = 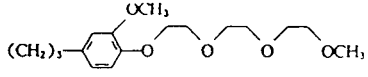				
	R = 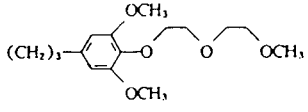				
	R = 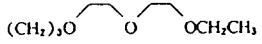			240	29
	R = 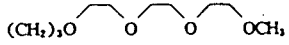			240	
	R = 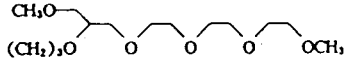			240	

[a] PVB-15C5 = poly(vinylbenzo-15-crown-5); VMSi17C6 = vinylmethylsila-17-crown 6; VMSi14C5 = vinylmethylsila-14-crown-4; PSO-11-18C6 = *n*-undecyloxymethyl-18-crown-6 polysiloxane; PSO-11-15C5 = *n*-undecyloxymethyl-15-crown-5 polysiloxane; PUAC-11-18C6 = *ω*-undecyleneaza-18-crown-6 polysiloxane; PUAC-11-15C5 = *ω*-undecyleneaza-15-crown-5 polysiloxane; PSOB-3-18C6 = 2,3-benzo-11-[(propenyloxy)methyl]-18-crown-6 polysiloxane; PSOB-3-15C5 = 2,3-benzo-9-[(propenyloxy)methyl]-15-crown-5 polysiloxane; PSO-DTB-3-15C5 = Di(*tert.*-butylbenzo)propyl-15-crown-5 polysiloxane; PSO-DB-15C5 = dibenzopropyl-15-crown-5 polysiloxane; PSO-DB-14C4 = dibenzopropyl-14-crown-4 polysiloxane; PAB-15C5 = 3-allylbenzo-15-crown-5 polysiloxane; PPATEG = *α*-propyl-*ω*-allyltriethylene glycol polysiloxane; PPADEG = *α*-propyl-*ω*-allyldiethylene glycol polysiloxane.

[b] Cross-linked with silicone *in situ* inside column.

crown ether polysiloxanes are very close for the two states at the glass transition temperature, the minimum allowable temperature will be much lower below the transition temperature. Hence the crown ether polysiloxane phases have a wide operating temperature range.

4. Conclusions

Crown ether (or non-cyclic polyether) polysiloxane stationary phases exhibit medium polarity and a selectivity similar to that of Carbowax 20M, but a much wider working temperature range. They also provide unique selectivity for polar compounds such as alcohols, aromatic amines and polar isomers. Especially samples having components covering a broad polarity range can be analysed using these phases. Moreover, the benzo-crown ether polysiloxanes show inistric thermostability and excellent resolution for polar isomers, and aza-crown ether polysiloxane phases can satisfy the need for an efficient basic stationary phase for open-tubular columns.

5. Acknowledgement

This work was supported by the National Science Foundation.

6. References

[1] K. Kimura and T. Shono, *J. Liq. Chromatogr.*, 5, Suppl. 2 (1982) 223.
[2] J.D. Lamb and R.G. Smith, *J. Chromatogr.*, 546 (1991) 73.
[3] W. Millen and S. Hawkes, *J. Chromatogr. Sci.*, 15 (1977) 48.
[4] R.V. Vigalok and A.L.F. Bubacahinkowa, *Usp. Gaz. Kromatogr. (Kazan)*, 6 (1981) 190.
[5] A. Ono, *Analyst*, 108 (1983) 1265.
[6] R. Li, *Wuhan Daxue Xuebao, Ziran Kexueban*, 4 (1985) 121.
[7] R. Li, *Sepu*, 4 (1986) 304.
[8] N.R. Ayyangar, A.S. Tambe and S.S. Biswas, *J. Chromatogr.*, 543 (1991) 179.
[9] A. Kohoutova, E.S. Keulemansova and L. Feltl, *J. Chromatogr.*, 471 (1989) 139.
[10] Y.H. Liu, D.P. Qiao and M. Li, *Sepu*, 10 (1992) 33.
[11] E.V. Zagorevskaya and N.V. Kovaleva, *J. Chromatogr.*, 365 (1986) 7.
[12] Y.H. Jin, R.N. Fu and Z.F. Huang, *J. Chromatogr.*, 469 (1989) 153.
[13] A.R.J. Andrews, Z. Wu and A. Zlatkis, *Chromatographia*, 34 (1992) 163.
[14] D.D. Fine, H.Z. Gearhart and H.A. Mottola, *Talanta*, 32 (1985) 751.
[15] C.Y. Wu, H.Y. Li, Y.Y. Chen and X.R. Lu, *J. Chromatogr.*, 504 (1990) 279.
[16] Z.R.Zeng, C.Y. Wu, X.H. Fang, Z.F. Huang and Y.T. Wang, *J. Chromatogr.*, 589 (1992) 279.
[17] Z.R. Zeng, C.Y. Wu, H. Yan, Z.F. Huang and Y.T. Wang, *Chromatographia*, 34 (1992) 85.
[18] Z.R. Zeng, C.N. Wang, C.Y. Wu and Z.F. Huang, *Chem. J. Chin. Univ.*, 13 (1992) 752.
[19] C.A. Rouse, A.C. Finlinson, B.J. Tarbet, J.C. Piston, N.M. Djordjevic, K.E. Markides, J.S. Bradshaw and M.L. Lee, *Anal. Chem.*, 60 (1988) 901.
[20] J.M. Bayona, B.J. Tarbet, H.C. Chang, C.M. Schregenberger, M. Nishioka, K.E. Markides, J.S. Bradshaw and M.L. Lee, *Int. J. Environ. Anal. Chem.*, 28 (1987) 263.
[21] C.Y. Wu, C.M. Wang, Z.R. Reng and X.R. Lu, *Anal. Chem.*, 62 (1990) 968.
[22] C.Y. Wu, C.M. Wang, Z.R. Reng and X.R. Lu, *Chem. J. Chin. Univ.*, 12 (1991) 173.
[23] C.Y. Wu, C.M. Wang, J.S. Cheng and X.R. Lu, *Sepu*, 8 (1990) 355.
[24] C.Y. Wu, X.C. Zhou, Z.R. Reng, X.R. Lu and L.F. Zhang, *Anal. Chem.*, 63 (1991) 1874.
[25] C.Y. Wu, L.S. Cai, Y.J. Hang, Z.R. Reng, Z.Y.Y. and H. Yuan, *Chromatographia*, 37 (1993) 374.
[26] C.Y. Wu, J.S. Cheng, W.H. Gao, Z.R. Reng, X.R. Lu and S.L. Gong, *J. Chromatogr.*, 594 (1992) 243.
[27] A.Q. Zhang, J.L. Ge, Z.X. Guan, J.H. Deng, H.W. Liu, J.Y. Zhu, R.N. Fu, Z.F. Huang and B. Zhang, *J. Chromatogr.*, 521 (1990) 128.
[28] J.L. Ge and R.W. Fu, *J. Microcol. Sep.*, 3 (1991) 211.
[29] B.J. Tarbet, J.S. Bradshaw, D.F. Johnson, A.C. Finlinson, C.A. Rouse, K. Jones, S.R. Sumpter, E.C. Huang, Z. Juvancz, K.E. Markides and M.L. Lee, *J. Chromatogr.*, 473 (1989) 103.
[30] J. Bradshaw, M. Schirmer, Z. Juvancz, K. Markides and M.L. Lee, *J. Chromatogr.*, 540 (1991) 279.
[31] L.S. Cai and C.Y. Wu, presented at *International Beijing Conference and Exhibition on Instrumental Analysis, Beijing*, 1993.
[32] K.E. Markides, M. Nichioka, B.J. Tarbet, J.S. Bradshaw and M.L. Lee, *Anal. Chem.*, 57 (1985) 1296.
[33] J.S. Bradshaw, C.M. Schregenberger, K.H.C. Chang, K.E. Markides and M.L. Lee, *J. Chromatogr.*, 358 (1986) 95.
[34] J.S. Bradshaw, S.K. Aggarwal, C.A. Rouse, B.J. Tarbet, K.E. Markides and M.L. Lee, *J. Chromatogr.*, 405 (1987) 169.

[35] K. Grob and G. Grob, *J. Chromatogr.*, 213 (1981) 121.
[36] P.A. Peaden, B.W. Wright and M.L. Lee, *Chromatographia*, 15 (1982) 335.
[37] E.L. Arancibia, C.R. de Schaeter and M. Katz, *Chromatographia*, 33 (1992) 41.
[38] C.Y. Wu, J.S. Cheng and Z.R. Zeng, *Chromatographia*, 35 (1993) 33.
[39] Y.W. Qiu, X.L. Zhang, F.H. Wang and H.Z. Wang, *Wuhan Daxue Xuebao, Ziran Kexueban*, 4 (1985) 71.
[40] G.Z. Tan and T.Q. Jiao, *Huaxue Xuebao*, 9 (1987) 52.
[41] C.J. Pederson, *J. Am. Chem. Soc.*, 89 (1967) 7017.
[42] B. Dietrich, J.M. Lehn and J.P. Sauvage, *J. Am. Chem. Soc.*, (1969) 2889.

Journal of Chromatography A, 662 (1994) 219–225
Elsevier Science B.V., Amsterdam

CHROM. 25 560

Enantiomeric separation of underivatized aliphatic β-amino alcohols by ligand-exchange chromatgraphy using barbital as an additive to the mobile phase

Shigeo Yamazaki*, Shoko Nagaya, Katsunori Saito and Takenori Tanimura

Laboratory of Analytical Chemistry, Toyama Medical and Pharmaceutical University, 2630 Sugitani, Toyama 930-01 (Japan)

(First received August 25th, 1992; revised manuscript received September 14th, 1993)

ABSTRACT

Underivatized aliphatic β-amino alcohols with a secondary alcohol moiety were separated into enantiomers by high-performance liquid chromatography using octadecylsilanized silica coated with N-*n*-dodecyl-L-hydroxyproline as the stationary phase and an aqueous solution containing copper(II) and barbital as the mobile phase.

INTRODUCTION

In previous papers we reported that underivatized aromatic β-amino alcohols (BAAs) could be separated into enantiomers by ligand-exchange chromatography (LEC) using a copper(II) solution as the mobile phase and octadecylsilanized silica gel (ODS) coated with N-*n*-dodecyl-L-hydroxyproline (C_{12}-Hyp) as the stationary phase [1,2]. On the other hand, for underivatized aliphatic BAAs, our attempts using this methodology were unsuccessful because of the low retention or a small separation factor.

In other studies, we found that not only aromatic but also aliphatic BAAs were separated into enantiomers by LEC using an ODS column and a chiral mobile phase containing copper(II), L-proline and barbital (BB). Although BB is a chiral, addition of BB to the mobile phase was critical for the separation [3].

In this work, BB addition was applied to the separation of underivatized aliphatic BAAs on a column packed with C_{12}-Hyp-coated ODS as a chiral stationary phase.

EXPERIMENTAL

Samples

The preparation of 1-amino-2-pentanol was accomplished by addition of ammonia to 1,2-epoxypentane according to the described method with minor modifications [4]. The epoxide was prepared by two methods: methylation of butyraldehyde using trimethylsulphonium iodide [5] or oxidation of 1-pentene with *m*-chloroperoxybenzoic acid [6]. The results of elemental analysis of the oxalate salt were as follows: calculated for $C_6H_{14}NO_3$, C 48.63, H 9.52, N 9.45; found, C 48.40, H 9.62, N 9.32%.

The preparation of chiral 1-amino-2-pentanol could not be accomplished by a fractional crystallization method using L-tartrate, dibenzoyl-L-tartrate, L-glutamate, *d*-camphor sulphonate or *d*-bromocamphorsulphonate as the chiral counter anion. However, it was achieved by using (*S*)-norvaline as the starting material to obtain the *S*-isomer as outlined in Fig. 1. The deamination

* Corresponding author.

0021-9673/94/$07.00
SSDI 0021-9673(93)E0992-4

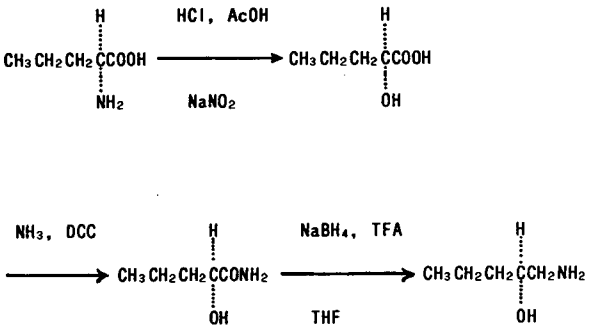

Fig. 1. Synthesis of (*S*)-1-amino-2-pentanol.

of (*S*)-norvaline [7] proceeds to (*S*)-2-hydroxyvaleric acid without racemization, as demonstrated by the chromatographic technique reported in a previous paper [8]. The solubility of lithium (*S*)-2-hydroxyvalerate is moderately low compared with the solubility of the sodium salt. Therefore, the reaction solution was poured into a cation-exchange column in the Li^+ form. The effluent from the column was concentrated and the lithium salt of the acid was obtained. After recrystallization, again using a cation-exchange column prepared in the acidic form, the lithium salt solution was converted into an acidic solution, which was dried and dissolved in chloroform. Using 1,3-dicyclohexcylcarbodiimide (DCC) and ammonia, the acid was derivatized to the amide [9]. Finally, the amide was reduced to the amine with sodium tetrahydroborate in trifluoroacetic acid–tetrahydrofuran [10]. After extraction with ethyl acetate, the amine was obtained as the oxalate salt. The results of elemental analysis of the oxalate salt were as follows: calculated for $C_6H_{14}NO_3$, C 48.63, H 9.52, N 9.45; found, C 48.46, H 9.38, N 9.37%; $[\alpha]_D^{27}$ + 7.7 (*c*, 0.60 in water).

The preparation of 1-amino-2-hexanol was accomplished by the method employed for the preparation of 1-amino-2-penatanol. 1,2-Epoxyhexene was commercially available. The results of elemental analysis of the oxalate salt were as follows: calculated for $C_7H_{16}NO_3$, C 51.90, H 9.95, N 8.33; found, C 51.83, H 9.94, N 8.64%.

(*S*)-1-Amino-2-hexanol was prepared according to the method employed for the preparation of (*S*)-1-amino-2-pentanol, but the results of elemental analysis were unsatisfactory. The crude product, however, was applicable for the determination of the elution order.

Other BAAs used were purchased from commercial sources.

Chromatography

The column used and the C_{12}-Hyp coating procedure have been described in a previous paper [1]. For the detection of BAAs a post-column reaction using *o*-phthalaldehyde to form a fluorophore was employed [1].

RESULTS AND DISCUSSION

The direct resolution of 1-amino-2-butanol, 1-amino-2-pentanol and 1-amino-2-hexanol, which contain an amino group attached to a primary carbon atom and a secondary alcohol group, was achieved. These 1-amino-2-ol type BAAs were all well resolved. Fig. 2 shows the chromatogram of 1-amino-2-pentanol. Conversely 2-amino-1-ol-type BAAs, which contain an amino group attached to a secondary carbon atom and a primary alcohol group, such as 2-amino-1-butanol and 2-amino-1-pentanol, could not be resolved under the conditions described in Fig. 2. A similar result, with the separation of 1-amino-2-ol-type aromatic BAAs being better than that of the corresponding 2-amino-1-ol-type aromatic BAAs on a column packed with C_{12}-Hyp-coated ODS, was reported in a previous paper [2]. These results indicate that the secondary alcohol group plays an important role in the separation mechanism in the present method. Fig. 3 shows that *trans*-2-aminocyclohexanol, which contains an amino group attached to a secondary carbon atom and a secondary alcohol group, could be separated even using a mobile phase containing no BB, but the separation was improved in the presence of BB. For 1-amino-2-propanol, only a partial separation was achieved even using three 15-cm columns in series and the mobile phase used in Fig. 2, because of the low retention.

We studied the influence of the BB, copper (II) and triethylamine(TEA) concentrations in the mobile phase and its pH on the separation of the three aliphatic 1-amino-2-ol-type BAA enantiomers.

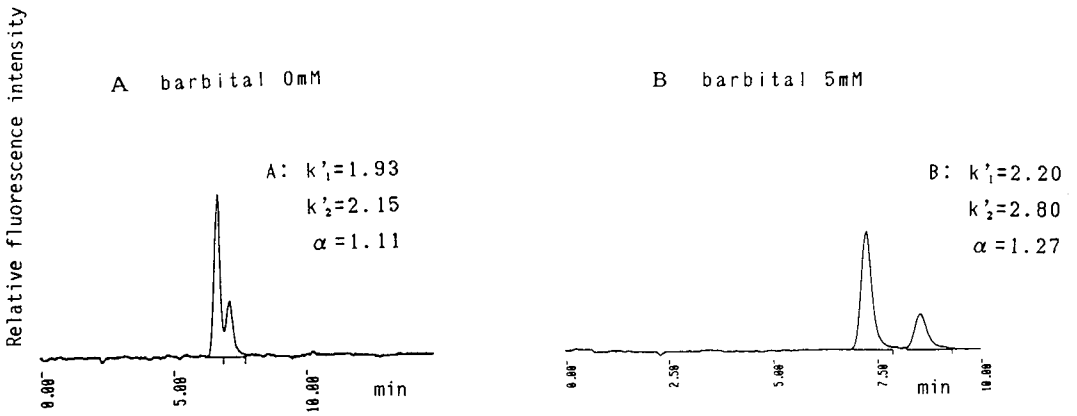

Fig. 2. (A) Chromatogram of 1-amino-2-pentanol. Column, Develosil ODS-5 coated with C_{12}-Hyp (150 mm × 4 mm I.D.); mobile phase, 12 m*M* copper(II) acetate and 20 m*M* TEA in 50 m*M* acetate buffer (pH 6.0, adjusted with acetic acid or NaOH); flow-rate, 0.5 ml/min; sample size, 20 μl, containing 0.1 μg of BAA ($S/R = 3:1$). Other conditions as in text. (B) Conditions as for (A) with the addition of 5 m*M* sodium barbital to the mobile phase.

The effect of BB concentration in the mobile phase on the capacity factor (k') and the separation factor (α) is shown in Fig. 4. The effect is concentration dependent in a non-linear and saturable manner. Maximum k' values were obtained at 5–10 m*M* BB, declining above 10 m*M* BB, but the α values above 10 m*M* BB remained approximately constant. BB can be replaced with other BB analogues such as amobarbital (Figs. 3 and 5).

The effect of addition of BB to the mobile phase on the separation of aromatic BAAs was also investigated. As shown in Figs. 5 and 6, the addition was effective for octopamine (1-amino-2-ol-type BAA) but not for phenylglycinol (2-amino-1-ol-type BAA). Although these structures are similar, the peaks of the octopamine enantiomers in Fig. 5 are tailing and those of phenylglycinol in Fig. 6 are fronting. The reason is not known.

Aldehydes and BAAs with a primary or secondary amine moiety can form an oxazolidine ring, and the oxazolidine could be separated into enantiomers [11]. BB has three carbonyl groups,

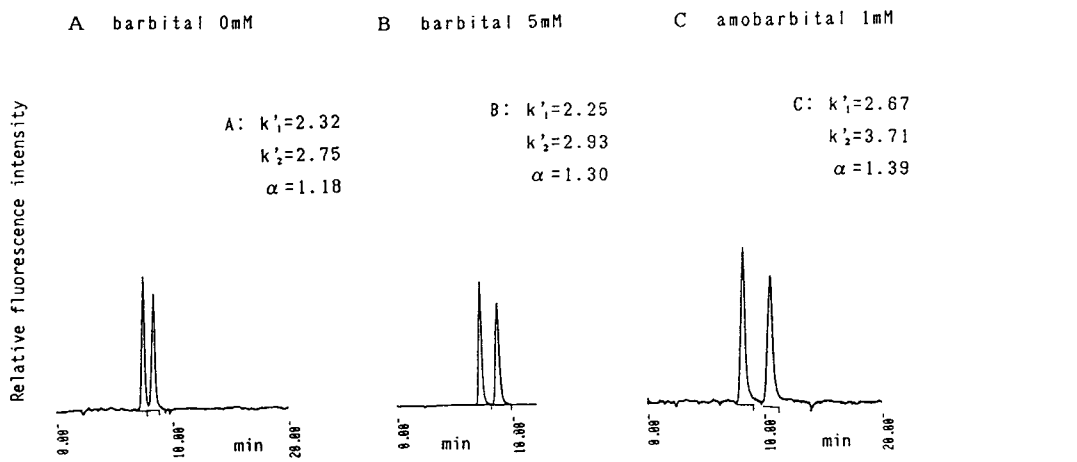

Fig. 3. (A) Chromatograms of *trans*-2-aminocyclohexanol. Conditions as in Fig. 2A. (B) Conditions as for (A) with the addition of 5 m*M* sodium barbital to the mobile phase. (C) Conditions as for (A) with the addition of 1 m*M* sodium amobarbital to the mobile phase.

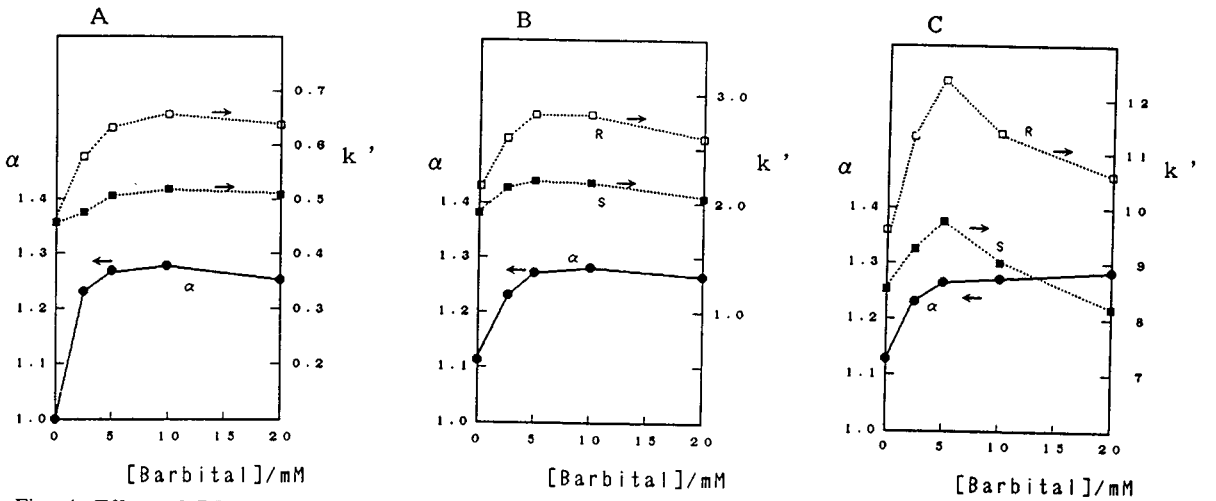

Fig. 4. Effect of BB concentration in the mobile phase on the enantiomeric separation of (A) 1-amino-2-butanol, (B) 1-amino-2-pentanol and (C) 1-amino-2-hexanol. Mobile phase, 8 m*M* copper(II) acetate, various concentrations of BB and 20 m*M* TEA in 50 m*M* acetate buffer (pH 6.0, adjusted with acetic acid or NaOH). Other conditions as in Fig. 2.

and the ring formation equilibrium between the BAA and BB may play some role in the separation. BAAs with a tertiary amine group cannot form such a ring; nevertheless, for the separation of 1-dimethylamino-2-propanol and 1-dimethylamino-2-butanol, a similar BB effect was also observed [12]. Hence oxazolidine formation does not seem to play a role in the separation. Although the exact role of BB is not clear, BB may coordinate with Cu(II). The use of BB as an additive is one of the advantages of the present method.

The separation was also strongly dependent on the copper(II) concentration, the TEA concentration and the pH of the mobile phase. Their influences on the separation of 1-amino-2-

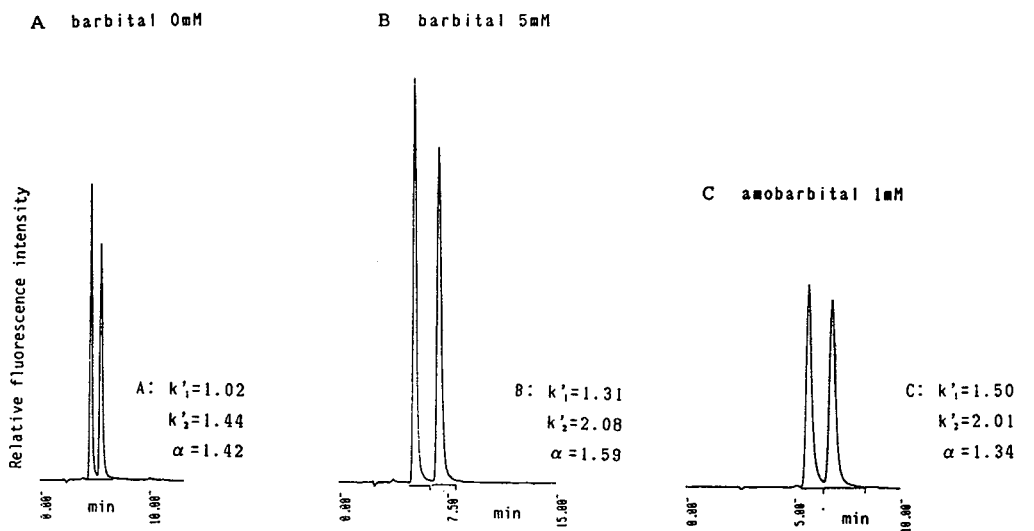

Fig. 5. (A) Chromatograms of octopamine. Conditions as in Fig. 2A. (B) Conditions as for (A) with the addition of 5 m*M* sodium barbital to the mobile phase. (C) Conditions as for (A) with the addition of 1 m*M* sodium amobarbital to the mobile phase.

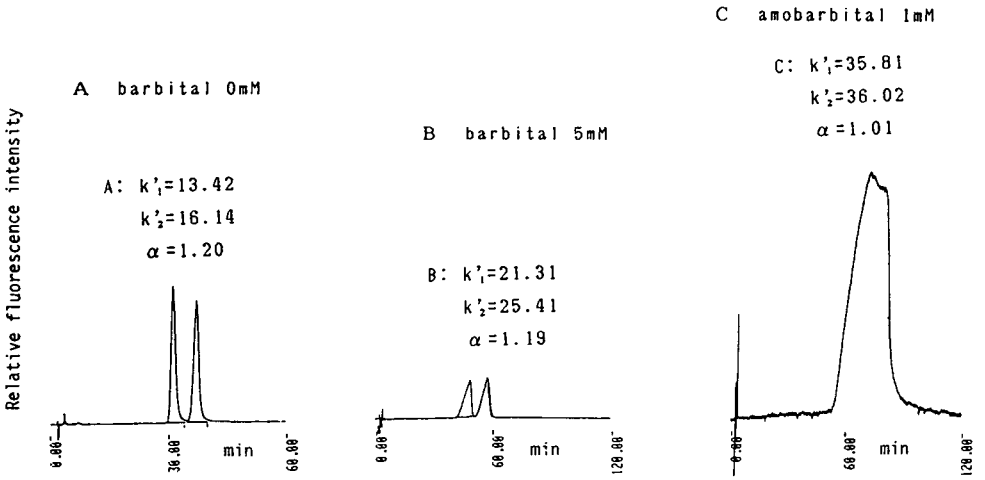

Fig. 6. (A) Chromatograms of phenylglycinol. Conditions as in Fig 2A. (B) Conditions as for (A) with the addition of 5 m*M* sodium barbital to the mobile phase. (C) Conditions as for (A) with the addition of 1 m*M* sodium amobarbital to the mobile phase.

butanol, 1-amino-2-pentanol and 1-amino-2-hexanol enantiomers were studied over the pH range 5–6 and with copper(II) concentrations in the range 1–16 m*M*. As shown in Figs. 7 and 8, increasing pH and copper(II) concentration of the mobile phase result in greater retention and better separation of the enantiomers. C_{12}-Hyp is an amino acid, and substantial complex formation with Cu^{2+} occurs at pH 5–6. With BAAs as solutes, the deprotonation of the BAAs is very low compared with that of the amino acid at this pH [13], and therefore the complex formation must increase as the pH increases. The strong dependence of retention and separation on pH 5–6 may be the reason. To avoid the precipitation of copper(II) hydroxide in the mobile phase, pH values above 6.2 were not studied.

The effect of TEA addition to the eluent on the k' and α values is shown in Fig. 9. It is well known that the addition of TEA to the mobile

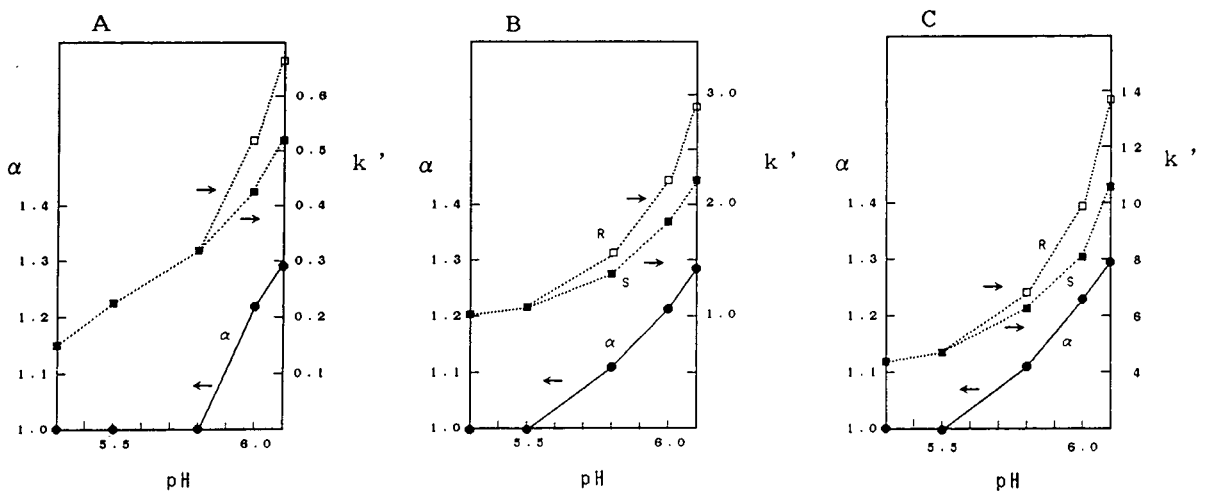

Fig. 7. Effect of pH of the mobile phase on the enantiomeric separation of (A) 1-amino-2-butanol, (B) 1-amino-2-pentanol and (C) 1-amino-2-hexanol. Mobile phase, 8 m*M* copper(II) acetate, 5 m*M* BB and 20 m*M* TEA in 50 m*M* acetate buffer (pH adjusted with acetic acid or NaOH). Other conditions as in Fig. 2.

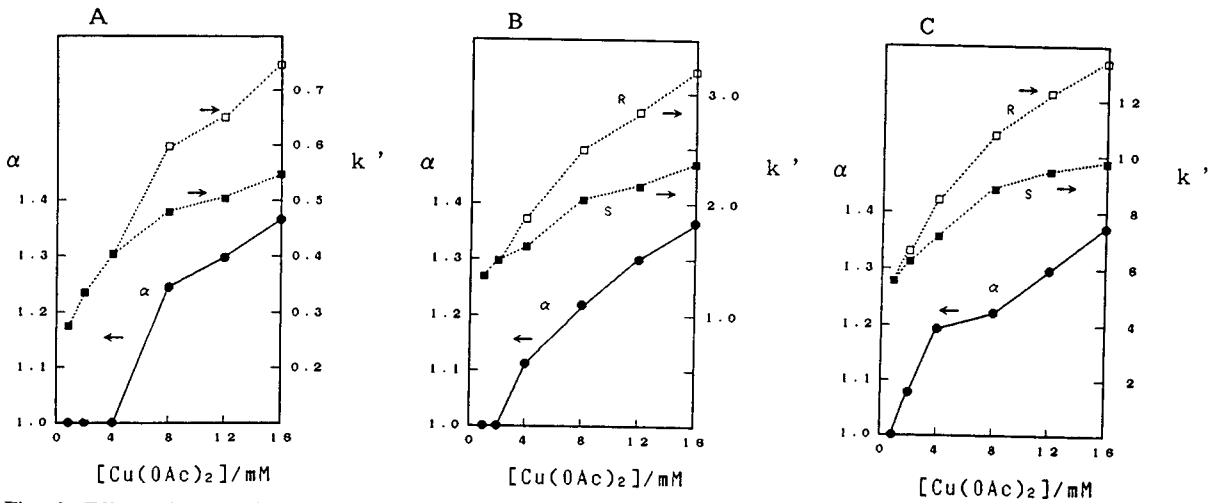

Fig. 8. Effect of copper(II) concentration in the eluent on the enantiomeric separation of (A) 1-amino-2-butanol, (B) 1-amino-2-pentanol and (C) 1-amino-2-hexanol. Mobile phase, various concentrations of copper(II) acetate, 5 m*M* BB and 20 m*M* TEA in 50 m*M* acetate buffer (pH 6.0, adjusted with acetic acid or NaOH). Other conditions as in Fig. 2.

phase improves the shape of amine peaks using a silica-based column. A 20 m*M* concentration of TEA resulted in an improvement in these separations, although it caused a decrease in the retention of the BAAs.

The final conditions selected were a mobile phase at pH 6 containing 8–16 m*M* copper(II), 5 m*M* barbital and 20 m*M* TEA, which provided a satisfactory separation of 1-amino-2-butanol, 1-amino-2-pentanol, 1-amino-2-hexanol and *trans*-2-aminocyclohexanol enantiomers. The results reported here show that the enantiomeric separation of underivatized aliphatic BAAs with a secondary alcohol moiety on a column packed with C_{12}-Hyp-coated ODS was improved by addition of BB to the mobile phase containing copper(II). Similarly, the separation of underivatized aromatic BAAs with a secondary alcohol

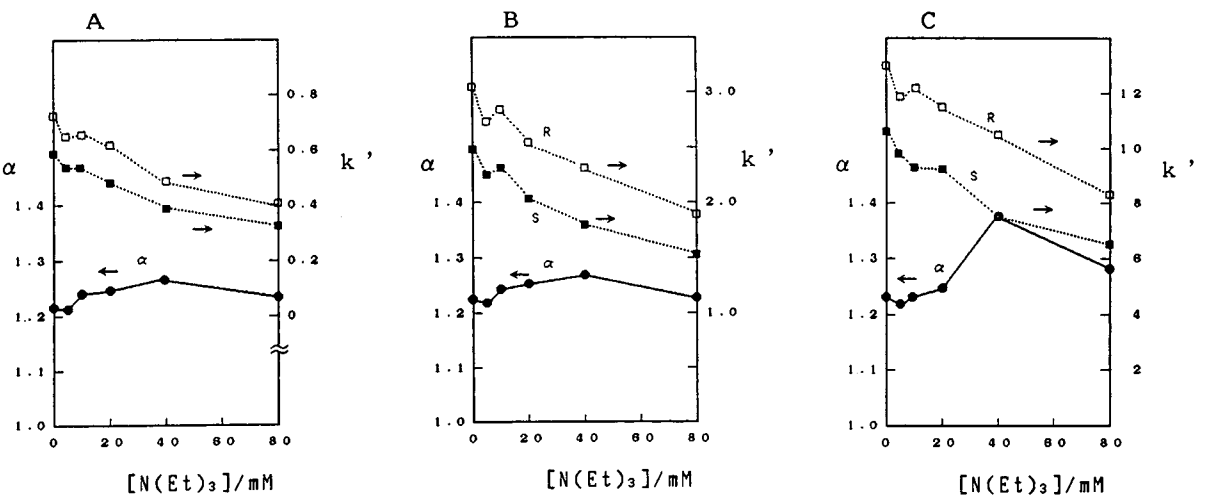

Fig. 9. Effect of TEA concentration in the eluent on the enantiomeric separation of (A) 1-amino-2-butanol, (B) 1-amino-2-pentanol and (C) 1-amino-2-hexanol. Mobile phase, 8 m*M* copper(II) acetate, 5 m*M* BB and various concentrations of TEA in 50 m*M* acetate buffer (pH 6.0, adjusted with acetic acid or NaOH). Other conditions as in Fig. 2.

moiety was improved. However, no improvements of the enantiomeric separation of 2-amino-1-ol-type BAAs, α-amino acids and β-amino acids were observed.

In subsequent work, we found that N-*n*-dodecylnorephedrine was also a useful coating reagent for ODS for the separation of both aliphatic 1-amino-2-ol- and 2-amino-1-ol-type BAAs into enantiomers. The details will be published elsewhere.

REFERENCES

1 S. Yamazaki, T. Takeuchi and T. Tanimura, *J. Liq. Chromatogr.*, 12 (1989) 2239.
2 S. Yamazaki, T. Takeuchi and T. Tanimura, *J. Chromatogr.*, 540 (1991) 169.
3 S. Yamazaki and T. Tanimura, *J. Liq. Chromatogr.*, submitted for publication.
4 A.J. Castro and C.R. Noller, *J. Am. Chem. Soc.*, 68 (1946) 203.
5 E. Borredon, M. Delmas and A. Gaset, *Tetrahedron Lett.*, 23 (1982) 5283.
6 N.N. Schwartz and J.H. Blumbergs, *J. Org. Chem.*, 29 (1964) 1976.
7 M. Winitz, L.B. Frankenthal, N. Izumiya, S.M. Birnbaum, C.G. Baker and J.P. Greenstein, *J. Am. Chem. Soc.*, 78 (1956) 2423.
8 R. Horikawa, H. Sakamoto and T. Tanimura, *J. Liq. Chromatogr.*, 9 (1986) 537.
9 Y.S. Klausner and M. Bodanzky, *Synthesis*, (1972) 453.
10 N. Umino, T. Iwakuma and N. Itoh, *Tetrahedron Lett.*, (1976) 763.
11 I.W. Wainer, T.D. Doyle, Z. Hamidzadeh and M. Aldridge, *J. Chromatogr.*, 261 (1983) 123.
12 S. Yamazaki, unpublished results.
13 C.W. Davies and B.N. Patel, *J. Chem. Soc. A*, (1968) 1824.

ELSEVIER

Journal of Chromatography A, 662 (1994) 227–233

JOURNAL OF CHROMATOGRAPHY A

On-line separation of phenylthiohydantoin derivatives of hydrophilic modified amino acids during sequencing☆

Daniel J. Strydom

Center for Biochemical and Biophysical Sciences and Medicine and Department of Pathology, Harvard Medical School, 250 Longwood Avenue, Boston, MA 02115, USA

(First received August 19th, 1993; revised manuscript received November 9th, 1993)

Abstract

All 20 commonly occurring phenylthiohydantoin (PTH) amino acids can be separated by a new reversed-phase chromatography method without interference from breakthrough peaks that prevail in other methods, and with good resolution from the most common reagent-related background peaks. Separation is compatible with automated sequencing in a cartridge sequencer. A large chromatographic area exists between the breakthrough peaks and the first- and second-eluting common PTH-amino acids, PTH-His and PTH-Asn, and is consequently available for detection and separation of hydrophilic amino acid derivatives. Derivatives such as phosphotyrosine, β-hydroxyaspartic acid and N-glycosylated asparagine elute as readily identifiable peaks. The method uses chromatography on octadecylsilane with isocratic elution followed by a simple linear gradient from acetonitrile–methanol to isopropanol–methanol to provide complete separation in 23 min. The turnaround time of 34 min includes a period of column washing to eliminate sequencer byproducts. PTH-Amino acids are generally detected with single pmol (1 to 4 pmol) sensitivity. PTH-His and PTH-Arg are eluted earlier than conventionally with a consequent sharpening of peaks and higher practical sensitivity.

1. Introduction

The identification and quantitation of phenylthiohydantoin (PTH) amino acids are at present fundamental to the process of protein and peptide sequencing, and provide a means to both recognize known modifications and point to the existence of unknown modifications. Chemical protein sequencing is therefore often used to examine potential post-translational modification of proteins. The availability of the protein of interest is often the limiting factor in such studies and therefore individual experiments should yield as much information as possible. Successful recognition of a modified residue at a specific position in a sequence presupposes the positive identification of a chromatographic peak during sequencing, and not merely the absence or low yield of normal residues, which may be caused by conventional losses inherent to the chemistry of the sequencing process.

Many post-translational modifications give rise to hydrophilic amino acid side chains and those are most likely to be missed or confused when using the common separation systems. Such modifications may be natural, such as glycosylation, phosphorylation, sulfation, hydroxylation and carboxylation, or synthetic, due to deliberate modifications, and are usually detected by

☆ Presented in part in a poster (S180) at the *7th Symposium of the Protein Society, San Diego, CA, July 24–28, 1993.*

0021-9673/94/$07.00
SSDI 0021-9673(93)E1215-L

alternative PTH separations, which are not used routinely. As an example acidic derivatives such as β-hydroxyaspartic acid may be analyzed by using 0.1% trifluoroacetic acid (TFA) as eluent [1]. Other derivatives that have been detected, but which elute in inconvenient positions for studies with low amounts of sample, are *e.g.* phosphotyrosine [2,3], γ-carboxyglutamic acid [4], and phosphoserine/threonine [5], although the latter derivatives may not survive the Edman chemistry [6,7]. Chemically modified residues studied by Edman degradation include degraded carboxyhistidines [8], azobenzene arsonate derivatives [9] and photoaffinity-modified residues, reacted with 8-azido ATP [5]. Glycosylation sites are frequently detected as "blank" sequencer cycles (see, *e.g.* ref. 10), although partial deglycosylation of protein samples allows extraction and identification of monoglycosidic PTH-amino acids [11] and the use of covalently immobilized samples in the sequencers allow extraction and chromatography of fully glycosylated residues [12,13].

Most current cartridge-style sequencers ("gas-phase sequencers") incorporate the on-line determination of PTH-amino acids by HPLC. The separation schemes have to accommodate the short cycle times of the sequencers and as a consequence most elute the first PTHs very early, in many cases within seconds of the sample breakthrough peaks and disturbances. In addition, the most common separations operate at a pH where PTH-Asp elutes first, thereby providing the characteristic "Asp-problem" for sequencing, which is the frequent loss of information on small amounts of Asp, or at best integration problems with the Asp peak eluting on or next to baseline disturbances. Hydrophilic (early-eluting) derivatives will consequently only be recognized with difficulty, if at all, in these early parts of the chromatograms.

Other difficulties experienced in PTH-amino acid separation schemes include the broadening of PTH-His and -Arg peaks and their consequently less sensitive detection, and the existence of reagent-related background peaks which may co-elute with PTH-amino acids.

We here developed a separation of PTH-amino acids that is compatible with a 34-min turn-around on a Millipore ProSequencer and that also provides disturbance-free chromatography in the early parts of the chromatogram as well as chromatographic space for detection of hydrophilic post-translational modifications. In addition PTH-His and -Arg are eluted much earlier and with sharper peaks than conventionally, thereby providing enhanced sensitivity. Many extraneous peaks [such as diphenylthiourea (DPTU)] are separated from the common PTH-amino acids.

2. Experimental

2.1. Materials

Standard PTH-amino acids, β-hydroxyaspartic acid and phosphotyrosine were from Sigma (St. Louis, MO, USA). Diphenylurea, diphenylthiourea, phenylthiourea and aniline were from Aldrich (Milwaukee, WI, USA). HPLC-grade solvents were from J.T. Baker (Phillipsburg, NJ, USA) and water was purified on a Milli-Q system (Millipore, Bedford, MA, USA) utilizing ion-exchange and Organex-Q cartridges. A glycopeptide, V2, was derived from a *Staphylococcus aureus* V8 digest of a ribonuclease homologue (unpublished). (The peptide contains significant amounts of mannose and glucosamine, and has the characteristic Asn–X–Thr sequence for potentially N-glycosylated Asn. Only the C-terminal Asp is found by conventional sequencing of the whole peptide, which has an amino acid composition that includes two aspartic acid or asparagine residues).

2.2. Sequencer

A Millipore ProSequencer [14] was used, employing the manufacturer's standard TFA-100 protocol which elutes anilinothiazolinone (ATZ) derivatives from the cartridge membrane with a pulse of TFA. Peptides were bound to arylamine

membranes (Sequelon-AA, Millipore), by carbodiimide (EDC) coupling [15–18].

2.3. HPLC

The HPLC equipment consisted of either (i) two M6000 pumps, a M680 gradient controller and a M440 detector (Millipore/Waters) and a PE Nelson interface/Nelson analytical chromatography software (Perkin-Elmer, Norwalk, CT, USA) for data collection or (ii) a Model 62M pump, 600E system controller and M486 tunable absorbance detector (Millipore) and Maxima software, on-line to a Millipore ProSequencer. The column was a Supelcosil LC-18-DB (25 × 0.46 cm; Supelco, Bellefonte, PA, USA), with a guard column of the same material.

Solvent A contained 0.33% (v/v) triethylamine (HPLC grade, Fisher, Pittsburgh, PA, USA), 9.5% (v/v) methanol and 10.5% (v/v) acetonitrile, and the pH was adjusted with orthophosphoric acid (HPLC-grade, Fisher) to 3.55 before addition of the organic solvents. Solvent B was methanol–isopropanol–water (60:20:20). The applied gradient is given in Table 1.

Table 1
Protocol for gradient-elution of PTH-amino acids

Time (min)	Flow-ate (ml/min)	Solvent A (%)	Solvent B (%)
0	1	95	5
7	1	95	5
22	1	33	67
23	1	0	100
25	1	0	100
25.5	1.2	0	100
28	1.2	0	100
29	1.2	95	5
33	1.2	95	5
33.5	1	95	5

The gradient segments are all linear. The column was a Supelcosil LC-18-DB (25 × 0.46 cm), with a guard column of the same material. Solvent A contained 0.33% (v/v) triethylamine, 9.5% (v/v) methanol and 10.5% (v/v) acetonitrile, and the pH was adjusted with orthophosphoric acid to 3.55 before addition of the organic solvents. Solvent B was methanol–isopropanol–water (60:20:20).

3. Results and discussion

3.1. Design and implementation of the PTH separation

An octadecylsilane column and methanol and isopropanol as solvents were taken as baseline conditions for the design of an improved PTH separation, based on prior experience over more than a decade in this laboratory with such a system in conjunction with a spinning cup sequencer [19]. Relatively few studies have used isopropanol as the major eluent for achieving separation of PTH amino acids (*e.g.* refs. 19–24). All of these demonstrate the same characteristic separation of the later-eluting PTH-amino acids which was again found in this study. Thus isopropanol provides a useful selectivity for the hydrophobic amino acids, allowing facile PTH-Met/Val separation and positioning PTH-(ε-PTC; phenylthiocarbamyl)-Lys and PTH-Trp conveniently earlier than PTH-Phe, in the large open chromatographic space after PTH-Val. The viscosity of isopropanol was accommodated and the consequent high chromatographic pressures were alleviated by the addition of a large ratio of methanol to the B solvent, and raising the temperature above room temperature. Notably the change from solely isopropanol in the second solvent to methanol–isopropanol (3:1) did not markedly change the relative elution positions of the amino acids Ala through Leu. The use of triethylamine phosphate as modifier of the chromatographic solvent allowed PTH-His and -Arg to elute at much earlier times than is commonly found, and the adjustment of pH to 3.55 delayed elution of PTH-Asp and PTH-Glu until *after* both PTH-His and -Arg. A mixture of acetonitrile and methanol was needed to separate the PTH-Thr, -Gln, -Gly triplet and the ratio of these two modifiers affects the position of those derivatives relative to one another.

The elution protocol is simple, starting with isocratic elution of the hydrophilic amino acids, followed by a single linear gradient in isopropanol–methanol, thereby allowing facile adjustment of conditions for different columns.

Two very different chromatographs were used during the development of this protocol —a single pump system with premixing of the gradient, and a dual pump system with post-delivery mixing of the solvents— and the separations are highly similar on both, suggesting ready applicability to other chromatographs.

The chromatographic separation achieved in the current studies is shown in Fig. 1. All the common amino acids are well resolved, and sequencer-derived byproducts of phenylisothiocyanate (PITC), such as DPTU and 1-phenyl-3-cyclohexylthiourea (PCHTU) (the latter derived from the scavenger, cyclohexylamine, added to wash solvents in the Millipore ProSequencer) are also separated from the PTH-amino acids (Fig. 2). Less commonly found byproducts such as aniline and phenylthiourea (PTU) elute respectively before and after PTH-His, completely separated from it. Methylphenylthiocarbamate, produced *i.a.* from methanol and PITC through incomplete drying of sequencer membranes, and sometimes seen in the first cycle of degradation, elutes midway between PTH-Met and -Val. Sequencer-derived PTH-Ile isomerizes to also yield PTH-*allo*-Ile, which elutes as a doublet with PTH-Ile. In this separation (Fig. 2) the shoulder preceding PTH-Ile indicates the elution position of PTH-*allo*-Ile, which is completely resolved from PTH-Phe. Although diphenylurea (DPU) creates difficulties for identification of PTH-Trp in some generally used systems [25], it elutes with PTH-*allo*-Ile in the present scheme. This does not prove to be a problem however, since (i) DPU, when present, is usually found only at the single picomol level, and (ii) PTH-Ile elutes as the two characteristic peaks, thereby allowing unequivocal identification and good quantitation.

The separation and identification of N-glycosylated PTH-Asn is demonstrated with the routine sequencer degradation of a peptide (V2, Arg–Arg–Asx–Met–Thr· · ·), from a digest of

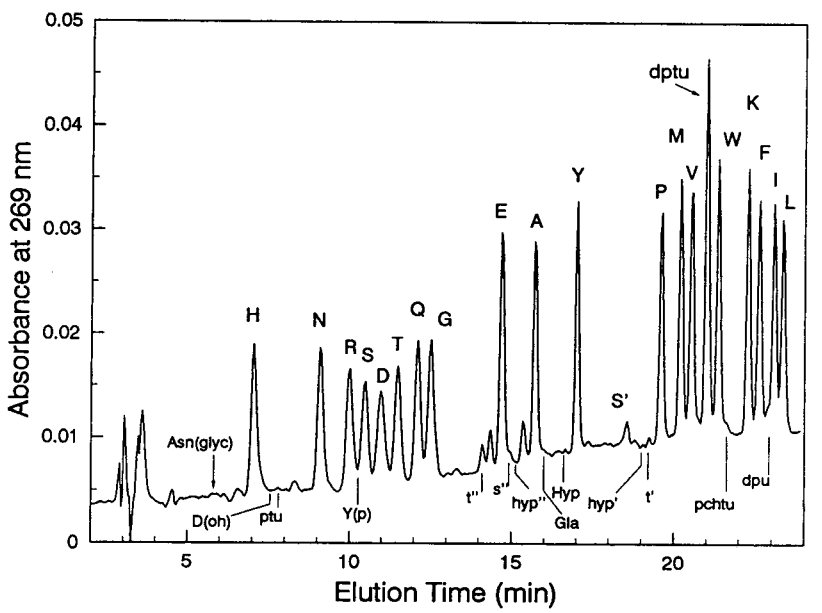

Fig. 1. Separation of 40 pmol of PTH-amino acids on a Supelcosil C_{18} column. The elution conditions are described in the text. The single letter notation for amino acids is used to identify the peaks corresponding to PTH-amino acids. Hyp = PTH-hydroxyproline, hyp′ and hyp″ = characteristic peaks also seen with hydroxyproline. S′, s″, t′ and t″ label the elution positions for characteristic degradation products of serine and threonine derivatives. The positions for phosphotyrosine [Y(p)], β-OH-Asp [D(oh)], γ-carboxy-Glu (Gla), glycosylated Asp and the phenylureas [diphenylthiourea (dptu), phenylthiourea (ptu), phenylcyclohexylthiourea (pchtu), diphenylurea (dpu)] are also indicated.

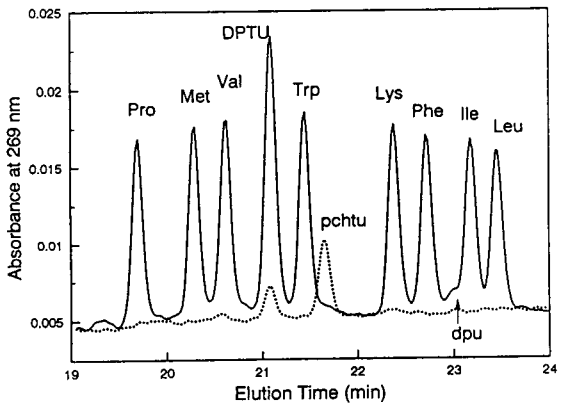

Fig. 2. Separation of the most hydrophobic PTH-amino acids on a Supelcosil C_{18} column. PTH Standards (40 pmol) and diphenylthiourea (DPTU) (solid line) are compared to a blank sequencer run (dotted line).

a ribonuclease homologue. Fig. 3 records the chromatograms of cycles 2 to 4 of Edman degradation on this peptide. The broad peak at 5.9 min is clearly the residue cleaved off in cycle 3, and is consistent with an expected N-glycosylated PTH-Asn. The asymmetry of this peak, also seen in a separate experiment on another peptide containing the same residue, probably reflects heterogeneity in the carbohydrate moiety.

The sensitivity of quantitation that can be achieved is illustrated by the separation of 4 pmol standard PTH-amino acids, dissolved in 100 μl sequencer-transfer buffer (20% acetonitrile, 0.1% acetic acid), in Fig. 4. All the PTH-amino acids are detected at the 4 pmol level, most are detectable at 1 pmol and with appropriate subtraction software the few residues such as PTH-Asn and PTH-Gly that are partly overlapped by small amounts of background compounds from the chemistry or HPLC buffers are also easily detected at 1 pmol.

3.2. Adjustment of separation

The chromatography is easily adaptable to other set-ups by consideration of a few specific aspects of the two-stage separation.

The more hydrophilic phenylthiohydantoins PTH-His, -Asn, -Arg, -Ser, -Asp, -Thr, -Gln and -Gly, are in effect eluted isocratically. PTH-Arg is positioned between PTH-Asn and -Ser by modifying the ionic strength of the A solvent

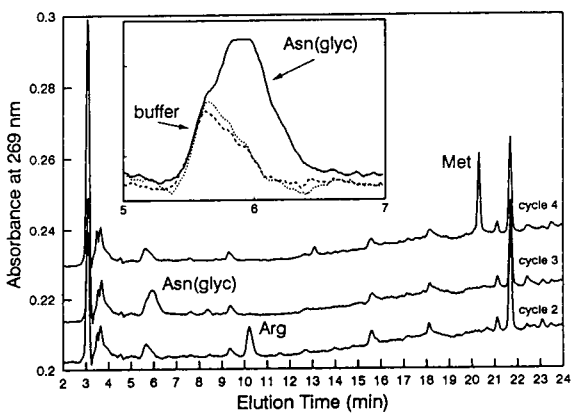

Fig. 3. Sequencer chromatograms for three cycles of degradation of a glycopeptide. Cycles 2, 3 and 4 each contain one major product which is identified as respectively Arg, an "unknown", and Met. The unknown elutes as a broad peak at 5.9 min (inset: the solid line is from cycle 3, the dashed and dotted lines are from cycles 2 and 4) which reflects its hydrophilicity and, as discussed in the text, would be N-glycosylated PTH-Asn, with heterogeneity in the carbohydrate.

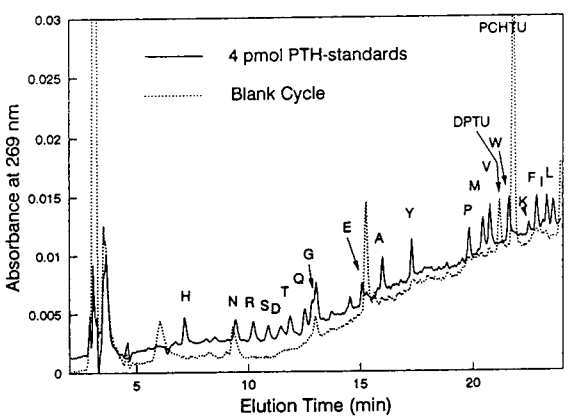

Fig. 4. Separation of 4 pmol of PTH-amino acids under conditions described in the text. A blank sequencer cycle (dotted line) is included to illustrate the background seen with a specific set of sequencer reagents.

(higher triethylamine concentrations allow earlier elution of PTH-Arg). The initial conditions are then adjusted to elute PTH-His at 4 ± 0.2 min after the solvent breakthrough. Changes in the initial state (2 to 7% B; lower amounts of B cause the PTHs to elute later) and/or temperature (higher temperatures cause earlier elution) should be used to position PTH-His. PTH-Gln is centered between PTH-Thr and -Gly by adjusting the methanol–acetonitrile ratio in solvent A. Thus ratios of 0.8 to 1.2 will move PTH-Gln from elution with PTH-Thr to elution with PTH-Gly in the specific system discussed here. Likewise, on changes of 0.15 to 0.2 pH unit from pH 3.55, PTH-Asp will coelute either with PTH-Ser (at higher pH) or with PTH-Thr (at lower pH) (as an example, with one new column we changed the pH to 3.70 to center PTH-Asp between PTH-Ser and -Thr; the rest of the separation remained the same). The start of the second stage, a linear gradient to high amounts of solvent B, is set to coincide with the elution of PTH-Arg. Thus if PTH-Arg elutes 7 min after the solvent breakthrough, the gradient portion of the elution should start at 7 min into the elution protocol. These gradient settings accommodate varying instrumental holdup volumes. Once this set of hydrophilic PTHs separates well the subsequent gradient can be adjusted to separate the later-eluting group.

The gradient portion of the protocol yields a robust separation of all the relevant PTH-amino acids and allows at least a 20% variation in gradient slope to be tolerated. The precise elution positions of DPTU and PCHTU however depend critically on the gradient and their positioning relative to PTH-Val and -Trp may require adjustments in the gradient slope. Additionally, lower temperatures or lower ratios of acetonitrile to methanol in the A solvent will move PCHTU further from DPTU, without much relative movement of the PTH-amino acids.

The washing cycle is important in the repeated analyses of sequencing cycles and since the organic content of the A solvent is high, reequilibration after washing is rapid, within 5 to 7 ml.

4. Conclusions

The primary requirements for a good PTH-amino acid separation system which will be compatible with on-line detection of sequencer products are: (i) a short turn-around time to accommodate sequencer cycle times; (ii) toleration of large injection volumes, compatible with automated transfer from the sequencer; (iii) a robust separation that can be installed and maintained with ease; (iv) separation of known reagent- and solvent-related peaks from common amino acids; (v) chromatographic space in which to elute and recognize known and unknown modifications; and (vi) detection sensitivity at low picomol level.

The separation developed here fulfills these requirements. The use of triethylamine phosphate as modifier of the elution solvent for PTH-amino acids provides very early elution of PTH-His and -Arg and, consequently, an opportunity to design a separation of PTH-amino acids that provides more chromatographic space early in the separation than conventionally used with on-line sequencers. This separation is easy to install and maintain. The very early elution of PTH-His and -Arg furthermore increases the sensitivity of detection of these usually problematic residues. Additionally, the sequencer byproducts DPTU, PTU, PCHTU and aniline are well separated from all common PTH-amino acids, including PTH-Trp. The extra chromatographic space is useful for the detection of hydrophilic post-translational modifications of proteins. Such modified residues of course need to be eluted from the sequencer cartridges under conditions that require covalent immobilization of the parent proteins [2,3,12,13]. The rapidly developing mass spectrometric sequencing technologies [26,27] are slated to supercede the traditional Edman chemistries in due course. The present high cost of the specialized instrumentation and the problems inherent in any youthful technology will, however, preclude many from immediate conversion to these technologies. The new capability of analyzing hydrophilic post-translational modifications of proteins during conventional

sequencing should therefore be immediately useful during this transition between methodologies.

5. Acknowledgements

I thank Dr. B.L. Vallee for continued support and Rebecca Ettling and Wynford Brome for expert technical assistance during various stages of this work. Dr. J.D. Dixon (Millipore Corp.) provided helpful discussions. These studies were supported by the Endowment for Research in Human Biology, Inc., Boston, MA, USA.

6. References

[1] T. Sugo, P. Fernlund and J. Stenflo, *FEBS Lett.*, 165 (1984) 102.
[2] R. Aebersold, J.D. Watts, H.D. Morrison and E.J. Bures, *Anal. Biochem.*, 199 (1991) 51.
[3] C.W. Turck, J. Herrmann, J.A. Escobedo and L.T. Williams, *Pept. Res.*, 4 (1991) 36.
[4] J.R. Cairns, M.K. Williamson and P.A. Price, *Anal. Biochem.*, 199 (1991) 93.
[5] J.E. Walker, I.M. Fearnley and R.A. Blows, *Biochem. J.*, 237 (1986) 73.
[6] J.C. Mercier, F. Grosclaude and B. Ribadeau-Dumas, *Eur. J. Biochem.*, 23 (1971) 41.
[7] M. Ikebe and S. Reardon, *J. Biol. Chem.*, 265 (1990) 8975.
[8] D.J. Welsch and G.L. Nelsestuen, *Biochemistry*, 27 (1988) 7513.
[9] B. Schwaller and H. Sigrist, *Anal. Biochem.*, 177 (1989) 183.
[10] K.J. Rutherford, K.M. Swiderek, C.B. Green, S. Chen, J.E. Shively and S.C. Kwok, *Arch. Biochem. Biophys.*, 295 (1992) 352.
[11] R.J. Paxton, G. Mooser, H. Pande, T.D. Lee and J.E. Shively, *Proc. Natl. Acad. Sci. U.S.A.*, 84 (1987) 920.
[12] J.L. Abernethy, Y. Wang, A.E. Eckhardt and R.L. Hill, in R.H. Angeletti (Editor), *Techniques in Protein Chemistry III*, Academic Press, San Diego, CA, 1992, p. 277.
[13] P.J. Neame and F.P. Barry, in R.H. Angeletti (Editor), *Techniques in Protein Chemistry IV*, Academic Press, San Diego, CA, 1993, p. 153.
[14] R.A. Laursen, J.D. Dixon, S.P. Liang, D.M. Nguyen, T. Kelcourse, L. Udell and D.J.C. Pappin, in B. Wittmann-Liebold (Editor), *Methods in Protein Sequence Analysis*, Springer, Berlin, 1989, p. 61.
[15] J.M. Coull, J.D. Dixon, R.A. Laursen, H. Köster and D.J.C. Pappin, in B. Wittmann-Liebold (Editor), *Methods in Protein Sequence Analysis*, Springer, Berlin, 1989, p. 69.
[16] D.J.C. Pappin, J.M. Coull and H. Köster, in J. Villafranca (Editor), *Current Research in Protein Chemistry*, Academic Press, San Diego, CA, 1990, p. 191.
[17] J.M. Coull, D.J.C. Pappin, J. Mark, R. Aebersold and H. Köster, *Anal.Biochem.*, 194 (1991) 110.
[18] D.J.C. Pappin, J.M. Coull and H. Köster, *Anal. Biochem.*, 187 (1990) 10.
[19] D.J. Strydom, J.W. Fett, R.R. Lobb, E.M. Alderman, J.L. Bethune, J. Riordan and B.L. Vallee, *Biochemistry*, 24 (1985) 5486.
[20] S.A. Cohen, *Application Brief: M3500*, Millipore–Waters, Milford, MA, 1985.
[21] H.V. Kolbe, R.C. Lu and H. Wohlrab, *J. Chromatogr.*, 327 (1985) 1.
[22] C. Fonck, S. Frutiger and G.J. Hughes, *J. Chromatogr.*, 370 (1986) 339.
[23] R. Murphy, J.B. Furness and M. Costa, *J. Chromatogr.*, 408 (1987) 388.
[24] A.B. Rawitch, H.G. Pollock and S.X. Yang, *Arch. Biochem. Biophys.*, 300 (1993) 271.
[25] T. Muller-Michel and P. Bohlen, *Anal. Biochem.*, 191 (1990) 169.
[26] A.L. Burlingame, in R.H. Angeletti (Editor), *Techniques in Protein Chemistry IV*, Academic Press, San Diego, CA, 1993, p. 3.
[27] B.T. Chait, R. Wang, R.C. Beavis and S.B.H. Kent, *Science*, 262 (1993) 89.

ELSEVIER

Journal of Chromatography A, 662 (1994) 235–241

JOURNAL OF CHROMATOGRAPHY A

Purification of tryptophan containing synthetic peptides by selective binding of the α-amino group to immobilised metal ions ☆

Per Hansen*, Gunnar Lindeberg

Department of Immunology, Biomedical Center, University of Uppsala, Box 582, S-751 23 Uppsala, Sweden

(First received June 28th, 1993; revised manuscript received November 15th, 1993)

Abstract

Immobilised metal ion affinity chromatography (IMAC) based on selective binding via the α-amino group to Cu^{2+} and Ni^{2+} ions has been used to purify tryptophan containing synthetic peptides. A free α-amino group, serving as an affinity handle, is present only in the target peptide when the peptides are synthesised by the solid-phase method and remaining amino groups after each coupling step are blocked by acetylation.

A free α-amino group is necessary to retain the peptide on the column. The tryptophan residue may contribute to the binding only if the peptide is simultaneously anchored via the α-amino group.

1. Introduction

Immobilised metal ion affinity chromatography (IMAC) was introduced by Porath *et al.* in 1975 [1] and has since been a useful tool for the purification of various proteins (*e.g.* refs. 2–11). The α-amino group is known to interact with immobilised metal ions [12–17], but it is generally assumed that it is histidine, cysteine and tryptophan that are largely responsible for the binding of proteins [1,18–20] and of peptides [15,16,21] in IMAC. Accordingly, these amino acids, when situated near the N-terminus, have been used as affinity handles for the purification by IMAC of synthetic peptides [22].

Crude peptides synthesised by the solid-phase method using a capping protocol contain, apart from the target peptide with its free α-amino function, truncated peptides with blocked α-amino groups. Affinity handles have been introduced on the free α-amino group of the target peptide [23–28] thus allowing the use of more specific separation methods than RP-HPLC, which is commonly used for purification of synthetic peptides. The limitations of this approach, and particularly the problems associated with the removal of the substituent, prompted us to investigate the use of the free α-amino group as an affinity handle [29]. We found that IMAC could be used for the purification, via the free α-amino group, of synthetic peptides lacking histidine, cysteine and tryptophan. Such peptides are retarded in IMAC only when a free α-amino group is present. The retention is pH dependent and increases from pH 5 to 7.5 (Cu^{2+}) and from pH 5 to 8.5 (Ni^{2+}) due to deprotonation of the

* Corresponding author.

☆ Part of this work was presented as a poster at the *22nd European Peptide Symposium, Interlaken, Switzerland, September 13–19, 1992.*

0021-9673/94/$07.00
SSDI 0021-9673(93)E1252-U

α-amino group. As the pH is further raised to 9–10 the retention drops as a result of metal ion transfer (MIT) from the chromatographic support to the peptide. At pH > 9 (on Cu^{2+}, but not Ni^{2+}) the retention of lysine containing peptides again increases due to deprotonation and binding of the ε-amino group.

We have now widened our study to determine if selective binding via the free α-amino group is also possible when a tryptophan residue is present in the peptide. Since tryptophan strongly contributes to the binding of peptides and proteins in IMAC [15,16,18,21,30,31], it could be expected that each peptide containing a tryptophan residue would bind to the IMAC adsorbent, thereby destroying the selectivity. In an attempt to reduce the presumed metal affinity of the indole function we decided to protect the indole nitrogen by formylation. However, such precautions proved to be unnecessary. Data presented in this report clearly show that the contribution by tryptophan to binding is of secondary importance and can be observed only when the peptide is simultaneously anchored to the IMAC support by a more efficient affinity handle such as the α-amino group.

2. Experimental

2.1 Chemicals

All chemicals were of analytical grade and used as purchased. *tert*-Butyloxycarbonyl (Boc) amino acids were obtained from Peninsula Laboratories Europe (St. Helens, UK) or Novabiochem (Läufelfingen, Switzerland). Boc-amino acyl resins were prepared according to Horiki *et al.* [32]. Chelating Superose was obtained from Kabi-Pharmacia (Uppsala, Sweden).

2.2 Buffers

The chromatographic buffers (pH range 5–11) contained 50 m*M* sodium dihydrogen phosphate, 50 m*M* boric acid and 1 *M* sodium chloride and were prepared as described previously [29].

2.3 Peptide synthesis

Solid-phase synthesis of peptides was performed on an Applied Biosystems 430A instrument as described previously [29]. Formylated tryptophan peptides were deprotected by reaction with 0.1 *M* aqueous piperidine at room temperature for 30 min, then desalted on a Sephadex G-10 gel filtration column (30 × 1 cm I.D.) equilibrated with 50 m*M* ammonium acetate pH 8.0 and recovered by lyophilization.

Spontaneous deformylation of peptides occurred in the upper pH range. After one week at pH 6.5 no deformylation was detected, at pH 8.5 partial deformylation was observed and at pH 10.0 peptides were completely deformylated. The peptide solutions were never prepared more than 8 h before use.

The peptides are listed in Table 1 and will hereafter be referred to in bold numbers with indication of a free (**A**) or blocked (**B**) α-amino group.

2.4 IMAC

An FPLC system (Kabi-Pharmacia, Uppsala, Sweden) was used for all chromatography and the conditions for IMAC were as described earlier [29]. The peptides (100 nmoles in 100 μl of the chromatographic buffer) were applied to the pre-equilibrated column and eluted isocratically. The capacity factor (k) was determined according to

$$k = V_e/V_0 - 1$$

where V_e is the retention volume for the peptide on a metal loaded column and V_0 the retention volume on a metal free column.

2.5 Mass spectrometry

Synthetic products and chromatographic fractions were analysed by plasma desorption mass spectrometry (PDMS) using a BioIon 20 instrument (Applied Biosystems, Uppsala, Sweden) as described earlier [29].

Table 1
Structures of peptides used in this investigation

Peptide	Structure
1A [a]	Gly–Ala–Thr–Lys–Gly–Pro–Gly–Arg–Val–Ile–Tyr–Ala
1B [a]	Ac–Gly–Ala–Thr–Lys–Gly–Pro–Gly–Arg–Val–Ile–Tyr–Ala
2A	Gly–Ala–Thr–Lys–Gly–Ile–Gly–Arg–**Trp**–Ile–Tyr–Ala
2B	Ac–Gly–Ala–Thr–Lys–Gly–Ile–Gly–Arg–**Trp**–Ile–Tyr–Ala
3A	Gly–Ala–Thr–Lys–Gly–Ile–Gly–Arg–**Trp**(For)–Ile–Tyr–Ala
3B	Ac–Gly–Ala–Thr–Lys–Gly–Ile–Gly–Arg–**Trp**(For)–Ile–Tyr–Ala
4A	Leu–Glu–Leu–Arg–Ser–Arg–Tyr–Val–Ala–Ile–Arg–Thr–Arg–Ser–Gly–Gly–NH_2
4B	Ac–Leu–Glu–Leu–Arg–Ser–Arg–Tyr–Val–Ala–Ile–Arg–Thr–Arg–Ser–Gly–Gly–NH_2
5A	Leu–Glu–Leu–Arg–Ser–Arg–Tyr–**Trp**–Ala–Ile–Arg–Thr–Arg–Ser–Gly–Gly–NH_2
5B	Ac–Leu–Glu–Leu–Arg–Ser–Arg–Tyr–**Trp**–Ala–Ile–Arg–Thr–Arg–Ser–Gly–Gly–NH_2
6A	Leu–Glu–Leu–Arg–Ser–Arg–Tyr–**Trp**(For)–Ala–Ile–Arg–Thr–Arg–Ser–Gly–Gly–NH_2
6B	Ac–Leu–Glu–Leu–Arg–Ser–Arg–Tyr–**Trp**(For)–Ala–Ile–Arg–Thr–Arg–Ser–Gly–Gly–NH_2

[a] Taken from ref. 29.

2.6 Trypsin digestion

Chromatographic fractions from IMAC were concentrated and desalted on a 10 × 1 cm I.D. Pep-RPC column. After adsorption, the column was washed with 0.1% aqueous TFA and the peptides eluted with a steep acetonitrile gradient (0–60% in 1 min). The material was recovered by lyophilization and then dissolved in 0.2 ml of 50 m*M* Tris–HCl, 50 m*M* glycine, pH 8.9. Trypsin (50 μg) was added and after 15 min at 37°C, samples were removed for PDMS analysis, none of the original material being detected after this time.

3. Results and discussion

Analogues of peptide **1** were synthesised with the Val in position 9 replaced with Trp (peptide **2**) or Trp(For) (peptide **3**). Peptides **5** and **6** were similarly derived from peptide **4**. The effect of the tryptophan residue on the retention of the peptides on Cu^{2+}- and Ni^{2+}-loaded columns was investigated (Fig. 1 and 2). The N-terminally blocked peptides **1B–6B** showed no retention on either metal over the entire pH range, with the exception of the lysine containing peptides **1B–3B** which were retained on Cu^{2+} above pH 9. That peptides **2B** and **5B** with unprotected tryptophan were not retained was surprising, challenging earlier assumptions about the importance of tryptophan in the binding of proteins and peptides in IMAC [15,16,18,21,30,31].

Peptides **1A–6A** with a free α-amino group showed increasing retention from pH 5 to 7.5 (Cu^{2+}) or pH 5 to 9 (Ni^{2+}), and decreasing retention from pH 7.5 to 9 (Cu^{2+}) or pH 9 to 9.5 (Ni^{2+}). Only the lysine containing peptides **1A–**

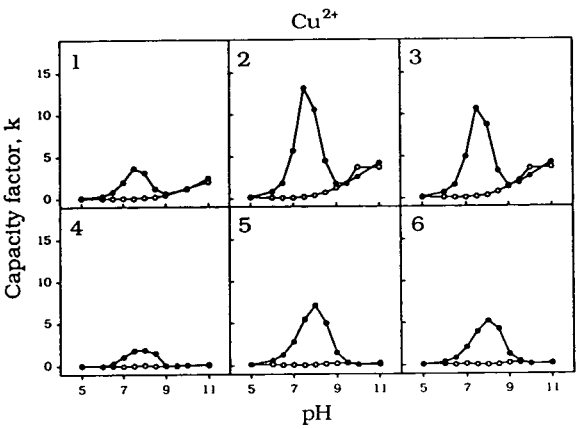

Fig. 1. Capacity factors *vs.* pH of peptides **1–6** on immobilised Cu^{2+}. The number in each square corresponds to the number of the peptide investigated (Table 1). Peptides with free α-amino groups are indicated with ● and blocked with ○. Column, Chelating Superose (1.8 × 1 cm I.D.) charged with Cu^{2+}. Elution, isocratic with 50 m*M* sodium phosphate/borate, 1 *M* NaCl at 1 ml/min. Sample, 100 nmoles of peptide dissolved in 100 μl of chromatographic buffer. Detection, UV at 280 nm.

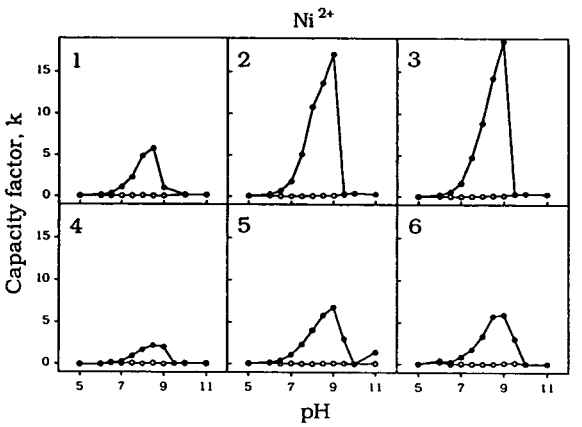

Fig. 2. Capacity factors *vs.* pH of peptides **1–6** on immobilised Ni^{2+}. Indications and chromatographic conditions as in Fig. 1.

3A were retained at pH 9–11 (Cu^{2+}). These findings suggest that the binding occurs by the mechanism proposed earlier [29], where the peptide is initially bound via the α-amino group and the neighbouring amide oxygen.

The tryptophan peptides **2A** and **3A** are structurally similar to peptide **1A** but their capacity factors are considerably higher (Fig. 1.1–1.3 and Fig. 2.1–2.3). In contrast, tryptophan contributes only moderately to the binding of peptides **5A** and **6A** (Fig. 1.4–1.6 and Fig. 2.4–2.6).

We can conclude from the results above that at least in the case of His- and Cys-free peptides a free α-amino group is necessary for binding to immobilised metal ions. The presence of a tryptophan residue in the sequence is in itself not sufficient for binding but can contribute in what seems to be a sequence dependent manner once the peptide has been anchored via the free α-amino group. It may be that other functional groups such as the imidazole of histidine could also serve as primary anchor points.

The capacity factors of peptides **2A** and **5A** are almost identical with those of the formylated peptides **3A** and **6A**, respectively, and not, as might be expected, significantly higher (Fig. 1 and Fig. 2). The increased retention is therefore unlikely to be caused by the indole nitrogen of the tryptophan residue complexing with a metal ion. The interaction could instead be hydrophobic in nature where the non-polar tryptophan side-chain interacts with the chromatographic support [33,34] or of charge-transfer character where the interaction occurs between the aromatic electrons of tryptophan and the metal ion [30]. The effect is only observed once the peptide has been anchored through the free α-amino group.

To confirm that the indole nitrogen is not contributing to the binding of peptides **2A**, **3A**, **5A** and **6A**, tryptamine and indole were included in the investigation. Tryptamine was used instead of tryptophan, since it is known that all amino acids chelate strongly as bidentate ligands to metal ions [12,16,35]. The binding of tryptamine to immobilised metal ions shows the typical pH dependence due to deprotonation of the amino group (Fig. 3). In addition there is a non-specific interaction with the chromatographic support causing *ca.* 2.5 times higher retention times on a metal free column than for peptides **1–6**. Indole, on the other hand, is retained in a pH independent manner equally on both metal loaded and metal free columns, with *ca.* 10-fold higher retention times than for peptides **1–6**. As in Fig. 1 and Fig. 2 the nitrogen of the indole is not seen to contribute to the binding over the pH range investigated. On the other hand, the metal independent binding of indole and tryptamine would suggest that the binding is due to non-specific hydrophobic interactions rather than charge transfer effects. However, when the indole function is present in a peptide these interactions are not as pronounced (only slightly higher retention times on a metal free column

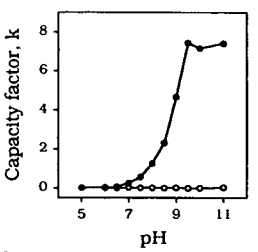

Fig. 3. Capacity factors *vs.* pH of tryptamine (●) and indole (○) on immobilised Cu^{2+}. Chromatographic conditions as in Fig. 1. On a Ni^{2+}-loaded support the capacity factors are close to zero over the entire pH range.

than for non-tryptophan containing peptides) and only contribute to the binding of a peptide that is already anchored to the matrix via a free α-amino group.

Yip *et al.* [15] studied the adsorption properties of several synthetic, biologically active peptides on IMAC columns. Two of these are of interest in the context of this report: human gastrin I (<Glu – Gly – Pro – Trp – Leu – Glu – Glu – Glu – Glu – Glu – Ala – Tyr – Gly – Trp – Met – Asp – Phe – NH_2) which despite the presence of two tryptophan residues is only slightly retarded at pH 7 and somatostatin (Ala – Gly – Cys – Lys – Asn – Phe – Phe – Trp – Lys – Thr – Phe – Thr – Ser – Cys) which shows a normal retention. These results support our findings that a peptide with a free α-amino group (somatostatin) will be bound in IMAC, while a peptide with a blocked α-amino group (human gastrin I) will not. In earlier purifications of synthetic cecropin A and a cecropin–mellitin hybrid the separation achieved was ascribed to the presence of a tryptophan residue in the N-terminal part of the sequence [22]. However, in view of the results presented here it seems that binding via the α-amino function, possibly amplified by hydrophobic interaction of the indole group, would provide a more likely explanation for the resolving power.

The usefulness of IMAC for the isolation of synthetic peptides via interaction of the α-amino group with an immobilised metal ion is demonstrated in the purification of the tryptophan containing peptide **2A**. The peptide was synthesised with formyl protected tryptophan, then the crude mixture subjected to deformylation as described above (Experimental). The crude peptide was applied on Ni^{2+}-loaded Superose and eluted with an increasing gradient of NH_4Cl at pH 8.5 (Fig. 4A). Two major fractions were obtained, which were further analysed by HPLC and mass spectrometry (Fig. 4B–E). As expected, peptide **2A** was detected in the main fraction (4A-II), together with a small amount of

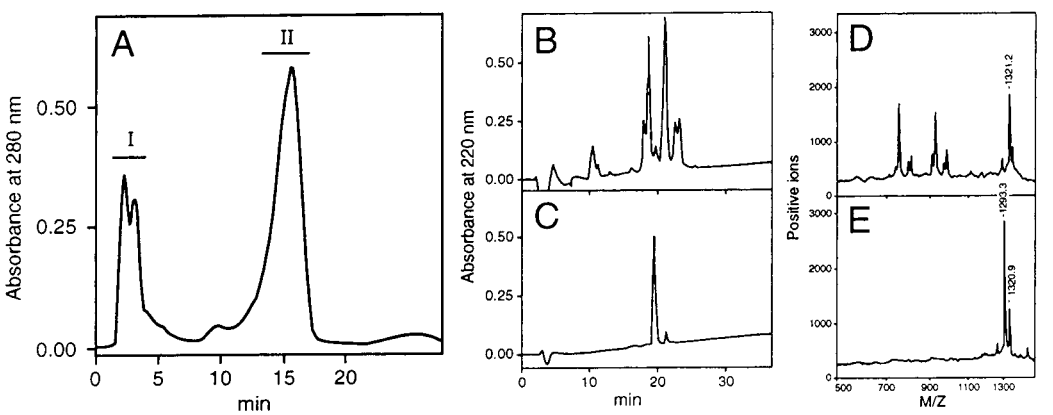

Fig. 4. (A) Chromatography of crude peptide **2A** on Chelating Superose-Ni^{2+}. Column dimensions, 1.8 × 1 cm I.D. Sample, 1.25 mg dissolved in 250 μl of 50 m*M* sodium phosphate/borate, 1 *M* NaCl, pH 8.5. Elution, 30-min gradient from 0 to 0.5 *M* NH_4Cl in the same buffer at 1 ml/min. For mass spectrometry the fractions indicated were concentrated and desalted on a 5 × 0.5 cm I.D. Pep-RPC column. After adsorption, the column was washed with 0.1% aqueous TFA and the peptides eluted with a steep acetonitrile gradient (0–60% in 1 min). (B) RP-HPLC of 1.5 ml (40%) of fraction 4A-I. Column, Pep-RPC (5 × 0.5 cm I.D.). Flow rate, 1 ml/min. Solvent A, 0.1% aqueous TFA. Solvent B, 0.1% TFA in acetonitrile. Gradient, 0–40% B in 30 min. (C) RP-HPLC of 200 μl (5%) of fraction 4A-II. Chromatographic conditions as in Fig. 4B. (D) PDMS of fraction 4A-I. The desalted sample (5 μl) was mixed with ethanol (2 μl) on a nitrocellulose coated aluminium foil, dried and rinsed with distilled water (20 μl). Most peaks can be attributed to various acetylated peptides and their fragment ions. The peak at 1321.2 mass units is due to migration of the formyl protecting group from the tryptophan residue to the α-amino group during deprotection. (E) PDMS of fraction 4A-II. Conditions as in Fig. 4D. The calculated molecular weight for peptide 2A is 1292.5. The peak at 1320.9 mass units is due to migration of the formyl protecting group from the tryptophan residue to the ϵ-amino group during deprotection.

formylated peptide presumably resulting from incomplete deprotection. Truncated peptides that had been acetylated in the capping steps were present in the non-retarded material (4A-I) together with a peptide of the same molecular weight as the formylated peptide **3A**. This surprising result could be explained by rearrangement of the formyl group from the tryptophan residue to the α-amino group during deprotection [36].

The following experiment was conducted to confirm that fraction 4A-I only contained peptides with blocked α-amino groups and that the anomalies mentioned above are artefacts of the deformylation procedure. The crude formylated peptide **3A** was applied to Ni^{2+}-loaded Superose and eluted with an increasing gradient of NH_4Cl at pH 8.5. The main fraction containing purified peptide **3A** was desalted and concentrated by RP-HPLC and then deformylated as outlined previously except that the sample was not desalted by gel filtration but diluted with 5–10 volumes of water prior to freeze drying. The deformylated material was then again applied on Ni^{2+}-loaded Superose (Fig. 5A) and the two major fractions analysed (Fig. 5B–E). As can be seen in Fig. 5, fraction 5A-II contains the expected product **2A** as the main component but also a small amount of formylated peptide. A formyl peptide is present also in fraction 5A-I. Tryptic digestion and PDMS analysis of fraction 5A-I and 5C-I (Table 2) revealed that neither peptide contained Trp(For). The formyl group must therefore have been relocated, either to the α- or to the ϵ-amino group. Since trypsin is unable to cleave the Lys–Gly bond in fraction 5C-I we may conclude that the ϵ-amino group is

Table 2
Trypsin digestion of GATKGIGRWIYA (**2A**)

Peptide fragment	Fraction 5A-I	Fraction 5C-I
GATK	For [a]	–
GIGR	+ [a]	–
WIYA	+	+
GATKGIGR	–	For
GIGRWIYA	–	–

The purified peptide GATKGIGRW(For)IYA was deformylated and separated using IMAC (Fig. 5A). The fractions 5A-I and 5C-I, both containing a peptide with an extra formyl group, were desalted and concentrated by RP-HPLC and then evaporated to dryness. The residues were dissolved in 0.2 ml of 50 m*M* Tris–HCl, 50 m*M* glycine, pH 8.9, and trypsin (50 μg) was added. After 15 min at 37°C the digests were analysed by PDMS.

[a] "+" indicates that a mass peak corresponding to the expected molecular weight was observed, "For" that the mass was 28 units higher than calculated.

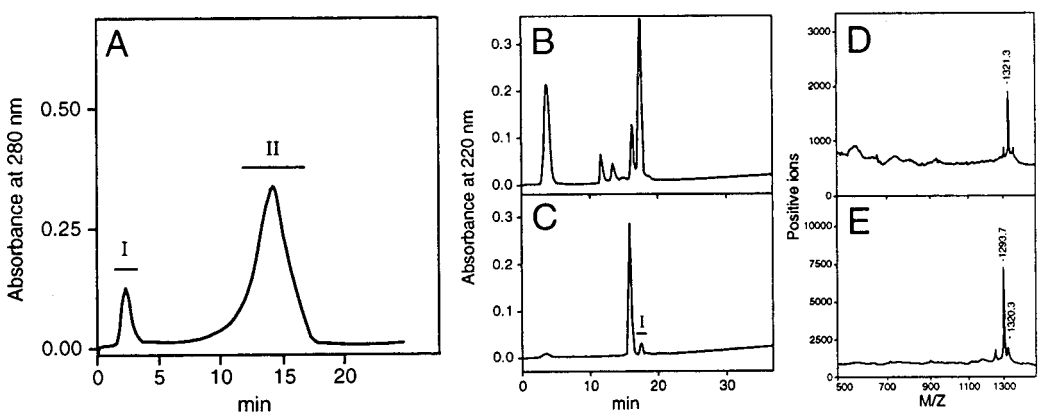

Fig. 5. (A) Chromatography of purified and deformylated peptide **3A** on Chelating Superose-Ni^{2+}. Chromatographic conditions as in Fig. 4A. (B) RP-HPLC of 1.2 ml (80%) of fraction 5A-I. Chromatographic conditions as in Fig. 4B. (C) RP-HPLC of 240 μl (4%) of fraction 5A-II. Chromatographic conditions as in Fig. 4B. (D) PDMS of fraction 5A-I. Conditions as in Fig. 4D. The peak at 1321.3 mass units is caused by rearrangement of the formyl protecting group to the α-amino function. (E) PDMS of fraction 5A-II. Conditions as in Fig. 4D. The calculated molecular weight for peptide **2A** (deformylated peptide **3A**) is 1292.5. The peak at 1320.3 mass units is due to migration of the formyl group to the ϵ-amino group.

modified (formylated). In fraction 5A-I the lysyl bond is cleaved in the normal way. In this case, the formyl group is most likely present as an α-amino substituent which explains why the peptide is not retarded on the IMAC support.

4. Conclusion

We have shown that IMAC based on metal binding via the α-amino group can be used for selective purification of synthetic peptides even when a tryptophan residue is present in the sequence. The target peptide with its free α-amino group will be well separated from the truncated peptides. The tryptophan residue alone is not sufficient for binding to immobilised metal ions; an effect may be observed only when the peptide is first anchored by the α-amino group. A particular advantage of this affinity method is that no modification of the target peptide is necessary. Consequently, material losses accompanying the introduction and removal of a specific affinity handle are avoided and the solubility is not affected.

5. Acknowledgements

We are grateful to Dr Lennart Andersson for helpful suggestions and valuable discussions and to Ms Judith Scoble for linguistic revision of the manuscript. This project was supported by The Swedish National Board for Industrial and Technical Development (NUTEK).

6. References

[1] J. Porath, J. Carlsson, I. Olsson and G. Belfrage, *Nature*, 258 (1975) 598.
[2] T. Kurecki, L.F. Kress and M. Laskowski, *Anal. Biochem.*, 99 (1979) 415.
[3] G. Muszynska, L. Andersson and J. Porath, *Biochemistry*, 25 (1986) 6850.
[4] L. Andersson, E. Sulkowski and J. Porath, *J. Chromatogr.*, 421 (1987) 141.
[5] L. Andersson, E. Sulkowski and J. Porath, *Cancer Res.*, 47 (1987) 3624.
[6] M.C. Smith, T.C. Furman, T.D. Ingolia and C. Pidgeon, *J. Biol. Chem.*, 263 (1988) 7211.
[7] D.J. Hilton, N.A. Nicola, N.M. Gough and D. Metcalf, *J. Biol. Chem.*, 263 (1988) 9238.
[8] F. Maisano, S.A. Testori and G. Grandi, *J. Chromatogr.*, 472 (1989) 422.
[9] G. Chaga, L. Andersson, B. Ersson and J. Porath, *Biotechnol. Appl. Biochem.*, 11 (1989) 424.
[10] T. Mantovaara, H. Pertorft and J. Porath, *Biotechnol. Appl. Biochem.*, 11 (1989) 564.
[11] J. Porath and P. Hansen, *J. Chromatogr.*, 550 (1991) 751.
[12] H. Sigel and R.B. Martin, *Chem. Rev.*, 82 (1982) 385.
[13] M.J. Smith, T.C. Furman and C. Pidgeon, *Inorg. Chem.*, 26 (1987) 1965.
[14] B. Monjon and J. Solms, *Anal. Biochem.*, 160 (1987) 88.
[15] T.-T. Yip, Y. Nakagawa and J. Porath, *Anal. Biochem.*, 183 (1989) 159.
[16] M. Belew and J. Porath, *J. Chromatogr.*, 516 (1990) 333.
[17] L. Andersson and E. Sulkowski, *J. Chromatogr.*, 604 (1991) 13.
[18] E. Sulkowski, *Trends Biotechnol.*, 3 (1985) 1.
[19] M. Belew, T.-T. Yip, L. Andersson and J. Porath, *J. Chromatogr.*, 403 (1987) 197.
[20] E.S. Hemdan, Y.-J. Zhao, E. Sulkowski and J. Porath, *Proc. Natl. Acad. Sci. USA*, 86 (1989) 1811.
[21] E.S. Hemdan and J. Porath, *J. Chromatogr.*, 323 (1985) 265.
[22] G. Lindeberg, H. Bennich and Å. Engström, *Int. J. Peptide Protein Res.*, 38 (1991) 253.
[23] D.E. Krieger, B.W. Erickson and R.B. Merrifield, *Proc. Natl. Acad. Sci. USA*, 73 (1976) 3160.
[24] R.B. Merrifield and A.E. Bach, *J. Org. Chem.*, 43 (1978) 4808.
[25] T.J. Lobl, M.L. Deibel and A.W. Yem, *Anal. Biochem.*, 170 (1988) 502.
[26] H.L. Ball and P. Mascagni, *Int. J. Peptide Protein Res.*, 40 (1992) 370.
[27] S. Funakoshi, H. Fukuda and N. Fujii, *J. Chromatogr.*, 638 (1993) 21.
[28] E. Bianchi, M. Sollazzo, A. Tramontano and A. Pessi, *Int. J. Peptide Protein Res.*, 42 (1993) 93.
[29] P. Hansen, G. Lindeberg and L. Andersson, *J. Chromatogr.*, 627 (1992) 125.
[30] J. Porath, *J. Chromatogr.*, 159 (1978) 13.
[31] M. Zachariou, I. Traverso and M.T.W. Hearn, *J. Chromatogr.*, 646 (1993) 107.
[32] K. Horiki, K. Igano and K. Inouye, *Chem. Lett.*, (1978) 165.
[33] D. Eaker and J. Porath, *Sep. Sci.*, 2 (1967) 507.
[34] B. Gelotte, *J. Chromatogr.*, 3 (1960) 330.
[35] E.S. Hemdan and J. Porath, *J. Chromatogr.*, 323 (1985) 255.
[36] D. Yamashiro and C.H. Li, *J. Org. Chem.*, 38 (1973) 2594.

ELSEVIER

Journal of Chromatography A, 662 (1994) 243–249

JOURNAL OF CHROMATOGRAPHY A

Separation of stereoisomeric oxindole alkaloids from *Uncaria tomentosa* by high performance liquid chromatography

Gerhard Laus*, Dietmar Keplinger

Immodal Pharmaka GmbH, Bundesstrasse 44, A-6111 Volders, Austria

(First received August 9th, 1993; revised manuscript received November 3rd, 1993)

Abstract

Two HPLC methods are presented that allow the rapid separation and determination of the stereoisomeric oxindole alkaloids present in the South American liana *Uncaria tomentosa* (Willd.) DC (Rubiaceae). Peak purities were established using a dual-wavelength technique. The effect of temperature on resolution was evaluated. The alkaloid pattern of individual plants changes with time. As these alkaloids are readily interconverted, a mild extraction procedure had to be established in order to retain the actual alkaloid composition.

1. Introduction

Although the alkaloids of the pantropical genus *Uncaria* have been surveyed extensively [1], only a few accounts have dealt with the constituents of the South American species *U. tomentosa* (Willd.) DC. In an early note, *U. tomentosa* was reported to contain tetracyclic indole and oxindole alkaloids [2]. Later, only pentacyclic oxindoles were found in plant material from Central Peru. However, it was not established whether the plant belonged to the species *U. tomentosa* or *U. guianensis*, both of which grow in that region [3]. The caryology of these two species was investigated [4], but difficulties in the correct identification of *Uncaria* species remained. Interrogation of locals from the Peruvian rain forest, who use *Uncaria* roots in traditional medicine, revealed that there were actually three varieties of *U. tomentosa*, which when freshly cut exhibit white-grey, yellow-brown or dark red root bark, and only the yellow-brown variety was used [5]. A reinvestigation showed the tetracyclic oxindoles rhynchophylline and isorhynchophylline to be the major alkaloids present in each of the three varieties, while the pentacyclic oxindole isopteropodine was found in high concentrations especially in the yellow-brown variety [6,7]. Recently, six pentacyclic oxindoles, namely pteropodine, isopteropodine, speciophylline, uncarine F, mitraphylline and isomitraphylline, have been identified in the root of *U. tomentosa*, but it was not specified which variety was used [8]. These inconsistent findings prompted us to develop reliable methods for the determination of above oxindole alkaloids.

2. Experimental

2.1. Equipment

A Merck–Hitachi HPLC system consisting of

* Corresponding author.

0021-9673/94/$07.00
SSDI 0021-9673(93)E1173-W

a Model L-6200 A pump, a Model L-4250 UV–Vis or Model L-4500 diode-array detector, a Model D-6000 interface and an IBM-compatible personal computer was used. The HPLC Manager Software D-6000 was from Merck–Hitachi. A Rheodyne Model 9125 sample injector fitted with a 200-μl polyether ether ketone (PEEK) loop was employed. LiChroCART 125 mm × 4 mm I.D. columns packed with LiChrospher 100 RP-18 (5 μm) were purchased from Merck (Darmstadt, Germany). The mixing chambers, injector and column were thermostated by a Peltier thermostat from Offenbeck Industrieelektronik (Langenzersdorf, Austria). The system suitability was checked by chromatographing a standard sample of pteropodine and determining the number of theoretical plates. A minimum of 7000 plates was found to be necessary in order to obtain the results reported here.

2.2. Reagents and materials

All reagents were of analytical-reagent grade, except acetonitrile, which was of HPLC grade, from Merck. Water was purified by use of Herco (Freiberg, Germany) Model HP40W reverse osmosis equipment. Eluents were gassed with helium. TLC plastic sheets (20 × 20 cm) precoated with a 0.2-mm layer of silica gel 60 F_{254} and silica gel 60 (70–230 mesh) for column chromatography were obtained from Merck. Plant material was collected and identified by K. Keplinger and D. Keplinger in the Province of Chanchamayo, Region of Andres Avelino Caceres (the former Departments of Junin and Pasco), Peru. Climate data (temperature, humidity, exposure to sunlight and rainfall) were also recorded [9].

2.3. Identification of alkaloids

The milled root bark of the yellow-brown variety was extracted with supercritical carbon dioxide and, after acid–base work-up of the fatty extract, the pure alkaloids were isolated by silica gel chromatography using mixtures of hexane, ethyl acetate and methanol with increasing polarity as the eluent. They were identified by analysis of two-dimensional correlated ^{1}H and ^{13}C NMR spectra and by comparison of melting points, mass spectra, hR_F values and isomerization behaviour with literature data [3,6,10–16]. Their structures and stereochemical notations are given in Table I. Additionally, natural mitraphylline and isomitraphylline were shown to be identical with the synthetic compounds prepared from ajmalicine [17].

2.4. Separation of oxindole alkaloids

We developed two elution programmes for the separation of oxindole alkaloids by HPLC. For system I, acetonitrile–*tert.*-butyl methyl ether–10 m*M* aqueous phosphate buffer (pH 6.7)

Table 1
Retention times, hR_F values, absorbance ratios and stereochemistry of oxindole alkaloids

Alkaloid	t_R (min)		hR_F	A_{245}/A_{230}	A_{245}/A_{260}	Chiral centre[a]					
	System I	System II				C-3	N-4	C-7	C-15	C-19	C-20
Pteropodine (**1**)	12.7	2.9	65	1.62	1.45	*S*	*R*	*R*	*S*	*S*	*S*
Isopteropodine (**2**)	24.1	4.4	73	1.57	1.44	*S*	*R*	*S*	*S*	*S*	*S*
Speciophylline (**3**)	6.7	2.0	7	1.44	1.45	*R*	*S*	*S*	*S*	*S*	*S*
Uncarine F (**4**)	7.9	2.6	48	1.36	1.53	*R*	*S*	*R*	*S*	*S*	*S*
Mitraphylline (**5**)	8.8	2.3	18	1.40	1.65	*S*	*R*	*R*	*S*	*S*	*R*
Isomitraphylline (46)	11.8	3.2	60	1.33	1.69	*S*	*R*	*S*	*S*	*S*	*R*
Rhynchophylline (**7**)	13.7	4.1	4	1.53	1.61	*S*	*R*	*R*	*S*	–	*R*
Isorhynchophylline (**8**)	15.6	4.3	67	1.52	1.61	*S*	*R*	*S*	*S*	–	*R*

[a] This notation of stereochemistry was proposed by Poisson and Pousset [18].

(34:1:65) was used as the eluent at a flow rate of 1.0 ml/min. The column temperature was 12°C and detection was carried out at 245 nm. The typical pressure build-up was 110 bar. For system II, acetonitrile–10 m*M* aqueous phosphate buffer (pH 7.0) (45:55)was used as the eluent at a flow-rate of 1.3 ml/min. The column temperature was 80°C and detection was carried out at 245 nm. The typical pressure build-up was 55 bar.

Chromatograms were developed with ethyl acetate–hexane (9:1) and the spots were detected with UV light at 254 nm.

The absorbance ratios $A_{245\ nm}/A_{230\ nm}$ and $A_{245\ nm}/A_{260\ nm}$ were determined using diode-array detection.

2.5. Sample preparation

The buffers were chosen according to the eluent system used. Stock standard solutions of the standard alkaloids in acetonitrile were prepared and diluted appropriately with 10 m*M* aqueous phosphate buffer. The root bark (1.000 g) was finely milled and leached with 20 ml of methanol–water–1.2 *M* hydrochloric acid (50:50:1) for 1 h at 20°C and the extract was decanted and filtered; this procedure was repeated four times, and the combined extracts were diluted to a final volume of 100 ml. An aliquot of this solution was diluted 1:5 with aqueous phosphate buffer. For validation purposes the root bark (1.000 g) was also exhaustively extracted in a Soxhlet apparatus with methanol (150 ml). All samples were filtered through solvent-resistant 0.45-μm filters from Sartorius (Göttingen, Germany) and degassed by ultrasonification just prior to injection.

2.6. Standard preparation

The alkaloid mixture was suspended in boiling *tert.*-butyl methyl ether, filtered and recrystallized twice to yield pteropodine (**1**) with a purity higher than 98% (HPLC and microanalysis). Equilibration of pure pteropodine by heating in aqueous methanol at pH 9 gave a mixture containing 70% isopteropodine (**2**) and at pH 2 a mixture containing 40% speciophylline (**3**). From these enriched mixtures, the pure isomers were obtained by column chromatography as described above and used as standards.

3. Results and discussion

3.1. Quantification

The purified alkaloids pteropodine (**1**), isopteropodine (**2**) and speciophylline (**3**) and synthetic mitraphylline (**5**) were used for calibration, giving identical plots within statistical error. A linear relationship between peak area and concentration of pteropodine was established in the ranges 0.05–20 μg/ml [system I; ten data points; correlation coefficient $R^2 = 0.998$; relative standard deviation (R.S.D.) = 1.07% for the five higher and 2.10% for the five lower concentrations] and 0.005–20 μg/ml (system II; twelve data points; $R^2 = 0.999$; R.S.D. was 0.65% for the six higher and 1.05% for the six lower concentrations). The detection limits were 5 ng/ml (system I) and 0.5 ng/ml (system II).

3.2. Precision and recovery

The precision (R.S.D.) was determined by analysis of six preparations of a root extract and was 0.90% (system I) and 1.03% (system II). The recovery was determined by spiking two preparations of the extract at two different levels of pteropodine before analysis. Extracts containing approximately 10 μg/ml of total alkaloids were spiked at levels of 15 and 20 μg/ml. The recovery ranged from 99 to 101% (system I) and from 99 to 103% (system II).

3.3. Chromatography

The constituents of *U. tomentosa* are of interest because this plant is used in traditional medicine in South America for the treatment of diseases that in our interpretation can be attributed to immune system disorders. We have isolated and identified eight oxindole alkaloids from *U. tomentosa* so far. A superior separation of

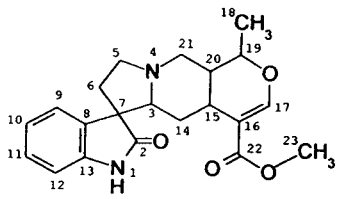

1-6

pteropodine (**1**), isopteropodine (**2**), speciophylline (**3**), uncarine F (**4**), mitraphylline (**5**) and isomitraphylline (**6**) was achieved by isocratic elution using HPLC system I. A typical chromatogram is given in Fig. 1a. In the course of validation, peak purity is an essential criterion. As the stereoisomeric compounds **1–6** exhibit virtually identical UV spectra, absorbance ratios at suitably selected wavelengths were calculated. Any impurities that co-eluted or overlapped with the peak of interest would be indicated by a distortion of the flat-topped peak

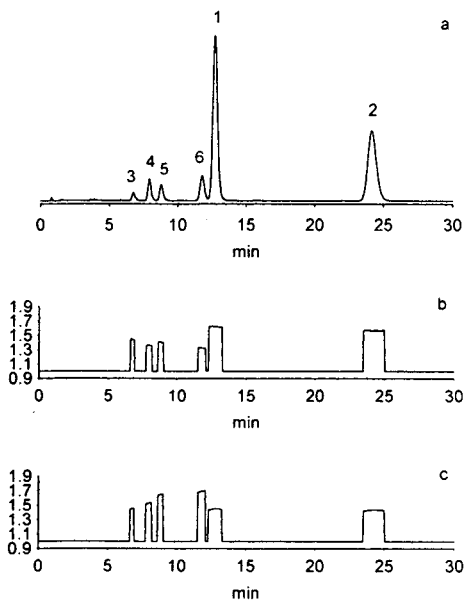

Fig. 1. (a) Chromatogram of the alkaloid mixture obtained by extraction of *Uncaria tomentosa* root bark with supercritical CO_2. Separation of pteropodine (**1**), isopteropodine (**2**), speciophylline (**3**), uncarine F (**4**), mitraphylline (**5**) and isomitraphylline (**6**) was carried out using HPLC system I (see text). Absorbance ratio plots using (b) 245/230 nm and (c) 245/260 nm, threshold set at 2% of highest peak.

in the ratiogram. We propose the use of 245 nm as the numerator wavelength because the absorption maxima of the alkaloids are between 243 and 247 nm. The denominator wavelength should be selected where the absorption is small, such that the resulting ratio exhibits a large value. We used 230 and 260 nm, respectively. It can be clearly seen in Fig. 1b and c that by this method the alkaloids can be distinguished and that the shapes of the peaks indicate homogeneity.

In contrast to a recently published method [8], the use of pure acetonitrile as the organic solvent instead of acetonitrile–methanol (1:1) led to better resolution. The admixture of a small amount of *tert.*-butyl methyl ether as a second modifier gave a further improvement in resolution. The effect of temperature on resolution has been reported in the range 9–30°C [8]. We found a different temperature dependance for our system I (Fig. 2a). It seemed of interest to evaluate the effect of higher temperatures also. These experiments led to the development of eluent system II. The temperature dependance of resolution using this system in the range 50–80°C is depicted in Fig. 2b. Complete separation of the alkaloids was achieved at 80°C within 5 min, as can be seen in Fig. 3. It is noteworthy that the sequence of elution of two pairs of alkaloids is reversed, namely that of **5–4** and **6–1**. The elution behaviour of these isomers, especially the fact that **2** is eluted so much later than the others, is not fully understood [19]. Retention times for both HPLC systems, hR_F values for TLC and absorbance ratio values are given in Table 1. As both methods use isocratic elution, no additional equilibration time is required. Thus, especially system II provides excellent resolution with a minimum turnaround time.

3.4. Sample preparation

Often, too little attention is paid to the extraction process in phytochemical research. It is known that oxindole alkaloids which are spiro structures undergo isomerization easily when heated with acids or bases [10,11]. We investigated the behaviour of these alkaloids in solu-

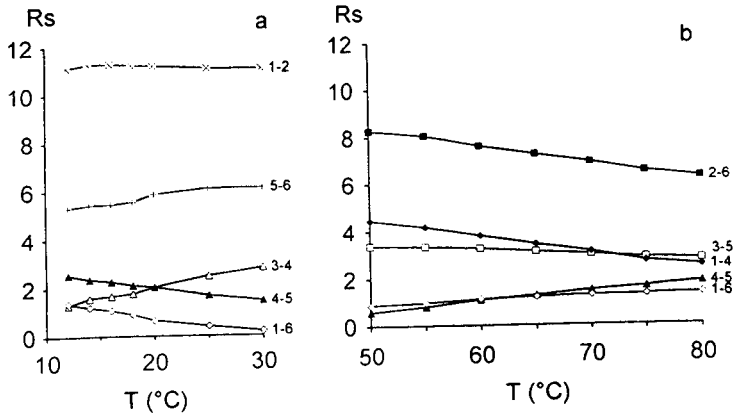

Fig. 2. Effect of temperature on resolution of the alkaloid pairs (a) **1–2**, **5–6**, **3–4**, **4–5** and **1–6** using HPLC system I (see text) in the range 12–30°C, and (b) **2–6**, **3–5**, **1–4**, **4–5** and **1–6** using HPLC system II (see text) in the range 50–80°C.

tions at different pH values and at different temperatures. We found that equilibration in neutral or basic solutions took place even at room temperature and proceeded rapidly under reflux conditions. However, in acidic solutions the isomerization was slower in general and almost ceased at room temperature. Hence, the usual continuous extraction technique in a Soxhlet apparatus, where the extracted material is in contact with a boiling solvent (methanol) during a prolonged period, could not be applied. The change of alkaloid distribution in a model mixture of pteropodine isomers **1–4** effected by boiling in methanol is shown in Fig. 4. The same applies for mitraphyllines and rhynchophyllines. Of course, these conversions also take place in the plant, but not after it has been dried. The mixture obtained by carbon dioxide extraction (Fig. 1a) has clearly undergone isomerization. It is evident that extracts obtained in this manner would not reflect the actual proportions of alkaloids as they occur in the plant. In contrast, when the root was extracted repeatedly with acid at room temperature, no isomerization was observed. Validation of the extraction techniques showed that the acid method yielded a 92.4% recovery (S.D. 3.7%) in authentic proportions compared with the Soxhlet method, which was assumed to give 100% (S.D. 2.8%) but showing artifacts.

The results of determinations using the different extraction methods are given in Table 2. All the following results were obtained by the acid extraction method.

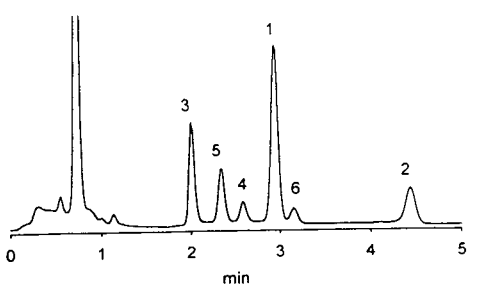

Fig. 3. Chromatogram of an acid extract of *Uncaria tomentosa* root bark containing the alkaloids **1–6** in authentic proportions. The separation was carried out using HPLC system II (see text).

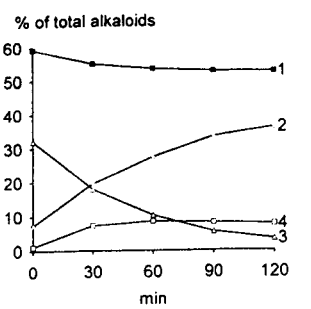

Fig. 4. Generation of artifacts by an unsuitable extraction procedure, *i.e.*, by boiling a model mixture of pteropodine isomers **1–4** in methanol.

Table 2
Comparison of extraction methods

Alkaloid	Soxhlet extraction		Acid extraction	
	mg/g root bark	% of total alkaloids	mg/g root bark	% of total alkaloids
Pteropodine (**1**)	6.51	51.62	5.75	49.01
Isopteropodine (**2**)	3.76	29.80	2.28	19.44
Speciophylline (**3**)	0.38	3.03	1.81	15.41
Uncarine F (**4**)	0.64	5.09	0.55	4.70
Mitraphylline (**5**)	1.03	8.15	1.13	9.65
Isomitraphylline (**6**)	0.29	2.30	0.21	1.79
Total alkaloids	12.61		11.73	

3.5. Plant analysis

It was found that the three varieties can be related to the climate, the dark red variety preferring a warm and moist environment, the white-grey variety preferring cool and dry conditions and the yellow-brown variety being in between. However, no correlation of alkaloid contents and the colour of the root bark could be established, as can be seen in Table 3, which gives the alkaloid content of three samples collected at the same time (July 1990). Only small stripes of the root bark were taken and the root was returned to the ground each time in order not to destroy the plant. Interestingly, samples from several individual plants harvested in different years displayed completely different alkaloid patterns. Only two major alkaloids were detected in these samples, rhynchophylline (**7**) and isorhynchophylline (**8**). Individual plants

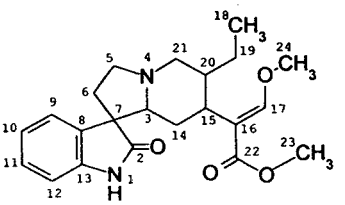

7,8

switched from one alkaloid pattern to the other over the years. In all instances either the pteropodine and mitraphylline isomers **1–6** or the rhynchophyllines **7** and **8** were found as major constituents (Table 4). The total alkaloid content varied from 0.036 to 3.83% (w/w) of dried root bark. The plant material was always collected from June to October, but there are reports of the Asian species *Mitragyna parvifolia* changing its oxindole alkaloids within several

Table 3
Alkaloid content of three differently coloured root bark samples of *Uncaria tomentosa*

Alkaloid	Alkaloid content (mg/g root bark)		
	White-grey root bark	Yellow-brown root bark	Dark red root bark
Pteropodine (**1**)	7.54	5.20	10.53
Isopteropodine (**2**)	3.94	2.49	2.99
Speciophylline (**3**)	8.16	2.80	4.06
Uncarine F (**4**)	3.00	0.79	0.86
Mitraphylline (**5**)	3.03	4.70	1.83
Isomitraphylline (**6**)	0.52	1.89	0.04
Total alkaloids	26.20	17.88	20.30

Table 4
Variation of alkaloid content in the root bark of *Uncaria tomentosa* collected at different times

Alkaloid	Alkaloid content (mg/g root bark)										
	Plant 1[a]				Plant 2[b]			Plant 3[c]			
	October 1985	July 1987	July 1990	July 1992	June 1983	October 1985	July 1987	August 1981	June 1983	October 1985	July 1987
Pteropodine (**1**)	3.14	2.65	6.18	0.04	1.29	3.83	0.04	0.48	0.04	0.48	0.43
Isopteropodine (**2**)	1.01	1.53	2.72	0.01	0.40	1.66	0.01	0.16	0.01	0.15	0.12
Speciophylline (**3**)	1.65	2.32	3.61	0.03	1.72	2.49	0.03	0.28	0.02	0.35	0.24
Uncarine F (**4**)	0.35	0.61	0.86	0.17	0.39	0.66	0.00	0.02	0.00	0.03	0.01
Mitraphylline (**5**)	1.91	3.59	5.48	0.11	1.07	3.62	0.07	0.76	0.04	1.04	0.60
Isomitrphylline (**6**)	0.80	1.63	2.17	0.04	0.66	1.52	0.08	0.26	0.05	0.38	0.24
Rhynchophylline (**7**)	0.01	0.08	0.05	13.82	20.33	0.09	12.53	3.36	0.08	7.12	4.52
Isorhynchophylline (**8**)	0.02	0.03	0.02	14.23	12.39	0.03	8.63	8.86	0.12	7.17	5.94
Total alkaloids	8.89	12.44	21.09	28.45	38.25	13.90	21.39	14.18	0.36	16.72	12.10

[a] Plant 1 is of the white-grey variety.
[b] Plant 2 is of the white-grey variety.
[c] Plant 3 is of the yellow-brown variety.

months [20,21]. Climate data also did not offer an explanation for this remarkable fact [9]. So far it cannot be deduced from our results whether seasonal or long-term fluctuations occur. At least it can be stated that the alkaloid distribution of the species *U. tomentosa* is subject to change, thus explaining the inconsistent findings of earlier investigations.

4. Acknowledgement

This work was supported by the Forschungsförderungs fonds für die gewerbliche Wirtschaft (Vienna).

5. References

[1] J.D. Phillipson, S.R. Hemingway and C.E. Ridsdale, *Lloydia (J. Nat. Prod.)*, 41 (1978) 503.
[2] S.R. Hemingway and J.D. Phillipson, *J. Pharm. Pharmacol.*, 26, Suppl. (1974) 113P.
[3] S. Montenegro de Matta, F. delle Monache, F. Ferrari and G.B. Marini-Bettolo, *Farmaco, Ed. Sci.*, 31 (1976) 527.
[4] H. Teppner, K. Keplinger and W. Wetschnig, *Phyton (Horn, Austria)*, 24 (1984) 125.
[5] K. Keplinger, *PCT Int. Appl.*, WO 82 01,130; *C.A.*, 97 (1982) 28587.
[6] H. Wagner, B. Kreutzkamp and K. Juric, *Planta Med.*, 51 (1985) 419.
[7] B. Kreutzkamp, *Ph.D. Thesis*, University of Munich, Munich, 1984.
[8] H. Stuppner, G. Sturm and G. Konwalinka, *Chromatographia*, 34 (1992) 597.
[9] M. Canayo-Payma, personal communication, 1992.
[10] A.F. Beecham, N.K. Hart, S.R. Johns and J.A. Lamberton, *Aust. J. Chem.*, 21 (1968) 491.
[11] K.C. Chan, F. Morsingh and G.B. Yeoh, *J. Chem. Soc. C*, (1966) 2245.
[12] E.J. Shellard, P. Tantivatana and A.H. Beckett, *Planta Med.*, 15 (1967) 366.
[13] W.H.M.W. Herath, M.U.S. Sultanbawa, G.P. Wannigama and A. Cave, *Phytochemistry*, 18 (1979) 1385.
[14] J.D. Phillipson and S.R. Hemingway, *J. Chromatogr.*, 105 (1975) 163.
[15] N.K. Hart, S.R. Johns and J.A. Lamberton, *J. Chem. Soc., Chem. Commun.*, (1967) 87.
[16] G.E. Martin, R. Sanduja and M. Alam, *J. Nat. Prod.*, 49 (1986) 406.
[17] H. Zinnes and J. Shavel, *J. Org. Chem.*, 31 (1966) 1765.
[18] J. Poisson and J.L. Pousset, *Tetrahedron Lett.*, 20 (1967) 1919.
[19] J.D. Phillipson, N. Supavita and L.A. Anderson, *J. Chromatogr.*, 244 (1982) 91.
[20] E.J. Shellard and P.J. Houghton, *Planta Med.*, 20 (1971) 82.
[21] E.J. Shellard and P.J. Houghton, *Planta Med.*, 21 (1972) 263.

Journal of Chromatography A, 662 (1993) 251–254
Elsevier Science B.V., Amsterdam

CHROM. 25 551

Determination of ajmaline stereoisomers by combined high-performance liquid and thin-layer chromatography

Maria E. Sosa

Institute of Pharmacy and Food Science, University of Havana, Ave. 222 and 25, La Coronela, Ciudad de la Habana (Cuba)

José R. Valdés*

Drug Research and Development Centre, Ave. 26 No. 1605, Esq. Puentes Grandes, Ciudad de la Habana (Cuba)

Jorge A. Martinez

Institute of Pharmacy and Food Science, University of Havana, Ave. 222 and 25, La Coronela, Ciudad de la Habana (Cuba)

(First received May 6th, 1993; revised manuscript received September 8th, 1993)

ABSTRACT

A procedure for the determination of ajmaline and its stereoisomers using a combined TLC–HPLC approach is described. TLC permitted the discrimination of ajmaline, isoajmaline and sandwicine or isosandwicine, whereas HPLC separated every pair of the alkaloids except for the normal series of bases (ajmaline–sandwicine). The analysis of several semipurified alkaloidal mixtures obtained from various *Rauwolfia* species is discussed.

INTRODUCTION

Ajmaline (**1**) is an indolic alkaloid first isolated from *Rauwolfia serpentina* Benth [1], that is currently used, together with several semi-synthetically derived drugs, for the treatment of cardiac arrhythmias [2]. This importance prompted several studies on the separation and determination of ajmaline in *Rauwolfia* extracts and official drugs containing this alkaloid, either by TLC [3–6] or HPLC techniques [7–13]. To our knowledge, none of these studies involved the determination of ajmaline in the presence of its stereoisomers, namely, isoajmaline (**2**), sandwicine (**3**) and isosandwicine (**4**) (Fig. 1), in spite of their co-occurrence in the roots of several *Rauwolfia* species.

In the course of our studies on *Rauwolfia*, looking for commercially and therapeutically important alkaloids, we have found that the above techniques were unsuccessful in resolving satisfactorily ajmaline and its stereosisomers. Some of them gave poorly reproducible experimental results. This paper describes our results on the application of TLC and HPLC

	R	R_1	R_2	R_3	R_4	R_5
[1] ajmaline	H	OH	OH	H	H	Et
[2] isoajmaline	H	OH	H	OH	Et	H
[3] sandwicine	OH	H	OH	H	H	Et
[4] isosandwicine	OH	H	H	OH	Et	H

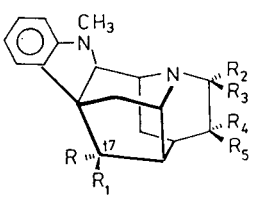

Fig. 1. Ajmaline stereoisomers.

* Corresponding author.

SSDI 0021-9673(93)E0974-Y

techniques for the separation and determination of the above alkaloids present in artificial and natural mixtures.

EXPERIMENTAL

Chemicals

Ajmaline was purchased from INFA (Milan, Italy). The stereoisomers **2–4** were prepared semi-synthetically using published procedures [14]. The products obtained were unequivocally characterized by physico-chemical and spectroscopic analysis.

Semi-purified alkaloidal mixtures, obtained from several available *Rauwolfia* species by previously reported procedures [15], were included in the analysis.

The products were dissolved in analytical-reagent grade methanol (Merck, Darmstadt, Germany) at concentrations of *ca.* 1 mg/ml. In each instance 25 μg of the samples were applied.

Chromatography

TLC was performed on thin-layer plates of silica gel G (Merck, Type 60, layer thickness 0.25 mm) previously activated at 110°C for 1 h. Among the solvent systems tried, the best separation was recorded with acetone–light petroleum (b.p. 40–60°C)–diethylamine (2:7:1). The chromogenic reagent used was a 1% solution of ammonium cerium(IV) sulphate in concentrated orthophosphoric acid [16].

HPLC was carried out on a Knauer (Berlin, Germany) system consisting of a variable-wavelength monitor, a high-pressure mixing chamber, two reciprocating pumps, a helium degasser and a cartridge column. For data processing a Facit S212-10 computer with specialized software was used. A Rheodyne Model 7125 valve with a 20-μl loop was employed for the introduction of the samples. The column (100 × 4 mm I.D.) was packed with Nucleosil SA (Knauer) of 5-μm particle size. The mobile phase was 0.1 mol/l dibasic ammonium phosphate (pH 7)–acetonitrile–2-propanol (80:20:7) at a flow-rate of 1 ml/min. Samples were injected in the range 0.2–5.0 μg. The detection wavelength was 290 nm.

RESULTS AND DISCUSSION

Under the above TLC experimental conditions we achieved the resolution of three of the four ajmaline stereoisomers (Fig. 2). However, none of the experiments developed, using a wide range of solvent mixtures, was successful in the separation of sandwicine and isosandwicine.

In the course of TLC analysis we observed that the C-17 (*S*) stereoisomers, **3** and **4**, yielded a more stable reddish pink colour with the chromogenic reagent employed for the detection of the alkaloidal spots. Instead, ajmaline and isoajmaline [the C-17 (*R*) series of stereisomers] showed a faint pink colour; the difference was useful in the analysis of alkaloidal mixtures.

As shown in Fig. 2, ajmaline was the only component detected in the root extracts of *Rauwolfia viridis* Roem. et Schult., ajmaline and sandwicine or isosandwicine being encountered in the root of the other species (*R. cubana* A. DC., *R. salicifolia* Griseb. and *R. linearifolia* Britt. et Wilson). None of these taxa gave spots corresponding to the isoajmaline reference sample by this method (see below, however).

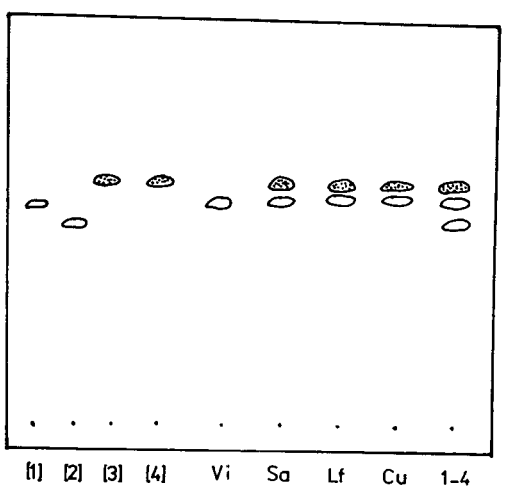

Fig. 2. TLC of ajmaline stereoisomers and several *Rauwolfia* root extracts. [1]–[4] = ajmaline stereoisomers **1–4**; Vi = *Rauwolfia viridis*; Sa = *R. salicifolia*; Lf = *R. linearifolia*; Cu = *R. cubana*. In each instance 25 μg of the samples were applied. Dotted spots indicate reddish pink colour with the chromogenic reagent employed; open spots indicate a faint pink colour with the same reagent (see text).

In the HPLC experiments, we did not obtain good results when employing the conditions reported by Flanagan *et al.* [11], who used non-aqueous developing systems with silica gel columns in separations of a wide variety of basic compounds, including ajmaline. In the course of the experiment, we found it difficult to stabilize the equipment under Flanagan *et al.*'s conditions, probably owing to the large amount of methanol present in the mobile phase and to difficulties usually encountered in conditioning silica gel columns [17]. We also tried several modifications of the conditions employed by Flanagan *et al.* [11], modifying the components (methanol–*n*-hexane, methanol–ethyl acetate and methanol–acetic acid) and the concentration of methanol in the mobile phase (17:3 to 7:3) and the length of the column (125 and 250 mm), but none of these approaches achieved the desired results in terms of resolution and reproducibility.

Jane *et al.* [12] reported analogous difficulties with the use of similar conditions of Flanagan *et al.*'s, owing to the asymmetry of the peaks and long retention times on silica gel columns.

It was therefore decided to follow the recomendations of Rogers [13], who reported good results for ajmaline resolution in *Rauwolfia* alkaloidal mixtures using long ion-exchange columns (1000 × 2.6 mm I.D.) with phosphate buffer–methanol as the mobile phase. After several adaptations of the experimental conditions in terms of pH, column dimensions, ionic strength and methanol content of the mobile phase, as described previously, we were able to obtain the results shown in Fig. 3. Thus, with the exception of the ajmaline–sandwicine pair, which always co-eluted, it is possible to separate and determine the stereoisomers.

Combined analysis using both TLC and HPLC allows better information to be obtained regarding the composition of these alkaloidal mixtures. For example, although in *R. viridis* crude root alkaloid mixture the HPLC results do not permit a distinction between ajmaline and sandwicine, TLC convincingly demonstrates the absence of **3**. For *R. linearifolia*, TLC results established the existence of ajmaline and one or both C-17 (*S*) stereoisomers (**3** or **4**); HPLC revealed the three components and, in trace amounts, the presence of isoajmaline (Fig. 3).

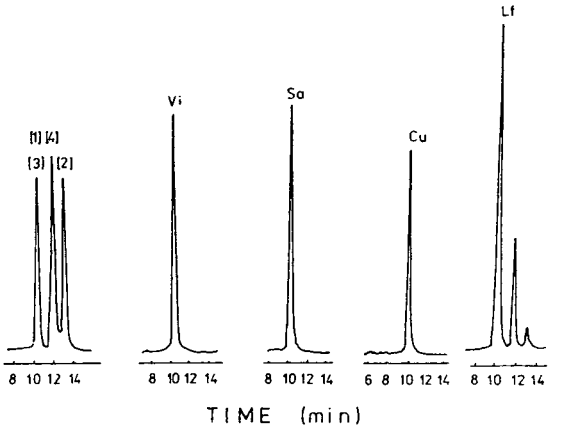

Fig. 3. HPLC of ajmaline stereoisomers and several *Rauwolfia* root extracts. Amount injected: **1–4**, 2 μg; *Rauwolfia* extracts, 5 μg. numbers and abbreviations as in Fig. 2.

In conclusion, in spite of the above-described limitations of each method for the separation of all natural ajmaline stereoisomers, the combination of the two techniques permits us obtain more information about the composition of alkaloidal mixtures containing these bases. Work is in progress on the application of HPLC for the complete resolution of ajmaline stereoisomers.

REFERENCES

1 S. Siddiqui and R.H. Siddiqui, *J. Indian Chem. Soc.*, 8 (1931) 667.
2 J.E.F. Reynolds (Editor), *Martindale, The Extra Pharmacopeia*, Pharmaceutical Press, London, 28th ed., 1982.
3 A. Baerheim-Svendsen and R. Verpoorte, *Chromatography of Alkaloids, Part A: Thin-Layer Chromatography*, Elsevier, Amsterdam, 1983.
4 M.J. Harris, A.F. Stewart and W.E. Court, *Planta Med.*, 16 (1968) 217.
5 W.E. Court and M.S. Habib, *J. Chromatogr.*, 80 (1973) 101.
6 M.S. Habib and W.E. Court, *Planta Med.*, 25 (1974) 331.
7 R. Verpoorte and A. Baerheim-Svendsen, *Chromatography of Alkaloids, Part B: Gas–Liquid and High-Performance Liquid Chromatography*, Elsevier, Amsterdam, 1984.
8 U.R. Cieri, *J. Assoc. Off. Anal. Chem.*, 66 (1983) 867.
9 L. Polz, H. Schubel and J. Stoeckigt, *Z. Naturforsch.*, Teil C, 42 (1987) 333.

10 P. Duez, S. Chamart, M. Vanhaelen-Fastré, M. Hanocq and L. Molle, *J. Chromatogr.*, 356 (1986) 334.
11 R.J. Flanagan, G.C.A. Storey, R.K. Bhamra and I. Jane, *J. Chromatogr.*, 247 (1982) 15.
12 I. Jane, A. McKinnor and R.J. Flanagan, *J. Chromatogr.*, 323 (1985) 191.
13 D.H. Rogers, *J. Chromatogr. Sci.*, 12 (1974) 742.
14 W.I. Taylor, in R.H.F. Manske (Editor), *The Alkaloids*, Vol. VII, Academic Press, New York, 1960, Ch. 22.
15 J.A. Martinez, C. Gómez, T. Santana and H. Vélez, *Planta Med.*, 35 (1989) 283.
16 N.R. Farnsworth, R.N. Blomster, D. Damratoski, W.A. Meer and L.V. Cammaroto, *Lloydia*, 27 (1967) 302.
17 Cs. Horváth, in C.F. Simpson (Editor), *Techniques in Liquid Chromatography*, Wiley, New York, 1982, Ch. 10.

ELSEVIER

Journal of Chromatography A, 662 (1994) 255–262

JOURNAL OF CHROMATOGRAPHY A

High-performance liquid chromatographic determination of chlordiazepoxide, its metabolites and oxaziridines generated after UV irradiation

V. Soentjens-Werts*[,a], J.G. Dubois[a], G. Atassi[b,c], M. Hanocq[a]

[a]*Laboratoire de Toxicologie, de Chimie Bioanalytique et de Chimie Physique Appliquée, Institut de Pharmacie, CP 205/1, Université Libre de Bruxelles, 1050 Brussels, Belgium*

[b]*Laboratoire de Pharmacologie Cellulaire, Institut de Pharmacie, Université Libre de Bruxelles, 1050 Brussels, Belgium*

[c]*Division Recherche Cancérologie, IDRS, 11 Rue des Moulineaux, 92150 Suresnes, France*

(First received July 21st, 1993; revised manuscript received October 25th, 1993)

Abstract

A reversed-phase high-performance liquid chromatographic (HPLC) procedure for the determination of chlordiazepoxide, its four metabolites and three unstable photoproducts (oxaziridines) generated by UV irradiation is reported. The influence of pH and acetonitrile (CH_3CN) and tetrahydrofuran (THF) percentages in the mobile phase was investigated. The optimum method uses a Nucleosil C_{18} column (5 μm) with a mobile phase consisting of CH_3CN–THF–0.06 *M* phosphate buffer (pH 5.8) (22:2:76). Eight drugs covering a wide range of lipophilicity and polarity were separated in 50 min. The absolute detection and quantification limits of benzodiazepines were less than 1 and 5 ng, respectively. The HPLC method alone or coupled with the UV irradiation procedure showed good precision (R.S.D. 1.7–4.0%) and excellent linearity in the range of 1.5–43 μg/ml ($r \geq 0.999$).

1. Introduction

Chlordiazepoxide (CDZ), used as a tranquillizer, undergoes extensive chain metabolization in man. The major metabolites are desmethylchlordiazepoxide (DES-CDZ) and demoxepam (DEM) and the minor metabolites are desmethyldiazepam (DES-DIAZ) and oxazepam (OXAZ), which are generally detected during chronic administration of CDZ [1] (Fig. 1).

Under UV irradiation, CDZ [2,3] and its two main metabolites isomerize to give photoproducts implicated in phototoxic effects (Fig. 1). Oxaziridine (OX) appeared to be the first and main drug formed if CDZ is irradiated with long-wavelength UV radiation. The N-oxide function of the parental 1,4-benzodiazepine is then transformed into an epoxy group [4–7]. When exposed to UV radiation, oxaziridine is transformed into quinoxaline and benzoxadiazocine [4] and when subjected to high temperature it is converted into the parent drug [8].

Reversed-phase high-performance liquid chromatographic (RP-HPLC) procedures have often been used to determine CDZ and its metabolites in biological fluids [9–16]. The determination of

* Corresponding author.

0021-9673/94/$07.00
SSDI 0021-9673(93)E1149-T

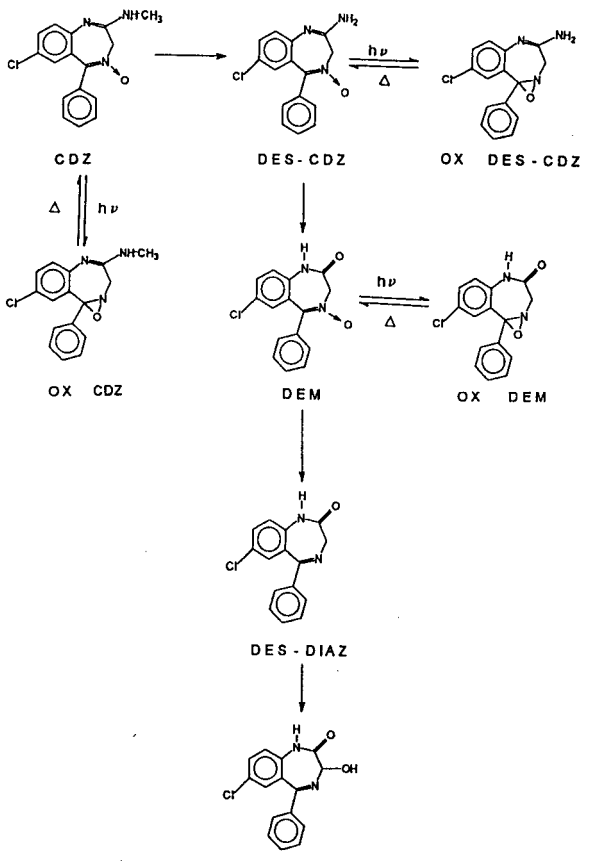

Fig. 1. Structures of chlordiazepoxide (CDZ), its metabolites (DES-CDZ, desmethylchlordiazepoxide; DEM, demoxepam; DES-DIAZ, desmethyldiazepam; OXAZ, oxazepam) and its photoproducts (OX CDZ, oxaziridine of chlordiazepoxide; OX DES-CDZ, oxaziridine of desmethylchlordiazepoxide; OX DEM, oxaziridine of demoxepam).

main decomposition products, namely demoxepam and 2-amino-5-chlorobenzophenone, in CDZ pharmaceutical formulations [17,18] and benzophenones in biological materials [19–21] have also been reported.

In this study, we developed and validated an RP-HPLC method for the separation and determination of CDZ, its four metabolites and three oxaziridines obtained after UV irradiation of CDZ, DES-CDZ and DEM or a mixture thereof. The production and separation of these drugs were the main objectives of this work for further investigations of their *in vitro* cytotoxicity mechanism and *in vivo* pharmacokinetics.

2. Experimental

2.1. Reagents and solutions

Chlordiazepoxide (CDZ) was kindly supplied by Hoffman-La Roche (Brussels, Belgium). Demoxepam (DEM) and desmethylchlordiazepoxide (DES-CDZ) were synthesized according to published methods [22–24] and their purity was monitored by IR and NMR spectrometry. Desmethyldiazepam (DES-DIAS) and oxazepam (OXAZ) were purchased from Sigma (St. Louis, MO, USA) and Federa (Brussels, Belgium), respectively.

Disodium hydrogenphosphate dihydrate and potassium monohydrogenphosphate were of analytical-reagent grade from Merck (Darmstadt, Germany). Acetonitrile (CH_3CN) and tetrahydrofuran (THF) were of HPLC grade from Lab-Scan Analytical Science (Dublin, Ireland) and Merck, respectively. Laboratory-purified HPLC-grade water was used in all mobile phases. The mobile phases were filtered through 0.2-μm membranes (Sartorius, Göttingen, Germany) and sonicated before use. Drugs were dissolved in acetonitrile.

2.2. HPLC system

The HPLC system consisted of a Gilson (Villiers le Bel, France) Model 305 pump, a Rheodyne (Cotati, CA, USA) Model 7125 loop injector and an HM holochrome UV monitor (Gilson) connected to a recorder (Kipp and Zonen, Brussels, Belgium). The reversed-phase chromatographic column (100 × 4.6 mm I.D.) was packed with Nucleosil C_{18} (5 μm) (Chrompack, Antwerp, Belgium) and operated at 20°C and a mobile phase flow-rate of 1 ml/min. The mobile phases tested to optimize the separation of CDZ, its metabolites and its photoproducts consist of CH_3CN, THF and phosphate buffer in various proportions, at different pH values and at different molarities. Volumes of 20–100 μl of sample solutions were injected; detection was performed at 265 nm. The selectivity of the method and the purity of the three photoproducts obtained were investigated with a

photodiode-array detector [Beckman (Fullerton, CA, USA) Model 168 System Gold and System Gold chromatography software (ASW 2)] connected to the HPLC system.

2.3. Irradiation system

The irradiation system was constructed in our laboratory. The materials (Oriel, Stratford, CT, USA) used were a Model 68806 arc lamp power supply which operates with a 150-W xenon lamp, a Photomax 60.100 lamp housing with the xenon lamp in the vertical position, a reflector provided with a demineralized water circulation cooling system, an RAL-UV mirror and lens system and a monochromator with a band pass of 6 nm and set at 350 nm.

2.4. Conditions for UV irradiation of CDZ and its metabolites

Irradiation was carried out at 350 nm to avoid subsequent photoisomerization of oxaziridine [4] (power supply of the lamp set at 6.5 A for a tension of 18 V). The optimum CDZ irradiation conditions to produce pure OX quantitatively were previously determined for concentrations up to 152 μg/ml: CH_3CN as irradiation solvent, a temperature of 10°C, a volume of 0.7 ml for the irradiated solutions and an irradiation time of 70–90 min for the CDZ solutions [25]. The optimum DES-CDZ and DEM irradiation conditions were the same as those for CDZ.

3. Results and discussion

3.1. Organic modifier concentration

In order to select a mobile phase able to separate CDZ and its metabolites, we studied the variation of the retention time (t_R), the peak resolution (R_s) and the separation factor (α) between drugs as a function of the decreasing percentage of CH_3CN and addition of THF. The first mobile phase tested [CH_3CN–0.06 *M* phosphate buffer (pH 5.4)] was previously used to study the kinetics of the photoisomerization of CDZ into oxaziridine and the determination of hydrolysis impurities, namely demoxepam, its oxaziridine and 2-amino-5-chlorobenzophenone, after UV irradiation [25]. The results showed that DES-CDZ and OXAZ are not separated ($R_s = 0.75$; $\alpha = 1.20$) with this mobile phase. Further, slight tailing of the peak of the oxaziridine derived from CDZ was observed (t_R = 15.50 min). Therefore, we first added THF, which works as a tailing suppressor but strongly decreases the retention time of CDZ and its oxaziridine (t_R of OX CDZ = 2.50 min). Therefore, we progressively decreased the proportion of CH_3CN to 23% to obtain a good separation and resolution of CDZ and its four metabolites in less than 20 min. However this mobile phase composition [CH_3CN–THF–0.06 *M* phosphate buffer (pH 5.4) (23:1:76)] was not able to separate OX CDZ and OX DEM after UV irradiation ($R_s = 0$; $\alpha = 1.03$).

3.2. Influence of pH

With a constant proportion of CH_3CN (23%), the influence of pH was tested (Table 1). In addition, for each pH tested, at least two percentages of THF were also investigated. pH was found to be a key parameter for the separation of CDZ, its metabolites and its photoproducts, as illustrated in Fig. 2. When the pH is in the range 5.4–6.0, the order of elution of the drugs in Table 1 is DEM, DES-CDZ, OXAZ, CDZ, DES-DIAZ, OX DES-CDZ, OX DEM and OX CDZ. A decrease in pH to 5.0 results in a reversed elution between the peaks of OX DEM and OX CDZ and also a weak resolution and separation of the two following peaks, DES-DIAZ and OX DES-CDZ, without any further changes (Table 1). At pH 4.5, other major modifications occur, namely, DEM and DES-CDZ are partly or not separated, OXAZ and CDZ co-elute, the four following peaks are separated but the retention times of OX DES-CDZ and OX CDZ have drastically decreased, whilst the retention times of DES-DIAZ and OX DEM do not vary (Table 1).

Mobile phases tested at pH 5.8 and 6.0 separated of all the drugs. We selected the following

Table 1
Influence of pH and THF percentage on the separation of CDZ, its metabolites and its photoproducts

Mobile phase	Parameter	Drug							
		DEM	DES-CDZ	OXAZ	CDZ	DES-DIAZ	OX DES-CDZ	OX DEM	OX CDZ
pH 6.0									
1% THF,									
23% CH_3CN	t_R	5.50	7.75	9.50	12.50	19.00	45.00	49.50	67.00
	R_s	2.86	2.00	3.00	5.27	8.96	1.67	4.97	
	α	1.50	1.26	1.35	1.57	2.44	1.10	1.36	
2% THF,									
23% CH_3CN	t_R	4.75	6.50	8.00	10.25	15.75	35.75	40.25	54.25
	R_s	3.50	2.80	3.00	6.00	7.73	1.48	4.46	
	α	1.47	1.27	1.32	1.59	2.36	1.13	1.36	
3% THF,									
23% CH_3CN	t_R	3.75	5.00	6.50	8.00	12.00	28.00	31.25	42.00
	R_s	1.50	1.58	1.33	3.00	6.29	1.09	3.75	
	α	1.45	1.38	1.27	1.57	2.45	1.12	1.36	
pH 5.8									
1% THF,									
21% CH_3CN	t_R	6.75	10.25	12.50	16.25	27.00	55.75	67.00	78.75
	R_s	2.33	1.43	2.27	4.20	7.74	2.40	2.08	
	α	1.61	1.24	1.33	1.70	2.11	1.21	1.18	
1% THF,									
22% CH_3CN	t_R	5.50	8.00	10.00	13.25	20.25	43.75	52.25	63.00
	R_s	1.83	1.08	2.00	3.88	6.43	2.05	2.00	
	α	1.56	1.29	1.36	1.57	2.22	1.20	1.21	
1% THF,									
23% CH_3CN	t_R	4.75	6.50	8.25	10.75	16.25	34.00	40.50	49.50
	R_s	2.00	1.09	1.67	3.57	10.14	2.07	2.48	
	α	1.47	1.32	1.34	1.56	2.16	1.20	1.23	
2% THF,									
22% CH_3CN	t_R	4.75	6.50	8.25	10.25	16.25	35.00	41.75	51.00
	R_s	1.60	1.40	2.00	3.57	5.90	1.94	2.32	
	α	1.47	1.32	1.28	1.65	2.23	1.20	1.23	
2% THF,									
23% CH_3CN	t_R	4.50	6.25	8.00	10.00	15.00	31.75	38.00	47.00
	R_s	2.00	1.56	1.64	3.38	6.80	2.00	2.55	
	α	1.50	1.33	1.29	1.56	2.20	1.20	1.24	
pH 5.0									
1% THF,									
23% CH_3CN	t_R	5.25	7.00	9.50	11.00	18.50	21.75	47.50	28.75
	R_s	1.40	1.50	1.50	3.88	0.81	2.07[a]	4.94	
	α	1.41	1.42	1.18	1.75	1.19	1.34[a]	1.68	
2% THF,									
23% CH_3CN	t_R	4.50	6.00	8.00	9.50	15.00	17.75	37.75	24.00
	R_s	1.25	2.25	1.00	3.57	1.05	2.47[a]	5.27	
	α	1.43	1.40	1.21	1.65	1.20	1.37[a]	1.60	

[a] Values between OX DES-CDZ and OX CDZ. Mobile phase composition: CH_3CN (21–23%)–THF (1–3%)–0.06 *M* phosphate buffer (pH 4.5–6.0) (78–74%).

Table 1 *(continued)*

Mobile phase	Parameter	Drug							
		DEM	DES-CDZ	OXAZ	CDZ	OX DES-CDZ	OX CDZ	DES-DIAZ	OX DEM
pH 4.5									
1% THF,									
23% CH_3CN	t_R	5.00	6.00	9.25	9.25	13.75	16.50	19.00	49.25
	R_s	0.40	3.00	0.00	2.43	2.00	1.50	11.27	
	α	1.25	1.65	1.00	1.55	1.22	1.16	2.68	
2% THF,									
23% CH_3CN	t_R	4.75	4.75	7.75	7.75	11.00	13.25	16.00	41.00
	R_s	0.00	2.67	0.00	1.29	1.29	1.87	9.27	
	α	1.00	1.69	1.00	1.48	1.23	1.22	2.67	

mobile phase composition to validate the method: CH_3CN–THF–0.06 *M* phosphate buffer (pH 5.8) (22:2:76). It was demonstrated that it maintained a good resolution and separation even if deterioration of the column or ambient temperature variations occurred. As our main objective was to determine low parent benzodiazepine concentrations after irradiation, we need chromatographic conditions that allow a very good separation between these peaks (DEM, DES-CDZ and CDZ) and those of drugs which have retention times close to them and which undergo no degradation (OXAZ and DES-DIAZ). The mobile phase chosen is suitable to resolve this problem and particularly to obtain a good resolution between CDZ and OXAZ. Moreover, these conditions provided a reasonable analysis time.

Fig. 3 illustrates the separation of CDZ and its metabolites before UV irradiation and Fig. 4

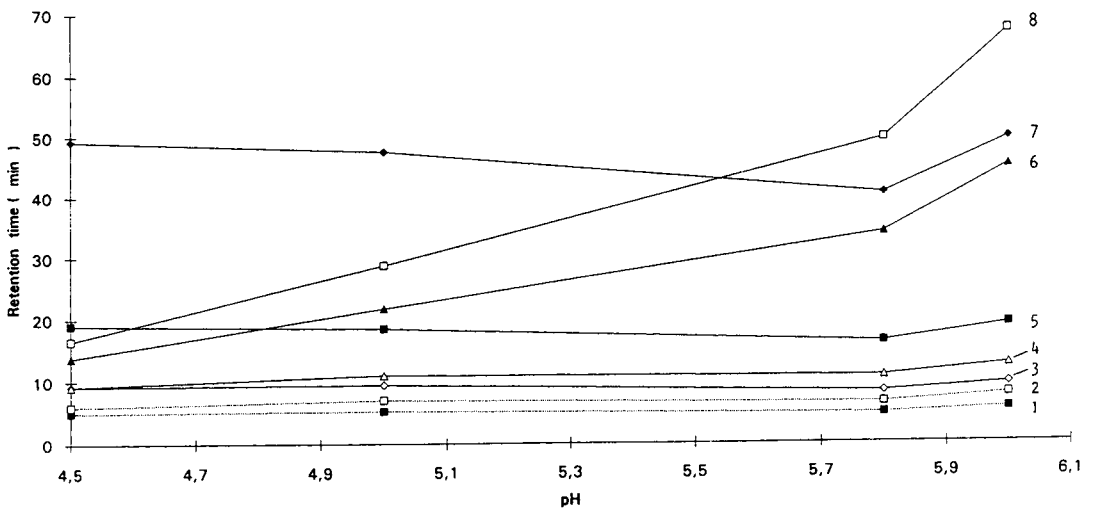

Fig. 2. Variation of retention times of CDZ, its metabolites and its photoproducts as a function of pH. Mobile phase composition: CH_3CN–THF–0.06 *M* phosphate buffer (pH 4.5–6.0) (23:1:76). 1 = DEM; 2 = DES-CDZ; 3 = OXAZ; 4 = CDZ; 5 = DES-DIAZ; 6 = OX DES-CDZ; 7 = OX DEM; 8 = OX CDZ.

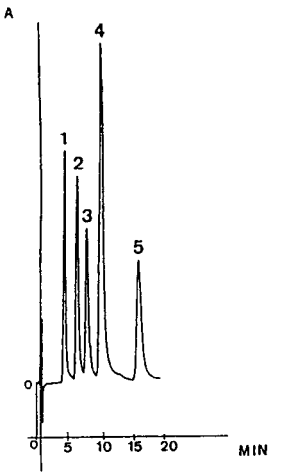

Fig. 3. HPLC separation of chlordiazepoxide (4) and its metabolites, namely desmethylCDZ (2), demoxepam (1), desmethyldiazepam (5) and oxazepam (3). Column temperature, 20°C; flow-rate, 1 ml/min; UV detection at 265 nm. Amounts injected: (1) 310; (2) 230; (3) 480; (4) 420; (5) 670 ng.

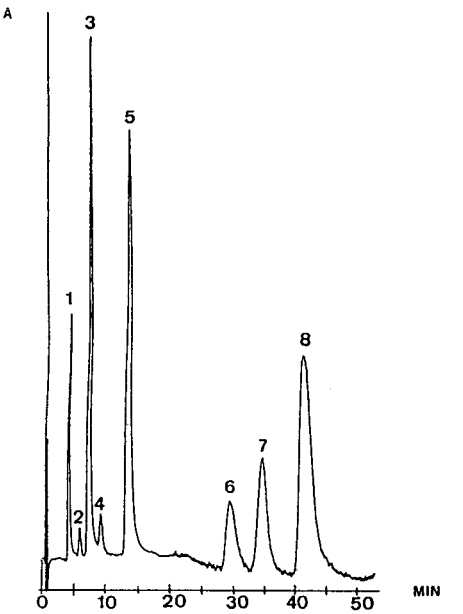

Fig. 4. HPLC separation of chlordiazepoxide (4), its metabolites, namely desmethylCDZ (2), demoxepam (1), desmethyldiazepam (5) and oxazepam (3), and its photoproducts after UV irradiation for 70 min at <10°C, namely oxaziridine of desmethylCDZ (6), oxaziridine of demoxepam (7) and oxaziridine of CDZ (8). Column temperature, 20°C; flow-rate, 1 ml/min; UV detection at 265 nm. Amounts injected: (1) 150; (2) 16; (3) 480; (4) 19; (5) 670 ng; (6–8) unknown.

shows the same separation but after UV irradiation and hence in presence of the three photoproducts.

We also tested different molarities of the phosphate buffer, *viz.*, 0.06, 0.10 and 0.20 *M*, but no advantages accrued. Indeed, the increase in the ionic strength induces a decrease in resolution. Moreover, it would decrease the column lifetime owing to phosphate crystallization.

3.3. Validation of the method

The results were linear over the following ranges: DEM, 0.2–31.8 μg/ml; DES-CDZ, 0.15–23.20 μg/ml; OXAZ, 0.31–49.10 μg/ml; CDZ, 0.27–43.00 μg/ml; and DES-DIAZ, 0.43–68.40 μg/ml. The equations of the calibration graphs and the regression coefficients are given in Table 2. The linearities were verified on three different days with the five drugs in a mixture dissolved in acetonitrile. The absolute detection and quantification limits for the five drugs were all less than 1 ng (for concentrations yielding a signal-to-noise ratio of 2) and less than 5 ng (for concentrations yielding a signal-to-noise ratio of 10), respectively, as illustrated in Table 3. These were determined using a diode-array detector, which also verified the specificity of the method and the purity of the eight substances present after UV irradiation.

The precision was determined by six replicate injections of a solution that contained CDZ and its four metabolites. Table 4 shows the results of the intra- and inter-day determination of these five drugs. There is a good intra-day precision with a mean R.S.D. lower than 2.8% for all the drugs and also a good inter-day precision with a mean R.S.D. lower than 4.1% (determined on four days).

Fig. 5 shows the linear response between the CDZ concentration before irradiation and the peak height of undecomposed CDZ for a constant irradiation time of 70 min. Therefore, the percentage of CDZ remaining is independent of

Table 2
Calibration graphs for CDZ and its metabolites

Compound	Range (μg/ml)	Slope (*m*)	Intercept (*c*)	*r**
DEM	0.2–31.8	0.2082	0.0075	0.9990
		0.2221	−0.0677	0.9995
		0.2191	−0.0781	0.9995
DES-CDZ	0.15–23.20	0.1665	0.0757	0.9986
		0.1777	−0.0053	0.9991
		0.1800	−0.0347	0.9996
OXAZ	0.31–49.10	0.5177	0.0388	0.9989
		0.5574	−0.1353	0.9992
		0.5538	−0.1479	0.9997
CDZ	0.27–43.00	0.1955	0.0113	0.9989
		0.2084	−0.0577	0.9994
		0.2080	−0.0893	0.9993
DES-DIAZ	0.43–68.40	0.8915	−0.0995	0.9989
		0.9500	−0.2101	0.9996
		0.9494	−0.2857	0.9993

$y = mx + c$, where y = concentration of the injected substance (μg/ml) and x = peak height of the substance (cm). r^* = regression coefficient.

Table 3
Absolute limits of detection and quantification of CDZ and its metabolites

Drug	Injected amount (ng)	
	Limit of detection	Limit of quantification
DEM	0.4	2.0
DES-CDZ	0.3	1.5
OXAZ	0.6	3.0
CDZ	0.5	2.5
DES-DIAZ	0.9	4.5

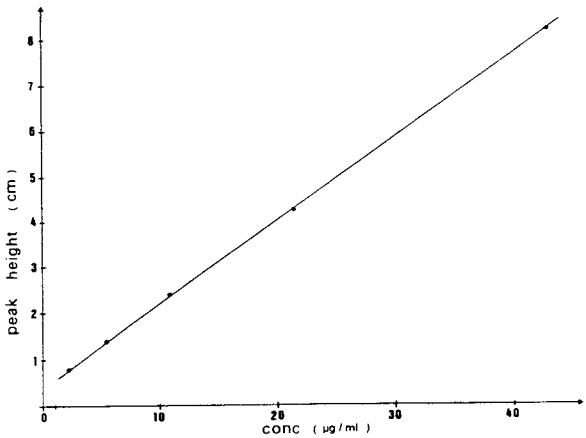

Fig. 5. Variation of the CDZ peak height after irradiation for 70 min at <10°C as a function of initial CDZ concentration dissolved in acetonitrile.

the initial CDZ concentration. These results confirm that the CDZ photoisomerization follows a first-order reaction [25]. Moreover, DES-CDZ and DEM were found to show the same kinetic behaviour. It is reasonable to consider that each mole of oxaziridine is stoichiometrically generated from 1 mol of the parent benzodiazepine as only one photoproduct was detected after irradiation of N-oxide derivatives and as the results show a linear response between the parent benzodiazepine concentration before irradiation and the peak height of OX generated during 70 min of irradiation.

The increase in the retention times of the drugs caused by modifications of the mobile phase did not change the photodegradation kinetics of the 1,4-benzodiazepines. This result shows that the unstable oxaziridines did not re-

Table 4
Within-assay reproducibility and day-to-day precision

Validation[a]	Drug[b]				
	DEM	DES-CDZ	OXAZ	CDZ	DES-DIAZ
Intra-assay R.S.D. (%) ($n = 6$)	1.7	2.6	2.2	2.0	2.7
Inter-assay R.S.D. (%) ($n = 4$)	3.5	3.0	4.0	2.7	4.0

[a] n = Number of injections.
[b] Concentrations: DEM 31.8, DES-CDZ 23.2, OXAZ 49.1, CDZ 43.0, DES-DIAZ 68.4 μg/ml.

form the parent drug on the column during the HPLC separation. The stability of the photoproducts was followed during their conservation in CH_3CN at −25°C in the dark. The results demonstrated that no degradation occurred during a 10-day period.

In conclusion, the reported and validated HPLC method separates CDZ, its metabolites and its photoproducts in spite of their wide ranges of lipophilicity and polarity. Further, the development of this assay (HPLC and irradiation systems) is a major step for further investigations of the production, stability, cytototoxicity mechanisms and pharmacokinetics of the oxaziridines.

4. Acknowledgements

This study was supported by the Institut de Recherche Servier, Suresnes, France. We thank Professor R. Collin for helpful discussions and his collaborators who made the irradiation system. The gift of chlordiazepoxide from Hoffman-La Roche, Basle, Switzerland, is gratefully acknowledged.

5. References

[1] M. Bourin and A. Lecalier, *Les Benzodiazépines Bases Pharmacocinétiques de la Prescription des Benzodiazépines*, Ellipses, Paris, 1981.
[2] L.H. Sternbach, B.A. Koechlin and E. Reeder, *J. Org. Chem.*, 27 (1962) 4671.
[3] G.F. Field and L.H. Sternbach, *J. Org. Chem.*, 33 (1968) 4438.
[4] P.J.G. Cornelissen, G.M.J. Beijersbergen van Henegouwen and K.W. Gerritsma, *Int. J. Pharm.*, 3 (1979) 205.
[5] P.J.G. Cornelissen, G.M.J. Beijersbergen van Henegouwen and G.R. Mohn, *Photochem. Photobiol.*, 32 (1980) 653.
[6] A. Bakri, G.M.J. Beijersbergen van Henegouwen and J.L. Chanal, *Photochem. Photobiol.*, 38 (1983) 177.
[7] A. Bakri, G.M.J. Beijersbergen van Henegouwen and J.L. Chanal, *Photodermatology*, 2 (1985) 205.
[8] H. De Vries, G.M.J. Beijersbergen van Henegouwen and P.J.H.H. Wouters, *Pharm. Weekblad, Sci. Ed.*, 5 (1983) 302.
[9] M.A. Peat, B.S. Finkle and M.E. Deyman, *J. Pharm. Sci.*, 68 (1979) 1467.
[10] V. Ascalone, *J. Chromatogr.*, 181 (1980) 141.
[11] T.B. Vree, A.M. Baars, Y.A. Hekster and E. Van der Kleijn, *J. Chromatogr.*, 224 (1981) 519.
[12] M. Divoll, D.J. Greenblatt and R.I. Shader, *Pharmacology*, 24 (1982) 261.
[13] A. Siouffi and J.P. Dubois, *J. Chromatogr.*, 531 (1990) 459.
[14] H.B. Greizerstein and I.G. McLaughlin, *J. Liq. Chromatogr.*, 3 (1980) 1023.
[15] R.G. Lister, *J. Chromatogr.*, 277 (1983) 201.
[16] F.T. Noggle, Jr., C. Clark and J. de Ruiter, *J. Liq. Chromatogr.*, 13 (1990) 4005.
[17] S.L. Ali, *Int. J. Pharm.*, 5 (1980) 85.
[18] S.E. Roberts and M.F. Delaney, *J. Chromatogr.*, 283 (1984) 265.
[19] K. Harzer and R. Barchet, *J. Chromatogr.*, 132 (1977) 83.
[20] C. Violon and A. Vercruysse, *J. Chromatogr.*, 189 (1980) 94.
[21] M. Chiarotti, N. de Giovanni and A. Fiori, *J. Chromatogr.*, 358 (1986) 169.
[22] L.H. Sternbach, E. Reeder, O. Keller and W. Metlesics, *J. Org. Chem.*, 26 (1961) 4488.
[23] L.H. Sternbach and E. Reeder, *J. Org. Chem.*, 26 (1961) 1111.
[24] S.C. Bell, T.S. Sulkowski, C. Gochman and S.J. Childress, *J. Org. Chem.*, 27 (1962) 562.
[25] V. Soentjens, J.G. Dubois, G. Atassi and M. Hanocq, *Int. J. Pharm.*, submitted for publication.

ELSEVIER

Journal of Chromatography A, 662 (1994) 263–267

JOURNAL OF CHROMATOGRAPHY A

High-performance liquid chromatographic purification of sodium bis(2-ethyl-1-hexyl)sulphosuccinate from commercial preparations containing near-UV absorbing and fluorescent impurities

Ettore Bismuto*, Gaetano Irace

Dipartimento di Biochimica e Biofisica, Seconda Università di Napoli, Via Costantinopoli 16, 80138 Naples, Italy

(First received July 19th, 1993; revised manuscript received October 20th, 1993)

Abstract

Commercial sodium bis(2-ethyl-1-hexyl)sulphosuccinate (Aerosol OT, AOT), a widely used surfactant forming reversed micelles in non-polar solvents, was found to contain some impurities with fluorescence characteristics, *i.e.*, absorption and emission spectra, similar to those of the tryptophan residues in proteins. Fluorescence lifetime determinations in the frequency domain confirmed the similarity between the emission decay of contaminants and that of tryptophan in proteins. A preparative procedure for the purification of commercial AOT by HPLC is described.

1. Introduction

Reversed micelles are spheroidal aggregates that are formed when certain surfactants are dissolved in apolar solvents. The polar head groups are directed towards the interior of the aggregate, thus forming a polar core that can solubilize water (water pool) [1]. Reversed micelles are capable of solubilizing a variety of proteins through encapsulation in the microaqueous phase. The observation that the catalytic activity of enzymes is retained in these systems has stimulated great interest as they provide a very useful model for studying the conformation and activity of biopolymers in membrane-like environments and has opened up new possibilities for investigations on enzymes at low temperatures [2]. Moreover, reversed micelles have been shown to provide new potential for technological applications [3].

The most common and best defined surfactant is the Aerosol OT (AOT), *i.e.*, sodium bis(2-ethyl-1-hexyl)sulphosuccinate. AOT molecules at a 3% concentration in hydrocarbon solutions are completely associated into uniformly sized micellar assemblies, each containing 23 AOT molecules. The addition of water to the micelle interior produces spheroidal particles. The structural and chemical homogeneity of such reversed micellar systems of AOT make them particularly convenient for studying biomembrane mimetic phenomena [4].

It has been reported that AOT preparations contain impurities as a result of the manufactur-

* Corresponding author.

0021-9673/94/$07.00
SSDI 0021-9673(93)E1201-A

ing processes [5]. AOT is often prepared by diesterification of maleic or fumaric acid with 2-ethylhexanol. The diester is then sulphonated with sodium hydrogensulphite. Possible impurities are sodium hydrogensulphite, various acidic monoesters as a result of incomplete esterification and 2-ethylhexanol. The existence of aromatic species has also been reported. The presence of acidic impurities may significantly affect reactions in microemulsions where pH is important. Aromatic impurities interfere with spectroscopic investigations, in particular in fluorescence studies. Although the quality of commercial AOT has been much improved, impurities at the 0.1% level are not easy to identify and their subsequent removal can pose considerable problems. In this paper, we report the existence of fluorescent impurities in commercial preparations of AOT with emission properties resembling those shown by tryptophan residues in proteins [6–8]. An HPLC procedure is suggested in order to remove these impurities from the AOT preparations.

2. Experimental

2.1. Chemicals and reagents

Sodium bis(2-ethyl-1-hexyl)sulphosuccinate (AOT) was obtained from Sigma (St. Louis, MO, USA). Solvents were of HPLC grade from Fluka (Buchs, Switzerland). Deionized water was generated in a Milli-Q plus system (Millipore).

2.2. Chromatographic apparatus

The chromatographic apparatus was a Beckmann System Gold 126 equipped with a diode-array detector module. A Beckmann ultrasphere ODS (d_p 5 μm) column (25 cm × 4.6 mm I.D.) was used for analytical separations. The preparative column (25 cm × 10 mm I.D.) was packed with Bio-Sil C_{18} HL silica (d_p 40–63 μm) from Bio-Rad (Hercules, CA, USA).

2.3. Spectral measurements

Absorption spectra were recorded with a Perkin-Elmer Lambda Array 3840 UV–Vis spectrophotometer. Steady-state fluorescence spectra were obtained using a Perkin-Elmer Model MPF-66 spectrofluorimeter.

2.4. Fluorescence lifetime determination

Lifetime measurements were made using a multi-frequency cross-correlation phase and modulation fluorimeter (ISS, Urbana, IL, USA) with a 300-W xenon lamp [9]. The emission was observed through a longwave pass filter (WG 330) with a cut-off wavelength at 330 nm to avoid Raman emission. The modulation frequency was variable from 1 to 200 MHz. A solution of *p*-terphenyl (Kodak) in cycloexane was placed in the reference cell to correct for colour error. A lifetime of 1.000 ns was assigned to the reference solution. At least twenty different modulation frequencies were used, and the data were collected until the standard deviations for each measurement of phase and modulation was below 0.25° and 0.004, respectively. The temperature of the solution was maintained constant at 18°C by using an external bath circulator. The observed phase shifts and demodulation values were analysed in order to obtain the lifetime of the emitting species according to the equations reported elsewhere [10].

3. Results and discussion

Inspection of the structure of aerosol OT (shown in the inset in Fig. 1) reveals the absence of chromophoric groups which may absorb and subsequently emit in the near UV region (270–350 nm). Nevertheless, commercial AOT shows the presence of near-UV-absorbing and -emitting components whose spectral properties are similar to those of the most common intrinsic protein chromophore, the indole moiety of the tryptophanyl residue. Fig. 1 shows the steady-state fluorescence spectrum of commercial AOT in methanol solution resulting from excitation at

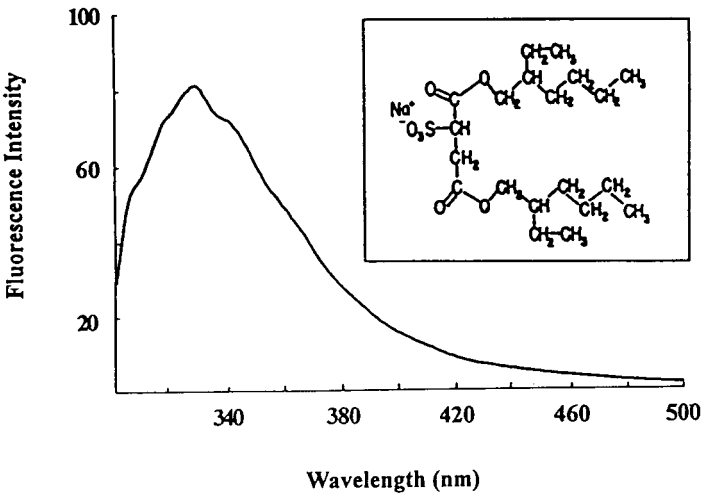

Fig. 1. Emission spectrum of commercial AOT dissolved in methanol. Excitation was at 290 nm. The sample absorbance at the exciting wavelength was less than 0.2. The inset shows the structure of AOT.

290 nm, a wavelength that is usually used to excite selectively the tryptophan residues in proteins. The shape of the emission spectrum is structured, suggesting the presence of aromatic impurities. The emission maximum, centred at about 330 nm, is coincident with that of tryptophan buried in the protein matrix.

The emission decay of commercial AOT preparations was investigated in the frequency domain. Fig. 2 shows the phase shifts and the demodulation factors *versus* the sinusoidal modulation frequency of the exciting light in the range 2–200 MHz [9]. The phase shift and the demodulation of the emission with respect to the exciting light are related to the fluorescence lifetime of the emitting species [10]. Table 1 shows the data fit obtained using a non-linear least-squares routine. The emission decay of commercial AOT in methanol is described by at least three discrete components with fluorescent lifetimes of 18.2, 4.4 and 0.7 ns, respectively. Table 1 also gives the results relative to the emission decays of reversed micelles formed by commercial AOT in isoctane and including an increasing water content. The average lifetime of the long-lived component is 11 ns whereas that of the second component is *ca.* 3 ns. This value is very close to that observed for the indole residue in several proteins [6–8] and may clearly affect the decay analysis of proteins included in AOT-formed reversed micelles. The very short lifetime

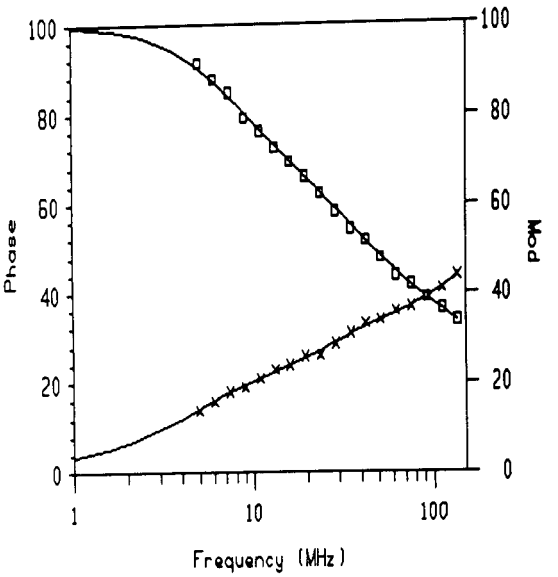

Fig. 2. Dependence of (×) phase shift and (□) demodulation factor on the modulation frequency of commercial AOT in methanol solution. Excitation was at 290 nm and emission was observed through a WG 330 filter. The absorbance of the sample at the exciting wavelength was less than 0.2. Solid lines were calculated from the tri-exponential fit parameters reported in Table 1.

Table 1
Emission decay analysis of commercial AOT as the sum of three exponentials

Sample	f_1	τ_1	f_2	τ_2	τ_3	χ^2
AOT, 0.5 *M* in methanol	0.37	18.2	0.33	4.38	0.70	2.13
Reversed AOT micelles, $R = 0$	0.36	11.2	0.37	2.52	0.60	1.98
Reversed AOT micelles, $R = 5$	0.33	10.9	0.41	1.75	0.05	1.85
AOT micelles, $R = 15$	0.27	11.7	0.55	2.61	0.02	2.20
Reversed AOT micelles, $R = 30$	0.40	8.2	0.46	2.14	0.03	2.01

f_i and τ_i are the fractions and the lifetimes (in nanoseconds), respectively. R is the H_2O:AOT molar ratio. The excitation wavelength was 295 nm and the temperature was maintained constant at 18°C.

component in Table 1 probably originates from weakly scattered light or other unpredictable instrumental contributions [11].

Recently there have been reports of studies of the dynamics of the water pool and enzymes encapsulated in reversed AOT micelles, most of which were based on the study of the emission decay [12–14]. Therefore, it appeared interesting to set up a rapid chromatographic procedure that eliminates the aromatic impurities that interfere with the emission decay of proteins.

The analytical separation of AOT from the near-UV-absorbing and -emitting impurities contained in the commercial preparations was carried out with a C_{18}-bonded silica column (25 cm × 4.6 mm I.D.). The column was eluted at a flow-rate of 0.7 ml/min with a binary linear gradient from 70 to 100% methanol in water in 40 min. All runs were performed at room temperature. Fig. 3 shows the chromatographic pattern of the separation detected by measuring the absorbance at 235 nm. The main peak centred at 5.34 min corresponds to the AOT molecule. Three other peaks are present in the chromatogram, at 3.9, 22.4 and 27.2 min. The absorption and emission spectra of the four fractions eluted from the column were recorded. The most important feature is that the main peak of the AOT preparation was virtually non-

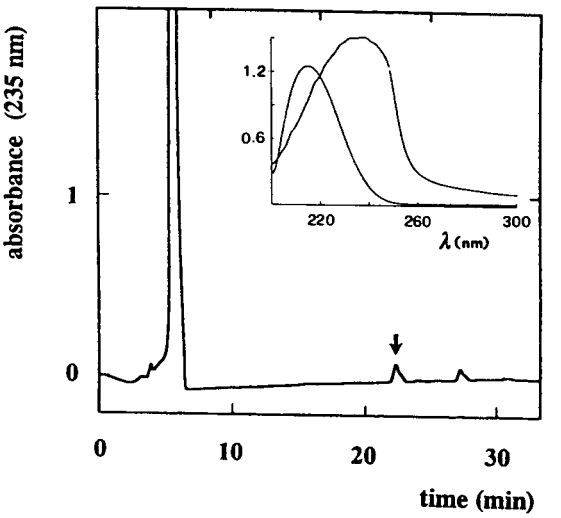

Fig. 3. Elution pattern of commercial AOT from the Ultrasphere ODS (5 μm) column (25 cm × 4.6 mm I.D.). The column was developed with a gradient from 60% to 100% methanol in water at a flow-rate of 0.7 ml/min. The inset compares the absorption spectra of commercial and HPLC-purified AOT. Both samples were dissolved in methanol–water (70:30).

fluorescent. Moreover, the absorption spectrum of purified AOT, shown in the inset in Fig. 3, revealed a strong decrease in near-UV-absorbing components compared with that of the commercial AOT in methanol solution. The absorption maximum of the purified AOT is shifted towards short wavelengths with a marked decrease in the near-UV region. The arrow in Fig. 3 indicates the fraction containing fluorescent material.

Large-scale AOT purifications from commercial preparations were performed on a chromatographic column (25 cm × 10 mm I.D.) packed with Bio-Sil C_{18} HL. The column was equilibrated with methanol–water (70:30). The flow-rate was maintained at 0.5 ml/min. Injections of 0.5–1 ml of commercial AOT [3.5 g per 10 ml of methanol–water (70:30)] were made. After the injection of the sample, the column was eluted with a linear gradient of from 70 to 100% methanol in water in 40 min and then with absolute methanol for 50 min. A typical elution pattern, obtained recording the absorbance at 235 nm, is shown in Fig. 4. As with the analytical separation, four components are resolved. The

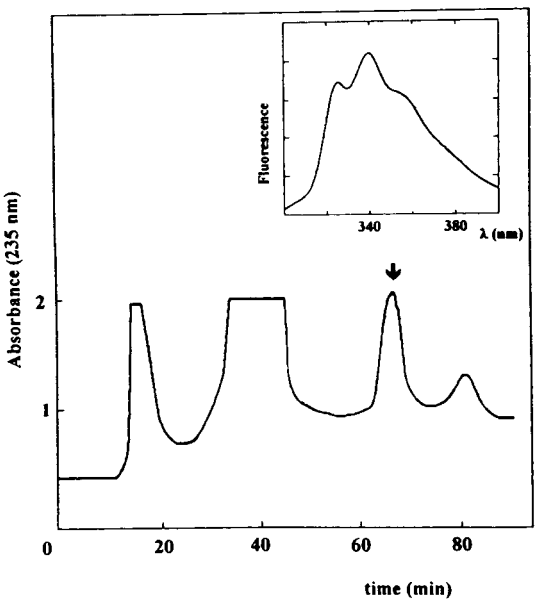

Fig. 4. Elution pattern of commercial AOT from the Bio-Sil C_{18} HL (40–63 μm) column (25 cm × 10 mm I.D.). The column was developed at a flow-rate of 0.5 ml/min with a gradient from 70 to 100% methanol in water in 40 min then with absolute methanol for 50 min. The emission spectrum of the AOT impurity corresponding to the peak marked with an arrow is shown in the inset.

inset in Fig. 4 shows the fluorescence spectrum of the third peak. It is worth noting that the first peak is much better separated from AOT using the preparative column. The collected main fraction corresponding to the purified AOT was vacuum dried. The recovery of AOT was 0.3 g for each run, an amount that is usually sufficient for performing a fluorescence lifetime determination of protein included in reversed micelles.

4. Acknowledgement

This research was supported by the Consiglio Nazionale delle Ricerche (Italy), grants 91.02478.CT14 and 92.02263.CT14.

5. References

[1] D. Langevin, in M.P. Pileni (Editor), *Structure and Reactivity in Reverse Micelles*, Elsevier, Amsterdam, 1989, pp. 13–42.
[2] P.L. Luisi, M. Giomini, M.P. Pileni and B.H. Robinson, *Biochim. Biophys. Acta*, 947 (1988) 209–246.
[3] R. Hilhorst, in M.P. Pileni (Editor), *Structure and Reactivity in Reverse Micelles*, Elsevier, Amsterdam, 1989, pp. 323–341.
[4] H.F. Eiche and Kvita, in P.L. Luisi and B.E. Straub (Editors), *Reverse Micelles*, Plenum Press, New York, 1984, pp. 21–35.
[5] P.D.I. Fletcher, A.M. Howe, B.H. Robinson and D.C. Steytler, in P.L. Luisi and B.E. Straub (Editors), *Reverse Micelles*, Plenum Press, New York, 1984, pp. 69–72.
[6] E. Bismuto, E. Gratton and G. Irace, *Biochemistry*, 27 (1988) 2132–2136.
[7] E. Bismuto and G. Irace, *Photochem. Photobiol.*, 47 (1989) 165–167.
[8] E. Bismuto, I. Sirangelo and G. Irace, *Arch. Biochim. Biophys.*, 287 (1991) 216–220.
[9] E. Gratton and M. Limkeman, *Rev. Sci. Instrum.*, 54 (1984) 294–299.
[10] E. Gratton, E. Limkeman, J. Lakowicz, B. Maliwal, H. Cherek and G. Laczko, *Biophys. J.*, 46 (1984) 479–486.
[11] B. Barbieri, F. De Piccoli and E. Gratton, *Rev. Sci. Instrum.*, 60 (1989) 3201–3206.
[12] E. Bismuto, I. Sirangelo and G. Irace, *Biophys. Chem.*, 44 (1992) 83–90.
[13] E. Bismuto, I. Sirangelo and G. Irace, *Biochim. Biophys. Acta*, 298-2 (1992) 83–90.
[14] V.N. Dorovska-Taran, C. Veeger and A.J.W.G. Visser, *Eur. J. Biochem.*, 211 (1993) 47–55.

Journal of Chromatography A, 662 (1994) 269–280
Elsevier Science B.V., Amsterdam

CHROM. 25 688

Estimation of gas–liquid chromatographic retention times from molecular structure

S.H. Hilal and L.A. Carreira*

Department of Chemistry, University of Georgia, Athens, GA 30602 (USA)

S.W. Karickhoff

Environmental Research Laboratory, U.S. Environmental Protection Agency, Athens, GA 30605 (USA)

C.M. Melton

Artificial Intelligence Group, University of Georgia, Athens, GA 30602 (USA)

(First received July 5th, 1993; revised manuscript received October 26th, 1993)

ABSTRACT

A new type of a computer program called SPARC (SPARC Performs Automated Reasoning in Chemistry) was developed to predict chemical reactivity parameters and physical properties of organic molecules from their molecular structures based on fundmental chemical structure theory. SPARC's physical models for vapor pressure and activity coefficient were used to calculate the Henry's constant, which can be related to the Kováts retention index. The Kováts indices for a wide range of compounds at any temperature on a squalane liquid phase were calculated. The Root Mean Square deviation error was found to be less than 7 Kováts units, a value that is close to interlaboratory experimental error.

INTRODUCTION

Despite some limitations, the Kováts index has found much greater usage than all other specialized retention specification schemes. The Kováts index is the only retention value in gas–liquid chromatography (GLC) in which two fundamental quantities, the relative retention and the specific retention volume are united [1]. Moreover, a series of explicit relationships between retention indices and a number of physicochemical quantities related to GLC have been developed. Also many different linear relationships between the Kováts index value for a molecule and other fundamental quantities such as carbon number, boiling point and refractive index have been derived [1,2].

The Kováts index [3] expresses the retention of a compound of interest relative to a homologous series of *n*-alkanes examined under the same isothermal conditions. The Kováts index for a particular compound of interest is defined as the carbon number (c) multiplied by 100 of a hypothetical *n*-alkane having exactly the same net retention volume characteristics of the compound of interest measured under the same conditions:

$$I = 100\left(\frac{\log V_{Nc} - \log V_{Nx}}{\log V_{Nc} - \log V_{N(c+1)}} + c\right) \quad (1)$$

where I is the Kováts Index of compound x, x is a compound with a retention between that of the first *n*-alkane and second *n*-alkane standard, c is

* Corresponding author.

0021-9673/94/$07.00
SSDI 0021-9673(93)E1160-2

the number of carbon atoms in the first *n*-alkane standard, c + 1 is the number of carbon atoms in the second *n*-alkane standard, V_{Nx} is the net retention volume of compound *x*, V_{Nc} is the net retention volume of the first *n*-alkane standard, and $V_{N(c+1)}$ is the net retention of the second *n*-alkane standard.

Numerous investigators have attempted to calculate or predict *I* using physicochemical descriptors like boiling point, density, dipole moment, etc. Unfortunately, all of the correlations of retention indices and the various physicochemical properties are either relatively limited in scope or their application is restricted to a particular chemical class. Other attempts to predict retention indices for a wide range of molecular structures using molecular bond length, molecular bond angle, topological indices [1,2,4], or other molecular characteristic have not been successful. Most of these studies also were restricted to a particular class of molecules on a specific stationary liquid phase.

Despite all the attempts to predict Kováts indices, no realistic scheme with widespread application for different classes of compounds or for different polarities of stationary liquid phase is available.

Our research goal is to develop mathematical models to calculate the Kováts index at any temperature based on a calculated Henry's constant for a wide range of different classes of compounds on different polar and non-polar stationary liquid phases. In the present study, we report the calculation of Kováts indices of organic compounds on a squalane liquid phase strictly from molecular structure by a new computer program called SPARC.

SPARC

SPARC (SPARC Performs Automated Reasoning in Chemistry) is a prototype computer program being developed by the U.S. Environmental Protection Agency and the University of Georgia for the estimation of chemical reactivities and physical properties from molecular structure for a broad range of compounds using computational algorithms based on fundamental chemical structure theory. This new computer program will cost the user only few minutes of computer time, to produce data that are more accurate and have a broader scope than can be obtained with conventional estimation techniques.

SPARC computational approach

The computational approach in SPARC is based on fundamental chemical structure theory to estimate a variety of reactivity parameters [5] (*e.g.*, ionization pK_a, rate constants, etc.) and physical properties [6] (*e.g.*, vapor pressure, distribution coefficient, heat of vaporization, etc.).

The approach involves primarily deductive reasoning and is theory/mechanism oriented. The SPARC program couples Perturbed Molecular Orbital theory [7], which estimates charge distribution and polarizabilities of π electrons with Linear Free Energy relationships [8] to predict the molecular properties of an almost unlimited range of molecular species.

SPARC presently predicts, for a large number of nonpolymeric organic molecules, ionization pK_a [5] and numerous physical properties [6] such as distribution coefficients between immiscible solvents, solubilities, vapor pressure, etc. The ultimate goal for SPARC is to model the chemical and physical behavior of molecules to predict chemical reactivity parameters and physical properties for the universe of organic and inorganic molecules strictly from molecular structure.

SPARC physical models

For all physical processes (*e.g.*, vapor pressure, activity coefficient, partition coefficient, etc.), SPARC uses one master equation to calculate characteristic process parameters:

$$\Delta G_{process} = \Delta G_{interaction} + \Delta G_{monomer} \quad (2)$$

where $\Delta G_{monomer}$ describes entropy changes associated with mixing, volume changes, or changes in internal (vibrational, rotational) energies going from the initial state to the final state. $\Delta G_{monomer}$ depends only on the phase change involved and in the present application is presumed to depend only on solute/solvent volumes in each phase. $\Delta G_{interaction}$ describes the change

in the intermolecular interactions in the initial state and final state. For example, for Henry's constant the interaction term describes the difference in the intermolecular interactions in the gas phase *vs.* those in the liquid phase. The interactions in the liquid phase are modeled explicitly, interactions in the gas phase are ignored, and molecular interactions in the crystalline phase are extrapolated from the sub-cooled liquid state using the melting point.

The intermolecular interactions in the liquid phase are expressed as a summation over all the intramolecular interaction forces between the molecules:

$$\Delta G_{\text{interaction}} = \Delta G_{\text{dispersion}} + \Delta G_{\text{induction}} + \Delta G_{\text{dipole}} + \Delta G_{\text{H-bonding}} \quad (3)$$

Each of these interactions is expressed in terms of a limited set of molecular-level descriptors (density-based volume, molecular polarizability, molecular dipole, and H-bonding parameters) which in turn are calculated from molecular structure.

SPARC molecular descriptors

The computational approach for molecular-level descriptors is constitutive with the molecule in question being broken at each essential single bond and the property of interest being expressed as a linear combination of fragment contributions as

$$\chi^0(\text{molecule}) = \sum_i (\chi_i^0 - A_i) \quad (4)$$

where χ_i^0 are intrinsic fragment contributions (which in most cases are tabulated in SPARC databases) and A_i are adjustments relating to steric or electrometric perturbations from contiguous structural elements for the molecule in question and process model or medium involved. Both χ_i^0 and A_i are empirically trained either on direct measurements of the descriptor in question (*e.g.*, liquid density based molecular volume) or on a directly related property (*e.g.*, index of refraction, which can be related to polarizability) for which large reliable data sets exit.

Average molecular polarizability

In SPARC, fragment polarizability factored into atomic contributions, χ_j, and the polarizability of fragment, i, is expressed as

$$\overline{\alpha_i} = \frac{1}{N_i} \cdot \left[\sum_j \chi_j \right]^2 \quad (5)$$

where the summation is over all the atoms in fragment i, χ_j is the intrinsic atomic hybrid polarizability contribution, and N_i is the number of electrons in fragment i. The χ_j are empirically determined from measured polarizabilities and stored in the SPARC database (with exception of hydrogen which is calculated from the measured polarizability of H_2).

The average molecular polarizability, α^0, is expressed as

$$\overline{\alpha^0} = 4 \sum_i (\overline{\alpha_i} - A_i) \quad (6)$$

where α_i is the polarizability of fragment i and A_i are the adjustments for the molecule in question. The only adjustment, A_i, currently implemented in SPARC is a 10% reduction in α_i for hydrocarbon fragments with an attached polar group or atom. The partition of polarizability into atomic contributions enables estimates to be made of molecular polarizabilities for any given molecular structure. The molecular polarizability can be calculated within less than 1% for a wide range of molecules. Fig. 1 shows the observed *vs.* SPARC-calculated refractive index at 25°C for alkane, alkene and aromatic

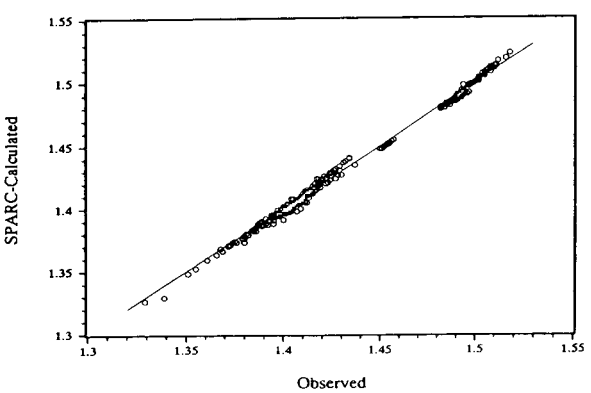

Fig. 1. Observed *vs.* SPARC-calculated refractive indices at 25°C.

systems. The root mean square (RMS) deviation for this set was found to be equal to $3 \cdot 10^{-3}$. Examples of the calculation of molecular polarizability and index of refraction are given in the appendix.

Molecular volume

The zero order density-based molecular volume is expressed as

$$V_{25}^{0} = \sum_{i} (V_i^{\text{frag}} - A_i) \tag{7}$$

where V^{frag} is the volume of the fragment and A_i is a correction to that volume based on both the number and size of fragments attached to it. The V^{frag} are determined empirically from the measured volume and then stored in the SPARC database. This zero order volume at 25°C is further adjusted for shrinkage resulting from dipole–dipole and H-bonding interactions:

$$V_{25} = V_{25}^{0} + A_{\text{d}} \frac{\sum_i D_i^2}{V_{25}^{0}} + A_{\text{HB}} \frac{\sum_i \alpha_i \sum_i \beta_i}{V_{25}^{0}} \tag{8}$$

where D_i is the dipole for the molecule, and α and β are the H-bonding parameters of potential proton donor and proton acceptor sites within the molecule, respectively.

The volume at temperature T is then expressed as a polynomial expansion in $(T-25)$ corrected as a function of H-bonding (HB), dipole (D) and polarizability (P) interactions as

$$V_T = V_{25}\left[1 + f(P, D, HB)\sum_n a_n (T-25)^n\right] \tag{9}$$

where a_n are variable parameters. The molecular volumes for a wide range of molecules can be calculated to better than 1%. Fig. 2 shows the observed versus SPARC-calculated density based molecular volumes for alkane, alkene, and aromatic systems. The RMS deviation was found to less than $4 \cdot 10^{-3}$. Examples of the calculation of molecular volume are given in the Appendix.

Solute–solvent interactions

Models for self interactions between like molecules and between solvent–solute molecules have been developed to calculate physical properties.

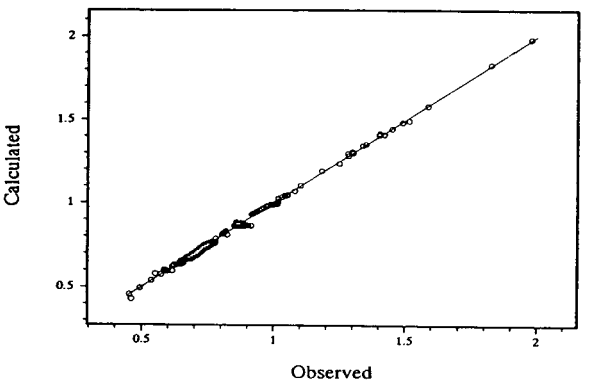

Fig. 2. Observed *vs.* SPARC-calculated densities at 25°C.

These interaction models build on the limited set of molecular-level descriptors (volume, polarizability, molecular dipole and H-bonding parameters) described above. These interaction models are dispersion, induction, dipole–dipole, and H-bonding. Dispersion interactions are present for all the molecules including non-polar molecules. Induction interactions are present between two molecules when at least one of them has a permanent dipole moment. Dipole–dipole interactions exist when both molecules have dipole moments. H-bonding interactions exist when $\alpha_i \cdot \beta_j$ or $\alpha_j \cdot \beta_i$ products are non-zero.

Dispersion interactions

In this paper we present our calculation of the Kováts retention indices for alkanes, alkenes and aromatics on a non-polar stationary phase squalane. For this reason, we shall not discuss the interaction mechanisms for dipoles and H-bonding. As such, this is a definitive test of our dispersion modeling.

Dispersion interactions occur between all molecules as a result of very rapidly varying dipoles formed between nuclei and electrons at zero-point motion of the molecules, acting upon the polarizability of other molecules to produce an induced dipole in the phase. The self interactions are expressed as

$$\Delta G_{ii}(\text{disp}) = \rho_{\text{disp}} (P_i^{\text{d}})^2 V_i \tag{10}$$

whereas solvent–solute interactions are expressed as

$$\Delta G_{ij}(\text{disp}) = \rho_{\text{disp}}\left(P_i^{\text{d}} - P_j^{\text{d}}\right)^2 V_i \quad (11)$$

$$P_i^{\text{d}}(\text{disp}) = \frac{\alpha_i + A_{\text{disp}}}{V_i} \quad (12)$$

where i and j designate the solute and squalane molecules respectively; P_i^{d} is the effective polarizability density of molecule i; ρ_{disp} is the susceptibility to dispersion; V_i and α_i are the molar volume and the average molecular polarizability described previously, respectively. $A_{(\text{disp})}$ is the polarizability adjustment for dispersion. $A_{(\text{disp})}$ differentiates the bulk polarizability α_i and the effective or microscopic polarizability that the molecule experiences at a point.

Dispersion is a short range interaction involving surface or near surface atoms and A_{disp} subtracts from the total polarizability, a portion of the contributions of sterically occluded atoms in the molecular lattice. Presently SPARC corrects for access judged to be less than afforded by a linear array of atoms (*i.e.*, for branched structures or rings small enough to prohibit intra penetration of the solvent).

Branched (ternary or quaternary) atoms in an alkane structure will lose a small part of their intrinsic molecular polarizability depending on the size and number of appended groups, and the proximity of other branched carbons. Similarly, carbons in rings may lose their intrinsic polarizability contributions depending on ring sizes and the presence of a ring appendage. Examples of the calculation of effective polarizability are given in the appendix.

Activity coefficient model

For a solute, i, in a liquid phase, j, at infinite dilution, SPARC expresses the activity coefficient as

$$-RT\ \log \gamma_{ij} = \Delta G_{\text{interactions}} + \Delta G_{\text{monomer}} \quad (13)$$

For the hydrocarbons in this study, the activity coefficient is given as

$$-RT\ \log \gamma_{ij}^{\infty} = \Delta G_{ij_{\text{disp}}} + RT\left(\log \frac{V_i}{V_j} + \frac{\left(1 - \frac{V_i}{V_j}\right)}{2.303}\right) \quad (14)$$

where the last term is the Flory–Huggins [9,10] excess entropy contributions of mixing in the liquid phase [beyond that of $\Delta G_{ij}(\text{disp})$] of placing a solute molecule in the solvent. When the solute and solvent have the same volume, the Flory–Huggins term will go to zero. Table I shows the observed *vs.* SPARC-calculated activity coefficients in squalane. It should be noted that the negative log values are a consequence of the large Flory–Huggins contributions. See the Appendix for sample calculations.

Vapor pressure model

The vapor pressure P_i of a solute, i, is expressed as

$$-2.303\ RT\ \log P_i = \Delta G_{i_{\text{disp}}} - 2.303\ RT(\log T + C) \quad (15)$$

where $RT(\log(T) + C)$ describes the change in the entropic contributions [14] associated with the volume changes between the liquid and the gas phases. Fig. 3 shows the observed *vs.* the SPARC-calculated values for the vapor pressure

TABLE I

OBSERVED *vs.* SPARC-CALCULATED VALUES FOR THE log ACTIVITY COEFFICIENT IN SQUALANE

Molecule	Activity coefficient	
	Obs.	Calc.
Pentane	−0.24	−0.20
Hexane	−0.19	−0.18
Heptane	−0.15	−0.16
Octane	−0.15	−0.15
Nonane	−0.17	−0.14
2-Methylpentane	−0.19	−0.16
2,4-Dimethylpentane	−0.14	−0.13
2,5-Dimethylhexane	−0.11	−0.12
2,3,4-Trimethylpentane	−0.17	−0.14
Cyclohexane	−0.28	−0.30
Ethylcyclohexane	−0.23	−0.22
Benzene	–	−0.15
Toluene	–	−0.16
1,3-Dimethylbenzene	–	−0.14
1,4-Dimethylbenzene	–	−0.14
1,3,5-Trimethylbenzene	–	−0.11

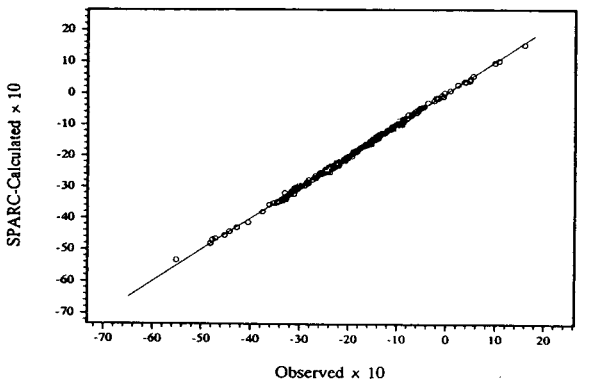

Fig. 3. Observed *vs.* calculated values for the vapor pressures at 25°C.

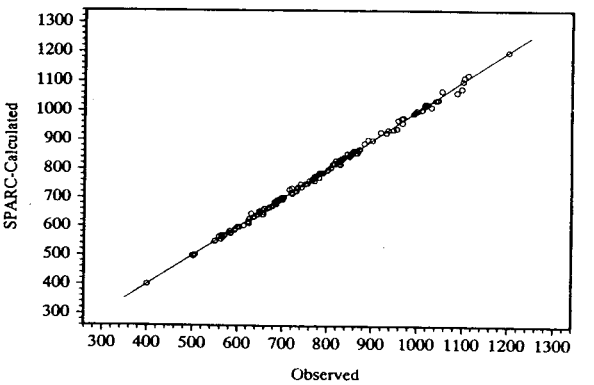

Fig. 4. Observed *vs.* calculated values for the retention indices at 25°C.

for various molecular structures at 25°C. The RMS deviation error for $\log P$ was 0.038.

See the Appendix for sample vapor pressure calculations.

Henry's constant

Henry's constant for a dilute solute, i, in a solvent, j, may be expressed as

$$H_x = P_i^0 \gamma_{ij}^{\infty} \tag{16}$$

where P_i^0 is the vapor pressure of pure solute i and γ_{ij}^{∞} is the activity coefficient of solute i in the squalane liquid phase at infinite dilution. SPARC vapor pressure and activity coefficient models are used to calculate Henry's constant for a solute in a squalane liquid phase.

Henry's constant can be related to the net retention volume, V_N, by

$$H_i = \frac{RT}{M} \cdot \frac{V_L}{V_N} \tag{17}$$

where M is the molecular weight of the solvent, and V_L is the volume of the stationary phase. Substituting in eqn. 1, we get

$$I = 100 \cdot \left(\frac{\log H_{Nx} - \log H_{Nz}}{\log H_{HN(z+1)} - \log H_{Nz}} + c \right) \tag{18}$$

where H_{Nx}, H_{Nz}, and $H_{N(z+1)}$ are Henry's constant for a compound x, first n-alkane standard, and second n-alkane standard, respectively.

Kováts indices at 25°C

Fig. 4 and Table II show the observed [11,12] versus the SPARC-calculated Kováts indices at 25°C. The RMS deviation was less than 7 Kováts units, a value that is close to the interlaboratory experimental error. We also calculated the Kováts index as a function of temperature using SPARC temperature dependence models discussed below.

SPARC calculates a physical property of interest at 25°C. In addition to the inherent temperature dependence described previously in eqns. 14 and 15 and the temperature dependence built in the volume calculator (eqn. 9), the susceptibility of dispersion at temperature T is modeled as a function of the polarizability density and the effective polarizability density. In effect, this describes the small temperature dependence of enthalpy. For temperature, an "activity-driven" process $\rho(t)$ is given by

$$\rho_T = \left[1 + \left(1 - \sum_n^5 a_n \left(\frac{298.15}{T} \right)^n \right) \cdot f(P, P') \right] \rho_{25} \tag{19}$$

where a_n are variable parameters. These parameters were inferred from boiling point measurements at 1, 10, 100, and 760 Torr (1 Torr = 133.322 Pa) for more than 400 compounds spanning a range of over 700°C. Table III and Fig. 5 show the observed *vs.* SPARC-calculated boiling point for wide range of molecules. The RMS deviation for this set was 3.4°C.

Based on these temperature dependent models we calculated the Kováts indices at 80°C as

TABLE II

OBSERVED *vs.* SPARC-CALCULATED RETENTION INDICES AT 25°C ON SQUALANE LIQUID PHASE

No.	Compound	Observed	Calculated	Difference
Kováts Bases				
1	*n*-Dodecane	1200.0	1200.0	0.0
2	*n*-Undecane	1100.0	1100.0	0.0
3	*n*-Decane	1000.0	1000.0	0.0
4	*n*-Nonane	900.0	900.0	0.0
5	*n*-Octane	800.0	800.0	0.0
6	*n*-Heptane	700.0	700.0	0.0
7	*n*-Hexane	600.0	600.0	0.0
8	*n*-Pentane	500.0	500.0	0.0
9	*n*-Butane	400.0	400.0	0.0
10	*n*-Propane	300.0	300.0	0.0
11	*n*-Ethane	200.0	200.0	0.0
12	*n*-Methane	100.0	100.0	0.0
Alkanes				
13	2,2-Dimethylbutane	534.8	525.1	9.7
14	2,3-Dimethylbutane	565.0	561.5	3.5
15	2-Methylpentane	569.4	569.0	0.4
16	3-Methylpentane	583.0	575.6	7.4
17	2,2,3-Trimethylbutane	636.2	634.8	1.4
18	3,3-Dimethylpentane	655.6	641.6	14.0
19	2-Methylhexane	666.2	663.0	3.2
20	2,3-Dimethylpentane	669.9	665.9	4.0
21	3-Methylhexane	675.2	670.2	5.0
22	3-Ethylpentane	684.7	678.4	6.2
23	2,2,4-Trimethylpentane	687.3	693.7	−6.4
24	2,2-Dimethylhexane	718.3	719.2	−0.9
25	2,5-Dimethylhexane	727.6	725.9	1.7
26	2,2,3-Trimethylpentane	733.2	738.4	−5.3
27	2,4-Dimethylhexane	730.8	732.9	−2.0
28	3,3-Dimethylhexane	740.0	737.0	3.0
29	2,3,4-Trimethylpentane	748.6	749.1	−0.5
30	2,3,3-Trimethypentane	753.9	750.8	3.0
31	2-Methyl-3-ethylpentane	757.9	760.1	−2.2
32	2,3-Dimethylhexane	758.5	761.4	−2.9
33	3-Methyl-3-ethylpentane	769.2	759.0	10.3
34	2-Methylheptane	764.6	762.5	2.1
35	3,4-Dimethylhexane	768.0	768.5	−0.4
36	4-Methylheptane	766.5	768.6	−2.1
37	2,2,4,4-Tetramethylpentane	769.7	775.7	−6.0
38	3-Ethylhexane	771.3	772.7	−1.4
39	3-Methylheptane	771.5	772.9	−1.4
40	2,2,5-Trimethylhexane	774.8	778.3	−3.5
41	2,2,4-Trimethylhexane	785.8	788.7	−2.9
42	2,3,5-Trimethylhexane	810.2	817.2	−7.0
43	2,2,3,4-Tetramethylpentane	814.1	821.1	−6.9
44	2,2,-Dimethyl-3-ethylpentane	817.1	830.5	−13.4
45	2,2-Dimethylheptane	814.7	817.5	−2.8
46	2,2,3-Trimethylhexane	817.7	828.7	−11.0

(*Continued on p. 276*)

TABLE II (*continued*)

No.	Compound	Observed	Calculated	Difference
47	2,4-Dimethylheptane	821.0	823.3	−2.3
48	4,4-Dimethylheptane	824.8	832.1	−7.3
49	2-Methyl-4-ethylhexane	823.4	824.2	−0.8
50	2,6-Dimethylheptane	826.6	826.3	0.3
51	2,4-Dimethyl-3-ethylpentane	832.1	833.7	−1.7
52	2,3,3-Trimethylhexane	835.2	840.2	−5.0
53	3,5-Dimethylheptane	832.5	835.8	−3.4
54	3,3-Dimethylheptane	833.7	836.5	−2.8
55	2,3,4-Trimethylhexane	842.6	851.9	−9.3
56	3,3,4-Trimethylhexane	847.8	843.3	4.4
57	3-Methyl-3-ethylhexane	849.4	848.8	0.6
58	2,3,3,4-Tetramethylpentane	852.1	850.6	1.5
59	3-Methyl-4-ethylhexane	851.1	855.6	−4.4
60	2,3-Dimethylheptane	853.6	858.7	−5.1
61	3,4-Dimethylheptane	855.7	861.9	−6.1
62	4-Ethylheptane	856.4	864.7	−8.3
63	2,3-Dimethyl-3-ethylpentane	865.7	856.1	9.6
64	4-Methyloctane	862.3	867.9	−5.6
65	2-Methyloctane	864.2	856.1	8.1
66	3,3-Diethylpentane	870.9	867.9	2.9
67	4-Ethylheptane	866.0	863.6	2.4
68	3-Methyloctane	869.7	870.0	−0.3
Alkenes				
69	*trans*-2-Pentene	501.0	496.3	4.7
70	4-Methyl-*trans*-2-pentene	561.9	555.4	6.5
71	*trans*-3-Hexene	593.4	591.2	2.2
72	3-Methyl-*trans*-2-pentene	612.6	603.9	8.7
73	2-Methyl-*trans*-3-hexene	648.0	655.4	−7.4
74	4-Methyl-*trans*-2-hexene	655.5	656.7	−1.2
75	3,3-Dimethyl-1-butene	505.2	501.4	3.8
76	4-Methyl-1-pentene	548.0	547.6	0.4
77	3-Methyl-1-pentene	549.4	549.9	−0.6
78	2,3-Dimethyl-1-butene	557.4	565.3	−7.9
79	2-Methyl-1-pentene	579.6	580.0	−0.4
80	1-Hexene	581.6	585.0	−3.3
81	2-Ethyl-1-pentene	592.0	586.7	5.4
82	4,4-Dimethyl-1-pentene	602.7	597.5	5.2
83	2-Methyl-2-pentene	598.0	598.5	−0.6
84	3,3-Dimethyl-1-pentene	623.5	617.7	5.8
85	2,3,3-Trimethyl-1-butene	625.6	627.4	−1.8
86	2,3-Dimethyl-2-butene	624.4	611.0	13.4
87	3,4-Dimethyl-1-pentene	634.6	632.6	2.0
88	3-Methyl-1-hexene	643.5	641.5	2.0
89	3-Ethyl-1-pentene	645.0	642.7	2.3
90	2,3-Dimethyl-1-pentene	648.1	652.2	−4.1
91	5-Methyl-1-hexene	648.8	647.2	1.6
92	4-Methyl-1-hexene	656.5	649.2	7.2
93	2-Methyl-1-hexene	677.5	674.7	2.8
94	1-Heptene	681.3	686.0	−4.7
95	2-Ethyl-1-pentene	681.7	679.2	2.6
96	2-Methyl-2-hexene	692.0	691.5	0.6

TABLE II (*continued*)

No.	Compound	Observed	Calculated	Difference
97	3-Ethyl-2-pentene	695.9	701.1	−5.1
98	2,3-Dimethyl-2-pentene	701.9	702.7	−0.7
99	2,4,4-Trimethyl-2-pentene	713.9	729.7	−15.8
100	1-Octene	780.3	788.3	−8.0
101	1-Nonene	881.2	888.9	−7.8
102	3-*trans*-Heptene	687.0	688.9	−1.9
103	2-*trans*-Heptene	698.7	693.5	5.2
104	4-*trans*-Octene	783.0	786.1	−3.1
105	3-*trans*-Octene	789.0	787.8	1.2
106	2-*trans*-Octene	798.6	794.8	3.8
Aromatics				
107	Benzene	629.9	645.7	−15.8
108	Tolune	739.1	748.7	−9.6
109	Ethylbenzene	828.2	835.7	−7.5
110	*p*-Xylene	842.5	854.6	−12.2
111	*m*-Xylene	845.7	846.9	−1.2
112	*o*-Xylene	862.7	856.4	6.3
113	Isopropylbenzene	889.5	902.5	−12.9
114	*n*-Propylbenzene	917.8	927.2	−9.5
115	1-Methyl-3-ethylbenzene	930.2	925.4	4.7
116	1-Methyl-4-ethylbenzene	934.4	934.5	−0.1
117	1-Methyl-2-ethylbenzene	946.1	935.7	10.4
118	1,3,5-Trimethylbenzene	953.1	939.1	14.1
119	*tert*-Butylbenzene	956.5	968.3	−11.8
120	*iso*-Butylbenzene	963.7	974.6	−10.9
121	1,2,4-Trimethylbenzene	965.9	959.6	6.3
122	*sec*-Butylbenzene	967.4	977.3	−9.9
123	1-Methyl-2-isopropylbenzene	994.6	996.2	−1.6
124	1-Methyl-3-isopropylbenzene	991.4	990.9	0.5
125	1-Methyl-4-isopropylbenzene	996.8	1001.6	−4.8
126	1,3-Dimethylbenzene	1009.4	1004.4	5.0
127	1-Methyl-4-*n*-propylbenzene	1015.7	1024.4	−8.7
128	1-Methyl-3-*n*-propylbenzene	1014.7	1015.6	−0.9
129	1,4-Diethylbenzene	1017.8	1020.3	−2.5
130	*n*-Butylbenzene	1018.5	1022.6	−4.1
131	1-Methyl-2-*n*-propylbenzene	1022.8	1023.0	−0.2
132	1,3-Dimethyl-5-ethylbenzene	1029.7	1013.4	16.3
133	1,4-Dimethyl-2-ethylbenzene	1039.3	1035.9	3.5
134	1,2-Dimethyl-4-ethylbenzene	1044.9	1037.6	7.3
135	1,3-Dimethyl-4-ethylbenzene	1044.1	1036.3	7.8
136	1-Methyl-4-*tert*-Butylbenzene	1053.1	1067.7	−14.6
137	1,2,3,5-Tetramethylbenzene	1086.4	1062.2	24.2
138	1,2,3,4-Tetramethylbenzene	1097.0	1074.8	22.2
139	1-Methyl-4-*n*-propylbenzene	1102.1	1111.7	−9.6
140	*n*-Pentylbenzene	1110.6	1121.2	−10.6
Cycloalkanes				
141	Cyclopentane	562.4	568.8	−6.4
142	Methylcyclopentane	624.6	625.7	−1.2

(*Continued on p. 278*)

TABLE II (*continued*)

No.	Compound	Observed	Calculated	Difference
143	1,1-Dimethylcyclopentane	669.3	668.5	0.8
144	1-*trans*-3-Dimethylcyclopentane	682.1	690.0	−7.9
145	1-*trans*-2-Dimethylcyclopentane	685.3	681.0	5.3
146	Cyclohexane	658.3	663.2	−4.9
147	1,1,3-Trimethylcyclopentane	718.9	734.4	−15.5
148	Methylcyclohexane	719.9	714.2	5.7
149	Ethylcyclopentane	729.3	723.2	6.1
150	1,1-Dimethylcyclohexane	779.8	771.3	8.5
151	1-*trans*-4-Dimethylcyclohexane	780.0	771.2	8.8
152	1-Methyl-2-*trans*-ethylcyclopentane	788.4	786.3	2.1
153	Isopropylcyclopentane	806.1	805.3	0.8
154	Ethylcyclohexane	827.5	816.8	10.7
155	*n*-Propylcyclopentane	825.6	818.1	7.5
156	1,1,3-Trimethylcyclohexane	833.8	840.9	−7.1

shown in Fig. 6. The RMS deviation was less than 8 Kováts units.

Models for predicting the Kováts index for polar and non-polar molecules on different polarity liquid phases (*e.g.*, OV-101, SE-30 and PEG-20M) are under development [13].

APPENDIX

Sample calculations

The following calculations will demonstrate the SPARC approach to calculating bulk polarizability, liquid density based volume, refractive

TABLE III

OBSERVED *vs.* SPARC-CALCULATED BOILING POINTS AT DIFFERENT PRESSURES

Molecule	Pressure					
	760 Torr		100 Torr		1 Torr	
	Obs.	Calc.	Obs.	Calc.	Obs.	Calc.
Pentane	36.1	36.6	−12.6	−12.6	−76.6	−76.3
Hexane	68.7	69.0	15.8	15.3	−54.0	−55.3
Heptane	98.4	99.0	41.8	41.8	−33.2	−35.2
Octane	125.7	126.8	65.7	66.8	−14.9	−15.7
Nonane	150.8	152.6	87.9	90.6	3.60	3.00
2-Methylpentane	60.3	55.8	8.10	5.00	−6.00	−6.40
2,4-Dimethylpentane	80.5	76.4	25.4	23.4	−4.70	−5.0
2,5-Dimethylhexane	109.1	106.0	50.5	45.5	−26.7	−31.4
2,3,4-Trimethylhexane	139.0	137.0	76.0	76.0	−7.00	−9.00
Cyclohexane	80.7	81.9	25.5	27.2	−47.0	−44.5
Ethylcyclohexane	131.8	128.7	69.0	67.8	−14.4	−14.7
Benzene	80.1	85.8	26.0	30.2	−45.0	−41.9
Toluene	110.6	113.5	51.9	54.5	−26.1	−23.1
1,3-dimethylbenzene	139.1	138.5	76.8	76.5	−7.2	−5.90
1,4-dimethylbenzene	138.4	140.3	75.9	78.1	−8.1	−5.0
1,3,5-trimethylbenzene	146.7	162.2	99.8	97.7	11.6	10.9

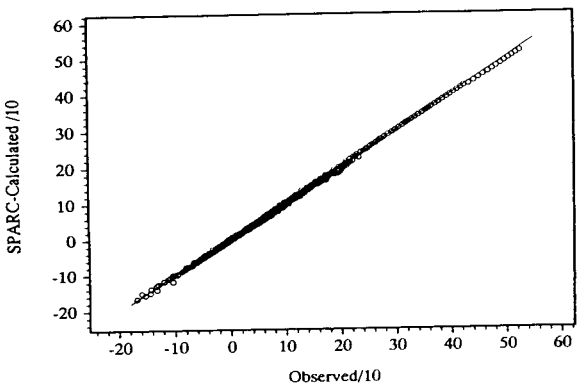

Fig. 5. Observed *vs.* SPARC-calculated values for the boiling points at 1, 10, 100 and 760 Torr.

index, effective molecular polarizability, vapor pressure and activity coefficient. Since the bulk of the molecules in this study are straight-chain and branched alkanes, the two molecules chosen for the sample calculations are *n*-pentane and 2,5-dimethylhexane.

Polarizability

The fragments for polarizability calculations are CH_x units for alkanes. Only two intrinsic atomic polarizabilities are needed, $\chi(\text{sp3–C}) = 1.25$ and $\chi(\text{H–C}) = 0.314$. From eqn. 5 α_i for the carbon is $(1.25 \cdot 1.25/6) = 0.260$ and α_i for each hydrogen is $(0.314 \cdot 0.314)/1 = 0.0986$. There are no corrections A_i (eqn. 6) for the alkanes since there are no connected polar groups. The bulk molecular polarizability for the alkanes, (C_nH_{2n+2}), from eqn. 6 can be written as $\alpha = 4 \cdot (n \cdot 0.260 + (2n+2) \cdot 0.0986)$ where the units are $Å^3$/molecule. For *n*-pentane this yields 9.94 and for 2,5-dimethylhexane the value is 15.43.

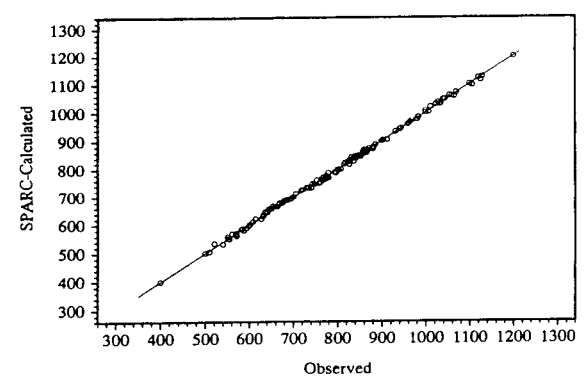

Fig. 6. Observed *vs.* SPARC-calculated values for the retention indices at 80°C.

Volume

For straight-chain and branched alkanes the fragment values V_{frag} in eqn. 7 are all that of $CH_x = 52.945$. The corrections A_i are due to the type, number and size of the substituents. For alkanes the type is always CH_x. The correction for this type is -19.2618. The correction for occluded volume from branching is 0 for branching <2, 3.31 for 2-branching and 8.42 for 3-branching. The size correction is 6.8 times the sum of the cone volumes [5].

n-pentane	V^{frag}	Subtr-type	Branch	Size	Frag-Total
C	52.945	-19.262	0	-6.8(0.113)	32.92
C	52.945	-19.262*2	3.3	-6.8(0.05+0.107)	16.66
C	52.945	-19.262*2	3.3	-6.8(0.091*2)	16.50
C	52.945	-19.262*2	3.3	-6.8(0.05+0.107)	16.66
C	52.945	-19.262	0	-6.8(0.113)	32.92
				Sum	115.6
				Obs	116.1
2,5 DMH					
C	52.945	-19.262	0	-6.8(0.213)	32.23
C	52.945	-19.262*3	8.4	-6.8(0.05*2+0.11)	2.16
C/	52.945	-19.262	0	-6.8(0.213)	32.23
C	52.945	-19.262*2	3.3	-6.8(0.131+0.126)	15.98
C	52.945	-19.262*2	3.3	-6.8(0.131+0.126)	15.98
C	52.945	-19.262*3	8.4	-6.8(0.05*2+0.11)	2.16
C/	52.945	-19.262	0	-6.8(0.213)	32.23
C	52.945	-19.262	0	-6.8(0.213)	32.23
				Sum	165.2
				Obs	166.1

Index of refraction

Index of refraction is a good way to check the polarizability density for the molecule. The polarizability and volume can be related to the index of refraction using the Lorentz–Lorenz equation. For our units of cm^3/mole for volume and $Å^3$/molecule for polarizability the Lorentz–Lorenz equation can be written as

$$\frac{n^2-1}{n^2+2} = \frac{4 \cdot \pi \cdot 0.6023\, P}{3\, V} \qquad \text{(A1)}$$

where n is the index of refraction, P is the molecular polarizability and V is the liquid density based volume. Eqn. A1 leads to a calculated index of refraction of 1.354 (obs 1.358) for *n*-pentane and a calculated index of refraction of 1.388 (obs 1.392) for 2,5-dimethylhexane.

Effective polarizability

Dispersion is a short range interaction involving surface or near-surface atoms and A_{disp} in eqn. 12 subtracts from the total polarizability, a portion of the contributions of sterically occluded atoms in the molecular lattice. Presently SPARC corrects for access judged to be less than afforded by a linear array of atoms. Branched (ternary or quaternary) atoms in an alkane structure will lose a small part of their intrinsic molecular polarizability depending on the size and number of appended groups, and the proximity of other branched carbons. For *n*-pentane there are no corrections so that the effective polarizability equals the calculated molecular polarizability of 9.94. For 2,5-dimethylhexane the polarizability of the 2 and 5 atoms are reduced by 1.72 times the sum of the sizes (see volume above) of the fragments attached to 2 and 5. Each atom is reduced by $1.72 \cdot (0.05 + 0.109 + 0.05) = 0.36$. The effective polarizability for 2,5-dimethylhexane is calculated to be $15.43 - 2 \cdot 1.72 \cdot (0.209) = 14.71$.

Vapor pressure

Once the molecular polarizabilty and volume are known we can use eqn. 10 to calculate the dispersion interactions. ϱ_{disp} is -2.571 (where this number has subsumed in it $-2.303 \cdot RT$) and the polarizability densities for *n*-pentane and 2,5-dimethylhexane are $9.94/115.6 = 0.086$ and $14.71/165.2 = 0.0891$, respectively. The dispersion contribution to the vapor pressure is calculated to be $-2.57 \cdot 0.086 \cdot 0.086 \cdot 115.6 = -2.20$ for *n*-pentane and $-2.57 \cdot 0.0891 \cdot 0.0891 \cdot 165.2 = -3.37$ for 2,5-dimethylhexane. The volume entropy terms $(\log(T) + C)$ are $\log(298) - 0.457 = 2.02$ at room temperature. Log (P) for *n*-pentane is then calculated to be $-2.20 + 2.02 = -0.18$. The observed vapor pressure for *n*-pentane is -0.17. Log(P) for 2,5-dimethylhexane is $-3.37 + 2.02 = -1.35$. The observed vapor pressure is -1.38.

Activity coefficient

In order to calculate the infinite dilution activity coefficient for *n*-pentane and 2,5-dimethylhexane in squalane we need the effective polarizability and volume for squalane. SPARC calculates the molecular polarizability of squalane to be 55.70, the effective polarizability to be 53.22 and the volume to be 530.0. The polarizability density of squalane is then calculated to be $53.22/530 = 0.10$. From eqn. 11 the dispersion contribution to the activity coefficient can be calculated. For *n*-pentane this is $-2.57 \cdot (0.086 - 0.10)^2 \cdot 115.6 = -0.06$ and for 2,5-dimethylhexane the value is $-2.57 \cdot (0.089 - 0.10)^2 \cdot 165.2 = -0.05$. The volume entropy terms from eqn. 15 are 0.26 and 0.17 for pentane and 2,5-dimethylhexane, respectively. The logs of the infinite dilution activity coefficients are $-(-0.06 + 0.26)$ or -0.20 and $-(-0.05 + 0.17)$ or -0.12 for *n*-pentane and 2,5-dimethylhexane, respectively.

REFERENCES

1 G. Tarjan, I. Timar, J.M. Takacs, S.Y. Meszaros, Sz. Nyiredy, M.V. Budahegyl, E.R. Lombosi and T.S. Lombosi, *J. Chromatogr.*, 271 (1982) 213.
2 J.K. Haken and M.B. Evans, *J. Chromatogr.*, 472 (1989) 93.
3 E.sz. Kováts, *Adv. Chrommatogr.*, 1 (1965) 31A.
4 L.S. Anker and P.C. Jurs, *Anal. Chem.*, 62 (1990) 2676.
5 S.W. Karickhoff, V.K. McDaniel, C.M. Melton, A.N. Vellino, D.E. Nute, L.A. Carreira, *Environ. Toxicol. Chem.*, 10 (1991) 1405.
6 S.W. Karickhoff, C.M. Melton, L.A. Carreira and S.H. Hilal, in preparation.
7 L.P. Hammett, *Physical Organic Chemistry*, McGraw Hill, New York, NY, 1970, 2nd ed.
8 M.J.S. Dewar, R.C. Dougherty, *The PMO Theory of Organic Chemistry*, Plenum Press, 1975, New York, NY.
9 P.J. Flory, *J. Chem. Phys.*, 10 (1942) 51.
10 M.L. Huggins, *J. Am. Chem. Soc.*, 64 (1942) 1712.
11 N. Dimov, *J. Chromatogr.*, 347 (1985) 366.
12 D. Papazova and N. Dimov, *J. Chromatogr.*, 356 (1986) 320.
13 S.H. Hilal, L.A. Carreira, S.W. Karickhoff and C.M. Melton, in preparation.
14 K.A. Sharp, A. Nicholls, R. Friedman and B. Honig, *Biochemistry*, 30 (1991) 9686.

Journal of Chromatography A, 662 (1994) 281–292
Elsevier Science Publishers B.V., Amsterdam

CHROM. 25 679

Indentification and quantification of mono-, di- and trihydroxybenzenes (phenols) at trace concentrations in seawater by aqueous acetylation and gas chromatographic–mass spectrometric analysis

Thomas J. Boyd*

0218, Marine Life Research Group, Scripps Institution of Oceanography, University of California, San Diego, La Jolla, CA 92093-0218 (USA)

(First received August 2nd, 1993; revised manuscript received October 22nd, 1993)

ABSTRACT

A method is described that uses aqueous acetylation with acetic anhydride, solid-phase extraction (SPE) and concentration, and gas chromatographic–mass spectrometric (GC–MS) analysis to identify and quantify mono-, di- and trihydroxybenzenes (phenols) at low concentrations in marine and waste waters. Phenolic compounds in water samples were buffered with $NaHCO_3$ and directly acetylated with acetic anhydride. Phenol acetates were then extracted using C_{18} SPE columns. The columns were eluted and the phenol acetates concentrated and analyzed by GC–MS. Detection of phenols in the ng l^{-1} concentration range can be obtained with 500 ml of sample. A large volume extraction setup is described from which detection limits in the upper pg l^{-1} range may be obtained. The method was applicable to a wide range of phenolic compounds but was not suitable for nitrophenols. Water samples from several coastal environments and wastewater treatment facilities were analyzed for phenols using this method. Phenol, cresols and catechols were the most common phenolic compounds identified. Concentrations ranged from 2.5 to 370 ng l^{-1} for these phenols in seawater sampled in San Diego Bay, in the vicinity of White's Point outfall off San Pedro (Los Angeles area) and outfalls off the Northern coast of California near Eureka.

INTRODUCTION

Phenolic materials are present in many environments. Their ubiquitous presence in industrial and municipal wastewaters, groundwaters, sediments, and soils [1–9] has made them of interest to chemists, waste managers, and public agencies such as the United States Environmental Protection Agency (EPA). Phenolic materials are also present in natural samples and have been identified in such environments as streams, lakes [10,11], estuaries [7,12], freshwater and marine sediments [13–17] and marine microlayers [18,19]. Phenolic moieties are also found in marine algae [20–22] and in humic materials from terrestrial sources [23,24].

Many analytical approaches have been used for the identification and quantification of phenolic materials under various environmental conditions. The EPA has approved several analytical methods for the analyses of these materials [25,26]. In addition, there is considerable interest from researchers and managers to devise new, definitive methods for phenolic analysis [27]. Most commonly, phenols are extracted from water samples by liquid extraction and quantified by gas chromatography (GC) or liquid chromatography (LC) [28–30]. Several colorimetric analyses also exist. Generally, most involve derivatizing the phenolic moiety with a

* Present address: Ocean Sciences Division, Room 725, National Science Foundation, 4201 Wilson Boulevard, Arlington, VA 22230, USA.

0021-9673/94/$07.00
SSDI 0021-9673(93)E1125-J

chromophoric substance for bulk colorimetric or LC separation and determination [31–33].

Derivatization of phenols, besides the potential to introduce chromophores, may also be used to introduce a halogenated group in the native molecule. Derivatized phenols thus become analyzable by extremely sensitive GC with electron-capture detection (ECD) [34,35]. Use of a derivatizer, such as a silanizing agent, makes phenols less polar, greatly increasing extraction efficiency [27,29]. Alteration of the phenolic molecule by acetylation may optimize GC analysis for a wide range of phenols on standard non-polar columns by affecting retention characteristics.

Recently, acetic anhydride has been used as a derivatizing agent for extracted phenols [30,34,36] and also for aqueous solutions [1,37,38]. Use of excess buffer and controlled conditions are essential for successful acetylation. Once acetylated, however, extraction efficiency of phenols is increased substantially. Use of acetic anhydride has several advantages that are exploited in this study: (1) addition of the acetyl group decreases the polarity of the phenolic analyte allowing for greater extraction efficiency [37], especially from di- and trihydroxybenzenes which are generally not extractable from aqueous samples by standard methods, (2) low cost of buffer salts and acetic anhydride makes the derivatization of large water samples economically feasible, (3) phenolic acetate formed by derivatization has very similar mass spectral characteristics to the original underivatized phenol, resulting in more successful spectral library searches, and (4) a characteristic peak 42 mass units higher than the parent phenol molecular ion peak may be used to identify an acetylated substance thus serving as a qualitative indicator of the phenolic moiety. Fragments showing a characteristic loss of ketene $M^+ - 42$, also may confirm the molecule as a phenol acetate.

Phenols in the marine environment are less well characterized than their terrestrial counterparts. Phenolic materials from terrestrial sources entering the ocean are subject to considerable physical, chemical and biological influence. Rapid dilution [39], photochemical bleaching [40–42], and possibly biodegradation [43–45] may lead to extremely low concentrations in coastal environments. The need to identify and quantitate phenolic and other toxic materials in marine waters has been set as a national objective and the development of new and improved techniques for its accomplishment are called for in the Federal Plan for Ocean Pollution Research, Development, and Monitoring [46]. This study was undertaken to develop a relatively rapid, accurate and reliable method for the determination of phenolic materials at extremely low concentrations in coastal marine environments.

EXPERIMENTAL

Chromatographic apparatus and scintillation counter

The gas chromatograph–mass spectrometer was a Hewlett-Packard 5988 Chemstation with a 7673A autosampler. The HPLC apparatus used to purify [2,6-^{3}H]*p*-cresol consisted of a Perkin-Elmer Series 410 LC pump, Wescan Model 272 UV absorbance detector (Japan Spectroscopic Co.), and a Hewlett-Packard Model 3390A integrator. The scintillation counter used in the purification of [2,6-^{3}H]*p*-cresol was a Beckman Model LS1801 (Beckman Instruments, Irvine, CA, USA).

Chromatographic conditions

A glass capillary AT-35 (65% methyl/35% phenyl) column, 25 m × 0.25 mm I.D. (Alltech, Deerfield, IL, USA) was used for all samples. A sample volume of 3 μl was used for each injection. The operating conditions were: column temperature: 40°C, hold 6 min; 40 to 275°C at 5°C min^{-1}, hold 5 min; injector port temperature, 190°C; linear velocity: 40 cm s^{-1} (set at 150°C), helium; mass spectrum with electron impact source tuned with perfluorotributylamine (PFTBA); source temperature, 180°C; scan 50–500 u with 100 abundance threshold; splitless injection. A 1 g l^{-1} solution of butylated hydroxytoluene was used as an external standard for day-to-day calibration of the instrument.

For HPLC purification of [2,6-^{3}H]*p*-cresol, a Waters Nova-Pak C_{18}, 4 μm particles, 150 mm × 3.9 mm steel column was used. The operating conditions were: 0 min, water (1% acetic acid)–

MeOH (1% acetic acid) (95:5) hold 2 min; 2–5 min ramp to water–MeOH (65:35), hold 10 min; detector set to 280 nm absorbance. Purified [2,6-^{3}H]*p*-cresol was analyzed in the scintillation counter and the specific activity (11 Ci mmol^{-1}) was calculated.

Large-volume extraction apparatus

For sample volumes over 1 l, a large-volume extraction apparatus consisting of the following components was used: A 19-l stainless-steel sample container (Cornelius, Anoka, MN, USA) fitted with PTFE O-rings and seals and stainless-steel sparger element, was employed to hold water samples. The container was sparged with nitrogen gas run through a Hewlett-Packard Model 19046A gas purifier within 1 h of sample collection. Containers were sparged soon after collection in an effort to inhibit aerobic microbial activity, particularly utilization of phenolic analytes. In addition, $NaHCO_3$ was also added soon after collection in an effort to alter the collected sample environment. The extra sodium load (0.35 *M* addition) was assumed to inhibit normal microbial activity. A PTFE hose connected to the stainless-steel container carried water flow through a 147 mm 0.3 μm precombusted glass fiber filter (Gelman Sciences, Ann Arbor, MI, USA) in a Millipore filter holder (Millipore, Bedford, MA, USA). Flow continued through a PTFE hose to a PTFE manifold and hose assembly and then into four pre-packed C_{18} solid-phase extraction (SPE) columns (see *Preparation of SPE columns* below). The columns were secured to a vacuum manifold through which extracted water flowed into a large (19 l) carboy trap (Corning, East Brunswick, NJ, USA).

Preparation of SPE columns

For sample volumes of 1 l or less, commercially available Prep-Sep C_{18} SPE columns (Fisher Scientific, Tustin, CA, USA) were used for extraction. For larger sample volumes, columns were constructed from 60-ml polypropylene syringes. Each syringe was fitted with a 20-μm pore frit (Varian, Harbor City, CA, USA) and loaded with 5 g of 40 μm C_{18} sorbent (Analytichem, Harbor City, CA, USA). The sorbent was capped with another frit. Columns were soaked for several minutes with Optima-grade methanol, vacuumed dry and immediately soaked with HPLC grade water prior to use.

Reagents

NaCl (pre-combusted at 550°C) was used to prepare 3 *M* artificial seawater (ASW). ASW was prepared freshly prior to use in preparations of standards. Water used in the preparation of all standards was HPLC grade from a Milli-Q purification apparatus (Millipore). Acetic anhydride, methanol, 2,7-dihydroxynaphthalene, $NaHCO_3$ and anhydrous Na_2SO_4 were of HPLC grade and purchased from Fisher Scientific. Butylated hydroxytoluene was purchased from Sigma (St. Louis, MO, USA). Na_2SO_4, used for drying organic extracts was pre-baked at 550°C. $NaHCO_3$ was cleaned by extraction with 35 volumes of CH_2Cl_2 (Fisher Scientific) in a Soxhlet extractor prior to use. Scintillation cocktail used was Ecoscint obtained from National Diagnostics, Manville, NJ, USA.

Preparation of standard solutions

Stock solutions of 1 g l^{-1} phenol (Mallincrodt, St. Louis, MO, USA), *o*-cresol, *m*-cresol, catechol, phloroglucinol (Sigma), *p*-cresol, 3-methylcatechol and 4-methylcatechol (Phaltz & Bauer, Waterbury, CT, USA) were prepared in methanol. A commercial standard containing 2,4,6-trichlorophenol, 4-chloro-3-methylphenol, 2-chlorophenol, 2,4-dichlorophenol, 2,4-dimethylphenol, 2-nitrophenol, 4-nitrophenol, 2,4-dinitrophenol and pentachlorophenol at concentrations of 0.5–2.5 g l^{-1} (Supelco, Bellefonte, PA, USA) was also used. These stock solutions were diluted in ASW to give the final standard concentrations listed in the following sections.

Preparation of standard test solutions

Two series of phenolic standard solutions were prepared as follows: one, in which the sample volume was kept constant and concentration was varied, and one, in which sample concentration was kept constant and the sample volume was varied. For constant-volume (0.50 l) standards, test solutions were made using ASW and phenol stock solutions to concentrations of 0.500, 1.00, 2.50, 5.00 and 10.0 μg l^{-1} for *o*-cresol, *m*-cresol, *p*-cresol, catechol, 3-methylcatechol, 4-methylcatechol and phloroglucinol; 0.250, 0.500, 1.25,

2.50 and 5.00 $\mu g\ l^{-1}$ for phenol, 2-chlorophenol, 2-nitrophenol, 2,4-dimethylphenol and 2,4-dichlorophenol; 1.25, 2.50, 6.25, 12.5 and 25.0 $\mu g\ l^{-1}$ for 4-chloro-3-methlyphenol, 4-nitrophenol and pentachlorophenol; and 0.750, 1.50, 3.75, 7.50 and 15.0 $\mu g\ l^{-1}$ for 2,4,6-trichlorophenol and 2,4-dinitrophenol.

For constant-concentration standards at 1.00 $\mu g\ l^{-1}$ for *o*-cresol, *m*-cresol, *p*-cresol, catechol, 3-methylcatechol, 4-methylcatechol and phloroglucinol; 0.500 $\mu g\ l^{-1}$ for phenol, 2-chlorophenol, 2-nitrophenol, 2,4-dimethylphenol and 2,4-dichlorophenol; 2.50 $\mu g\ l^{-1}$ for 4-chloro-3-methlyphenol, 4-nitrophenol and pentachlorophenol; and 1.50 $\mu g\ l^{-1}$ for 2,4,6-trichlorophenol and 2,4-dinitrophenol, solutions were made up using ASW to volumes of 0.50, 1, 5 and 18 l.

Derivatization, extraction and solvent evaporation

Phenol acetates were prepared using the following protocol:

Standards of 500 ml and 1 l. Standard phenolic solutions and blanks were prepared with ASW and stored in a 4-l flask, 10 μg of 2,7-dihydroxynaphthalene were added per liter as an internal standard and 8 g of $NaHCO_3$ buffer were added and allowed to dissolve. Two 1-ml aliquots of acetic anhydride were added per liter with vigorous shaking and allowed to react for 2 min. After the reaction, the water sample was poured through Prep-Sep columns under vacuum. The columns were dried with purified nitrogen gas and eluted with 1 ml of ethyl acetate and two 1-ml aliquots of CH_2Cl_2. The extracts were combined, dried over anhydrous sodium sulfate, placed in a conical centrifuge tube, and the volume gently reduced to 100 μl under a vortical stream of purified nitrogen gas. All standards were run in triplicate

Standards of 5 l and 18 l. Standard phenolic solutions and blanks were prepared with ASW and stored in 19-l stainless-steel vessels. Both 10 μg of 2,7-dihydroxynaphthalene as an internal standard and 8 g of $NaHCO_3$ were added per liter as above. Two 1-ml aliquots of acetic anhydride were added per liter with vigorous shaking and allowed to react for 2 min. After the reaction, the sample vessel was pressurized to approximately 130 kPa to force sample through 60-ml C_{18} extraction columns. In addition, the columns were seated in a vacuum manifold to facilitate sample flow. The columns were then dried with purified nitrogen gas and eluted with 5 ml of ethyl acetate followed by two 5-ml aliquots of CH_2Cl_2. The extracts were combined, dried over anhydrous sodium sulfate, and reduced in volume as above. Standards were run in triplicate.

Collection of natural seawater and wastewater samples

Water samples were collected with a 30-l Niskin bottle (White's Point), 4-l amber solvent bottles (Hyperion and JWPCP effluents), or in the 19-l stainless-steel vessels (all other). See Table III for summary of sampling locations and depths. Internal standard, $NaHCO_3$ and acetic anhydride were added as above. The sample vessel was then pressurized to approximately 130 kPa to force sample water through a 0.3-μm pre-combusted glass fiber filter and 60-ml C_{18} extraction columns. The columns were seated in a vacuum manifold as with standards. The columns were then dried and eluted as above. Extracts were reduced to 500 μl.

Calculation of extraction efficiency for p-cresol

[2,6-^{3}H]*p*-Cresol was obtained from Amersham (Arlington Heights, IL, USA), purified by HPLC and added at 500 ng l^{-1} to each of 6 250-ml flasks containing 75 ml of natural seawater collected of the Scripps Institution of Oceanography pier in La Jolla, CA, USA. Three flasks were reacted with acetic anhydride as above to acetylate *p*-cresol. Samples were filtered through 0.3-μm Millipore 25 mm type PH filters to remove cells and the filtrate poured through C_{18} Prep-Sep columns. Effluent from the columns was collected and 1 ml was transferred to scintillation vials. Columns were eluted with 1 ml of MeOH and the eluent transferred to a scintillation vial. Filters, flowthrough water, and column eluent were counted for ^{3}H dpm. Percent efficiency (E) was calculated as:

$$\%E = 1 - \frac{\mathrm{dpm}_{\mathrm{flowthrough}}}{(\mathrm{dpm}_{\mathrm{total}} - \mathrm{dpm}_{\mathrm{filter}})} \times 100\%$$

RESULTS AND DISCUSSION

Gas chromatography–mass spectroscopy

The separation of standards of analyzed phenolic materials is shown in Fig. 1. Shown is the mass spectrum for catechol diacetate. Table I shows characteristic GC–MS data for phenolic standards. Peaks were identified by mass spectral conformational analysis as acetate esters. The molecular ion for catechol is 110 and Fig. 1 shows the addition of two 42 mass unit peaks, 152 and 194. The acetylation allows for identification of phenols based not only on the native mass spectrum (in this case 110 and lower), but also on the addition of the 42 mass unit peak additions. With standards of 0.50 l and varied concentrations, peak area values for each phenolic standard were plotted as a function of concentration. For constant concentration standards, peak area values were plotted as a function of volume. Fig. 2 shows examples for *o*-cresol, *m*-cresol and *p*-cresol. Nitrophenols such as 2-nitrophenol, 4-nitrophenol and 2,4-dinitrophenol were not adequately derivatized and extracted by this method. The acidity of the $-NO_2$ group may hinder extraction efficiency. For this reason, the nitrophenols were not included in the analysis. During preliminary de-

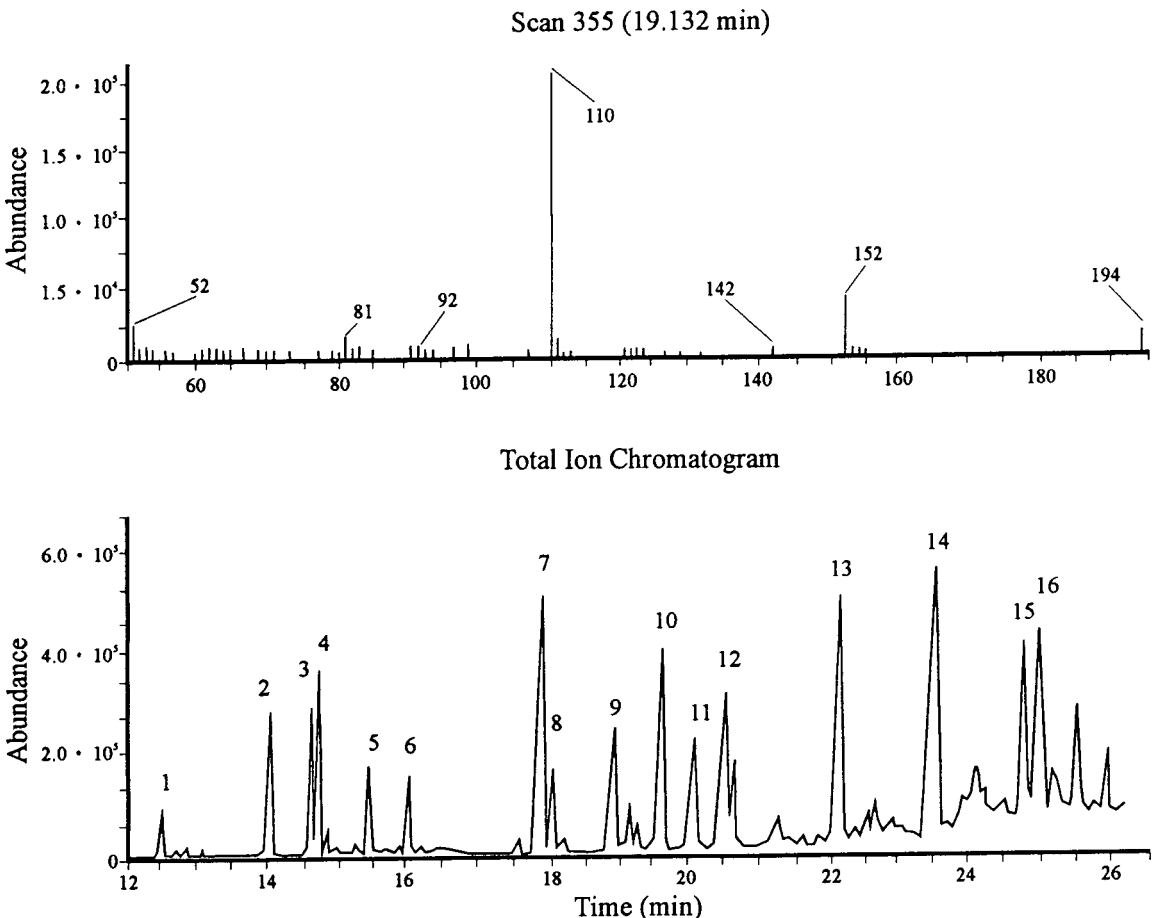

Fig. 1. Total ion chromatogram of standard solution of phenols. Illustrated is scan 355 (19.132 min), mass spectrum for catechol diacetate. Identified phenols (as acetate esters) are: 1 = phenol; 2 = *o*-cresol; 3 = *m*-cresol; 4 = *p*-cresol; 5 = 2-chlorophenol; 6 = 2,4-dimethylphenol; 7 = 4-chloro-3-methylphenol; 8 = 2,4-dichlorophenol; 9 = catechol; 10 = 2,4,6-trichlorophenol; 11 = 3-methylcatechol; 12 = 4-methylcatechol; 13 = internal standard; 14 = diethylphthalate (contaminant); 15 = pentachlorophenol; 16 = phloroglucinol.

TABLE I

CHARACTERISTIC IONS AND RELATIVE ABUNDANCES FOR ACETYLATED PHENOLS

Substrate	Ion (abundance)
Phenol	51 (4), 65 (13), 66 (16), 94 (100), 95 (6), 136 (12)
o-Cresol	51 (10), 77 (22), 79 (13), 107 (40), 108 (100), 150 (14)
m-Cresol	51 (6), 77 (18), 79 (13), 107 (45), 108 (100), 150 (13)
p-Cresol	51 (9), 77 (18), 79 (10), 107 (54), 108 (100), 150 (11)
2-Chlorophenol	63 (14), 64 (11), 73 (11), 128 (100), 130 (33), 170 (11)
2,4-Dimethylphenol	77 (17), 91 (15), 107 (57), 121 (22), 122 (100), 164 (10)
4-Chloro-3-methylphenol	51 (14), 77 (24), 107 (52), 142 (100), 144 (29), 184 (10)
2,4-Dichlorophenol	63 (22), 133 (10), 162 (100), 164 (62), 166 (10), 204 (8)
Catechol	52 (8), 81 (4), 110 (100), 111 (6), 152 (17), 194 (3)
2,4,6-Trichlorophenol	97 (26), 167 (11), 196 (100), 198 (98), 238 (10), 240 (10)
3-Methylcatechol	78 (6), 123 (7), 124 (100), 125 (7), 166 (14), 208 (3)
4-Methylcatechol	78 (6), 123 (8), 124 (100), 125 (7), 166 (13), 208 (3)
Pentachlorophenol	164 (20), 264 (64), 266 (100), 268 (62), 270 (20), 308 (13)
Phloroglucinol	97 (5), 126 (100), 127 (6), 168 (28), 210 (13), 252 (4)

velopment of this method, standard solutions were reduced to pH 2 with HCl prior to extraction in an effort to protonate acidic groups and bolster extraction efficiency. Nitrophenols are able to be resolved, although not quantitatively, over the concentration range used for method development. Severe bubble formation and possible foaming over and loss of the buffered seawater sample may occur with acid addition. Therefore, this manipulation was not incorporated into the final method.

Statistical parameters for the analysis of standards are shown in Table II. The retention time index was calculated by dividing the retention time of the standard phenolic acetate by the retention time of the external standard, butylated hydroxytoluene. A molecular ion peak percent for the parent phenol was calculated by dividing the abundance of the parent molecular ion by the total peak area for all of the standards. The values were averaged and the mean multiplied by 100%. This value was calculated for use with natural seawater extracts which, in some cases, contained compounds that co-eluted within the same retention time period as the analytes. Linear regression analyses were conducted for peak areas plotted against both varying concentration and varying volume (Fig. 2).

Based on analyses of the GC–MS data, the following general formula was used to calculate concentration (x) of phenolics in samples of unknown phenolic composition and concentration:

$$zv^{-1}ynm^{-1}l_{orig}{}^{-1}V_{fin} = x \pm s\%$$

where z = correction value for external and internal standards, v = correction value for the use of large volume samples calculated from the deviation between theoretical and actual slope values for peak area *vs.* volume extracted plots (see Fig. 2), y = parent phenol molecular ion peak area, n = parent phenol molecular ion peak percent, m = slope normalized to 1 l of sample (see Fig. 2), l_{orig} = original sample volume, V_{fin} = final extract volume (in μl) and s = percent error calculated by the addition of regression coefficients $(1-r)_{concentration}$ and $(1-r)_{volume}$. See linear regression equations in Fig. 2. Table II lists the standard parameters outlined above for standard compounds analyzed in this study.

Analysis of phenolics in natural samples

Water samples were taken from several coastal locations off California (see Table III). In addition, composite effluent from Hyperion and the Joint Water Pollution Control Plant were analyzed. Results are summarized in Table III. Putative identifications are based primarily on mass spectral evidence. Unknown peak spectra

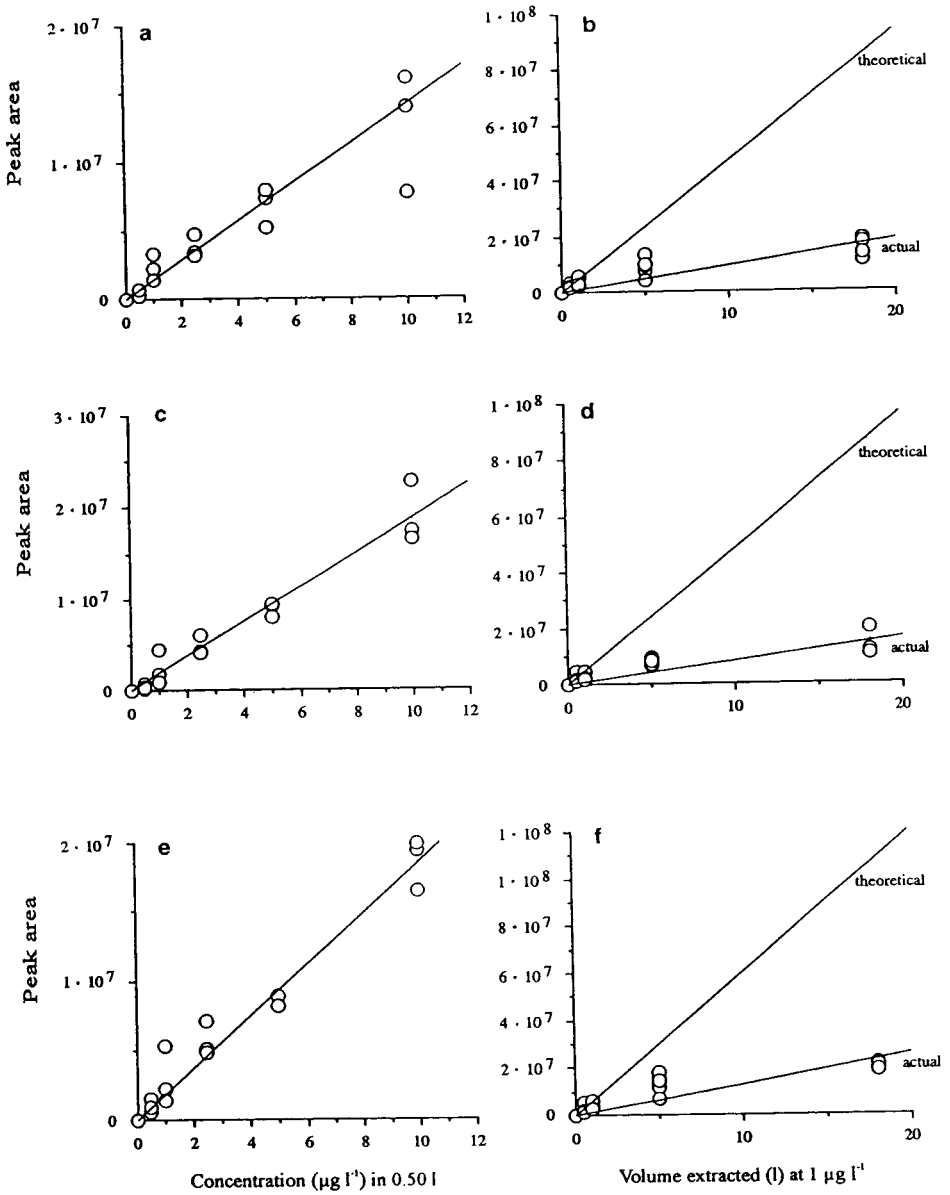

Fig. 2. Peak areas for phenolic standards (a, b) *o*-cresol, (c, d) *m*-cresol and (e, f) *p*-cresol calculated from (a, c, e) constant volume and varied substrate concentration and (b, d, f) constant concentration and varied volume. Theoretical peak area *vs.* volume slope calculated using peak area values for 0.50 l standard volume. Equations: (a) $y = 1.42 \cdot 10^6 x$, $r^2 = 0.98$; (b) $y = 9.33 \cdot 10^5 x$, $r^2 = 0.95$; (c) $y = 1.87 \cdot 10^6 x$, $r^2 = 0.98$; (d) $y = 8.25 \cdot 10^5 x$, $r^2 = 0.94$; (e) $y = 1.86 \cdot 10^6 x$, $r^2 = 0.98$; (f) $y = 1.30 \cdot 10^6 x$, $r^2 = 0.98$.

were searched on the HP 5988 Chemstation spectral data library for suspected matches. Matches were assessed by comparison of molecular ion abundance of the parent phenol and the presence of an $M^+ + 42$ mass unit (acetyl group) peak. Fig. 3 shows a putative identification of 2-methoxyphenol. A library search produced an 80% similarity index with 2-methoxyphenol ($M_r = 124$). The presence of a identifiable peak at 124 + 42 (166) presents strong evidence for

TABLE II

ANALYTICAL AND STATISTICAL PARAMETERS FOR PHENOLIC STANDARDS

Values are used in the generalized equation: $zv^{-1}ynm^{-1}l_{orig}{}^{-1}V_{fin} = x \pm s\%$, where z = correction value for external and internal standards, v = correction value for the use of large volume samples, y = parent phenol molecular ion peak area, n = parent phenol molecular ion peak percent, m = slope normalized to 1 l of sample (see Fig. 4), l_{orig} = original sample volume, V_{fin} = final extract volume (in μl) and s = percent error.

Substrate	Retention time index	Parent phenol molecular ion	Parent phenol molecular ion peak percent (n)	Volume correction (v)	Slope ($m \times 10^6$)	Percent error (s)
Phenol	0.601	94	1.83	1.55	0.62	6
o-Cresol	0.697	108	1.28	0.20	2.84	4
m-Cresol	0.707	108	1.37	0.17	3.74	5
p-Cresol	0.713	108	1.33	0.22	3.72	3
2-Chlorophenol	0.750	128	1.28	0.50	3.10	4
2,4-Dimethylphenol	0.778	122	0.77	1.66	2.92	4
4-Chloro-3-methylphenol	0.867	142	0.71	0.54	4.16	4
2,4-Dichlorophenol	0.880	162	0.94	0.46	3.88	4
Catechol	0.923	110	1.11	0.27	4.90	7
2,4,6-Trichlorophenol	0.957	196	0.51	0.70	3.74	5
3-Methylcatechol	0.981	124	1.14	0.26	3.48	4
4-Methylcatechol	1.010	124	1.15	0.58	5.46	4
Pentachlorophenol	1.230	266	0.42	0.45	2.18	4
Phloroglucinol	1.240	126	0.96	0.41	2.50	9

identification as 2-methoxyphenol. Other phenols identified qualitatively (Table III) were assessed in a similar manner.

Samples were also taken from "pristine" coastal (5 m depth off Scripps Institution of Oceanography pier) and open ocean (Station M, 34°48.51 N × 123°00.86 W) at 200 m sites. No recognizable phenols were detected in these samples (concentrations greater than 100 pg l^{-1}). Brown algae such as *Fucus* spp. are known to contain phenolic materials, generally thought to be polymers of phloroglucinol [21,47,48]. In nearshore environments, degradation of these materials is most likely rapid, perhaps facilitated by solar radiation [40–42] or through pathways that do not include phloroglucinol as an intermediate. Phenolic compounds appear, from the results of this study, to be confined predominantly to nearshore marine environments where terrestrial input is considerable or dilution is hampered by physical enclosure, such as in San Diego Bay.

Concentration ranges for putative identifications were determined by the largest range of deviation from the known standards analyzed, the lowest value from the equation for *o*-cresol and the highest from the equation for 2,4-dimethylphenol. These ranges are only estimates and definitive results require the use of identified compounds as a series of analyzed standards. Phenols identified in this way were all from the Simpson and Louisiana–Pacific outfall sites, and are generally consistent with phenolic compounds previously isolated from pulp mill facilities [9,49,50].

The use of single ion monitoring (SIM) acquisition during GC–MS might improve sensitivity in quantitative analysis, especially if only a narrow range of phenolic materials is suspected to be in a particular sample. For the purposes of the qualitative analysis performed in this work, scan mode was chosen for the widest possible detection ability.

Calculation for derivatization and extraction efficiency

Percent efficiency was calculated using radiolabeled *p*-cresol. This allowed for a direct com-

TABLE III

SAMPLING SITES AND PHENOLS INDENTIFIED

Phenols in italics are putative identifications based on mass spectral data. See text.

Sampling location; coordinates; date	Depth	Phenols identified	Concentration ($ng\ l^{-1}$)
Spanish Landing, San Diego Bay; 32°43′40″ × 117°12′42″; April 4, 1992	Surface	*o*-Cresol	3 ± 0.5
		Catechol	130 ± 21
		3-Methylcatechol	33 ± 5
		4-Methylcatechol	22 ± 3
Sweetwater Channel, San Diego Bay; 32°38′43″ × 117°07′25″; December 9, 1992	11 m	Phenol	228 ± 36
		o-Cresol	5 ± 1
		Catechol	188 ± 30
Simpson Outfall; 40°48′03″ × 124°12′50″; June 24, 1992	Surface	Phenol	32 ± 5
		o-Cresol	22 ± 3
		p-Cresol	15 ± 2
		2-Methoxyphenol	*390–6600*
		2,3,5,6-Tetramethylphenol	*12–200*
		2-Methoxy-4-methylphenol	*17–280*
		4-Ethyl-2-methoxyphenol	*110–1900*
		2-Methoxy-4-isopopenylphenol	*13–220*
		4-Hydroxy-3-methoxybenzaldehyde	*82–1400*
		4,5-Dichloro-2-methoxyphenol	*19–320*
		1,1-Dimethylethylcatechol	*66–1100*
Louisiana-Pacific Outfall; 40°49′05″ × 124°12′10″; June 24, 1992	Surface	Phenol	12 ± 2
		o-Cresol	9 ± 1
		Catechol	100 ± 16
		2-Methoxyphenol	*34–580*
White's Point Outfall 33°41′40″ × 118°19′30″; March 10, 1993	34 m	Phenol	328 ± 52
		o-Cresol	8 ± 1
		p-Cresol	60 ± 10
JWPCP effluent; N/A; March 9, 1993	N/A[a]	Phenol	7000 ± 1120
		o-Cresol	2000 ± 320
		p-Cresol	2400 ± 380
Hyperion effluent; N/A; February 3, 1993	N/A	*o*-Cresol	170 ± 27
		p-Cresol	516 ± 83

[a] N/A = Not applicable.

parison of derivatization–extraction efficiency between unreacted and acetic anhydride derivatized *p*-cresol. Extraction efficiency for derivatized *p*-cresol was calculated at 97% while underivatized *p*-cresol was extracted at 86%. These results are consistent with published efficiencies calculated for the acetate esters of *o*- and *m*-cresol extracted with liquid solvent (CH_2Cl_2) [37]. Derivatizing was necessary in this experimental protocol for the extraction of catechol, 3-methylcatechol, 4-methylcatechol and phloroglucinol. Recoveries were essentially 0% for these unreacted compounds. During optimization of buffer addition, it was noted that under

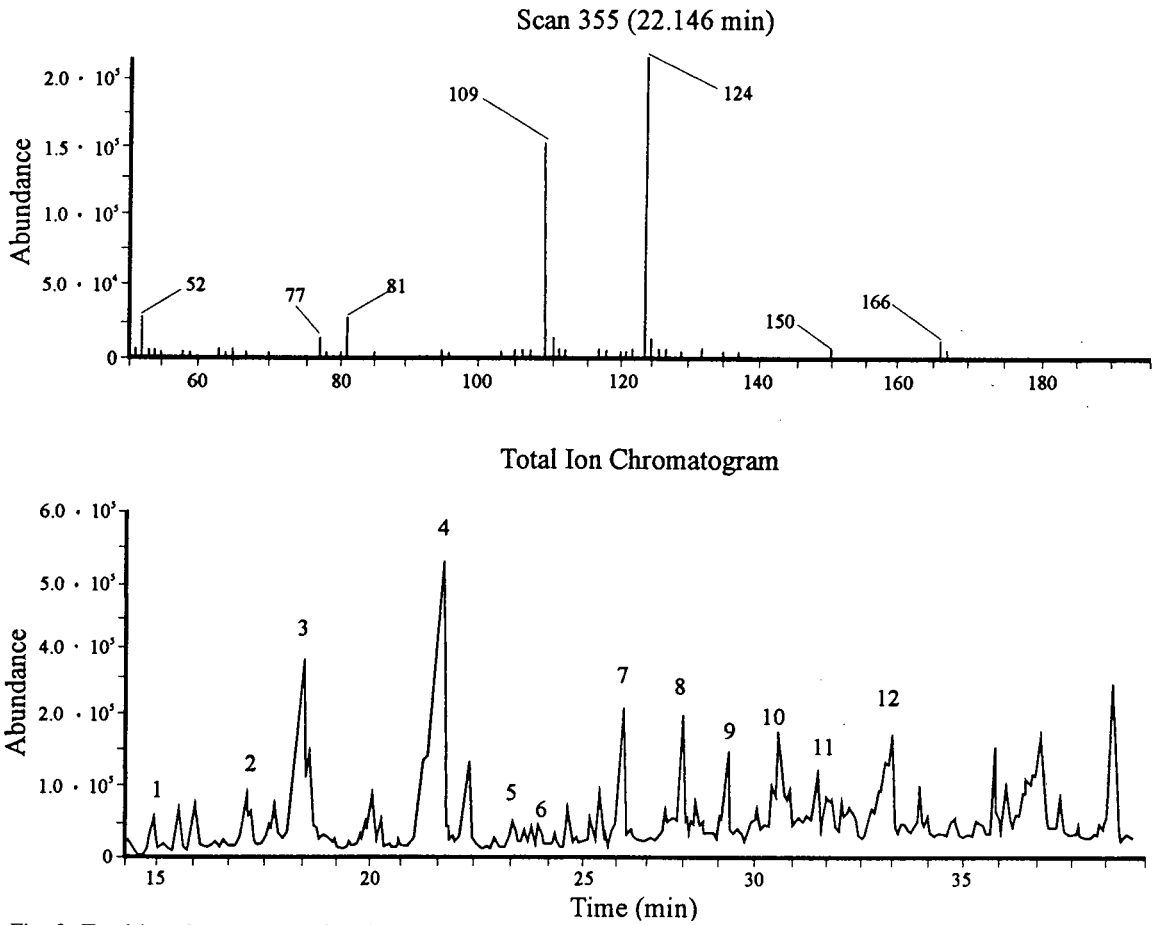

Fig. 3. Total ion chromatogram for Simpson outfall extract. Illustrated is scan 469 (22.146 min), identified as 2-methoxyphenol acetate. Other identified phenols (as acetate esters) are: 1 = phenol; 2 = *o*-cresol; 3 = *p*-cresol; 4 = 2-methoxyphenol (above); 5 = 2,3,5,6-tetramethylphenol; 6 = 2-methoxy-4-methylphenol; 7 = 4-ethyl-2-methoxyphenol; 8 = 2-methoxy-4-isopropenylphenol; 9 = 4-hydroxy-3-methoxyphenol; 10 = 4,5-dichloro-2-methoxyphenol; 11 = 1,1-dimethylethylcatechol; 12 = internal standard.

less than optimal conditions (too little buffer added), acetylation of one hydroxyl group in dihydroxybenzenes occurred allowing for only partial recovery.

CONCLUSIONS

A method is described which uses acetic anhydride for the direct acetylation of phenols in aqueous solutions. The use of this rapid and relatively inexpensive method was optimized for large volume samples using SPE and GC–MS qualitative and quantitative analysis. The advantages of this modification are (1) the ability to extract, qualify and quantify large volumes (tens of liters) of sample suspected of containing phenolic materials; (2) the increased extraction efficiency obtained with aqueous acetylation prior to extraction such that polar phenols such as catechols and phloroglucinol are extractable; (3) the reduction in use of expensive and toxic solvents; and (4) the ability to screen mass spectral data for conformational analysis and putative identification of unknown phenols in a water sample.

ACKNOWLEDGEMENTS

Research was funded in part by a grant from the National Sea Grant College Program, Na-

tional Oceanic and Atmospheric Administration (NOAA), US Department of Commerce, under grant number NA89AA-D-SG138, project number R/CZ-98 through the California Sea Grant College, and in part by the California State Resources Agency. The views expressed herein are those of the author and do not necessarily reflect the views of NOAA or any of its subagencies. The US Government is authorized to reproduce and distribute for governmental purposes. Funds and logistical support were also provided by the Office of Naval Research under grant N00014-87-K-0148 and by the Marine Life Research Group at Scripps Institution of Oceanography. Special thanks are given to the County Sanitation District of Los Angeles County and the crew of the vessel *RV Ocean Sentinel*, the Los Angeles Sanitation District and the crew of the vessel *RV La Mer*, and John D. Faulkner and Russel Vernon-Clark for review and comments on this manuscript.

REFERENCES

1 E.E. Hargesheimer and R.T. Coutts, *Environ. Sci. Technol.*, 5 (1984) 433.
2 D.J. McDermott, *Southern California Coastal Water Research Project Annual Report 1974*, Southern California Coastal Water Research Project, Long Beach, CA, 1974, p. 89.
3 J.N. Cross and D.M. Wiley (Editors), *Southern California Coastal Water Research Project Annual Report 1989–90*, Southern California Coastal Water Research Project, Long Beach, CA, 1990, p. 9.
4 T.W. Federle, *Can. J. Microbiol.*, 34 (1988) 1037.
5 H.A. Schafer, *Southern California Coastal Water Research Project Annual Report 1978*, Southern California Coastal Water Research Project, Long Beach, CA, 1978, p. 97.
6 H.R. Harvey, J.H. Tuttle, R. Dawson and J.T. Bell, in D.A.C. Manning (Editor), *Organic Geochemistry Advances and Applications in Energy and the Natural Environment*, St. Martin's Press, New York, 1991, p. 237.
7 I. Tolosa, J.M. Bayona and J. Albaigés, *Mar. Poll. Bull.*, 22 (1991) 603.
8 J. Perez, T. de la Rubia, J. Moreno and J. Martinez, *Environ. Toxicol. Chem.*, 11 (1992) 489.
9 A. Morales, D.A. Birkholz and S.E. Hrudey, *Water Environ. Res.*, 64 (1992) 669.
10 P. Larsson and K. Lemkemeier, *Water Res.*, 23 (1989) 1081.
11 L. Tranvik, P. Larsson, L. Okla and O. Regnell, *Environ. Toxicol. Chem.*, 10 (1991) 195.
12 J.K. Whelan, M.E. Tarafa and E.B. Sherr, *Org. Mar. Geochem.*, 1986 (1993) 62.
13 G.M. King, *Appl. Environ. Microbiol.*, 54 (1988) 3079.
14 G.M. King, *Nature*, 323 (1986) 257.
15 B. Charriere, F. Gadel and L. Serve, *Hydrobiologia*, 222 (1991) 89.
16 S.M. Steinberg, M.I. Venkatesan and I.R. Kaplan, *Mar. Chem.*, 21 (1987) 249.
17 K. Abrahamsson and S. Klick, *Mar. Pollut. Bull.*, 22 (1991) 227.
18 D.J. Carlson, *Nature*, 296 (1982) 426.
19 D.J. Carlson and L.M. Mayer, *Nature*, 286 (1980) 482.
20 V.N. Kozitskaya, *Hydrobiol. J.*, 3 (1984) 54.
21 P.D. Steinberg, *Oecologia*, 78 (1989) 373.
22 J.McN. Sieburth and A. Jensen, *J. Exp. Mar. Biol. Ecol.*, 3 (1969) 275.
23 R.L. Malcolm, *Anal. Chim. Acta.*, 232 (1990) 19.
24 K.J. Meyers-Schulte and J.I. Hedges, *Nature*, 321 (1986) 61.
25 *Method of Organic Chemical Analysis of Municipal and Industrial Wastewater, US EPA-600/4-83-057*, EPA, Cincinnati, OH, 1982.
26 *Fed. Reg.*, 49, No. 209 (Oct. 26, 1984).
27 E. Tesarová and V. Pacáková, *Chromatographia*, 17 (1983) 269.
28 R.C. Quackenbush, D. Bunn and W. Lingren, *Aquat. Bot.*, 24 (1986) 83.
29 K. Abrahamsson and T.M. Xie, *J. Chromatogr.*, 279 (1983) 199.
30 A. Alfieri, G. Crawford and I. Ahmad, *J. Assoc. Off. Anal. Chem.*, 72 (1989) 760.
31 H.O. Friestad, D.E. Ott and F.A. Gunther, *Anal. Chem.*, 41 (1969) 1750.
32 C. Baiocchi, E. Campi, M. Gennaro, E. Mentasti and P. Mirti, *Chromatographia*, 15 (1982) 660.
33 W.M. Walter, Jr. and A.E. Purcell, *J. Agric. Food Chem.*, 27 (1979) 942.
34 G. Bengtsson, *J. Chromatogr. Sci.*, 23 (1985) 397.
35 L. Renberg, *Chemosphere*, 10 (1981) 767.
36 L. Renberg and K. Lindstrom, *J. Chromatogr.*, 214 (1981) 327.
37 R.T. Coutts, E.E. Hargesheimer and F.M. Pasutto, *J. Chromatogr.*, 179 (1979) 291.
38 H.-B. Lee, L.-D. Weng and A.S.Y. Chau, *J. Assoc. Off. Anal. Chem.*, 67 (1984) 789.
39 T.J. Hendricks, *Southern California Coastal Water Research Project Annual Report 1977*, Southern California Coastal Water Research Project, Long Beach, CA, 1977, p. 41.
40 K. Lin and D.J. Carlson, *Mar. Chem.*, 33 (1991) 9.
41 H. Kawaguchi, *J. Contam. Hydrol.*, 9 (1992) 105.
42 H.M. Hwang, R.E. Hodson, R.F. Lee, R.G. Zika and W.J. Cooper, *Photochem. Environ. Aquat. Syst.*, 327 (1987) 27.
43 A.V. Palumbo, F.K. Pfaender and H.W. Paerl, *Environ. Toxicol. Chem.*, 7 (1988) 573.
44 T.J. Boyd and A.F. Carlucci, *Aquat. Toxicol.*, 25 (1993) 71.
45 G.W. Bartholomew and F.K. Pfaender, *Appl. Environ. Microbiol.*, 45 (1983) 103.

46 National Ocean Pollution Program Office, *Federal Plan for Ocean Pollution Research, Development, and Monitoring; Fiscal Years 1992–1996*, US Department of Commerce, Washington, DC, 1991, p. 9.
47 D.J. Carlson and L.M. Mayer, *Can. J. Fish. Aquat. Sci.*, 40 (1983) 1258.
48 J. Tuomi, H. Ilvessalo, P. Niemela, S. Siren and V. Jormalainen, *Botanica Marina*, 32 (1989) 505.
49 M.M. Haeggblom, J.H.A. Apajalahti and M.S. Salkinoja-Salonen, *Wat. Sci. Tech.*, 20 (1988) 205.
50 J.L. Sarmiento and E.T. Sundquist, *Nature*, 356 (1992) 589.

Journal of Chromatography A, 662 (1994) 293–299
Elsevier Science B.V., Amsterdam

CHROM. 25 678

Separation and identification of partially ethylated galactoses as their acetylated aldononitriles and alditols by capillary gas chromatography and mass spectrometry

Marcelo R. Cases, Carlos A. Stortz[☆] and Alberto S. Cerezo[*,☆]

Departamento de Química Orgánica, Facultad de Ciencias Exactas y Naturales, UBA, Ciudad Universitaria, 1428 Buenos Aires (Argentina)

(First received June 29th, 1993; revised manuscript received October 22nd, 1993)

ABSTRACT

As an aid to the structural determination of naturally methylated galactans, the separation and identification by capillary gas chromatography and the mass spectral features of ethylated galactoses as their aldononitrile and alditol acetate derivatives are presented and compared with those of their methylated counterparts. Data for some ethylated mono-O-methylgalactose derivatives are also included.

INTRODUCTION

The determination of the position of glycosidic linkages in oligo- and polysaccharides is usually achieved by methylation analysis [1]. The mixtures of partially methylated sugars released by hydrolysis of the methylated polysaccharides are generally derivatized to the alditol acetates [2] or, less frequently, to the aldononitrile acetates [3,4] to produce volatile derivatives for gas chromatographic analysis of the mixtures.

For polysaccharides containing naturally methylated sugars in addition to their non-methylated counterparts, methylation analysis leaves uncertainties in the structural determination. This has been overcome by the use of trideuteriomethyl iodide as alkylating agent [5], but as deuterium labelling does not change retention times, the use of coupled gas chromatography–mass spectrometry (GC–MS) is necessary for unequivocal interpretation of the chromatograms [5].

Another approach is ethylation (or propylation) [6], which produces a significant change in chromatographic behaviour, and therefore can be used without the need for MS. Albersheim and co-workers [7,8] have used ethylation as an alternative to methylation to achieve better chromatographic separations of alditol acetates in packed columns and a laboratory-made, wide-bore capillary column. An advantage of ethylation is that ethyl iodide is far cheaper than trideuteromethyl iodide, and can be synthesized and purified easily.

Seaweed polysaccharides usually contain variable amounts of galactoses naturally methylated at one of the four available positions [9,10]. We now report capillary column GC retention times and the main mass spectral features of partially ethylated D-galactononitrile acetates and galactitol acetates. The data are compared with those for their methylated counterparts. Data for the products of ethylation of some mono-O-methylgalactoses (generated by ethylation of

* Corresponding author.
☆ Research Member of the National Research Council of Argentina (CONICET).

0021-9673/94/$07.00
SSDI 0021-9673(93)E1124-I

naturally methylated seaweed galactans) are also included.

EXPERIMENTAL

Gas chromatography–mass spectrometry

Separations were carried out on a Hewlett-Packard HP 5890 apparatus. Volumes of 1 μl of chloroform solutions of derivatives were introduced via the injector in the split mode (*ca.* 1:100) on a Supelco (Bellefonte, PA, USA) SP-2330 vitreous-silica capillary column (30 m × 0.25 mm I.D., 0.20 μm film thickness), using nitrogen as the gas carrier (100 kPa, flow-rate *ca.* 1 ml/min). Temperature program A was isothermal at 210°C and in program B the temperature was programmed from 160 to 210°C at 2°C/min and from 210 to 240°C at 5°C/min [11]. A flame ionization detector was used, at 230 and 245°C, respectively. For MS, the same apparatus and column were used but using helium as gas carrier (64 kPa), interfaced to a Trio-2 VG Masslab (Manchester, UK) mass spectrometer. Mass spectra were recorded at 70 eV with scan times of 0.90 s (0.10 s reset).

TABLE I

RELATIVE RETENTION TIMES OF ETHYLATED GALACTOSES AS THEIR ACETYLATED ALDONONITRILES ON AN SP-2330 CAPILLARY COLUMN

Retention times relative to 3,4,5-tri-O-acetyl-2,6-di-O-ethylgalactononitrile = 1000.

Acronym	Position of O-ethyl	Programme A	Programme B
1N	2,3,4,6	358	460
2N	3,4,6	568	714
3N	2,4,6	587	729
4N	2,3,4	640	777
5N	2,3,6	662	796
6N	2,6	1000	1000
7N	4,6	1024	1008
8N	3,6	1046	1016
9N	2,4	1283	1098
10N	2,3	1352	1115
11N	6	1537	1155
12N	2	2085	1260
13N	3	2329	1299
14N	4	2554	1333
	–	*ca.* 3400	1488
Xylitol[a]		1505 (19.38 min)	1152 (30.54 min)

[a] Absolute and relative retention times of xylitol pentaacetate are given for comparison.

TABLE II

RELATIVE RETENTION TIMES OF ETHYLATED GALACTOSES AS THEIR ACETYLATED ALDITOLS ON AN SP-2330 CAPILLARY COLUMN

Retention times relative to 1,3,4,5-tri-O-acetyl-2,6-di-O-ethylgalactitol = 1000.

Acronym	Position of O-ethyl	Programme A	Programme B	Ref. 7[a]
1A	2,3,4,6	418	518	588
3A	2,4,6	652	771	804
2A	3,4,6	659	781	810
5A	2,3,6	676	796	810
4A	2,3,4	738	847	889
6A	2,6	1000	1000	1000
7A	4,6	1016	1005	967
8A	3,6	1128	1061	1018
10A	2,3	1287	1120	1065
9A	2,4	1375	1145	1092
11A	6	1501	1172	1105
12A	2	1952	1264	1209
13A	3 (=4)	2421	1337	1294
	–	3095	*ca.* 1440	1490
Xylitol[b]		1778	1233	1176

[a] Reported data on a 1% PEGS, 1% PEGA, 4% XF-1150 capillary column [7].
[b] Relative retention times of xylitol pentaacetate are given for comparison; absolute values are given in Table I.

General methods

Xylogalactans from *Corallina officinalis* were isolated, fractionated, purified and characterized as described previously [10]. They were composed of xylose, galactose and four mono-O-methylgalactoses [10]. Cystocarpic carrageenans from *Iridaea undulosa* were isolated and fractionated by means of potassium chloride; they are devoid of methylated galactoses [12]. These seaweed polysaccharides were ethylated as their triethylammonium salts, as described previously for methylation [12,13], but a second addition of methylsulphinyl carbanion and iodoethane was made. Carbanion was allowed to react for 150 min and iodoethane for 1 h each time. Iodoethane was synthesized from iodine, ethanol and red phosphorus [14], purified by distillation and found by ^{1}H NMR to be pure.

Ethylated polysaccharides were hydrolysed with 45% formic acid at 100°C for 16 h and divided into two roughly equal portions: one was derivatized as the alditol acetates [7] and the other as the aldononitrile acetates [3]. Samples of α-methyl galactopyranoside (Sigma, St. Louis, MO, USA) were ethylated using variable but limiting amounts of iodoethane [7], and hydrolysed as described.

RESULTS AND DISCUSSION

Table I gives the GC relative retention times of different O-acetyl-O-ethyl-D-galactononitriles on an SP-2330 capillary column using two different conditions. Table II gives the same data for the corresponding alditols. Both tables were constructed using ethylation data for several carrageenans and other galactans (see Experimental) for which methylation data are available [12,15], and complemented with intentionally underethylated samples of methyl α-D-galactopyranoside [7]. In the former case, the general pattern after ethylation was similar to that of methylation. Sweet *et al.* [7] reported the retention times of ethylated galactitol acetates on three different packed columns and a laboratory-made capillary ("wide-bore") column. Their results are included in Table II.

The retention times of the same polysaccharide components, as their partially methylated galactononitrile and galactitol acetates, are presented in Tables III and IV, respectively. A previous publication reported the data for the former derivatives in packed columns [3], and for the latter derivative several reports have been made [11,16], one of which (using an SP-2330 column) is included in Table IV. To aid comparison between Tables I–IV, the retention time of xylitol pentaacetate with respect to each standard is included in each table.

SP-2330 is regarded as an excellent support for separating methylated alditol acetates [11]. Good separation is achieved for all ethylated galactononitrile acetates (Table I), being comparable to the corresponding methylated derivatives (Table III). In spite of the molecular mass increment, ethylated aldononitrile derivatives appear earlier than corresponding methylated derivatives, owing to their lower polarity. The order of elution for the derivatives is, however, not the same: there are reversals for 3,4,6- and 2,4,6-tri-O-alkyl, the 2,3,4- and 2,3,6-tri-O-alkyl and the 6-mono- and 2,3-di-O-alkyl derivatives.

TABLE III

RELATIVE RETENTION TIMES OF METHYLATED GALACTOSES AS THEIR ACETYLATED ALDONONITRILES ON SP-2330 CAPILLARY COLUMNS

Retention times relative to 3,4,5-tri-O-acetyl-2,6-di-O-methylgalactononitrile = 1000. Data for an older and a newer column are presented (see text).

Position of O-methyl	Programme A		Programme B	
	ca. 3 years	<1 year	*ca.* 3 years	<1 year
2,3,4,6	411	393	576	536
2,4,6	624	612	785	755
3,4,6	678	664	832	803
2,3,6	748	737	878	852
2,3,4	794	782	911	883
2,6	1000	1000	1000	1000
4,6	1082	1082	1028	1030
3,6	1132	1129	1042	1046
2,4	1356	1361	1099	1116
2,3	1458	1461	1125	1139
6	1423	1433	1123	1132
2	1898	1916	1209	1223
3	2357	2372	1292	1298
4	2571	2590	1325	1328
–	2858	2912	1377	1380
Xylitol[a]	1254		1077	

[a] Relative retention times of xylitol pentaacetate are given for comparison; absolute values are given in Table I.

TABLE IV

RELATIVE RETENTION TIMES OF METHYLATED GALACTOSES AS THEIR ACETYLATED ALDITOLS ON SP-2330 CAPILLARY COLUMNS

Retention times relative to 1,3,4,5-tri-O-acetyl-2,6-di-O-methylgalactitol = 1000. Data for an older and a newer column are presented (see text).

Position of O-methyl	Programme A		Programme B		
	ca. 3 years	<1 year	*ca.* 3 years	<1 year	Ref. 11[a]
2,3,4,6	487	466	663	626	606
2,4,6	699	687	840	817	803
3,4,6	752	740	880	859	847
2,3,6	773	760	892	871	859
2,3,4	942	928	982	970	964
2,6	1000[b]	1000[b]	1000	1000	1000
4,6	1005[b]	1005[b]	1000	1000	1000
3,6	1153	1159	1051	1059	1073
2,3	1433	1436	1119	1136	1175
2,4	1474	1486	1127	1148	1188
6	1270	1283	1079	1094	1150
2	1795	1822	1187	1208	1262
3 (=4)	2305	2342	1273	1287	1342
–	2352	2406	1282	1298	1353
Xylitol[c]	1361		1101		1160

[a] Literature data [11] using programme B are included.
[b] Unresolved peaks.
[c] Relative retention times of xylitol pentaacetate are given for comparison; absolute values are given in Table I.

TABLE V

RELATIVE RETENTION TIMES OF ETHYLATED MONO-O-METHYLGALACTOSES AS THEIR ACETYLATED ALDONONITRILES AND ALDITOLS ON AN SP-2330 CAPILLARY COLUMN

Retention times relative to the derivative of the corresponding 2,6-di-O-methylgalactose = 1000.

Position of O-ethyl	Position of O-methyl	Aldononitriles			Alditols		
		Acronym	Programme A	Programme B	Acronym	Programme A	Programme B
3,4,6	2	**15N**		478	**15A**	461	570
2,3,6	4	**16N**	398	514	**16A**	470	583
2,4,6	3	**17N**		520	**17A**		595
2,4	6	**18N**	633	762			
3,6	4	**19N**	651	780			
3,6	2	**20N**	705	823	**20A**	774	864
2.4	3	**21N**		868			
2,6	3	**22N**	776	876	**22A**	800	884
4	2				**23A**	1588	1198
	2,6[a]		1000 (15.45 min)	1000 (28.36 min)		1000 (14.24 min)	1000 (27.74 min)

[a] Absolute retention times of the derivatives of the corresponding 2,6-di-O-methylgalactose are given for comparison.

TABLE VI

MAIN PEAKS IN THE MASS SPECTRA OF THE O-ACETYL-O-ETHYL-D-GALACTONONITRILES ($m/z > 44$)

m/z	Compound																				
	1N	**15N**	**16N**	**17N**	**2N**	**19N**	**3N**	**18N**	**4N**	**21N**	**5N**	**20N**	**22N**	**6N**	**7N**	**8N**	**9N**	**10N**	**11N**	**12N**	**13N**	**14N**
45	15	23	16	23				78		26			48							18		
57				17															100			
59	57	43	69	83	25	58	33	21		30	64	58	31	74	51	41				16		
71			41	28		27												17		33	15	
73	15	19		18								15										
85	51	42	60	70	18	24	19	24	23	26	30	27	19	23	20		15	100		85	100	
87			37	36		29		16					31									
97																					27	
98								20							24						38	26
99				18						20			33					15		16	16	
101	19	23	14	24	18	15	14	14	18	38	100	100	100	100	23	100	10	25	57	29	29	16
102										14		18	25									
103		24	15	24						14				12				20		84	26	
109															16							
113	10	10				16	25	27	43	43	19	16	15	49			27	94		11	82	
114											10							21			17	
115	14	22	54	34		50	12	65	11	18		12	13	77	10		14	32	28	89	52	14
116	17	13	11									12						26		14		
117	16						11	18									14					
126					16		59	61						18	71		85			10		85
127				10									52	19			11	60		69	55	31
128																					29	
129	46	32	100	100	25	100	100	17					15	12	100					28		
131			33	36		23				13	10			32				13	14		16	
140						24	10	14							18		16					17
141											44	31				12						
142				14						11	13							11				
143	100	100		94	100	22	56	100	100	100	66	70	58	51	63	59	100		20	13		100
145	19	17		22	17								29		10		10			85	12	12
152														13					9			
153														21								
154					18		9	12						6			11					
155											6							8		11		
156	6					6			6							20					84	
157								5			5			19					9	21	15	
159	5									9	26	23			7	23						
161											6	7	7			6						
168							58	73						19	79		61		6	9		54
169							5								13		5		10	11	5	11
173			24	26					5	6				48			20	10	21		13	
175			55	33		72		48													5	
186		5								8										8		
187	15	15								6			12					5		100	9	
189	59	75		50	65		29								27							
196														6								
197														34								
198														24	7	6				56	9	
200	2					8			3													
201						2			10	3	10	7				3						
203						5			32	29	3	5	6	9		3	27		2			14
211																			37	10	4	
212						2													11	3		
214				2	6		48	85						17			73					
215														6				13			12	
217																		4		11	10	
228													3		60							26
229																						3
230												2	4									
233			10	12																		
239														15								
240																3						
244											2											
247	10	6								6			10									
256														3								
261									4		7	4				2						
275														3			2	3			3	

TABLE VII

MAIN PEAKS IN THE MASS SPECTRA OF THE O-ACETYL-O-ETHYL-D-GALACTITOLS ($m/z > 44$)

m/z	Compound																	
	1A	**15A**	**16A**	**17A**	**2A**	**3A**	**4A**	**5A**	**20A**	**22A**	**6A**	**7A**	**8A**	**9A**	**23A**	**10A**	**11A**	**12A**	**13A**
57		27	15	20															
59	56	66	42	66	18	21		22	68			44	28				100		
71			18																
73	35	31	21	38			30					21				17			
85	87	91	60	71	19		21	17	41			64				32	27		41
87		44	25	27					34										
89	24	15		24											19				
97																	21	12	
98																	29		
99				17												28			
101	52	36	39	52	16		50	24	34	11	13	32	33	10	19	26	96		17
103	17	21	16	38		12	12			10		16		10		17	24		
113	11	16		14	17	10	75	11	24			90	10		10	34	13		47
114												12				10			
115	16	88	30	53	11				47	13		22	10		10		85		16
116		10		13															
117	26	80		41					100						100				11
127				11						27		59				20	16		30
129	100	67	100	100	13	20	63	18	10	20		57				13			
130	14	11		10															
131	89	29	97	57		100	100	100	33	100	100	17		100	21	100	25	100	17
139																	58	17	
141	11	11						30	59				21						
143	90	100	19	37	100	44	50	30	32		22	100	100	55	56		90	12	100
145	16	22	12	30	10							18					29		
153																	13		
156									5							9	24		
157				13					5			5					64		
159	8	7		5				16	38				12						
170																	7		
171						6					10								
173			31	39								8				6	16		7
175		31	20	32					15										
185									3								9	6	
187	28	26		5											5		6		
189	70	53	24	13	36	29	15	5				58							
198																	25		
199																	12		
201	3	3		2	2	7	10	7	15				5	5	7				
203	2	2		3	18		14						32	14	19		5		36
213											7								
215						4						17		2		11	2	2	17
217				4													6		
231						2					2								
233			30	28															
245																	2		2
247	31	26	2	2	2				2	9					13				
259																	4		
261				2	2	11	8	14	29				10	6					
275												28				20			20
333											2								
347																	3		

Compared with methylation, ethylation improves the separation between 6- and 2,3-di-O-alkyl galactose derivatives, but worsens that between 2,6-, 4,6- and 3,6-di-O-alkyl derivatives, even though the resolution is not impaired.

The ethylated alditol acetates (Table II) show more overlapping peaks (*e.g.*, 2,4,6- and 3,4,6-tri-O-ethylgalactitol and 2,6- and 4,6-di-O-ethylgalactitol) than the aldononitrile derivatives; the same trend was observed for methylated products [3]. The only reversal found in the elution order is for the 6-O-alkyl derivative, which appears earlier than some dialkylated products in methylation (Table IV), but later when comparing ethylated derivatives, *i.e.*, the number of alkyl groups has a greater effect on the elution order in the ethylated derivative series.

As noted previously for methylated derivatives on packed columns [3], ethylated galactononitrile acetates yield better separations than the alditol derivatives. However, each run takes longer as they are less volatile (*cf.*, their retention times relative to xylitol pentaacetate).

Table V reports the retention times of several ethylated mono-O-methylgalactoses separated as their aldononitrile and alditol acetates encountered in the ethylation of the polysaccharides from *Corallina officinalis* [15]. As shown, aldononitrile derivatives allow better separations.

Tables III and IV show the differences in retention times recorded on a newer (less than 1 year old) and an older (*ca.* 3 years old) column. It is noteworthy that as the SP-2330 column ages, the retention times become closer to the standard, *i.e.*, resolution diminishes. However, this effect is not large (Tables III and IV), and even with the 3-year-old column good resolution of peaks is achieved. For Tables I, II and V only the retention times for an aged column (2–3 years old) are shown.

Tables VI and VII show mass spectral data for ethylated galactoses and mono-O-methylgalactoses as aldononitrile acetates and alditol acetates, respectively. The fragmentation patterns are similar to those already predicted for methylated derivatives [2,3] and ethylated alditols [8], *i.e.*, the fission takes place mainly between carbon atoms carrying vicinal alkoxyl groups, and the primary fragments generated eliminate simple molecules to yield secondary fragments. Another fragmentation pathway which arises by loss of neutral fragments from the molecular ion, yielding radical ions, was postulated earlier [3] for aldononitriles and is supported by the ethylation data. Inspection of all the data shows that unambiguous characterization of the products is possible.

ACKNOWLEDGEMENTS

The authors are indebted to UMYMFOR (FCEyN-CONICET) for technical assistance. This work was supported by grants from CONICET and OAS.

REFERENCES

1 G.O. Aspinall, in G.O. Aspinall (Editor), *The Polysaccharides*, Vol. 1, Academic Press, Orlando, 1982, p. 36.
2 H. Björndal, C.G. Hellerqvist, B. Lindberg and S. Svensson, *Angew. Chem., Int. Ed. Engl.*, 9 (1970) 610.
3 C.A. Stortz, M.C. Matulewicz and A.S. Cerezo, *Carbohydr. Res.*, 111 (1982) 31.
4 G.R. Tanner and I.M. Morrison, *J. Chromatogr.*, 299 (1984) 252.
5 B. Lindberg, J. Lönngren and W. Nimmich, *Acta Chem. Scand.*, 26 (1972) 2231.
6 M.H. Saier and C.E. Ballou, *J. Biol. Chem.*, 243 (1968) 992.
7 D.P. Sweet, P. Albersheim and R.H. Shapiro, *Carbohydr. Res.*, 40 (1975) 199.
8 D.P. Sweet, R.H. Shapiro and P. Albersheim, *Biomed. Mass Spectrom.*, 1 (1974) 263.
9 T.J. Painter, in G.O. Aspinall (Editor), *The Polysaccharides*, Vol. 2, Academic Press, Orlando, 1982, p. 195.
10 M.R. Cases, C.A. Stortz and A.S. Cerezo, *Phytochemistry*, 31 (1992) 3897.
11 E.M. Shea and N.C. Carpita, *J. Chromatogr.*, 445 (1988) 424.
12 C.A. Stortz and A.S. Cerezo, *Carbohydr. Res.*, 242 (1993) 217.
13 T.T. Stevenson and R.H. Furneaux, *Carbohydr. Res.*, 210 (1991) 277.
14 B.E. Hunt, *J. Chem. Soc.*, 117 (1920) 1592.
15 M.R. Cases, C.A. Stortz and A.S. Cerezo, *Int. J. Biol. Macromol.*, submitted for publication.
16 J. Klok, H.C. Cox, J.W. de Leeuw and P.A. Schenck, *J. Chromatogr.*, 253 (1982) 55.

ELSEVIER

Journal of Chromatography A, 662 (1994) 301–321

JOURNAL OF CHROMATOGRAPHY A

Application of gas chromatography–mass spectrometry and gas chromatography–tandem mass spectrometry to the analysis of chemical warfare samples, found to contain residues of the nerve agent sarin, sulphur mustard and their degradation products

Robin M. Black *, Raymond J. Clarke, Robert W. Read, Michael T.J. Reid

Chemical and Biological Defense Establishment, Porton Down, Salisbury, Wiltshire SP4 0JQ, UK

(First received October 5th, 1993; revised manuscript received November 15th, 1993)

Abstract

Samples of clothing, grave debris, soil and munition fragments, collected from the Kurdish village of Birjinni, were analysed by GC–MS with selected ion monitoring (SIM) for traces of chemical warfare agents and their degradation products. Positive analyses were confirmed, where possible, by full scan mass spectra, or at low concentrations by additional GC–MS-SIM analysis using chemical ionisation, by higher resolution GC–MS-SIM, and by GC–tandem mass spectrometry using multiple reaction monitoring. Sulphur mustard and/or thiodiglycol were detected in six soil samples; isopropyl methylphosphonic acid and methylphosphonic acid, the hydrolysis products of the nerve agent sarin, were detected in six different soil samples. Trace amounts of intact sarin were detected on a painted metal fragment associated with one of these soil samples. The results demonstrate the application of different GC–MS and GC–MS–MS techniques to the unequivocal identification of chemical warfare agent residues in the environment at concentrations ranging from low ppb to ppm (w/w). They also provide the first documented unequivocal identification of nerve agent residues in environmental samples collected after a chemical attack.

1. Introduction

The prime requirement in analytical investigations of the use of chemical warfare (CW) agents is for the unequivocal detection and identification of the agents concerned and/or their degradation products [1]. The recent use of chemical warfare agents in the Iran–Iraq conflict has been well documented [2–4] and corroborated or confirmed by the chemical analysis of samples retrieved from bomb craters and unexploded weapons [2–4], and from human casualties [5–7]. Subsequent allegations of CW use against the Kurdish community within Iraq were substantiated by the analysis of samples obtained from a ruptured munition collected from the mountainous region of Northern Iraq [8]. In all but one of these incidents, positive analyses have revealed the presence of sulphur mustard and/or its degradation products such as thiodiglycol and 1,4-dithiane. Most of the positive environmental samples were obtained soon after the event, from bomb craters or unexploded munitions, and contained relatively high concentrations of agent or degradation

* Corresponding author.

0021-9673/94/$07.00
SSDI 0021-9673(93)E1214-K

products enabling unequivocal identification to be obtained by full-scan GC–MS and other less sensitive techniques such as NMR. In a single case [2], a virtually neat sample of the nerve agent tabun (GA) was given to UN investigators, reported as being the fill of an unexploded munition, although the more widespread use of nerve agents was strongly suspected during the Iraq–Iran war and against Kurdish communities in northern Iraq during 1987 and 1988 [4].

In October 1992, the Chemical and Biological Defense Establishment (CBDE) was asked to analyse a number of samples which had been collected in June 1992 from the Kurdish village of Birjinni, in the mountainous region of northern Iraq, by a team of forensic scientists from the Physicians for Human Rights and Middle East Watch Organisations [1]. The village was reported to have been subjected to a chemical attack on August 25th, 1988, almost four years earlier. Four villagers were reported to have died after the attack; surviving casualties reported feelings of suffocation, temporary blindness, muscular paralysis and spasms. The investigating team collected samples of clothing, soil and insect pupae from the exhumed skeletal remains of two of the victims, an old man and a young boy. Additional samples of soil and metal fragments were collected from four out of twelve bomb craters present in or near the village.

In this paper we report full details of the analytical methods employed to identify nerve agent and sulphur mustard residues in these samples. The results demonstrate the utility of different GC–MS and GC–MS–MS techniques for the unequivocal identification of CW agent residues in authentic environmental samples at concentrations ranging from low ppb to ppm (w/w).

2. Experimental

2.1. Samples

The samples, sealed inside plastic bags tagged with police forensic labels, were transported from Iraq, unopened, at ambient temperature via Boston (USA), and received at CBDE on October 5th, 1992. A fully documented audit trail was maintained from collection to analysis. After receipt, the samples were stored at 4°C prior to analysis. The samples consisted of the following: *sample 1*, a shirt plus intrathoracic contents (soil, insect pupae) from burial 1; *sample 2*, trousers from burial 2; *sample 3*, a shirt and vest from burial 2; *samples 4A–4L*, dry, stony, light brown soil samples collected from four bomb craters; some metal fragments, believed to be from munitions, were associated with some of these soil samples (4D, 4H, 4I, 4J). The fragment associated with soil sample 4H consisted of a twisted piece of double skinned metal (iron), *ca.* 7×5 cm, mass 35 g, coated with green paint.

Each sample was divided into appropriate subsamples for analysis and assigned unique CBDE identification numbers. Small sections were cut from the shirts, vest and trousers for analysis. Soil containing tiny pupae was removed from sample 1 and analysed separately. Fragments of metal present in soil samples 4D, 4H, 4I and 4J were analysed separately from the soil.

2.2. Standards and solvents

Samples of 1,1-thiobis(2-chloroethane) (sulphur mustard), O-ethyl N,N-dimethylphosphoramidocyanidate (tabun, GA), isopropyl methylphosphonofluoridate (sarin, GB), pinacolyl methylphosphonofluoridate (soman, GD), cyclohexyl methylphosphonofluoridate (GF), O-ethyl S-2-diisopropylaminoethyl methylphosphonothiolate (VX), isopropyl methylphosphonic acid (iPMPA), pinacolyl methylphosphonic acid, cyclohexyl methylphosphonic acid and ethyl methylphosphonic acid were synthesised in the Organic Chemistry Section, CBDE and were 99% pure by NMR and GC–MS or MS. Thiodiglycol (TDG) (99%) was purchased from Aldrich (Gillingham, UK) and methylphosphonic acid (MPA) (98%) from Lancaster Synthesis (Morecambe, UK). Fisons (Lough borough, UK) Distol-grade solvents were used. Water was distilled and purified using a Milli-Q system (Millipore, Bedford, MA, USA).

2.3. General analytical procedures

The samples were extracted with dichloromethane for the analysis of intact CW agents and with water for the analysis of hydrolysis products. For screening purposes the dichloromethane extracts were analysed specifically for sulphur mustard and nerve agents (tabun, sarin, soman, GF, VX) using GC–MS with selected ion monitoring (SIM) employing electron ionisation (EI). The aqueous extracts were derivatised and analysed specifically for TDG, the hydrolysis product of sulphur mustard, and for MPA and alkyl methylphosphonic acids, the hydrolysis products of nerve agents (except tabun). Additional analysis by full-scanning GC–MS was used to identify other significant volatile contaminants present. Positive analyses were confirmed following the procedures for unambiguous identification suggested in the series of Blue Books for the identification of CW agents [9], *i.e.* by full-scan EI and chemical ionisation (CI) mass spectra where obtainable, or by higher-resolution GC–MS-SIM (EI) and GC–tandem mass spectrometry (GC–MS–MS) to confirm low-resolution GC–MS-SIM data. In the single case of sarin detection, the analysis was confirmed by GC–MS–MS using both EI and ammonia CI on two GC columns of differing polarity. Quality control checks were run at least daily and glassware blanks were run before each sample.

2.4. Sample preparation

Soil samples

Screening for intact agents and other volatiles. Samples were allowed to reach ambient temperature before opening. Aliquots of soil (1–5 g, according to the size of the sample) were weighed into 3-ml vials or 15-ml tubes (for the larger aliquots) fitted with PTFE-lined screw caps. The soil was extracted by tumbling for 1 h with dichloromethane (2 or 5 ml). After standing for 2–3 min, 1-ml aliquots of the dichloromethane extracts were transferred to screw capped vials for GC–MS analysis and concentrated, if required, to small volume under nitrogen at 40°C.

Screening for hydrolysis products. Fresh aliquots (1–4 g) of soil were weighed into 15-ml tubes with PTFE-lined screw caps. Water (2 or 5 ml) was added and the soil extracted by tumbling for 1 h. After centrifuging at 1600 rpm (270 *g*) for 30 min, 1- or 2-ml aliquots of extract were transferred to 1-ml vials and concentrated to dryness using a Gyrovap centrifugal evaporator (Howe, Banbury, UK) at 60°C. To improve recovery of MPA, the extractions with water were repeated on fresh aliquots but were eluted through Dowex 50W-X8 cation-exchange resin (H^+ form, 200–400 mesh, 40–80 μm) (Fluka, Gillingham, UK) [500 mg, pre-washed with deionised water (2 × 2 ml), 0.01 *M* hydrochloric acid (2 × 2 ml) and deionised water (1 ml)] contained in a 3-ml Bond Elut reservoir.

Extractions for confirmation of initial screening results. Fresh aliquots (1–3 g) of soil were weighed into 15-ml tubes and extracted with dichloromethane (3 ml) as above. After standing for 2–3 min the dichloromethane extract was filtered through a 0.45-μm PVDF filter (Gelman, Ann Arbor, MI, USA) into 4-ml screw-capped vials. Residual dichloromethane was removed from the soil by evaporation in a centrifugal evaporator at 35°C. The soil was then extracted with water (3 ml) as above. Extracts were centrifuged at 1600 rpm for 30 min and as much of the aqueous fraction as possible filtered through 0.45-μm PVDF filters into 4-ml screw capped vials. Aliquots (1 ml) were transferred to 1-ml vials and concentrated to dryness in a centrifugal evaporator at 60°C.

2.4.2. Metal fragments

Samples were weighed into suitably sized small beakers or screw capped jars and dichloromethane added just to cover the sample. Beakers were covered with sealing film and placed in an ultrasonic bath for 1 h. Aliquots (2 ml) of the extracts were removed, filtered through 0.45-μm PVDF filters into 4-ml screw-capped vials and concentrated if required under nitrogen. Residual dichloromethane was removed from the fragments by evaporation under nitrogen at 40°C. Water was then added just to cover the fragment and extraction carried out as above.

Aliquots (1 or 2 ml) of extract were filtered through 0.45-μm PVDF filters into 1-ml vials and concentrated to dryness in a centrifugal evaporator at 60°C.

2.4.3. Clothing samples

Aliquots of cloth (1–3 g) were weighed into 24-ml Wheaton vials with PTFE-lined screw caps. The samples were extracted by tumbling for 1 h with dichloromethane (10 ml). As much of the dichloromethane extract as possible was filtered through 0.45-μm PVDF filters into 4-ml screw capped vials. Residual dichloromethane was removed from the samples by evaporation in a centrifugal evaporator at 35°C. The samples were then extracted by tumbling for 1 h with water (10 ml). After centrifuging at 1000 rpm (100 *g*) for 10 min, aliquots (1 or 2 ml) of the aqueous layer were filtered through 0.45-μm filters into 1-ml vials and concentrated to dryness in a centrifugal evaporator at 60°C. Larger samples of cloth (4–10 g) were similarly extracted with water (50 ml) and 25-ml aliquots concentrated to dryness using a rotary evaporator. Residues were transferred to 1-ml vials in 1-ml volumes of water and concentrated to dryness as above.

2.4.4. Derivatisation of dried aqueous extracts

Acetonitrile (50 μl) and N-methyl-N-(*tert.*-butyldimethylsilyl)-trifluoroacetamide–1% *tert.*-butyldimethylchlorosilane (Fluka) (50 μl) were added to the dried residues and the samples heated in a heating block for 1 h at 60°C [10].

GC–MS, SIM and full scan, of dichloromethane extracts

Dichloromethane extracts were screened using a Finnigan MAT TSQ 700 mass spectrometer (Finnigan MAT, Hemel Hempstead, UK) interfaced to a Varian 3400 gas chromatograph. The gas chromatograph was fitted with a 30 m × 0.25 mm I.D. DB-5 (J & W) bonded phase column, film thickness 0.25 μm, inserted directly into the ion source, with a 1 m × 0.25 mm I.D. retention gap (phenyl methyl deactivated). Helium at 103 kPa was used as carrier gas. The oven was heated at 40°C for 0.5 min, from 40 to 300°C at 15°C/min, and held at 300°C for 2 min. Aliquots (1 μl) were injected through a Varian SPI injector, heated at 35°C for 0.5 min, from 35 to 250°C in 1.5 min, and held at 250°C for 30 min. The transfer line was heated at 300°C. The TSQ 700 was operated in Q1MS mode using EI and SIM. Electron energy was 70 eV, emission current 400 μA, electron multiplier 1500 V, conversion dynode − 5 kV and source temperature 150°C. Ions monitored were *m/z* 99 (sarin, soman, GF), 109 (mustard), 114 (VX), 125 (sarin), 126 (soman), 133 (tabun), 158 (mustard) and 162 (tabun). Dwell time was 0.125 s each ion, total scan time 1 s.

Confirmation of sulphur mustard, 1,4-dithiane, 1,4-thioxane and tetryl, by full-scan GC–MS, was performed under similar GC conditions but employing a 25 m × 0.22 mm I.D. BP5 column (SGE, Milton Keynes, UK), film thickness 0.25 μm, using 1-μl splitless injections, injector temperature 220°C, split delay 0.5 min. The mass spectrometer was scanned from *m/z* 40–400 at 1 s per scan using EI as above, or using methane CI with electron energy 150 eV, source pressure 930 Pa (gauge reading), source temperature 150°C.

For confirmation of sarin by SIM, GC conditions were as above. Using EI, ions monitored were *m/z* 81, 99, 125, dwell time 0.33 s each ion, total scan time 1 s. Using ammonia CI (source conditions as for methane CI), ions monitored were *m/z* 141 (MH^+), 158 ($M + NH_4^+$), dwell time 0.5 s each ion, total scan time 1 s.

2.6. GC–MS, SIM and full scan, of water extracts

Water extracts were screened for the *tert.*-butyldimethylsilyl (TBDMS) derivatives of the hydrolysis products of sulphur mustard, sarin, soman, GF and VX, using a Finnigan MAT 4600 GC–MS system operated in the selected ion mode. The gas chromatograph was fitted with a 25 m × 0.22 mm I.D. BP5 column, film thickness 0.25 μm, with 50 cm × 0.25 mm retention gap (phenyl methyl deactivated). Helium at 103 kPa was used as carrier gas. The oven was heated at 90°C for 1 min, from 90 to 250°C at 10°C/min,

and held at 250°C for 1 min. Splitless injections (1 μl) were used, injector temperature 275°C, split delay 0.5 min. The GC–MS interface was heated at 250°C. EI at 70 eV was employed, emission current 300 μA, electron multiplier 1500 V, source temperature 150°C. Ions monitored were *m/z* 153 (MPA, iPMPA, pinacolyl MPA, cyclohexyl MPA, ethyl MPA), 267 (MPA), 293 (TDG). Dwell time was 0.3 s each ion, total scan time 1 s.

Confirmation by full-scan GC–MS was performed under similar conditions. The mass spectrometer was scanned from *m/z* 40–400 at 1 s per scan using EI as above, or using methane CI with electron energy 150 eV, source pressure 107 Pa, source temperature 120°C.

2.7. GC–MS-SIM (CI)

Confirmation of TDG, MPA and iPMPA, where concentrations were too low to obtain satisfactory full-scan data, was performed using methane CI as above with SIM of five ions per analyte. Ions monitored were TDG-$(TBDMS)_2$, *m/z* 219, 293, 294, 335, 336; MPA-$(TBDMS)_2$, *m/z* 267, 309, 310, 325, 326; iPMPA-TBDMS, *m/z* 153, 195, 211, 239, 253. Dwell time was 0.16 s each ion, total scan time 1 s.

2.8. Higher-resolution GC–MS-SIM

Confirmation using higher-resolution (HR) SIM was performed using a VG Autospec Q instrument (VG Analytical, Wythenshawe, UK) interfaced to a Hewlett-Packard 5890 series II gas chromatograph. The gas chromatograph was fitted with a 25 m × 0.22 mm I.D. BP5 column, film thickness 0.25 μm, or with a 25 m × 0.25 μm I.D. Ultra 2 column (Hewlett-Packard), film thickness 0.25 μm. For confirmation of the TBDMS derivatives of TDG, MPA and iPMPA, the oven was heated at 90°C for 0.5 min, from 90 to 260°C at 10°C/min and held at 260°C for 2 min. Splitless injections (1 μl) were used, injector temperature 250°C, split delay 0.5 min. For confirmation of sarin the oven was heated at 35°C for 2 min, from 35 to 300°C at 15°C/min, injection as above, split delay 2 min. The mass spectrometer was operated at 5000 resolution using EI, source temperature 220°C. Ions monitored were TDG-$(TBDMS)_2$, *m/z* 233.1395 ($C_{11}H_{25}OSSi$), 293.1427 ($C_{12}H_{29}O_2SSi_2$), *m/z* 242.9856 (perfluorokerosene) was used as mass lock; MPA-$(TBDMS)_2$, *m/z* 195.0063 ($C_4H_{12}O_3PSi_2$), 267.1002 ($C_9H_{24}O_3PSi_2$), 309.1471 ($C_{12}H_{30}O_3PSi_2$); iPMPA-TBDMS, *m/z* 153.0137 ($C_3H_{10}O_3PSi$), 195.0606 ($C_6H_{16}O_3PSi$), 237.1076 ($C_9H_{22}O_3PSi$), *m/z* 218.98562 (perfluorokerosene) was used as mass lock; sarin, *m/z* 99.0011 (CH_5O_2FP), 125.0168 ($C_3H_7O_2FP$), *m/z* 118.9920 (perfluorokerosene) was used as mass lock. Dwell time was 80 ms per ion, 20 ms delay.

2.9. GC–MS–MS multiple reaction monitoring

A Finnigan MAT TSQ 700 instrument interfaced to a Varian 3400 gas chromatograph was employed, operated in the multiple reaction monitoring (MRM) mode. For the confirmation of TDG, MPA and iPMPA, the GC was fitted with a 25 m × 0.22 mm I.D. BP-5 column, film thickness 0.25 μm; GC conditions were as in the screening procedure except that 1-μl splitless injections were used, injector temperature 220°C, 0.5 min split delay. Methane CI was employed, source conditions as above. Collision-activated decomposition (CAD) was performed using argon as collision gas at 0.13 Pa, collision offset − 20 eV. Reactions monitored were TDG-$(TBDMS)_2$, *m/z* 335→231, 189, 159, 147; MPA-$(TBDMS)_2$, *m/z* 325→309, 267; iPMPA-TBDMS, *m/z* 253→211, 195, 153. Dwell times were 0.2 s (TDG), 0.33 s (MPA) and 0.25 s (iPMPA) each ion, including undissociated parent ion, total scan time 1 s.

For the confirmation of sarin, GC–MS–MS analysis was performed under four different conditions. GC separation was performed using a non-polar BPX5 column (dimensions and conditions as for BP5), or using a polar 15 m × 0.25 mm I.D. DBWAX column, film thickness 0.5 μm, with 50 cm × 0.25 mm I.D. retention gap (phenyl methyl deactivated). For the latter the oven was heated at 40°C for 0.5 min, from 40 to 240°C at 10°C/min, and held at 240°C for 1 min.

Splitless injections (1 μl) were used, injector temperature 220°C, split delay 0.5 min. The transfer line was heated at 240°C. EI, ammonia CI [11] and CAD conditions were as described above. Reactions monitored were EI, *m/z* 125→99, 81; CI, *m/z* 158→141, 99. Dwell time was 0.33 s each ion including undissociated parent ion, total scan time 1 s.

2.10. Quantitation

No attempt was made at accurate quantitation; soil samples were considerably heterogeneous. Crude estimation of the amounts of analyte extracted from soil samples was performed by comparing peak areas of selected ions used in the GC–MS-SIM (EI) screening procedure [TDG-$(TBDMS)_2$, *m/z* 293; MPA-$(TBDMS)_2$, *m/z* 267; iPMPA-TBDMS, *m/z* 153; sulphur mustard, *m/z* 109] with the peak areas from appropriate standards (0.5 or 1 ng injected). In those cases where sulphur mustard was detected in the dichloromethane extract, TDG-$(TBDMS)_2$ was determined in the water extracts, using GC–MS-SIM (CI), *m/z* 293, after sequential extraction of the sample with dichloromethane (to remove sulphur mustard) and water. Sarin on fragment 4H(M) was estimated using the transition *m/z* 125→99 in the GC–MS–MS (EI) procedure.

2.11. Quality control

Glassware blanks (*i.e.* solvent taken through the entire extraction and derivatisation procedure) were run prior to the extraction of each sample.

Blanks, either the glassware blank for the next sample or a solvent or reagent blank, were analysed after every positive sample or standard to ensure that no cross-contamination occurred. System performance was checked by the analysis of standards at least daily or every 3–5 samples. Any problems identified were rectified and standards repeated before continuing with the analysis of samples. For the analysis of intact agents, samples of sulphur mustard, tabun, sarin, soman, GF and VX (100 pg or 1 ng of each) were injected in dichloromethane. For the analysis of hydrolysis products, TBDMS derivatives of TDG, iPMPA and MPA (0.5 or 1 ng of each) were injected in acetonitrile.

3. Results

3.1. Standards

Representative reconstructed ion chromatograms (*i.e.* summations of SIM chromatograms) for standard solutions of sulphur mustard, nerve agents and their derivatised hydrolysis products, as used for screening purposes, are shown in Fig. 1. Limits of detection were estimated as being in the range 10–50 ng extracted per sample based on a *S/N* ratio of *ca.* 3:1, with the exception of VX for which the screening procedure is less sensitive due to its poor chromatographic properties. Representative GC–MS-SIM (CI), GC–HRMS-SIM and GC–MS–MS-MRM chromatograms are shown below for the sample analyses. CAD spectra for the TBDMS derivatives of TDG, MPA and iPMPA, and for sarin, used for the selection of product ion monitoring for GC–MS–MS analysis, are shown in Fig. 2.

3.2. Grave samples 1, 2 and 3

No traces of nerve agents, sulphur mustard or their hydrolysis products were detected in any of the samples from the graves. Increasing the amounts of clothing extracted was not beneficial since the relatively large chemical background present increased proportionately. A repeat of the aqueous extraction with removal of cations by ion exchange also gave negative results for MPA.

3.3. Soil and metal fragments 4A–4L

The results for soil samples 4A–4L plus associated metal fragments are shown in Table 1.

Soil samples 4A, 4B and 4D

Soil samples 4A, 4B and 4D contained sulphur mustard at concentrations (0.6–10 ppm) suffi-

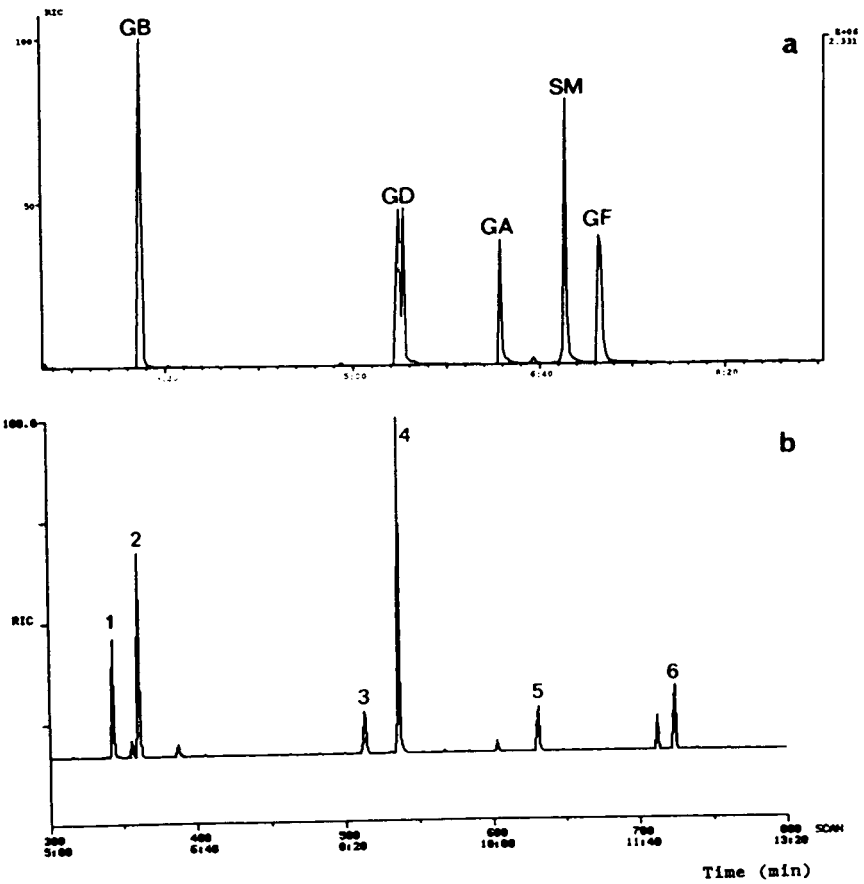

Fig. 1. Reconstructed ion current chromatograms for (a) nerve agents GA, GB, GD, GF and sulphur mustard (SM) (1 ng injected) and (b) TBDMS derivatives of (1) ethyl MPA, (2) iPMPA, (3) pinacolyl MPA, (4) MPA, (5) cyclohexyl MPA and (6) TDG (500 pg injected).

cient to obtain full-scan data. The dichloromethane extracts of samples 4A, 4B and 4D gave qualitatively similar total ion current (TIC) chromatograms; that from sample 4A is shown in Fig. 3 together with a full-scan EI mass spectrum obtained for sulphur mustard. In addition to sulphur mustard, small amounts of related cyclic degradation products, 1,4-thioxane and 1,4-dithiane, were present. The major component of the dichloromethane extracts was the explosive tetryl (N-methyl-N,2,4,6-tetranitroaniline), which chromatographs as the thermal decomposition product N-methyl-2,4,6-trinitroaniline [12], apparent as a very intense peak in Fig. 3. Two related products were also tentatively identified, 2,4,6-trinitroaniline (or possibly the N-nitro derivative) and 2,4,6-trinitrohydrazine (or possibly 2,4,6-trinitro-1,3-benzenediamine). One major peak remained unidentified in the extracts although it did not appear to be a CW-related material. TDG was detected at sub-ppm levels in the aqueous extracts of these samples, and on the metal fragment associated with soil sample 4D, and confirmed by GC–MS-SIM and GC–MS–MS data as shown in Table 1.

Soil samples 4C, 4E and 4F

No sulphur mustard was detected in the dichloromethane extracts of samples 4C, 4E and 4F, but its hydrolysis product TDG was detected

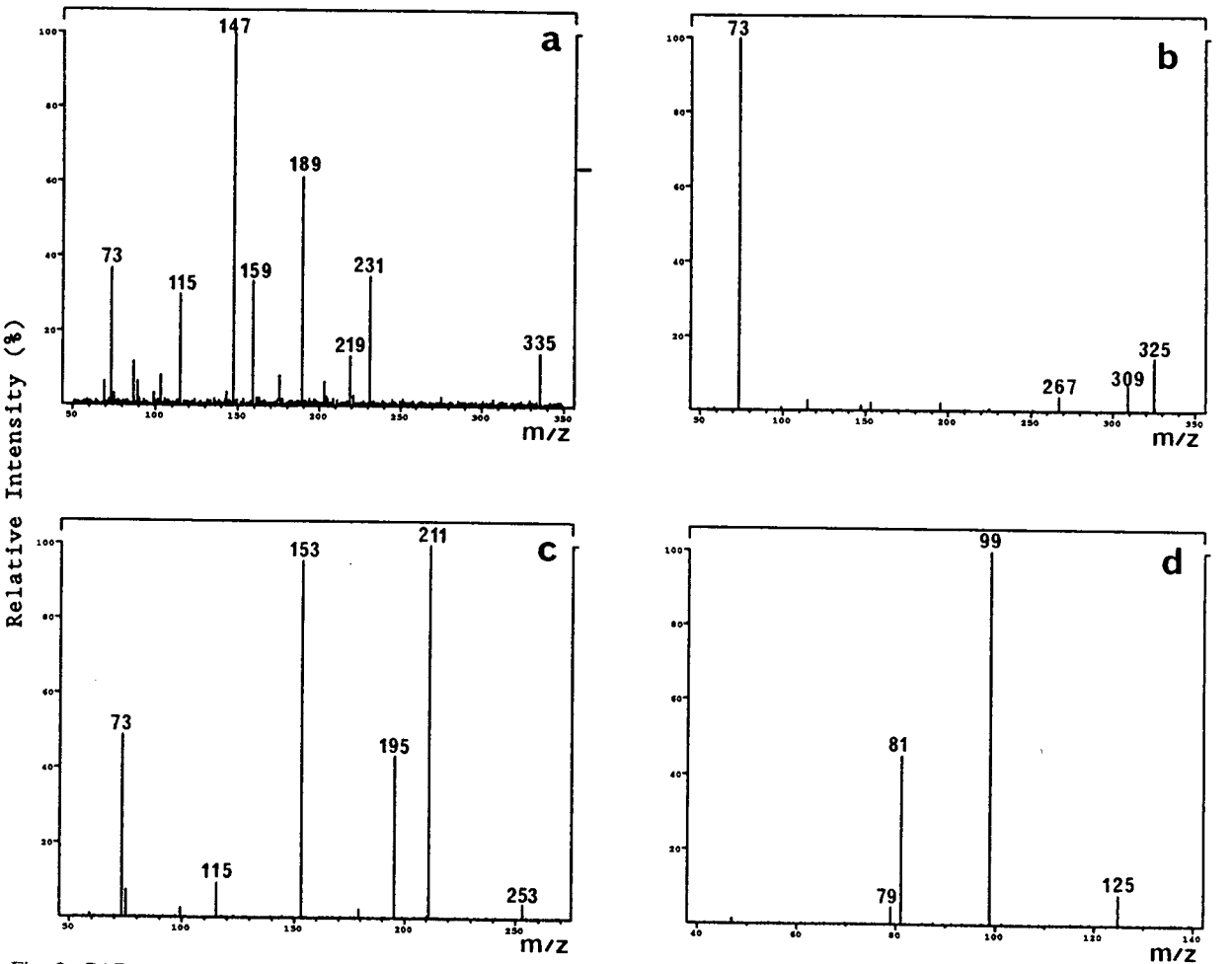

Fig. 2. CAD spectra of (a) TDG-$(TBDMS)_2$, *m/z* 335, (b) MPA-$(TBDMS)_2$, *m/z* 325, (c) iPMPA-TBDMS, *m/z* 253 (all CH_4 CI) and (d) GB, *m/z* 125 (EI).

in the aqueous extracts. It was confirmed by full-scan EI and CI spectra of the TBDMS derivative at the higher concentrations (3 ppm) present in sample 4C, shown in Fig. 4. Samples 4E and 4F contained low-ppb concentrations which were confirmed by GC–MS-SIM (CI) monitoring five ions, by higher-resolution GC–MS-SIM (EI), and by GC–MS–MS. The data for sample 4E, at concentrations estimated as 20 ppb, are shown in Fig. 5.

Soil samples 4G, 4H, 4I, 4J, 4K and 4L

Soil samples 4G, 4H, 4I, 4J, 4K and 4L, plus the metal fragments associated with samples 4H, 4I and 4J, were each found to contain iPMPA and MPA using the SIM screening procedure. Using simple aqueous extraction neither were extracted at levels sufficient to obtain good quality full-scan spectra of the TBDMS derivatives, and neither were observable above baseline noise in full-scan total ion current chromatograms. Confirmation of both MPA and iPMPA was initially obtained using GC–MS-SIM (CI) monitoring five ions, by higher-resolution GC–MS-SIM and by GC–MS–MS. Data for iPMPA in sample 4G are shown in Figs. 6, 7 and 8 together with the glassware blank for iPMPA under GC–MS–MS conditions. Following a re-

Table 1
Analysis of soil samples 4A–L

Sample	Number[a]	SIM screen	Confirmed by	Approximate concentration[b]
Soil	4A	Mustard	Full-scan EI, CI[c]	3 ppm
		TDG	CI-SIM, HR-SIM, MS–MS	200 ppb
Soil	4B[d]	Mustard	Full-scan EI, CI[c]	10 ppm
		TDG	CI-SIM, HR-SIM, MS–MS	300 ppb
Soil	4C	TDG	Full-scan EI, CI	3 ppm
Soil	4D	Mustard	Full-scan EI, CI[c]	600 ppb
		TDG	CI-SIM, HR-SIM, MS–MS	100 ppb
Metal	4D(M)	TDG	CI-SIM, HR-SIM, MS–MS	
Soil	4E	TDG	CI-SIM, HR-SIM, MS–MS	20 ppb
Soil	4F	TDG	CI-SIM, HR-SIM, MS–MS	100 ppb
Soil	4G[d]	iPMPA	CI-SIM, HR-SIM, MS–MS	80 ppb
		MPA	CI-SIM, HR-SIM, MS–MS	60 ppb[e]
Soil	4H	iPMPA	HR-SIM	6 ppb
		MPA	Full-scan EI, CI[e]	600 ppb[e]
Metal	4H(M)	iPMPA	CI-SIM, HR-SIM, MS–MS	
		MPA	CI-SIM, HR-SIM, MS–MS	
		GB	CI-SIM, HR-SIM, MS–MS[f]	
Soil	4I	iPMPA	CI-SIM, HR-SIM, MS–MS	100 ppb
		MPA	Full-scan EI, CI[e]	40 ppm[e]
Metal	4I(M)	iPMPA	CI-SIM, HR-SIM, MS–MS	
		MPA	CI-SIM, HR-SIM, MS–MS	
Soil	4J	iPMPA	CI-SIM, HR-SIM, MS–MS	30 ppb
		MPA	Full-scan EI, CI[e]	60 ppm[e]
Metal	4J(M)	iPMPA	CI-SIM, HR-SIM, MS–MS	
		MPA	CI-SIM, HR-SIM, MS–MS	
Soil	4K	iPMPA	CI-SIM, HR-SIM	200 ppb
		MPA	Full-scan EI, CI[e]	4 ppm[e]
Soil	4L	iPMPA	CI-SIM, HR-SIM	50 ppb
		MPA	Full-scan EI, CI[e]	7 ppm[e]

Abbreviations: CI-SIM = GC–MS-selected ion monitoring, methane CI, five ions; HR-SIM = GC–MS-selected ion monitoring, resolution 5000, EI, two or three ions; MS–MS = GC–MS–MS multiple reaction monitoring, two or three product ions.
[a] Numbers as received; additional CBDE numbers were assigned.
[b] Estimated to 1 significant figure.
[c] Additional volatiles 1,4-dithiane, 1,4-oxathiane, tetryl plus degradation products of tetryl, also identified by full-scan GC–MS.
[d] Mostly stones.
[e] After ion-exchange clean up.
[f] Using EI and ammonia CI on non-polar and polar GC columns.

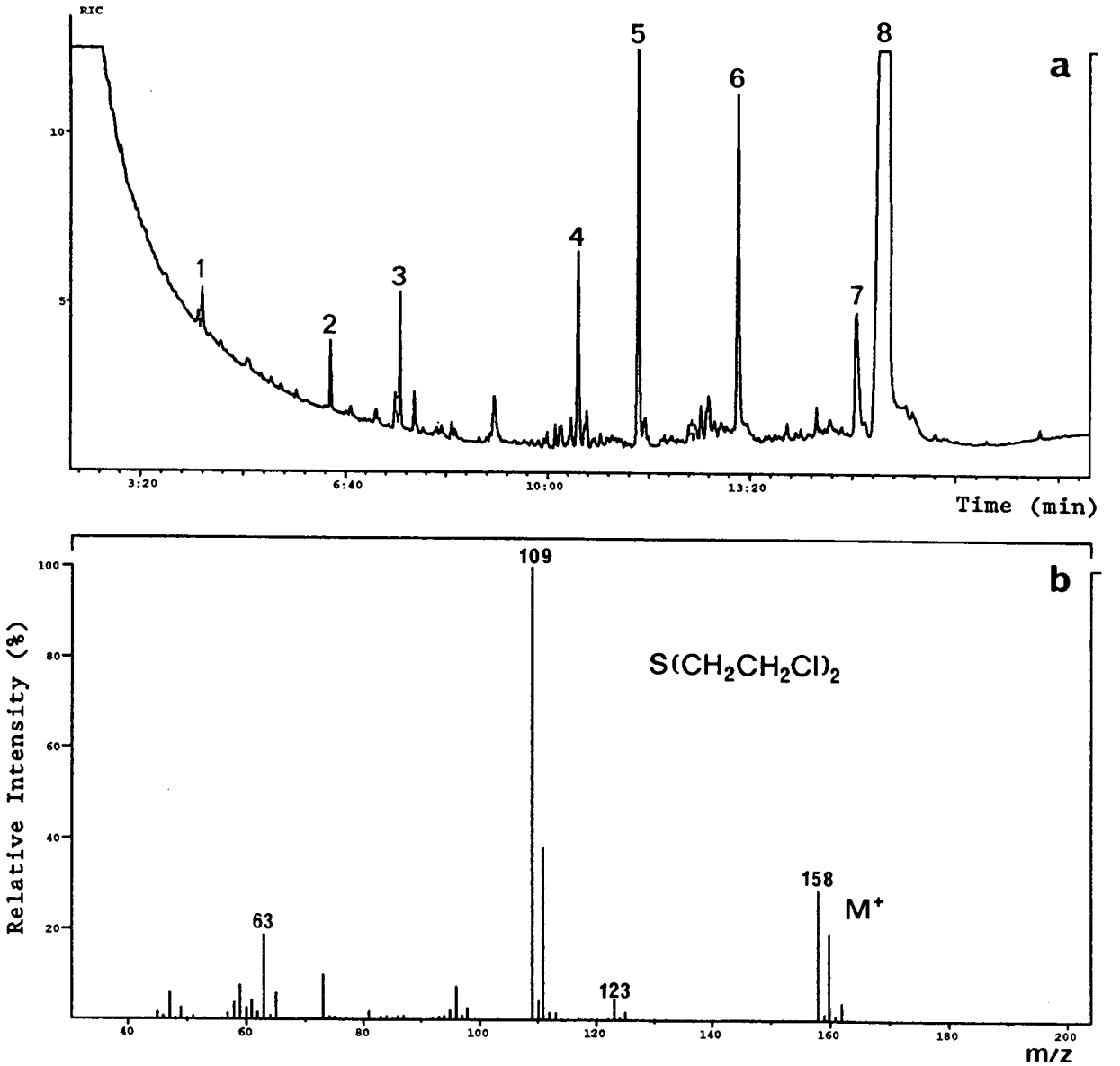

Fig. 3. (a) Total ion current chromatogram from the dichloromethane extract of soil sample 4A showing the presence of (1) 1,4-thioxane, (2) 1,4-dithiane, (3) sulphur mustard, (4) 2,6-bis(1,1-*tert.*-butyl)-2,5-cyclohexadiene-1,4-dione, (5) unidentified, (6) 2,4,6-trinitrophenylhydrazine (tentative identification), (7) 2,4,6-trinitroaniline and (8) tetryl. (b) Full-scan EI spectrum confirming the identification of sulphur mustard.

cent round robin exercise it was reported [13] that recoveries of MPA could be increased by passage of the aqueous extract through an acidic cation-exchange resin prior to derivatisation, which removes metal ions, possibly calcium which binds strongly to MPA. When this modified procedure was applied to these samples the concentrations of MPA found in the extracts increased substantially (up to 1000-fold) and good quality EI and CI full-scan data were

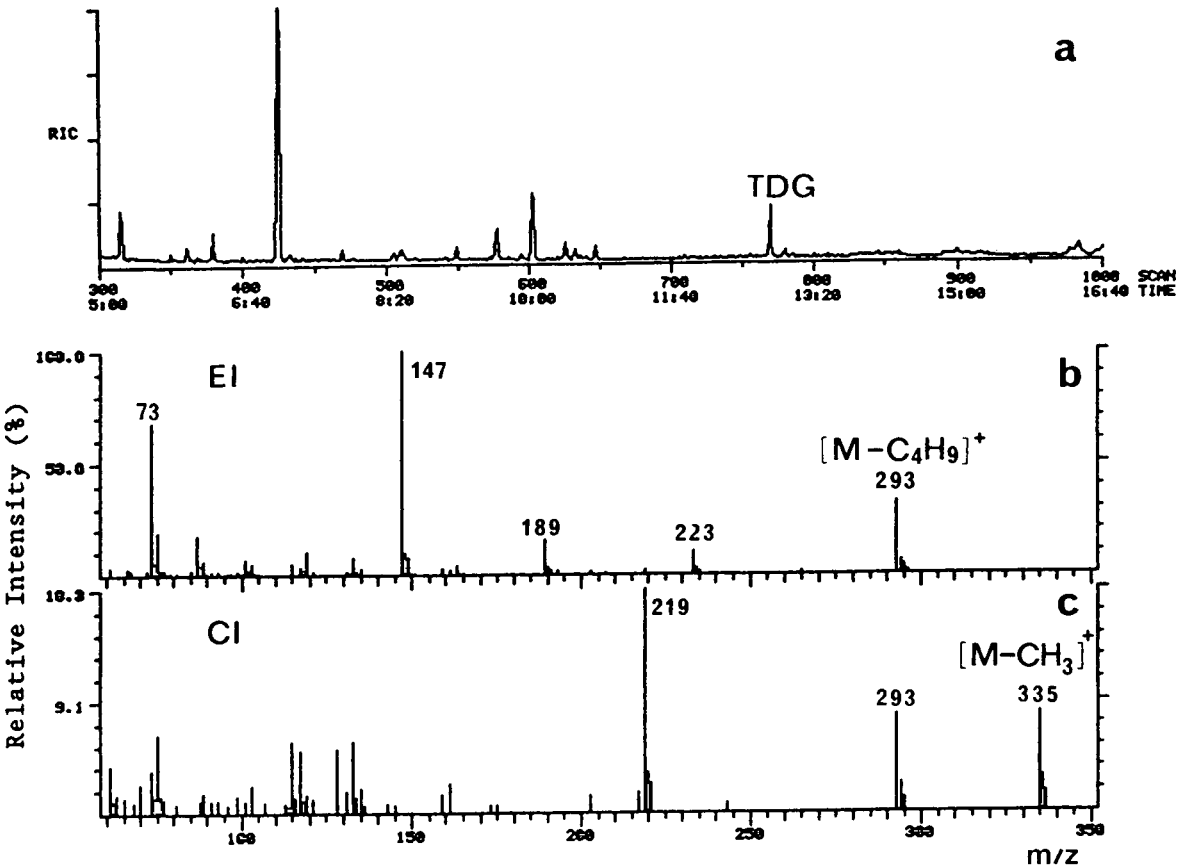

Fig. 4. (a) Total ion current chromatogram from the aqueous extract of soil sample 4C, with (b) EI and (c) CH_4 CI full-scan spectra confirming the identification of TDG-$(TBDMS)_2$.

obtained except for soil sample G which consisted mainly of stones. The total ion current chromatogram and EI and CI mass spectra of MPA-$(TBDMS)_2$, obtained from the aqueous extract of sample 4J after ion-exchange clean up and derivatisation, are shown in Fig. 9. Elution through the cation-exchange resin made little difference to the recoveries of iPMPA which remained in the extracts at concentrations below those required to obtain good quality full-scan data.

Metal fragment 4H(M)

In the case of a single metal fragment, associated with soil sample 4H, a relatively weak response at the retention time of sarin was observable in the selected ion screening procedure. After further concentration of the extract, additional evidence for the presence of sarin was obtained by GC–MS-SIM using both EI and ammonia CI [11] and by higher-resolution GC–MS-SIM (Fig. 10). To provide unequivocal evidence for the unexpected identification of intact sarin the sample was further analysed by GC–MS–MS, using both EI and ammonia CI, and employing two columns of widely differing polarity (methyl–5% phenyl silicone and Carbowax). Responses corresponding to those of a standard were obtained under each experimental condition. Chromatographic peak shape and S/N ratios on two or three product ions were superior using the polar

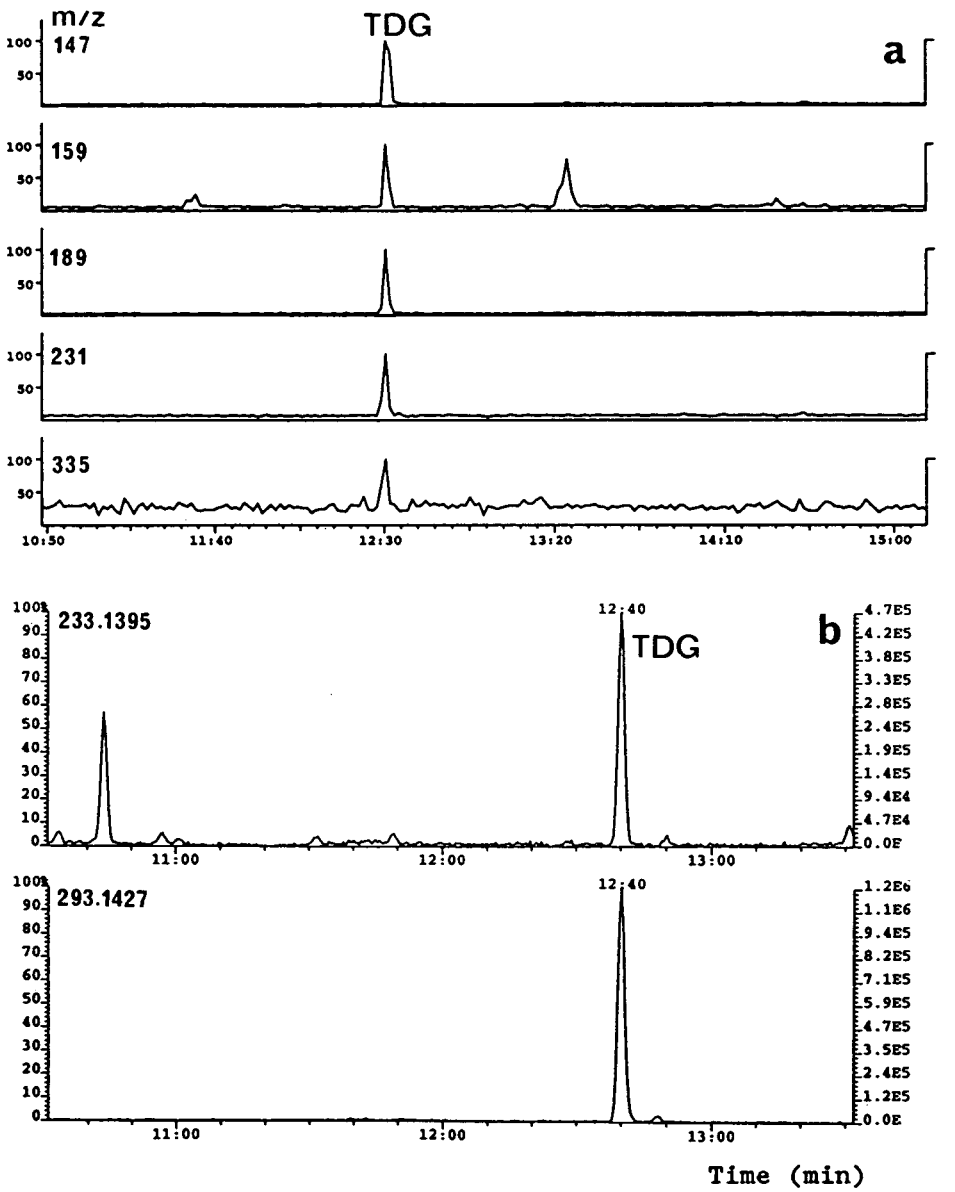

Fig. 5. (a) GC–MS–MS-MRM chromatograms (CH_4 CI) and (b) high-resolution SIM (EI) chromatograms confirming the identification of TDG-$(TBDMS)_2$ in the aqueous extract of soil sample 4E.

DBWAX column as shown in Fig. 11. MRM chromatograms, obtained using EI with a BP5 column and ammonia CI with a DBWAX column, are shown in Fig. 12. The total amount of sarin extracted from the 35-g fragment was estimated as 170 ng by GC–MS–MS. Both MPA and iPMPA were detected in the aqueous extract of the fragment; the GC–MS–MS response for iPMPA extracted from the metal fragment is shown in Fig. 13.

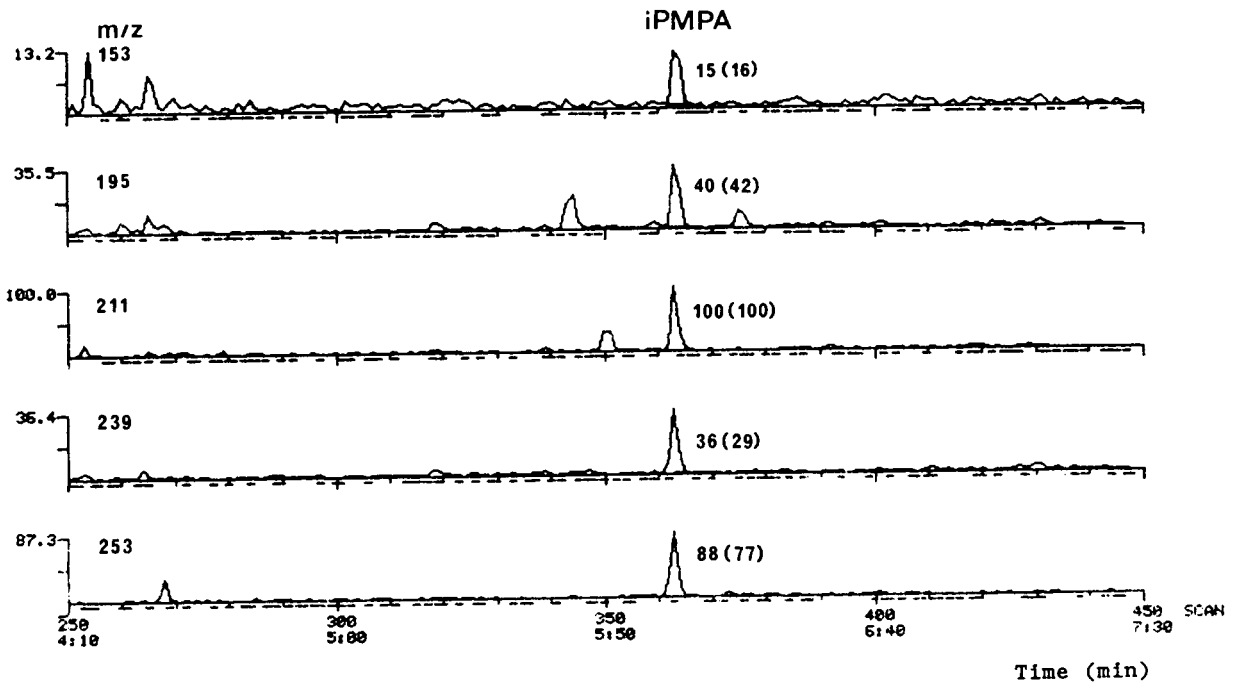

Fig. 6. Selected ion current chromatograms (CH_4 CI) confirming the identification of iPMPA-TBDMS in the aqueous extract of soil sample 4G. Relative peak intensities are shown together with those obtained from a standard in parentheses.

4. Discussion

The results demonstrate the utility of the different GC–MS and GC–MS–MS techniques which can be applied to forensic-type analyses to detect and unambiguously identify environmental contaminants at concentrations ranging from ppm to low ppb. At ppm levels, good quality full-scan mass spectra are usually obtainable and these provide the most desirable data where possible. At lower concentrations, where the more sensitive technique of GC–MS-SIM is required for detection, the combination of GC retention time (± 2 s) with the response for three characteristic ions, with ratios within 15–20% of those for a standard, have generally been accepted as proof of identification, the chances of a second compound responding in exactly the same manner having being calculated as extremely low [14]. Ion ratios for GC–MS-SIM using methane CI were generally reproducible within 20% limits when compared to standards at similar concentrations, but the relative intensities of the two most intense ions for iPMPA-TBDMS derivative were sometimes reversed at low concentrations. However, as recommended [9], the additional use of higher resolution GC–MS-SIM and/or GC–MS–MS-MRM adds an additional degree of certainty to the analysis and makes confirmation unequivocal within reasonable limits of probability. For samples such as the metal fragment, found to contain trace levels of sarin against a fairly noisy background, GC–MS–MS proved invaluable for improving S/N ratios and the specificity required for an unambiguous identification. The additional use of GC columns of widely differing polarity in combination with GC–MS–MS reinforced the results for sarin. The combination of EI, DBWAX column and GC–MS–MS appears to offer an excellent system for the confirmation of sarin. GC–MS–MS was also particularly useful

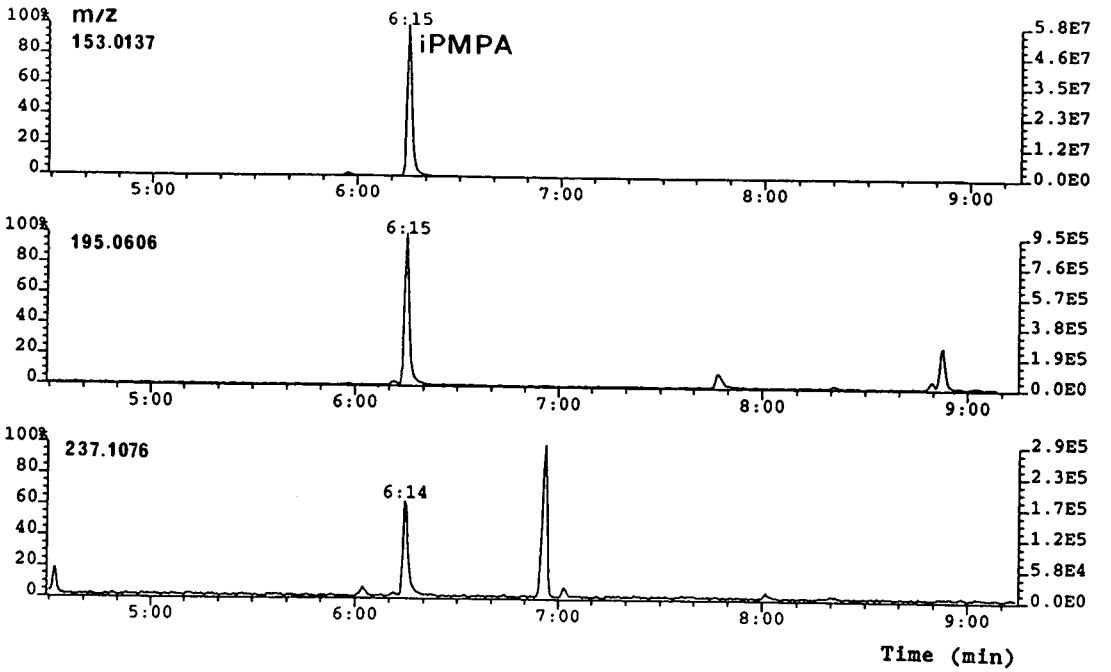

Fig. 7. Selected ion current chromatograms (EI) at 5000 resolution confirming the identification of iPMPA-TBDMS in soil sample 4G.

for the confirmation of iPMPA-TBDMS and gave superior S/N ratios and cleaner traces than higher-resolution SIM (Figs. 7 and 8). Similarly GC–MS–MS was useful for confirmation of TDG and MPA TBDMS derivatives although a disadvantage under the MS conditions used was that most of the product ion current from the protonated molecular ion of MPA-$(TBDMS)_2$ was concentrated in the non-characteristic ion m/z 73, which is derived from the TBDMS moiety. D'Agostino and co-workers [15–17] have demonstrated the advantages of GC–MS–MS using ammonia CI for the detection of sarin spiked into air and concrete samples, and other laboratories have reported exploratory work applying MS–MS techniques to CW agent detection [18–20]. In cases where identification was still in doubt the use of LC–MS [21,22] or an alternative derivative for GC–MS may be useful, *e.g.* pentafluorobenzoyl [23], heptafluorobutyryl [24] or trimethylsilyl [25] for thiodiglycol, and methyl [26,27], pentafluorobenzyl [26,28] or trimethylsilyl esters [25] for methylphosphonic acids. We prefer to use TBDMS derivatives for screening for TDG and methylphosphonic acids because of their ease of preparation, stability and mass spectral properties [10]. They have the added advantage over methyl or pentafluorobenzyl esters that TDG can be screened for simultaneously with methylphosphonic acids.

The absence of any traces of nerve agents, mustard or their hydrolysis products in the samples collected from the graves was not unexpected. Any agent which may have originally been present would most likely have been well dispersed and therefore more likely to be degraded and leached from the clothing and soil, although the results on the soil samples suggest that MPA is fairly persistent in soil. In contrast, all of the soil samples 4A–4L and their associated metal fragments, collected from bomb craters, gave positive results for sulphur mustard, TDG or sarin hydrolysis products. Information obtained following completion of the initial analyses indicated that the results correlated well with the sampling of different bomb craters. Soil

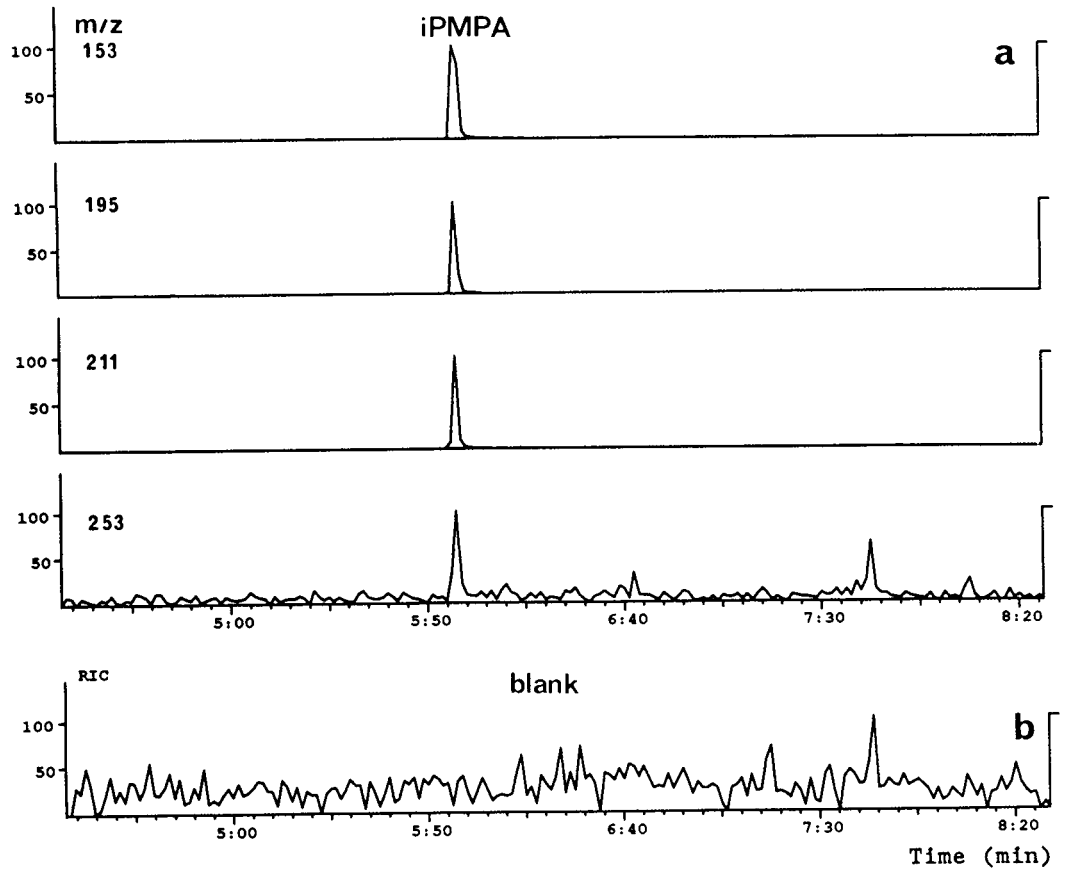

Fig. 8. GC–MS–MS-MRM chromatograms (CH_4 CI), (a) confirming the identification of iPMPA-TBDMS in soil sample 4G and (b) the reconstructed ion current trace from the preceding glassware blank.

samples 4A, 4B, 4C, and 4D, 4E, 4F, which contained sulphur mustard and/or TDG, were obtained from the first two craters sampled. Soil samples 4G, 4H, 4I, and 4J, 4K, 4L, which contained the hydrolysis products of sarin, were obtained from the third and fourth craters sampled. Samples 4A, 4D, 4G and 4J were collected from the centres of the respective craters, samples 4B, 4E, 4H and 4K from the southern edges and samples 4C, 4F, 4I and 4L from the northern edges of the craters.

In addition to sulphur mustard, samples 4A, 4B and 4D contained 1,4-dithiane, 1,4-thioxane and the explosive tetryl. These same compounds were found in the residues from a ruptured bomb, collected from the Kurdish region of northern Iraq, analysed at CBDE in 1988 [8]. The relatively high concentrations of tetryl present in these three samples caused some column degradation during the analysis of concentrated extracts. Samples 4G–4L, and the accompanying metal fragments in the case of samples 4H, 4I and 4J, all contained iPMPA and MPA, the hydrolysis products of sarin, at variable concentrations in the ppb (iPMPA) to ppm (MPA) range. iPMPA is the more important of these hydrolysis products since it is the initial product of rapid hydrolysis which confirms that the agent used was GB. MPA, which is formed by further hydrolysis of iPMPA, is the end product of hydrolysis of other organophosphorus nerve agents (*e.g.* soman, GF, VX). It may also arise

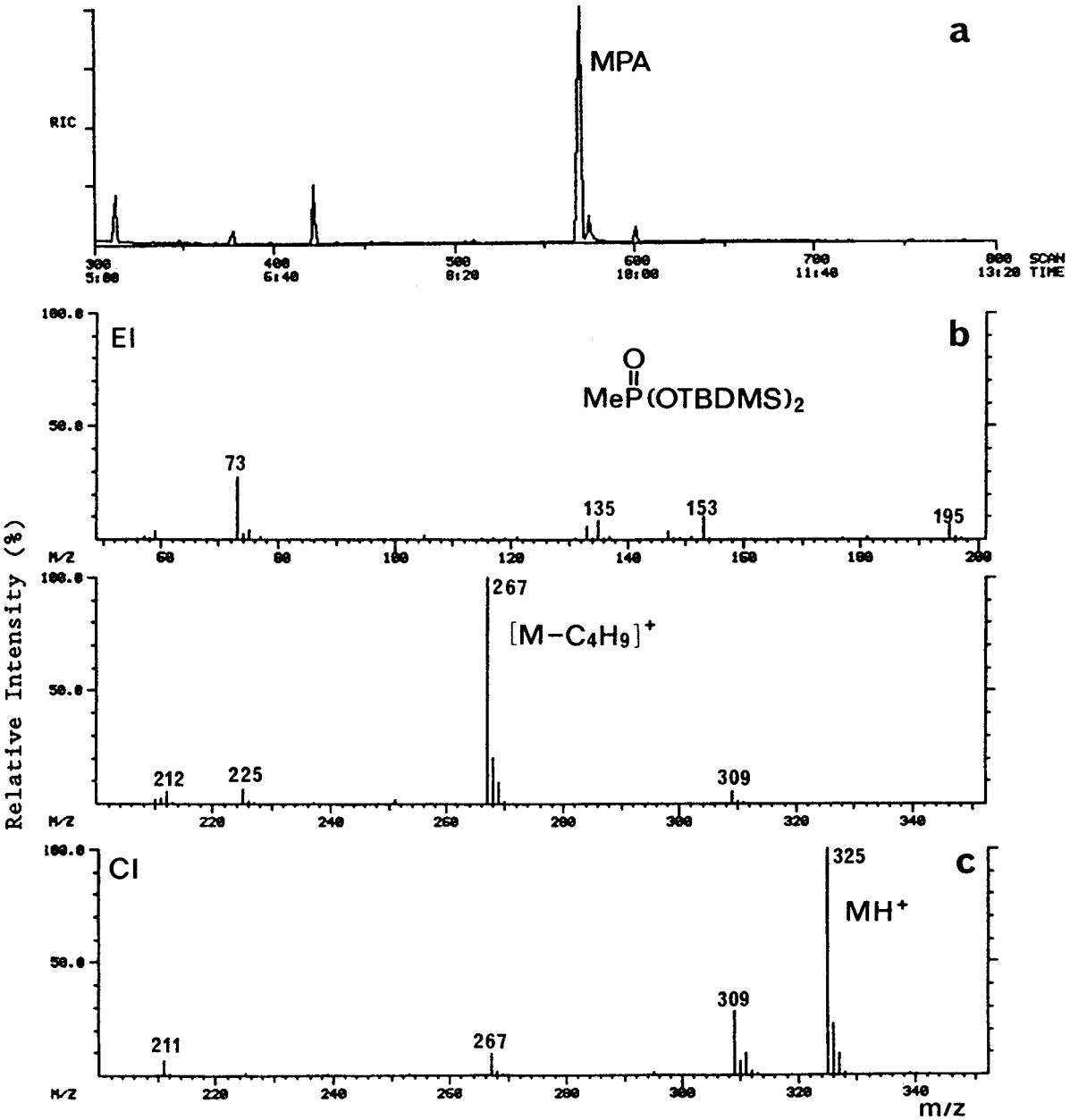

Fig. 9. (a) Total ion current chromatogram from the aqueous extract of soil sample 4J after passage through cation-exchange resin, with (b) EI and (c) CH_4 CI full scan spectra confirming the identification of MPA-$(TBDMS)_2$.

from the hydrolysis of other compounds such as fire retardants and one or two pesticides containing P–CH_3, although its presence in soil is most likely to be associated with CW use. No intact sarin was detected in any of the soil samples. In contrast to sulphur mustard, sarin is miscible with water and complete hydrolysis in a soil environment would be expected. Hydrolysis

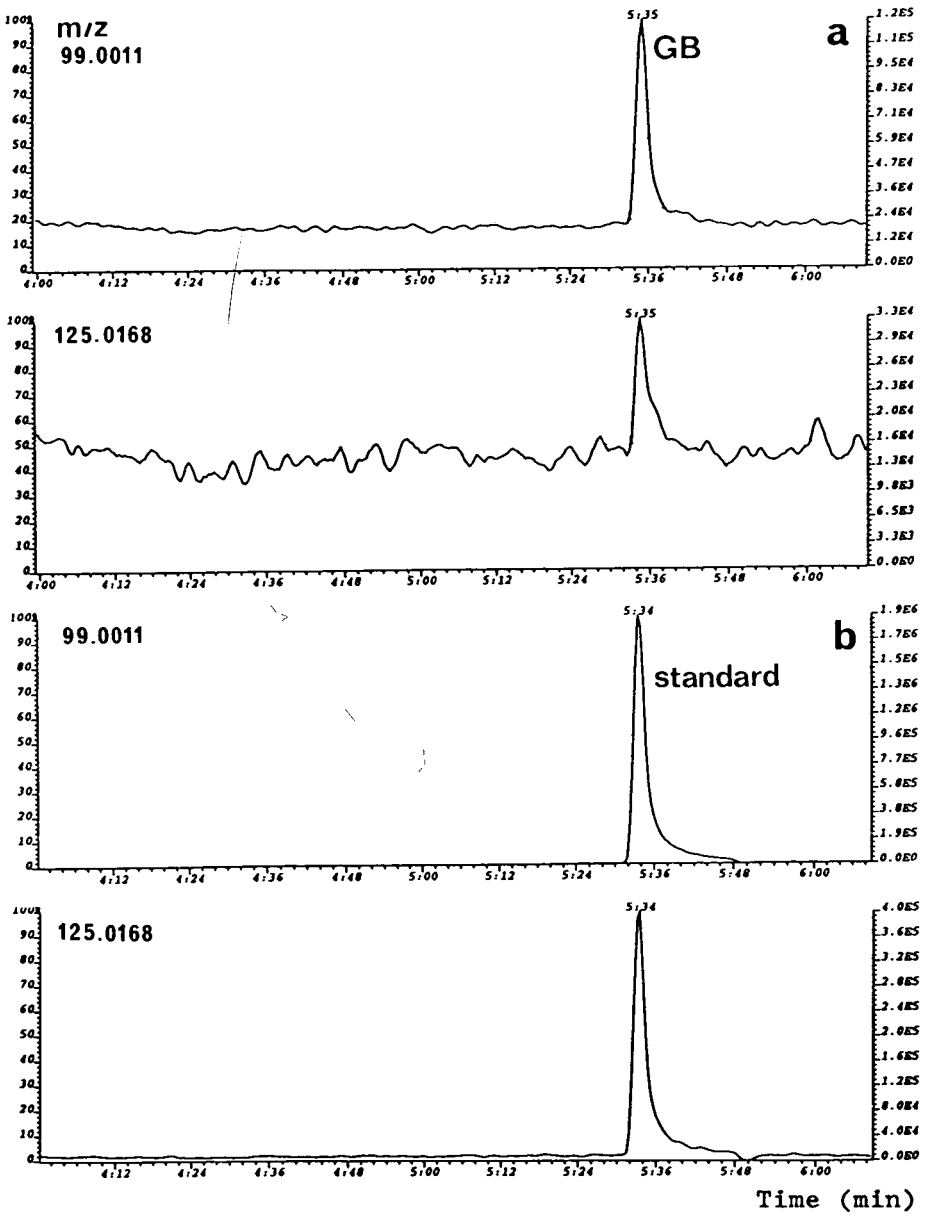

Fig. 10. Selected ion current chromatograms (EI) at 5000 resolution showing (a) the detection of GB in the dichloromethane extract of metal fragment soil 4H(M) and (b) the response from a standard (1 ng injected).

products alone were detected in nine of the twelve soil samples and these results once again emphasise the importance of analysing for hydrolysis products of CW agents in environmental samples.

The presence of sarin on the metal fragment after four years in the environment was unexpected. The GC–MS–MS data were unequivocal and clean glassware blanks were obtained for all of the analyses. This particular sample was unique in that the metal was coated with a military-type green paint. Sarin is readily

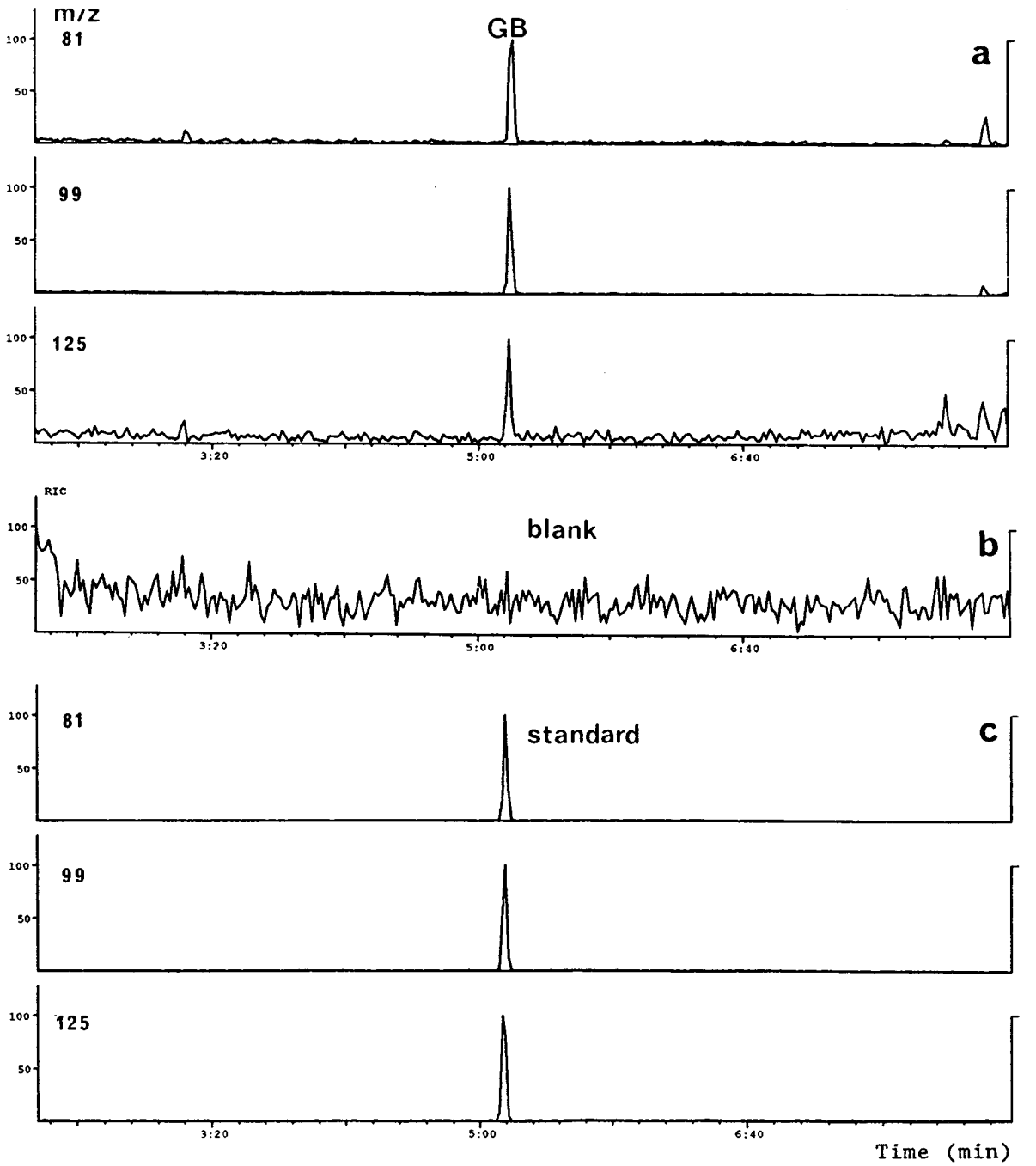

Fig. 11. GC–MS–MS-MRM chromatograms (EI, DBWAX polar column), (a) confirming the identification of GB in dichloromethane extract of metal fragment 4H(M), (b) the reconstructed ion current trace for the glassware blank and (c) the response from a standard (1 ng injected).

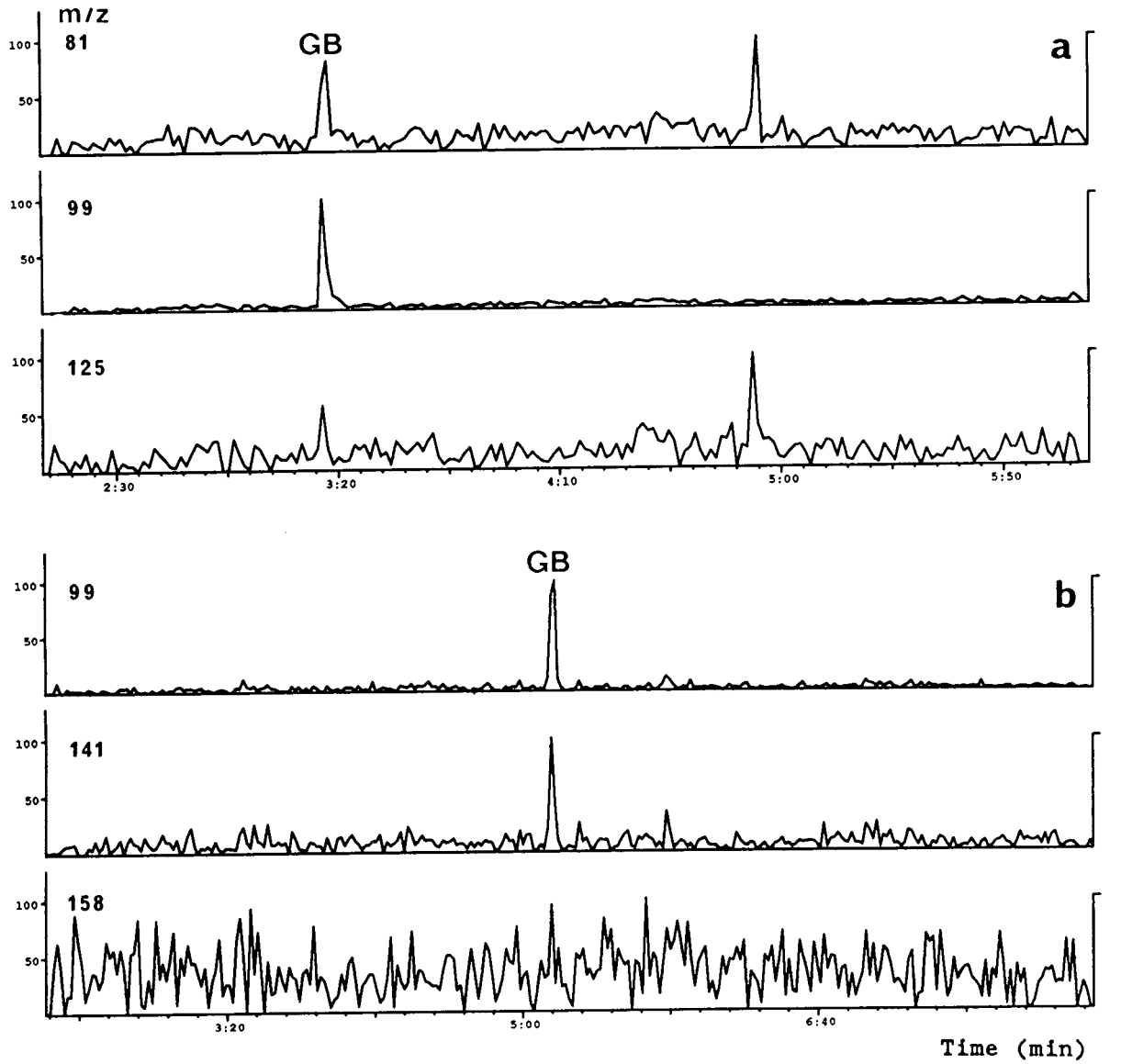

Fig. 12. GC–MS–MS-MRM chromatograms confirming the identification of GB in the dichloromethane extract of metal fragment 4H(M). (a) EI, BPX5 non-polar column; (b) NH_3 CI, DBWAX column.

absorbed into paints where it would be protected from moisture. A less likely explanation is that the sarin had been protected from environmental degradation by penetration of the double skinned layer of metal of which the fragment was composed. The detection of intact sarin on the metal fragment after four years in the environment suggests that paint may be a useful material to analyse in future investigations of alleged CW use. To our knowledge, these analyses provide the first example of an unequivocal confirmation of nerve agent residues in environmental samples collected after an alleged use of chemical weapons. It is particularly encouraging for the

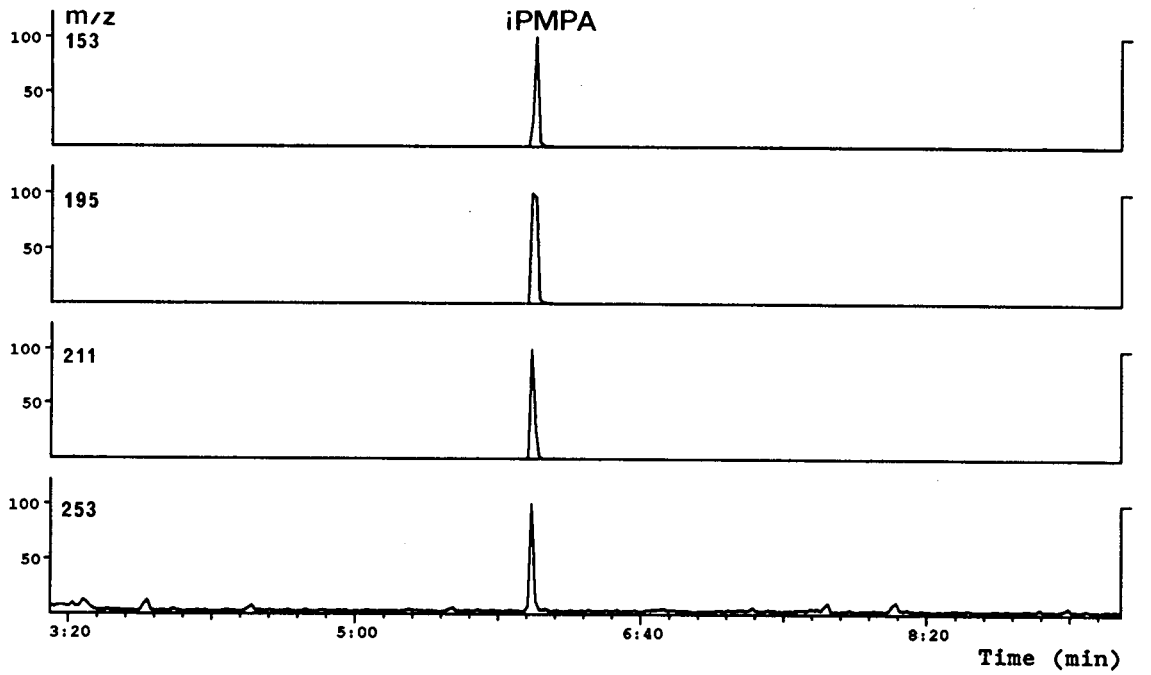

Fig. 13. GC–MS–MS-MRM chromatograms (CH_4 CI) confirming the identification of iPMPA-TBDMS in the aqueous extract of metal fragment 4H(M).

Chemical Weapons Convention that the use of both sulphur mustard and the much less persistent nerve agent sarin may be confirmed several years after the event provided that samples are collected from a point of high initial contamination.

5. Acknowledgements

The grave samples were collected by a forensic team under the leadership of Dr. Clyde Snow of the Physicians for Human Rights Organisation. The samples from bomb craters were collected by the team archeologist Dr. Jim Briscoe. Liason with CBDE was organised by Dr. Alistair Hay, Leeds University.

6. References

[1] R.M. Black and G.S. Pearson, *Chem. Br.*, 29 (1993) 584.

[2] *Report S-16433*, United Nations Security Council, New York, 1984.

[3] J.P. Perry Robinson, in *SIPRI Yearbook (1985), World Armaments and Disarmament*, Taylor & Francis, 1985, London, Ch. 6.

[4] S.J. Lundin, in *SIPRI Yearbook (1989), World Armaments and Disarmament*, Taylor & Francis, 1989, London, Ch. 4.

[5] E.R.J. Wils, A.G. Hulst and J. van Laar, *J. Anal. Toxicol.*, 12 (1988) 15.

[6] W. Vycudilik, *Forensic Sci. Int.*, 35 (1987) 67.

[7] G. Drasch, E. Kretschmer, G. Kauert and L. Von Meyer, *J. Forensic Sci.*, 32 (1987) 1788.

[8] R.M. Black, R.J. Clarke, D.B. Cooper, R.W. Read and D. Utley, *J. Chromatogr.*, 637 (1993) 71.

[9] *International Inter-Laboratory Comparison (Round-Robin) Test for the Verification of Chemical Disarmament, F.3, Testing of Procedures on Simulated Military Facility Samples*, Ministry for Foreign Affairs of Finland, Helsinki, 1992.

[10] J.G. Purdon, J.G. Pagotto and R.K. Miller, *J. Chromatogr.*, 475 (1989) 261.

[11] P.A. D'Agostino and L.R. Provost, *Biomed. Environ. Mass Spectrom.*, 13 (1986) 231.

[12] S.D. Harvey, R.J. Fellows, J.A. Campbell and D.A. Cataldo, *J. Chromatogr.*, 605 (1992) 227.

[13] E.R.J. Wils, presented at *4th International Round Robin Exercise, Meeting of Participating Laboratories, CBDE, May 1993.*

[14] B.J. Millard, *Quantitative Mass Spectrometry*, Heyden, London, 1978, pp. 127–131.
[15] P.A. D'Agostino, L.R. Provost, J.F. Anacleto and P.W. Brooks, *J. Chromatogr.*, 504 (1990) 259.
[16] P.A. D'Agostino, L.R. Provost and P.W. Brooks, *J. Chromatogr.*, 541 (1991) 121.
[17] P.A. D'Agostino and C.J. Porter, *Rapid Commun. Mass Spectrom.*, 6 (1992) 717.
[18] A. Hesso and B. Kostiainen, *Proceedings of the 2nd International Symposium on Protection Against Chemical Warfare Agents, Stockholm*, National Defence Research Institute, Umeå, 1988, p. 257.
[19] S.N. Ketkar, S.M. Penn and W.L. Fite, *Anal. Chem.*, 63 (1991) 457.
[20] C.S. Harden, A.P. Snyder and G.A. Eiceman, *Org. Mass Spectrom.*, 28 (1993) 585.
[21] E.R.J. Wils and A.G. Hulst, *J. Chromatogr.*, 454 (1988) 261.
[22] E.R.J. Wils and A.G. Hulst, *J. Chromatogr.*, 523 (1990) 151.
[23] R.M. Black and R.W. Read, *J. Chromatogr.*, 449 (1988) 261.
[24] E.M. Jakubowski, C.L. Woodard, M.M. Mershon and T.W. Dolzine, *J. Chromatogr.*, 528 (1990) 184.
[25] P.A. D'Agostino and L.R. Provost, *J. Chromatogr.*, 589 (1992) 287.
[26] *Identification of Degradation Products of Potential Organophosphorus Warfare Agents —An Approach for the Standardization of Techniques and Reference Data*, Ministry for Foreign Affairs of Finland, Helsinki, 1992.
[27] J.Aa. Tornes and B.A. Johnsen, *J. Chromatogr.*, 467 (1989) 129.
[28] M.L. Shih, J.R. Smith, J.D. McMonagle, T.W. Dolzine and V.C. Gresham, *Biol. Mass Spectrom.*, 20 (1991) 717.

Journal of Chromatography A, 662 (1994) 323–327
Elsevier Science B.V., Amsterdam

CHROM. 25 686

Separation of T-MAZ ethoxylated sorbitan fatty acid esters by supercritical fluid chromatography

Ming Y. Ye* Kim D. Hill and Ron G. Walkup

ManTech Environmental Technology, Inc. P.O. Box 1198 Ada, OK 74820 (USA)

(First received June 23rd, 1993; revised manuscript received October 27th, 1993)

ABSTRACT

The application of supercritical fluid chromatography (SFC) to the analysis of T-MAZ ethoxylated sorbitan fatty acid esters is described. SFC separation methods utilize a density programming technique and a 50 μm I.D. capillary column. This work demonstrates that capillary column SFC is a powerful technique for the analysis of complex mixtures of many derivatives of ethoxylated sorbitan fatty acids which is not amenable to gas chromatography or gel permeation chromatography. This work also demonstrates that complex distributions of polyethylene glycol can be resolved. The results of this study show how changes in chromatographic parameters affect the SFC analysis.

INTRODUCTION

T-MAZ Ethoxylated sorbitan fatty acid esters (T-MAZ) are emulsifiers with a wide range of hydrophilic characteristics. They are used to cover a wide range of oil in water and water in oil emulsification systems. They are excellent solubilizers of essential oils, wetting agents, viscosity modifiers, antistats, stabilizers and dispersing agents. They are used to prepare numerous products in the food, cosmetic, drug, textile and metalworking industries. Because their molecules contain hydrophilic and hydrophobic moieties, T-MAZ are surface-active and concentrate at interfacial regions: oil–water, for example. They are generally referred to as surfactants. Recently, there has been considerable interest in using surfactants to remediate subsurface contamination, *e.g.* to immobilize contaminants for subsequent *in situ* treatment, to release contaminants from mineral surfaces, or redistribute immobile organic phases into the mobile aqueous phase [1–3].

T-MAZ is an industrial chemical which is a complex mixture of many derivatives of ethoxylated sorbitan fatty acids. According to the manufacturer the major component, T-MAZ 60, has a molecular mass of 1300. Because of the high molecular mass and low volatility of T-MAZ, this material is difficult to analyze by GC. High-temperature GC was used to analyze sucrose fatty acid ester fractions [4]; however, a derivatization procedure has to be performed prior to analysis. Gel permeation chromatography (GPC) is a technique used for polymer analysis to determine the molecular mass distribution. However, GPC is usually used for high-molecular-mass polymers and does not give a complete separation of all the oligomers in the polymer samples. T-MAZ does not have UV-absorbing chromophores which prohibits the use of high-performance liquid chromatography (HPLC) with UV detection. Capillary column supercritical fluid chromatography (SFC) with large solute diffusion coefficients, gas-like viscosities and liquid-like densities allows high-resolution analysis of many less volatile or labile compounds [5–8]. The greater densities of supercritical fluids compared to gases lead to elution based on solute solubility, and mobile and

* Corresponding author.

0021-9673/94/$07.00
SSDI 0021-9673(93)E1151-O

stationary phase selectivity. When used with capillary columns and mobile phase density programming, many components in this complex mixture of the fatty acid esters were resolved.

EXPERIMENTAL

The SFC instrumentation is a Dionex (Sunnyvale, CA, USA) 600-D supercritical fluid/gas chromatography system which includes a syringe pump to generate the high-pressure fluid flow, a chromatograph oven for temperature control, and a data acquisition and processing system. Pressure and density programs were generated by using a Dell 486 33 MHz personal computer which allowed a variety of density gradients. Dionex data acquisition and processing system includes an advanced computer interface (ACI), a Dell 433DE computer (Dell, Austin, TX, USA) and an Epson FX-850 printer (Epson America, Torrance, CA, USA). Detection was via flame ionization detection (FID). To obtain maximum sensitivity, the hydrogen–air ratio (1:10) was optimized and the detector operated in the most sensitive range. The flow-rates were hydrogen: 30 ml/min, air: 300 ml/min and nitrogen: 25 ml/min. The detector body was heated to 390°C. Samples were introduced into the chromatographic system using a Valco (Houston, TX, USA) injector. The injection mode used was time split with the injection duration of 0.1 s. A 1-μl volume of the sample was loaded to the injector loop which has a volume of 0.5 μl. With 0.1-s time split injection, 0.3 μl (60% of 0.5 μl) sample was loaded to the SFC column. The injector was cooled at 10°C with a NesLab constant temperature circulator (NesLab, Portsmouth, NH, USA).

Separations were accomplished by using a SB-Biphenyl-30 capillary column from Dionex which is 50 μm I.D. coated with approximately 0.25 μm film thickness. The column length was 10 m. Prior to detection the supercritical fluid was decompressed and the mobile phase linear velocity controlled to approximately 1.5 cm/s by connecting the terminal end of the capillary column to a frit restrictor attached through a fused butt connector.

Supercritical carbon dioxide was used as the supercritical mobile phase. SFE-grade carbon dioxide was purchased from Scott Specialty Gases (Plumsteadville, PA, USA). T-MAZ60K POE(20) sorbitan monostearate was purchased from PPG Industries (Gurnee, IL, USA). T-MAZ is a registered trademark of PPG Industries. Polyethylene glycol standards with molecular masses of 600, 960 and 1470 were from Polymer Labs. (Foster City, CA, USA). Methanol was from Burdick & Jackson (Baxter Healthcare Corporation, Muskegon, MI, USA). All solutions were made with methanol.

RESULTS AND DISCUSSION

T-MAZ oligomers

The molecular structure of T-MAZ ethoxylated sorbitan fatty acid esters is given in Fig. 1A. The complexity of this product is mainly due to the ethoxylation of sorbitan fatty acid with various lengths of polyoxyethyl groups, $(OCH_2CH_2)_n$. One of the major components,

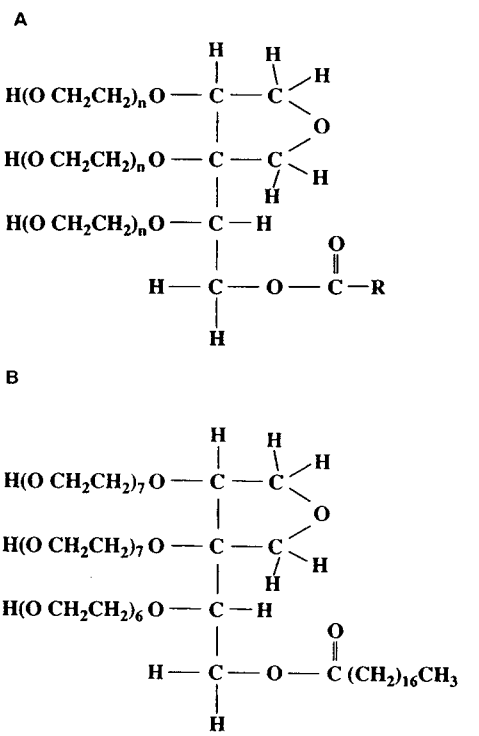

Fig. 1. Molecular structure of T-MAZ ethoxylated sorbitan fatty acid esters. (A) T-MAZ, (B) T-MAZ 60.

according to the manufacturer, is T-MAZ 60 (Fig. 1B) with total polyoxyethyl groups of 20. The molecular mass of T-MAZ 60 is about 1300. Fig. 2A shows the SFC chromatogram of T-MAZ ethoxylated sorbitan fatty acid esters, which clearly demonstrates the complexity of this product. A capillary column (10 m) with biphenyl stationary phase was used. Linear density program was taken in two steps: (1) from 0.3600 g/ml [157 atm (1 atm = 101 325 Pa), at 100°C] to 0.7000 g/ml (329 atm, at 100°C) at ramp rate of 0.01 g/ml per min and held for 20 min; (2) from 0.7000 g/ml to 0.7574 g/ml (400 atm, at 100°C) at ramp rate of 0.02 g/ml per min and then held for 50 min. The slower ramp rate of the first step allows the separation of the components in T-MAZ with the average molecular mass in the range of 1000, which will be discussed shortly.

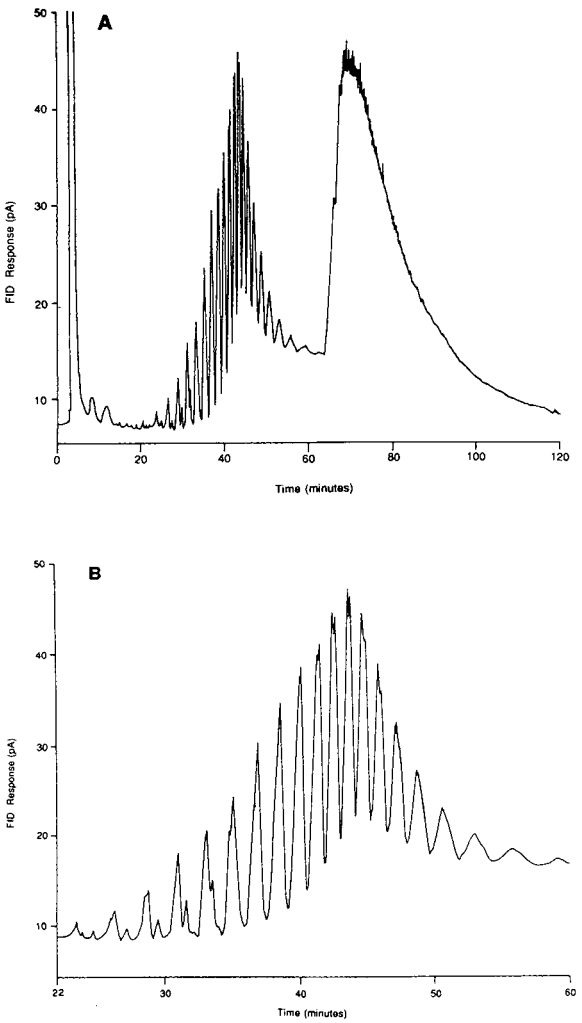

Fig. 2. SFC chromatograms of T-MAZ ethoxylated sorbitan fatty acid esters. Conditions: 10 m × 50 μm I.D. biphenyl column; CO_2 mobile phase at 100°C; Two steps linear density program: (1) from 0.3600 g/ml (157 atm, at 100°C) to 0.7000 g/ml (329 atm, at 100°C) at ramp rate of 0.01 g/ml per min and hold for 20 min; (2) from 0.7000 g/ml to 0.7574 g/ml (400 atm, at 100°C) at ramp rate of 0.02 g/ml per min and then hold for 50 min; FID at 390°C. (B) is the detail part of (A).

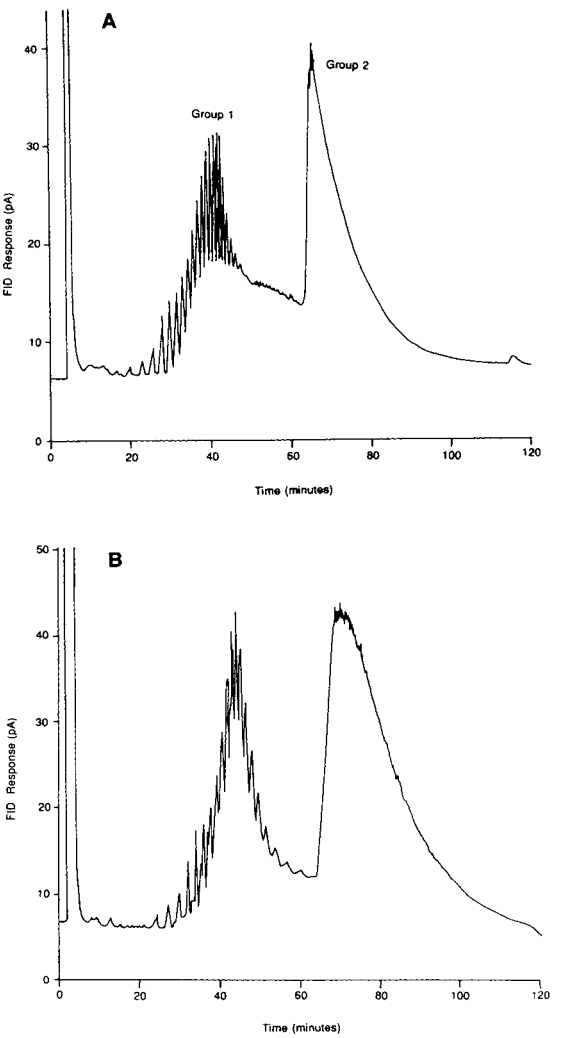

Fig. 3. SFC chromatograms of T-MAZ ethoxylated sorbitan fatty acid esters run under similar conditions except for oven temperature (A) at 80°C and (B) at 110°C, multi-step linear density program.

The column was kept at temperature of 100°C. The detail part of the chromatogram in Fig. 2A is shown in Fig. 2B. The chromatogram shows the distribution of 22 groups of oligomeric isomers eluting between 22 and 60 min. When this T-MAZ sample was analyzed by GPC, only one peak was observed [9]. The separation was also performed at 80°C and 110°C, shown in Fig. 3A and B. At 80°C the oligomers were not resolved as well as that at 100°C, and a lower ratio of peak area of group 1 and group 2 was observed, which suggests that there were more oligomers eluted at later time. This can be attributed to the lower solvating power of supercritical carbon dioxide at 80°C than that at 100°C. At 110°C, the peak resolution was significantly reduced (Fig. 3B). The experiment was also carried out at a lower FID temperature, 350°C, and the result indicated that the detector response for later-eluting peaks (high-molecular-mass components) was 20 to 40% lower at 350°C than that at 390°C. This is probably due to the condensation of

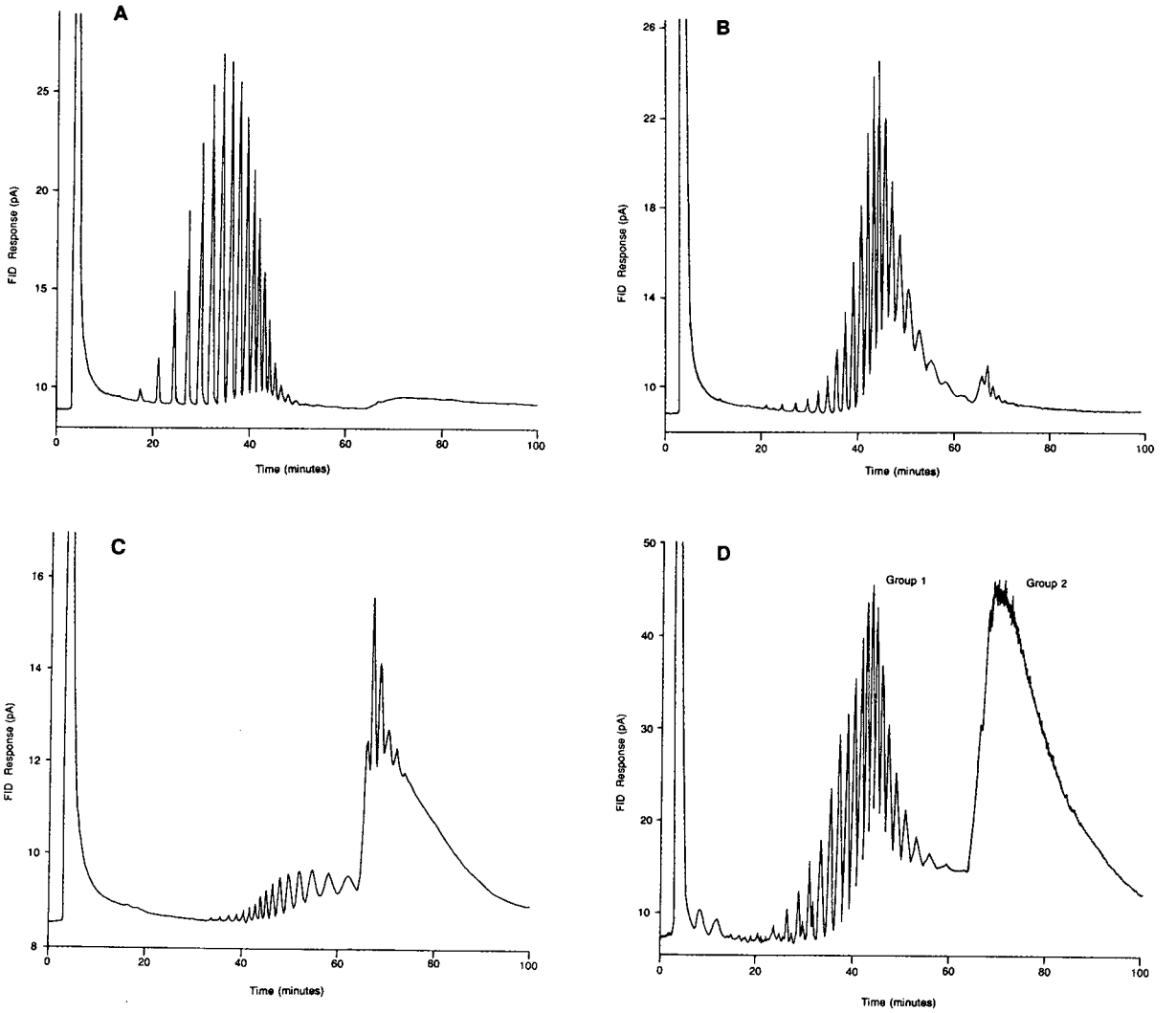

Fig. 4. SFC chromatograms of polyethylene glycol (PEG) and T-MAZ ethoxylated sorbitan fatty acid esters run under the same conditions as in Fig. 2. (A) PEG 600 at concentration, 31.4 mg/ml; (B) PEG 960, 38.0 mg/ml; (C) PEG 1470, 36.5 mg/ml; (D) T-MAZ, 35.4 mg/ml.

high-molecular-mass components in the restrictor [8].

Polyethylene glycol standards

Three PEG standards with molecular masses 600, 960 and 1470, were used to estimate the molecular mass of T-MAZ. Their chromatograms, along with a T-MAZ chromatogram, are shown in Fig. 4A–D. The SFC conditions used in the analysis of PEG standards and T-MAZ were identical. As seen from the chromatograms, SFC demonstrates excellent separation of PEG oligomers in each PEG standard. A total of 18 oligomers were found in PEG 600, 23 in PEG 960, and at least 22 in PEG 1470. With the traditionally used GPC method, only one peak can be seen in each of these PEG standards [9]. Since the molecular mass of each peak in the PEG standards is unknown, it is impossible to make a specific estimation of molecular mass for each peak found in T-MAZ. However, the molecular mass of the oligomers in T-MAZ as groups can be estimated. Assuming that the oligomers of the PEG standards and the oligomers of T-MAZ with the same molecular mass have similar solubility in supercritical carbon dioxide at the same density and have similar interaction with the stationary phase of the capillary column, then the molecular mass of the first group of oligomers in T-MAZ (Fig. 3A) was estimated to be in the range of 900 to 1000, and the second group in the range of 1000 to 1500.

ACKNOWLEDGEMENTS

The authors wish to think Dr. Candida West of US Environmental Protection Agency, Dr. Dennis Fine of ManTech Environmental Technology, Inc., David E. Knowles and Nathen Porter of Dionex Corporation for valuable suggestions and discussions.

DISCLAIMER

Although the research described in this article has beenfunded wholly or in part by the US Environmental Protection Agency through Contract 68-C8-0025 to ManTech Environmental Technology, Inc., it has not been subjected to Agency review and therefore does not necessarily reflect the views of the Agency and no official endorsement should be inferred.

REFERENCES

1 C.C. West and J.H. Harwell, *Environ. Sci. Technol.*, 26 (1992) 2324.
2 M. Harper and C.J. Purnell, *Environ. Sci. Technol.*, 24 (1990) 55.
3 J. Lee, J.R. Crum and S.A. Boyd, *Environ. Sci. Technol.*, 23 (1989) 1365.
4 R. Karrer and H. Herberg, *J. High Resolut. Chromatogr.*, 15 (1992) 585.
5 B.W. Wright, H.T. Kalinoski and R.D. Smith, *Anal. Chem.*, 57 (1985) 2823.
6 R.D. Smith, J.C. Fjeldsted and M.L. Lee, *J. Chromatogr.*, 247 (1982) 231.
7 H.T. Kalinoski, H.R. Udseth, E.K. Chess and R.D. Smith, *J. Chromatogr.*, 394 (1987) 3.
8 D.E. Knowles, L. Nixon, E.R. Campbell, D.W. Later and B.E. Richter, *Fresenius' Z. Anal. Chem.*, 330 (1988) 225.
9 M.Y. Ye, K.D. Hill and R.G. Walkup, *Chromatographia*, in press.

Journal of Chromatography A, 622 (1994) 329–340
Elsevier Science B.V., Amsterdam

CHROM. 25 697

Chromium determination by supercritical fluid chromatography with inductively coupled plasma mass spectrometric and flame ionization detection

Jeffrey M. Carey[☆], Nohora P. Vela and Joseph A. Caruso*

University of Cincinnati, Department of Chemistry, Cincinnati, OH 45221-0172 (USA)

(First received July 2nd, 1993; revised manuscript received October 26th, 1993)

ABSTRACT

Supercritical fluid chromatography (SFC) has been investigated for the separation of a pair of β-ketonate chromium compounds and a thermally labile organochromium dimer. A limited comparison between flame ionization detection (FID) and inductively coupled plasma mass spectrometric (ICP-MS) detection of these compounds is presented. The β-ketonate complexes were observed with both detectors, while the thermally labile dimer was not observed with ICP-MS detection. Detection limits for these compounds with ICP-MS were in the range of 0.9 to 3 pg with FID giving values between 10 and 250 pg. Reproducibility of the method is between 1 and 4% relative standard deviation (R.S.D.). The technique provided a linear response over approximately three orders of magnitude. The effect of two mobile phases (nitrous oxide and carbon dioxide) on the detection by each of the detectors are presented in a qualitative manner. Finally, the SFC–ICP interface heating method and the manner in which the restrictor is heated in the FID system are compared and there effect on the chromatography discussed.

INTRODUCTION

Coupling supercritical fluid chromatography (SFC), as well as other chromatographic methods, to inductively coupled plasma mass spectrometry (ICP-MS) has received increasing interest in recent years as the need for speciation information on a particular sample begins to rival the need to achieve ultra-trace level detection [1–3]. This increasing demand comes from the dependence of the chemical form or environment of a given element on its toxicity. An important example of such an element is chromium. Chromium(III) is an essential element for good nutrition and health while chromium(VI) is a known carcinogen; therefore, a total chromium level determination for a given sample is not sufficient. In order to accurately assess the toxicological concern of the sample, a determination of the chromium form is required for an accurate assessment of the toxicological and environmental concern.

While the trivalent form of chromium is the most innocuous and common form, the hexavalent form is the most industrially important. Sodium chromate and dichromate are principal materials in the production of all chromium containing chemicals. These chromates are produced by a smelting, roasting, and extraction process from chromite ore. The major uses of chromium, and therefore, environmental sources, are: the production of stainless steel; leather tanning; pigment production; wood preservatives; and anti-corrosives in cooking systems and boilers [4].

A number of different liquid chromatographic

* Corresponding author.
☆ Present address: The Lubrizol Corporation, 29400 Lakeland Boulevard, Wickliffe, OH 44092, USA.

0021-9673/94/$07.00
SSDI 0021-9673(93)E1144-O

methods have been employed for speciation of the different chromium oxidation states and different complexed forms of chromium [5–10]. Because of the limitations in the analysis of highly polar compounds via SFC, for analysis of ionic compounds, it may be necessary to complex the chromium prior to injection into the SFC system. For these reasons, β-ketonate compounds were chosen for this study. Chromium β-ketonate complexes have previously been used with reversed-phase LC to provide chromophores for the UV detector [5,6].

Reports have appeared on the use of supercritical fluid chromatography for the separation of metal β-ketonate complexes using ICP atomic emission spectroscopy and UV absorption spectrometric detection [11–13]. These reports, however, use packed column SFC instruments which may not be the most advantageous for ICP detection. The higher flow rates, relative to capillary systems, of mobile phase may cause severe perturbations in the plasma relative to those found with capillary SFC sample introduction. A review of SFC–plasma spectrometry has appeared [14], and the coupling of capillary SFC to ICP-MS has been performed successfully previously in our laboratory and been reported [15–17].

When using a new detector for a chromatographic method (such as ICP-MS) it is important to have a grasp on the detector's effect on the separation. Flame ionization detection (FID) was chosen as the detection method for comparison to ICP-MS due to its preferred usage for capillary SFC. The work presented in this report will investigate the effect of pressure programming with both ICP-MS and FID, the effect of mobile phase, and the effect of the SFC–ICP interface on the analysis.

EXPERIMENTAL

SFC Instrumentation

The supercritical fluid chromatograph used has been described in detail previously [15] (Fig. 1). It consisted of a Hewlett-Packard 5890 Series II gas chromatograph (Hewlett-Packard, Avondale, PA, USA) and a Lee Scientific Series 600 supercritical fluid pump (Lee Scientific Division of Dionex, Salt Lake City, UT, USA) controlled by an XT-clone computer. Mobile phases used were supercritical fluid grade liquid carbon dioxide and supercritical fluid-grade liquid nitrous oxide (Scott Specialty Gases, Plumsteadville, PA, USA). The column used was a 4 m long capillary which had an internal diameter of 50 μm. The stationary phase, which had a film thickness of 0.25 μm, was SB-biphenyl-30 (Dionex). A 1.5 cm/s linear velocity frit restrictor was used which had a length of 1.5 m (Dionex). The SFC–ICP interface has also been described previously [15] and differed only in that the interface was constructed from brass, rather than stainless steel; to avoid chromium contamination. The injector and pump were cooled, through the use of a recirculating chiller, to approximately 0°C.

FID

The chromatographic conditions to be compared to those obtained with ICP-MS were obtained with FID (Hewlett-Packard). The FID signal obtained was collected using a Hewlett-Packard 3396 Series II integrator. The integrator data were then collected by a 386SX computer, equipped with Hewlett-Packard's Peak96 software.

ICP-MS Instrument

The inductively coupled plasma mass spectrometer used in this study was a VG PlasmaQuad II STE (Fisons Instruments, Winsford, UK). SFC was coupled to ICP-MS by removing the pneumatic nebulizer and spray chamber, and replacing them with the SFC–ICP interface. No other modifications to the instrument were necessary. The ICP-MS operating conditions are shown in Table I. It is important to note that since the SFC sample introduction method produces a "dry plasma", it is necessary to tune on either a background spectral feature (such as the peak at $m/z = 56$ resulting from ArO^+) or an element which has a high vapor pressure and can be introduced into the dry plasma (such as mercury).

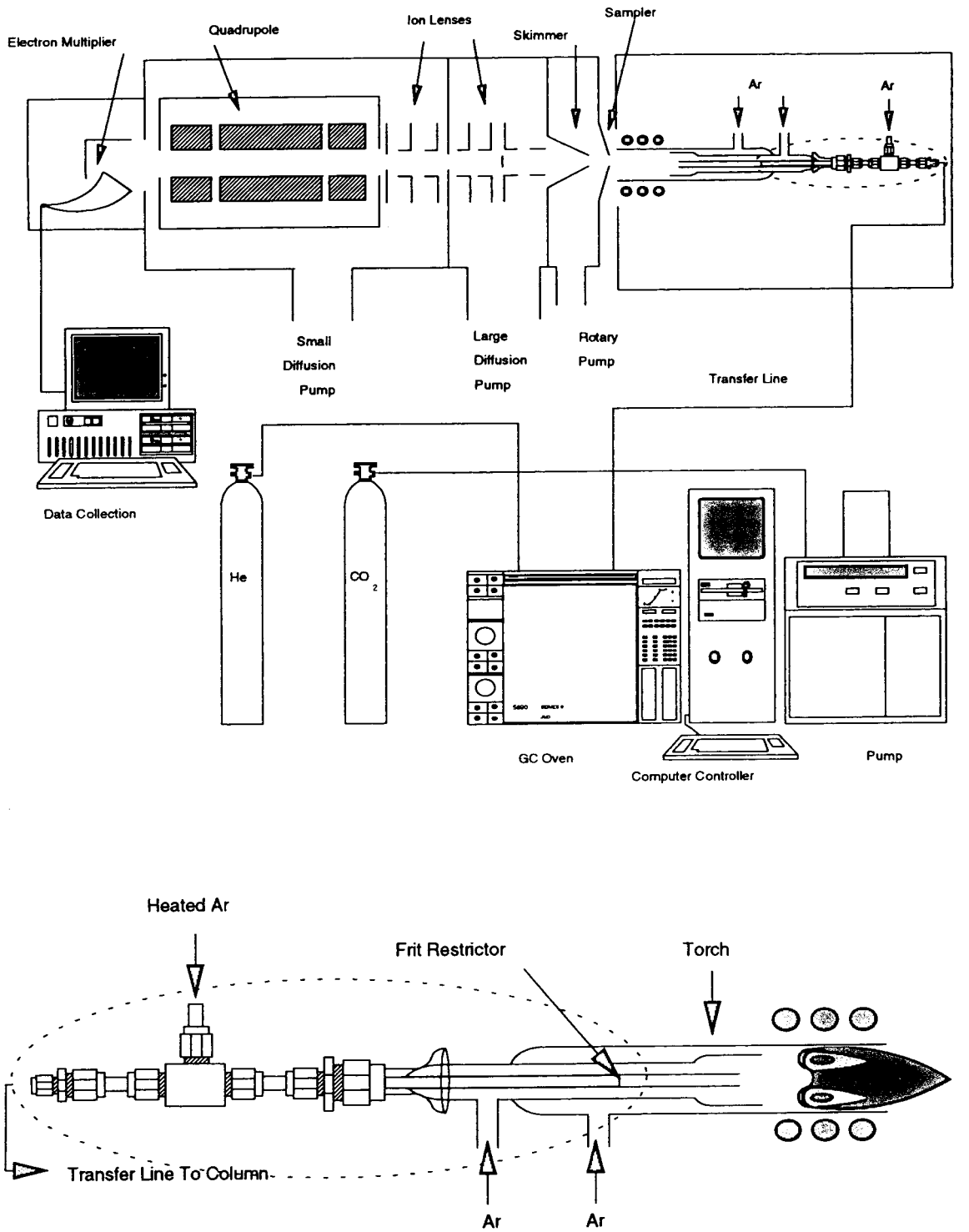

Fig. 1. SFC–ICP-MS instrument diagram showing the SFC–ICP interface.

TABLE I

FID AND ICP-MS OPERATING CONDITIONS

FID Conditions		
Temperature[a]	375°C	
Nitrogen flow	31 ml/s	
Hydrogen flow	50 ml/s	
Air flow	400 ml/s	
ICP-MS Conditions		
Interface temperature[a]	300°C	
Transfer line temperature[a]	80°C	
Injector gas flow	0.9 l/min	
Auxillary gas flow	1.5 l/min	
Coolant gas flow	15 l/min	
Forward power	1.35 kW	
Reflected power	Less than 5 W	
Ion lens tuning	m/z 56 (ArO^+)	
Expansion pressure	Less than 2 mbar	
Intermediate pressure	Less than 10^{-4} mbar	
Analyzer pressure	Approximately $5 \cdot 10^{-6}$ mbar	
SFC Conditions		
Ramp rate[a]	30 atm/min (FID) or	70 atm/min (ICP-MS)
Initial pressure[a]	85 atm	
Initial hold time[a]	4 min	
Oven temperature[a]	70°C	

[a] Optimized condition.

Reagents

Chromium(III) 2,4-pentanedionate [$Cr(C_5H_7O_2)_3$, PDC, M_r 349] was purchased from Alfa Products (Ward Hill, MA, USA) and was used without further purification. Chromium(III), 2,2,6,6-tetramethyl-3,5-heptanedionate [$Cr(C_{11}H_{19}O_2)_3$, MHDC, M_r 602] and pentamethylcyclopentadienylchromium dicarbonyl dimer {$[(CH_3)_5C_5Cr(CO)_2]_2$, MCCD, M_r 757, decomposes at 200°C} were obtained from Strem Chemicals (Newburyport, MA, USA) and were also used without further purification. All solutions were prepared in optima-grade methylene chloride (Fisher Scientific, Fairlawn, NJ, USA).

RESULTS AND DISCUSSION

FID Separation optimization

The chromatographic conditions, initial hold time, initial pressure, ramp rate, oven temperature and FID temperature, for these compounds were optimized using FID. A univariate optimization approach was used for the investigation. The parameters studied were the initial hold time, initial pressure, ramp rate, oven temperature and detector temperature. The optimum conditions found for the optimized parameters are shown in Table I. Optimum conditions were chosen to allow for the shortest analysis time with the best separation.

When no hold time was initially used (no period of constant pressure) the first eluting peak (MHDC) was not observed and was assumed to be co-eluting with the solvent peak. This assumption was based on the expected elution order due to the relative polarities and sizes of the compounds in question. Therefore, in order to effectively resolve the relatively non-polar MHDC from the solvent peak it was necessary to utilize a period of constant pressure prior to the start of any pressure ramp (times of 3.5 to 6 min were investigated). The four-minute hold time was chosen for the separation of MHDC from the solvent peak, and allowed for good resolution of the latter eluting PDC and MCCD peaks.

The next parameter investigated was the initial pressure. As previously stated, the initial hold time used was 4 min while each of the other parameters had the same values as used in the preceeding optimization. While holding these parameters constant, the initial pressure was varied between 70 and 120 atm (1 atm = 101 325 Pa). At pressures below 85 atm, the two later eluting peaks are not observed during the time the signal was acquired. At pressures above 110 atm, the MHDC peak is not observed and is assumed to be co-eluting with the solvent peak. Both sets of peaks (MHDC/solvent and PDC/MCCD) are nearly baseline resolved at 85 atm, and therefore this pressure was chosen for future use.

The ramp rate was also optimized in a univariate manner by varying the rate from 10 to 60 atm/min. Each of the previously optimized parameters were used (initial hold time of 4 min and an 85 atm initial pressure) and the other variables were also held constant. Unlike the previous optimizations, all three of the com-

pounds were observed under each of the conditions. When both analysis time considerations and resolution of the peaks were considered, the optimal condition for the ramp rate was chosen to be 30 atm/min. This value was chosen due to the increased resolution over faster ramp rates, compared to the improvement in analysis times.

An important parameter with SFC (besides the pressure) is the temperature of the supercritical fluid. The previously determined conditions were used for the optimization, along with a FID temperature of 325°C. As the oven temperature is increased, the density is decreased, and, therefore, the capacity factor for each of the compounds in question increases. Another aspect is that the solvent is not affected to as large an extent as the three compounds due to the decreased mobile phase densities at higher temperatures and the less volatile nature of the compounds.

From an analysis of the capacity factors alone, it might be assumed that for these compounds, the lower temperatures might be optimal. However, the separation between PDC and MCCD is greatly affected by the oven temperature. This is probably due to the more polar nature of these compounds. Since they are more polar, they have a greater affinity for the induced dipoles of the stationary phase. Therefore, a stronger solubilizing ability of the mobile phase is required to elute these compounds, leading to larger differences in elution at lower densities (and longer retention times). Given that PDC and MCCD are nearly baseline resolved and that the resolution between the solvent peak and MHDC is not overly large at 70°C, this was chosen as the optimum condition for the separation.

FID Temperature optimization

Previous work has shown that the temperature of the restrictor may have a marked effect on the chromatographic performance of the system [19]. This has been particularly observed with the previously described SFC–ICP interface. These effects have included losses in signal, particularly for less volatile compounds, changes in retention times, and freezing of the restrictor tip. In this study, the effect of the restrictor temperature, through the FID temperature, on the peak areas of the three compounds and on the capacity factors for each of the three compounds was investigated. This will allow a clearer determination of whether or not the restirctor is being heated in the same manner with the SFC–ICP interface, as it is with a well-defined detection method such as FID.

Fig. 2 illustrates the effect of different FID temperatures on each of the three compounds. Fig. 2A shows a decreasing trend for the capacity factors as the FID temperature is increased. This is to be expected because as the FID temperature is increased the frit in the restrictor expands, causing further restriction of the flow of carbon dioxide. This has the effect of increasing the analysis times with increasing FID temperature. Fig. 2B illustrates the effect of the FID

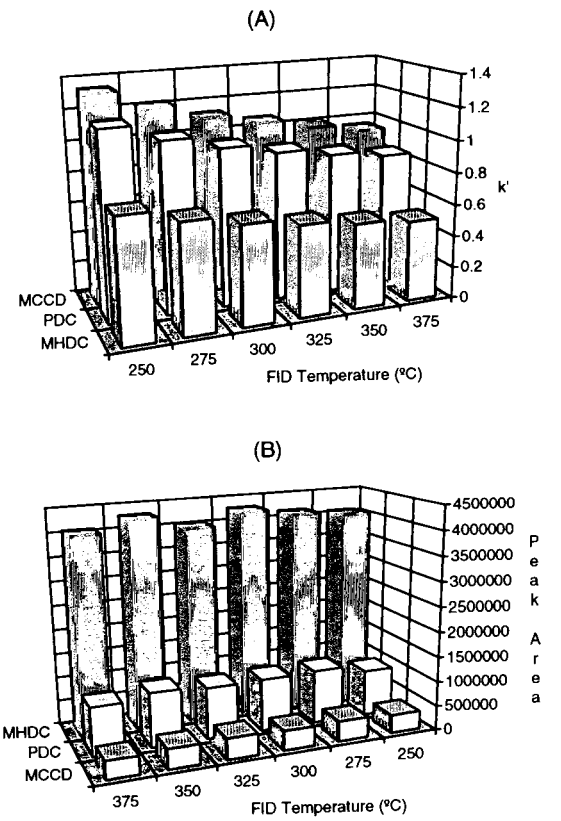

Fig. 2. SFC–FID detector temperature optimization: (A) indicates the capacity factors for each of the three compounds (MHDC, PDC and MCCD) and (B) indicates the peak areas for each of the compounds.

temperature on the area of each of the peaks. It is interesting to note that the detector temperature seems to have no effect on the peak areas obtained. This result is important since a different result was expected using the SFC–ICP interface [19]; indicating that if this is indeed the case, the restrictor is heated in a different manner with the SFC–ICP interface requiring further study of the interface fundamentals. Because the FID temperature seemed to have little effect on the analysis, and 375°C gave the fastest analysis times, it was decided that this temperature would be used as the optimal.

SFC–FID Mobile phase considerations

The chromatograms found using the conditions described previously are shown in Fig. 3 for a carbon dioxide mobile phase and Fig. 4 for a nitrous oxide mobile phase. Carbon dioxide is, by far, the most commonly used mobile phase for SFC due to its non-toxic nature, availability in highly purified forms, and relative low cost. An additional factor in the favorable nature of carbon dioxide as a SFC mobile phase is that it produces minimal FID signal, the most common detection method for reasons previously described. Indeed, as is shown in Fig. 3, a good separation for the compounds was achieved with minimal background signal. The peaks shown, in order of increasing retention time, are methylene chloride, MHDC, PDC, and MCCD.

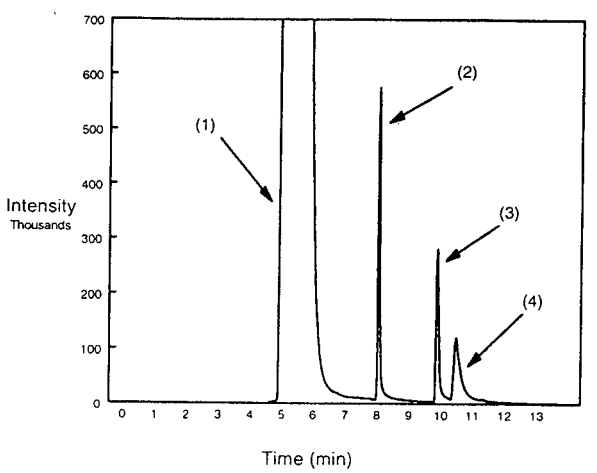

Fig. 3. SFC–FID chromatogram using a carbon dioxide mobile phase for a 10 ng mixture of MHDC (2), PDC (3) and MCCD (4) in methylene chloride (1).

Despite the successful separation of the compounds with the flame ionization detector using a carbon dioxide mobile phase, there were expected difficulties with the use of carbon dioxide for ICP-MS detection. These difficulties result from an expected isobaric interference at m/z 52 (the major isotope of chromium) from the polyatomic species $^{40}Ar^{12}C^{+}$. For this reason, the use of an alternative mobile phase, nitrous oxide, was investigated. Nitrous oxide was chosen due to its similar solvating properties to those of supercritical carbon dioxide. The main difference between the two fluids is that nitrous oxide has a slight dipole moment, making it somewhat polar.

As can be observed in Fig. 4, this mobile phase is not ideal for FID, as sufficient ionization of the nitrous oxide occurs to cause a fairly intense background signal. The background signal mirrors the pressure program, as a greater amount of nitrous oxide is introduced into the flame ionization detector at higher pressures. This background signal obscures the detection of the later eluting compounds at lower concentrations. It can be observed, however, in Fig. 4 that for a 100 ng mixture, the chromatographic separation is maintained.

SFC–ICP-MS Mobile phase backgrounds

When switching of ICP-MS detection, it was hoped that minimal differences in the chromato-

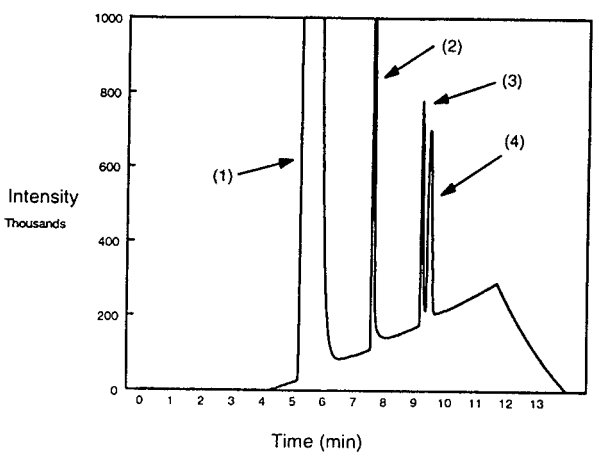

Fig. 4. SFC–FID chromatogram using a nitrous oxide mobile phase for a 100 ng mixture of MHDC (2), PDC (3) and MCCD (4) in methylene chloride (1). The large baseline increase is due to ionization of the nitrous oxide mobile phase.

graphic conditions would be observed. Therefore, it would be desirable to use the same mobile phase as is most favorable for FID. However, as previously mentioned, this was not believed to be possible. In order to determine the feasibility of using both carbon dioxide and nitrous oxide mobile phases, background scans of the plasma while introducing each of the mobile phases at a given pressure were acquired. These scans are shown in Fig. 5 for the introduction, from an isobaric pressure program at 100 atm, of carbon dioxide (A) and nitrous oxide (B). Fig. 5A clearly shows that the detection of chromium at the major isotope (m/z 52) would be extremely difficult due to the large background signal at this mass from ArC^+. In addition, large argon oxygen polyatomic species are observed which may interfere with the determination of iron at m/z 56. A large peak is also

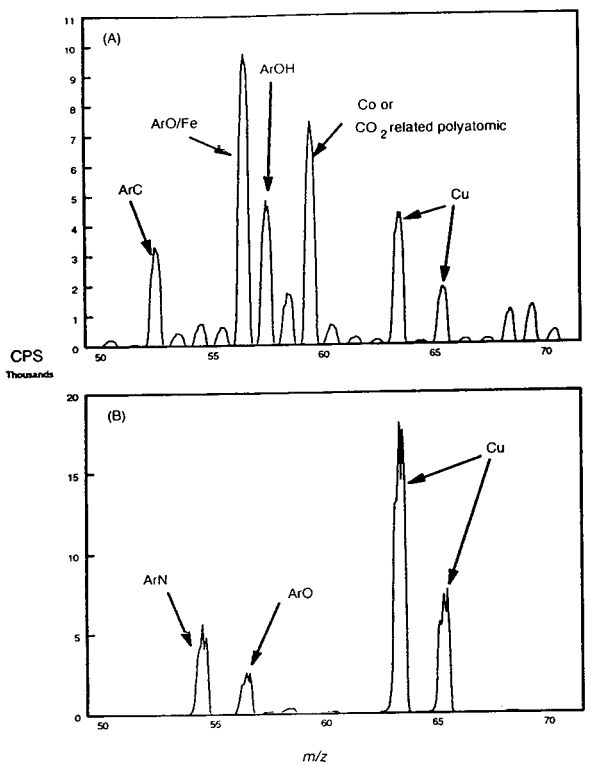

Fig. 5. ICP-MS background scans: (A) is the resulting background from introducing carbon dioxide from a constant pressure program at 100 atm; (B) is the resulting background from introducing nitrous oxide from a constant pressure program at 100 atm.

observed at m/z 59 which corresponds to cobalt. However, a cobalt contamination source was not found, and this peak is believed to be resulting from an unknown carbon dioxide related polyatomic (possibly $HNCO_2^+$).

From Fig. 5B it is observed that with nitrous oxide a much simpler background spectrum is observed. The main peak of note occurs at m/z 54 corresponding to $^{40}Ar^{14}N^+$. This particular mass to charge ratio does not correspond to the major isotope of any elements. Despite not interfering with the major isotope of any elements, this background feature may interfere with isotope ratio determinations for both iron and chromium. Large peaks associated with copper in both of the scans are from the brass SFC–ICP interface. The peaks for the copper in the nitrous oxide scan are larger because the interface was brand new. As the interface ages and is heated for a period of time this signal begins to decrease as the copper surface is oxidized. The carbon dioxide scan shown in Fig. 5A was acquired after the interface had been used for several days.

Problems with thermally labile MCCD

Once it was determined that a nitrous oxide mobile phase would be necessary for ICP-MS detection, each of the three compounds were injected to determine what changes, if any, were observed with their elution. Both of the β-ketonate complexes were found to elute with similar characteristics to FID (with slightly shorter retention times); however, no peak was observed for the MCCD compound. This was unexpected since the compound was easily observed with FID, and peak identification could be made based on retention time. There are several possible causes for the "loss" of this compound including thermal decomposition of the compound in the restrictor followed by irreversible binding to the capillary tube walls and an oxidatively driven decomposition of the compound (using a N_2O mobile phase) with irreversible binding to the capillary walls.

The second of these possibilities is the most unlikely, primarily due to the observation of the compound (albeit in high concentrations) on FID with the nitrous oxide mobile phase. This conclusion is based on the fact that MCCD is known to

decompose at 200°C. Since the interface is heated for a length of nearly 30 cm, the compound is exposed to the high temperatures for a longer period of time than in the FID detector (approximately 8 cm). This will most likely cause the decomposition of the compound, and the chromium is then in an inorganic, or highly polar organic, form which irreversibly binds to the deactivated fused silica capillary tubing walls. The supercritical nitrous oxide then does not have sufficient solvating power to elute the remaining chromium.

A further possibility for the loss of the MCCD is that the interface temperature is too low and the compound is freezing in the restrictor. This type of behavior has been observed previously with non-volatile tin compounds [19]. Because of this possibility, the interface temperature was optimized while injecting the MCCD. However, the compound was not observed at any of the temperatures investigated, reducing the possibility of this being the cause of the loss.

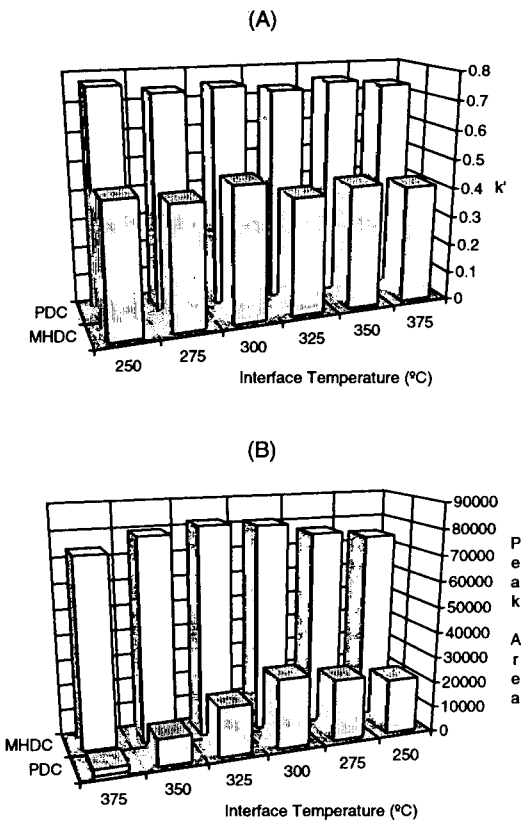

Fig. 6. SFC–ICP interface temperature optimization: (A) indicates the capacity factors for both of the detected compounds (MHDC and PDC); (B) indicates the peak areas obtained for the compounds.

SFC–ICP Interface temperature optimization

Despite the loss of the MCCD compound, it was necessary to optimize the interface temperature, to achieve optimum sensitivity, for the pair of β-ketonate complexes. Fig. 6 illustrates the effect of this parameter on both PDC and MHDC. Since the solvent is a carbon-containing compound, it gives an ArC^+ signal in the ICP-MS allowing the determination of capacity factors. It is interesting that the trends observed are not at all the same as those observed for FID. The capacity factors, Fig. 6A, increased on FID with increasing frit temperature, (the interface and FID temperatures are both essentially the temperature of the frit restrictor) while with ICP-MS detection there is no effect with increasing restrictor temperature on the capacity factor. The retention times were observed to increase; however, the void volume time (solvent peak) increased accordingly. A further difference is that for the more polar PDC, the peak widths were larger at higher temperatures than those observed with FID. Clearly the restrictor in the ICP-MS interface is being heated in a manner different from that in the FID system.

This conclusion is further illuminated by the results shown in Fig. 6B. The peak areas, particularly for the PDC compound, are affected by the SFC–ICP interface temperature. At higher temperatures the PDC compound gives a much smaller peak than at temperatures less than about 325°C. The reason for the significant effect on the signal from PDC is the more polar nature of the compound requiring greater solvating power of the nitrous oxide, which is not available at the higher temperatures (PDC is slightly soluble in water while MHDC is only soluble in relatively non-polar organic solvents).

Since the MCCD compound was not observed with the ICP-MS and no immediate solution to this problem was found, the ramp rate was re-optimized to improve the analysis time. At a ramp rate of 70 atm/min good resolution was found with a sufficiently fast separation (less

than 7 min) and, therefore, this value was chosen as optimal. The chromatographic conditions chosen for the SFC–ICP-MS analyses are shown in Table I.

SFC–ICP-MS Chromatogram and figures of merit

Fig. 7 shows the chromatogram achieved for a 10 ng injection of MHDC and PDC in methylene chloride. This chromatogram was acquired using a nitrous oxide mobile phase and the conditions listed in Table I for ICP-MS, while monitoring m/z 52. Analytical figures of merit for these compounds are listed in Table II. The detection limit for MHDC was less tan one picogram while the detection limit for the PDC was approximately three picograms. These detection limits were calculated using three times the standard deviation of the blank and dividing by the slope of the calibration curve. The linearity of the calibration curves was tested between 0.1 and 100 ng and was found to be quite linear for both compounds. Linearity of the curves was confirmed through the correlation coefficient (R^2) values and the slope of the log–log calibration curve being near one. Finally, the reproducibility of the measurements was tested for five replicate injections of 1 ng of each of the compounds (as chromium). The relative standard deviation (R.S.D.) was found to be less than 3% for the peak area of both compounds.

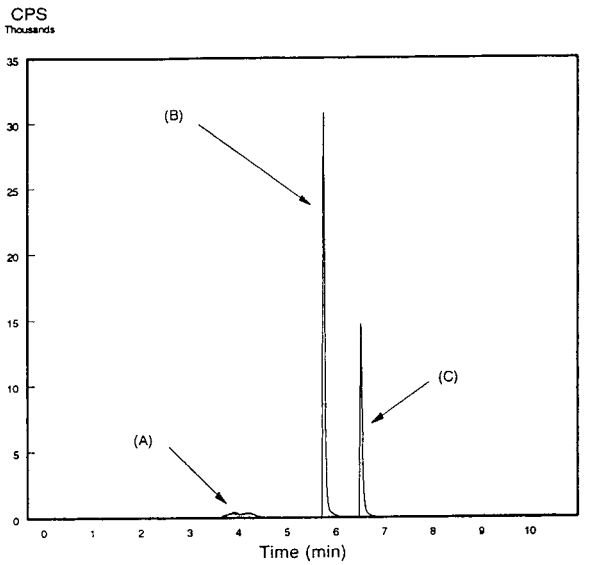

Fig. 7. SFC–ICP-MS chromatogram at m/z 52 using the optimal conditions and a 10 ng mixture. A = Solvent; B = MHDC; C = PDC.

Peak shape analysis

A measure of comparison between the chromatographic efficiency of the two methods is the extra-column variance (or peak broadening in the interface). As can be seen in Table III the expected peak broadening in the SFC–ICP interface was not observed for either MHDC or PDC. The variance was analyzed by normalizing the signal intensity and time scale, while measur-

TABLE II

SFC–ICP-MS ANALYTICAL FIGURES OF MERIT

Detection limits based on 3σ calculations.

	Chromium(III) 2,2,6,6-tetramethyl-3,5-heptanedionate	Chromium(III) 2,4-pentanedionate
Detection limit	0.9 pg	3 pg
Relative standard deviation (%)	1.4	2.6
Linear range	0.1–100 ng	0.1–100 ng
Log–log slope	0.99	0.98
Correlation coefficient	0.999	0.999

TABLE III

PEAK SHAPE INFORMATION FOR FID AND ICP-MS DETECTION OF SFC

Peak shape factor	FID	ICP-MS
MHDC		
Asymmetry factor	1.1	1.5
Total system variance (σ^2)	22 mm^2	15 mm^2
Variance difference (σ_{ex})	2.7 mm	N/A[a]
PDC		
Asymmetry factor	1.4	1.8
Total system variance (σ^2)	31 mm^2	24 mm^2
Variance difference (σ_{ex})	2.6 mm	N/A

[a] N/A = Not applicable.

ing the peak widths at half maximum (see Fig. 8). The differences in the system variance result from differences in analysis times and from differences in the heating of the restrictor. A result such as this probably means that the observed differences in peak widths are due to an increase in the variance from the analytical column (increased retention time) rather than any extra column effects, *per se*.

A final measure of the quality of the chromatogram is the deviation from a Gaussian peak, the asymmetry factor. Table III clearly indicates a difference in the peak shape for PDC and MHDC with FID and ICP-MS. This conclusion is further born-out by a visual inspection of the peaks shown in Fig. 8 for MHDC and PDC. The skewed peak shapes for ICP-MS may result from the use of the carrier gas to sweep the analyte from the restrictor into the plasma.

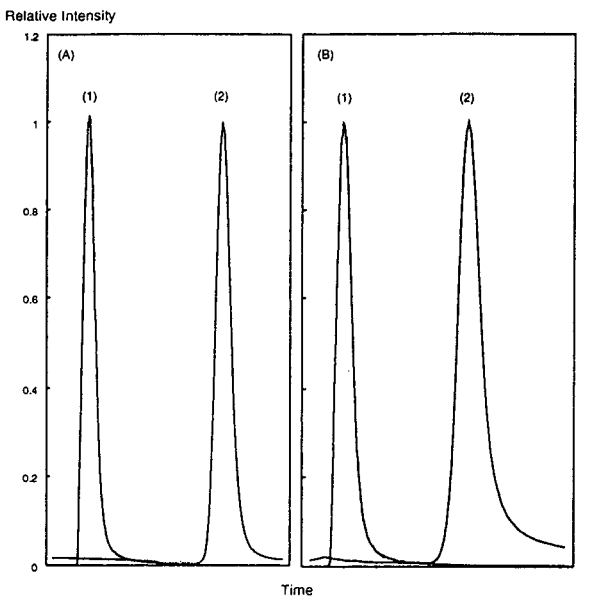

Fig. 8. Peaks for MHDC (A) and PDC (B) using both ICP-MS (1) and FID (2); note that the intensities have been normalized for comparison purposes.

Comparison to other methods

A brief comparison of the figures of merit obtained with this method, to those achieved with other methods is listed in Table IV. The chromatographic methods listed are for β-ketonate chromium complexes. The detection limits shown for FID are the range for the three compounds used in this study. The large difference in reported retention times is due to the slower pressure ramp used for FID. It is clear that the nitrous oxide is not a desirable mobile phase for FID and that ICP-MS provides for better detectability in both cases. Although the retention times for the chromium compounds are somewhat less for the other SFC reports, they are for a packed column, which may not be the most advantageous for plasma detection. In addition, in these analyses a methanol modifier was added to the carbon dioxide, while with the current investigation pure carbon dioxide and nitrous oxide were used. Finally, the use of MS allows for greater detectability compared to the ICP-AES and UV detectors described although no detection limits were presented in these reports.

When compared to liquid chromatographic methods, the advantages of SFC for these compounds, if ICP-MS detection were used, is found in the mobile phase. Upon decompression, the supercritical fluid is a gas which causes minimal plasma perturbations, while HPLC mobile phases can cause problems with plasma quenching, low nebulizer transport efficiency, and clogging of the nebulizer, skimmer and/or sampler cone orifices. Finally, a comparison of the detection limits to another dry plasma, transient signal sample introduction method (electrothermal vaporization, ETV) is provided. It can be seen that the detection limits are improved for the ETV

TABLE IV

COMPARISON OF SFC–FID AND SFC–ICP-MS TO OTHER METHODS

AES = Atomic emission spectroscopy; ETV = electrothermal vaporization; MIP = microwave induced plasma.

Technique	Detector	Detection limit	Retention time (min)	Ref.
SFC (capillary, N_2O)	ICP-MS	0.9–3 pg	6–7	This work
SFC (capillary, N_2O)	FID	50–250 pg	8–11	This work
SFC (capillary, CO_2)	FID	10–70 pg	8–11	This work
SFC (packed)	UV and ICP-AES	N.R.[a]	9	14
SFC (packed)	UV	N.R.	1–4	12
HPLC	UV	N.R.	6–14	5
HPLC	UV	N.R.	6–12	6
ETV	ICP-MS	0.2 pg	N.A.[b]	18
ETV	MIP-AES	1.5–4.2 ng	N.A.	18
ETV	ICP-AES	0.009–1.0 ng	N.A.	18

[a] N.R. = Not reported.
[b] N.A. = Not applicable.

measurements; however, electrothermal vaporization is a total element analysis method, not a speciation method. This is not desirable since as previously indicated; chromium is an element whose concern is highly species dependent.

CONCLUSIONS

The ability to analyze organochromium compounds by SFC–ICP-MS has been demonstrated. However, the technique does not allow for the use of the most common SFC mobile phase, carbon dioxide, due to an isobaric interference in the mass spectrometer resulting from the formation of ArC^+ at m/z 52. This mass to charge ratio corresponds to the major isotope of chromium so detection is severely limited when sufficiently high levels of carbon containing materials are used. The use of ICP-MS detection does not change the optimal chromatographic conditions to any considerable extent. However, the interface heating method does degrade the peak shapes to some degree. Perhaps the most severe limitation of the SFC–ICP interface is that the restrictor is heated over a relatively long distance which may hinder the analysis of thermally labile compounds such as MCCD.

Further investigations are needed into the ability to analyze ionic chromium and speciate the different oxidation states. This should be feasible through complexation of the chromium with a common organic ligand such as the β-ketonates illustrated here. In addition, the method in which the restrictor is heated, with the interface, needs to be investigated on a fundamental level so a better understanding of the processes which are occurring can be gained. Studies such as these may lead to an interface with a more efficient method of heating the restrictor, which also may possess better chromatographic compatibility with other detectors and better chromatographic performance.

ACKNOWLEDGEMENTS

The authors would like to acknowledge Dr. Jiangsheng Wang, Dr. G. Paul Sutton, Mr. Jeffrey J. Giglio and Ms. Sandra L. Cleland for their assistance in the preparation of this manuscript. In addition the financial support of the United States Environmental Protection Agency, under grant RP-2963, the National Institute of Environmental Health Sciences under grants ES03221 and ES04908 are greatly appreciated.

REFERENCES

1 D.T. Heitkemper and J.A. Caruso, in I.S. Krull (Editor), *Trace Metal Analysis and Speciation*, Elsevier, Amsterdam, New York, 1992, Ch. 3.
2 L.K. Olson, D.T. Heitkemper and J.A. Caruso, in P. Uden (Editor), *Element-Specific Chromatographic Detection by Atomic Emission Spectroscopy*, American Chemical Society, Washington, DC, 1992, Ch. 17.
3 J.M. Carey, F.A. Byrdy and J.A. Caruso, *J. Chromatogr. Sci.*, 31 (1993) 330.
4 C.D. Klaassen, M.O. Amdur and J. Doull, *Toxicology: The Basic Science of Poisons*, MacMillan, New York, 1986.
5 R.C. Gurira and P.W. Carr, *J. Chromatogr. Sci.*, 20 (1982) 461.
6 W. Mastowska and S. Starzynski, *Chromatographia*, 9/10 (1989) 519.
7 L.H. Lajunen, E. Eijarvi and T. Kenakkala, *Analyst*, 109 (1984) 699.
8 B. Maiti and S.R. Desai, *Analyst*, 111 (1986) 809.
9 J.J. Thompson and R.S. Houk, *Anal. Chem.*, 58 (1986) 2541.
10 I.S. Krull, D. Bushee, R.N. Savage, R.G. Schleicher and S.B. Smith, *Anal. Lett.*, 15 (1982) 267.
11 M. Ashraf-Khorassani, J.W. Hellgeth and L.T. Taylor, *Anal. Chem.*, 59 (1987) 2077.
12 C. Fujimoto, H. Yoshida and K. Jinno, *J. Microcol. Sep.*, 2 (1990) 146.
13 K. Jinno, H. Mae and C. Fujimoto, *J. High Resolut. Chromatogr.*, 13 (1990) 13.
14 J.M. Carey and J.A. Caruso, *Trends Anal. Chem.*, 11 (1992) 287.
15 J.M. Carey, N.P. Vela and J.A. Caruso, *J. Anal. At. Spectrom.*, 7 (1992) 1173.
16 N.P. Vela and J.A. Caruso, *J. Anal. At. Spectrom.*, 7 (1992) 971.
17 W.L. Shen, N.P. Vela, B.S. Sheppard and J.A. Caruso, *Anal. Chem.*, 63 (1991) 1491.
18 J.M. Carey and J.A. Caruso, *Crit. Rev. Anal. Chem.*, 23 (1992) 397.

Journal of Chromatography A, 662 (1994) 341–361
Elsevier Science B.V., Amsterdam

CHROM. 25 650

Determination of lipophilicity by means of reversed-phase thin-layer chromatography

I. Basic aspects and relationship between slope and intercept of TLC equations

G.L. Biagi*, A.M. Barbaro and A. Sapone

Dipartimento di Farmacologia, Università di Bologna, Via Irnerio 48, 40126 Bologna (Italy)

M. Recanatini

Dipartimento di Scienze Farmaceutiche, Università di Bologna, Via Belmeloro 6, 40126 Bologna (Italy)

(First received July 25th, 1993; revised manuscript received October 13th, 1993)

ABSTRACT

The main aspects of the authors' chromatographic work are reviewed. The determination of lipophilicity by means of TLC techniques is mainly based on the linear relationship between R_M values and organic solvent concentrations in the mobile phase, as described by the TLC equation. The very good correlation between experimental and extrapolated R_M values supports the validity of the extrapolation technique. Another interesting aspect is that the nature of the organic solvent does not affect the measurement of lipophilicity. However, the main purpose of this paper was to re-examine all the TLC equations in order to assess whether the relationship between intercepts and slopes is a basic feature of the chromatographic determination of lipophilicity. The analysis of more than 700 TLC equations showed that the above relationship holds only when dealing with series of strictly congeneric compounds. The structural meaning of chromatographic congenerity is discussed.

INTRODUCTION

Lipophilic character often seems to be the most important physico-chemical parameter in accounting for the variations of biological activity within series of chemical agents. As an expression of the lipophilic character of a given compound, its partition coefficient, P, between an aqueous and a non-aqueous phase, can be used. The partitioning between water and *n*-octanol, as proposed by Hansch, has been established as the reference system, with log P defined as the logarithm of the ratio of concentration of a neutral, non-ionized substance, in *n*-octanol to that in water [1]. Boyce and Milborrow [2] suggested using the chromatographic R_M value in order to avoid the practical difficulties that often arise in the direct determination of the partition coefficient. The R_M value can be shown to be related to the logarithm of the partition coefficient between the polar mobile phase and the non-polar stationary phase of a TLC system [3]. In our laboratory we have been using the R_M values as measured by means of a reversed-phase TLC system, where the mobile phase is represented by aqueous buffers alone or in various proportions with acetone, acetonitrile or methanol, and the non-polar stationary phase is a silica

* Corresponding author.

0021-9673/94/$07.00
SSDI 0021-9673(93)E1086-F

gel G layer impregnated with silicone oil [4,5].

The determination of lipophilicity by means of the chromatographic technique is mainly based on the linear relationship between the R_M values and the organic solvent concentrations in the mobile phase. In fact, from the linear equations a theoretical R_M value at 0% organic solvent in the mobile phase can be calculated even for those compounds which do not migrate with an aqueous buffer alone. For the more hydrophilic compounds, which migrate even at 0% organic solvent, one can measure an experimental R_M value and calculate an extrapolated value. The very good correlation between experimental and extrapolated R_M values supports the validity of the extrapolation technique [4].

Another interesting point is that the nature of the organic solvent does not affect the measurement of the lipophilic character. In fact, the extrapolated R_M values are the same whether the organic solvent of the mobile phase is acetone, acetonitrile or methanol [4]. The above features of the TLC technique contributed to establishing the reliability of the R_M values as lipophilicity parameters. Their usefulness was finally supported by the very good correlations between R_M and log P values [4,5]. Similar relationships between log k' and log P values have been shown in reversed-phase HPLC [4,6–11]. In fact, log k' values are currently used as a measure of lipophilicity [12]. Attention has been drawn by several workers [13–19] to the relationship between intercepts and slopes of the equations relating the capacity factor (log k') to the composition of the mobile phase (percentage of organic modifier). As regards the TLC system, this point was taken into consideration by Kuchar and co-workers [20,21] and Cserháti [22].

The purpose of this paper is to review the main aspects of our chromatographic work and re-examine all our TLC equations in order to assess whether the relationship between intercepts and slopes is a basic feature of the chromatographic determination of lipophilicity. For the present study, the data provided by recent chromatographic investigations on series of naphthalenes and quinolines, 4-nitropyrazoles and 1,4-dihydropyridines and some unpublished data on prostaglandins were also used.

EXPERIMENTAL

The reversed-phase TLC technique was described previously [23]. The details of the chromatographic determination of the R_M values for the recently investigated series of naphthalenes and quinolines, 4-nitropyrazoles and 1,4-dihydropyridines will be described in a further paper. In any case, for these classes of compounds and for all others listed in Table I a non-polar stationary phase was obtained by impregnating a silica gel GF_{254} layer (E. Merck, Darmstadt, F.R.G.) with silicone DC 200 (350 cSt) from Applied Science Labs. (State College, PA, USA). The choice of silicone oil as impregnating agent was initially made because most organic substances can be detected on siliconized silica G by charring with an alkaline solution of potassium permanganate. This offers the possibility of detecting very different classes of compounds without the need for any specific reagent [23]. The impregnation was carried out by developing the plates in a 5% silicone solution in diethyl ether. The mobile phases, saturated with silicone, were water or aqueous buffers alone or mixed with various amounts of acetone, acetonitrile or methanol. The pH of the mobile phase was chosen on the basis of the ionization profiles of the test compounds, in order to measure, whenever possible, the R_M value of their non-ionized form. The compositions of the mobile phases used for the determination of the R_M values of the compounds taken into consideration are reported in Table I. The general formulae for the chemical series listed in Table I are reported in Fig. 1.

RESULTS

TLC equations

In a typical reversed-phase TLC experiment, the detection of the compounds on the developed plate results in the appearance of round spots at different distances from the starting line. For the more hydrophilic compounds a reliable R_F value, *i.e.*, the ratio between the distance travelled by the compound on the TLC plate and the distance travelled by the solvent front, can be measured even when the mobile phase is

TABLE I

COMPOSITION OF THE TLC MOBILE PHASES FOR MEASUREMENT OF R_M VALUES

Chemical class	Compound No.	TLC mobile phase		Ref.
		Organic solvent	Aqueous component	
Steroids	88	Acetone	Water	24
Naphthalenes and quinolines	57	Acetone	Glycine (pH 9.0)[a]	25
		Methanol	Glycine (pH 9.0)[a]	25
Nitroimidazo-thiazoles	47	Acetone	Glycine (pH 9.0)	26
β-Carbolines	15	Acetone	Glycine (pH 9.0)	27
Penicillins	18	Acetone	Sodium acetate–veronal (pH 7.0)	28
		Acetone	Glycine (pH 1.2)	28
Benzodiazepines	39	Acetone	Water	29
Phenols	28	Acetone	Sodium acetate–veronal (pH 7.4)	30
Triazines	20	Acetone	Sodium acetate–veronal (pH 7.0)	31
		Acetonitrile	Sodium acetate–veronal (pH 7.0)	32
		Methanol	Sodium acetate–veronal (pH 7.0)	31
4-Nitropyrazoles	32	Acetone	Sodium acetate–veronal (pH 7.4)	25
		Acetone	Glycine (pH 1.2)	25
Prostaglandins	12	Acetone	Sodium acetate–veronal (pH 7.0)	33
		Methanol	Sodium acetate–veronal (pH 7.0)	33
		Acetonitrile	Sodium acetate–veronal (pH 7.0)	25
1,4-Dihydropyridines	53	Acetone	Sodium acetate–veronal (pH 7.4)	25
Cardiac glycosides	41	Acetone	Sodium acetate–veronal (pH 7.2)	34
Xanthones	41	Methanol	Glycine (pH 9.0)	35
Xanthines and adenosines	44	Acetone	Sodium acetate–veronal (pH 7.0)[b]	36
Cephalosporins	20	Acetone	Sodium acetate–veronal (pH 7.0)	28
		Acetone	Glycine (pH 1.2)	28
5-Nitroimidazoles	22	Methanol	Ammonium chloride (pH 9.0)[c]	37
Dermorphins	23	Acetone	Sodium acetate–veronal (pH 7.0)	38
		Methanol	Sodium acetate–veronal (pH 7.0)	38

[a] For the hydroxy derivatives, sodium acetate–veronal (pH 7.4) was used.
[b] For some derivatives, glycine buffer (pH 1.2) was used.
[c] For one compound, sodium acetate–veronal (pH 3.6) was used.

water or an aqueous buffer. The addition of an organic solvent to the mobile phase induces longer migrations of the compound and therefore higher R_F values. On the other hand, when the mobile phase is represented by an aqueous buffer only, the more lipophilic compounds tend not to move from the starting line ($R_F = 0$), and the addition of an organic solvent is necessary in order to obtain a reliable R_F value, *i.e.*, $0 < R_F < 1$. At higher organic solvent concentrations all the compounds tend to move with the solvent front and therefore to yield R_F values close to 1.

Because of the relationship $R_M = \log(1/R_F - 1)$ from lower or higher R_F values higher or lower R_M values, respectively, are obtained. Since the R_F values range from 0 to 1, R_M values ranging from $+\infty$ to $-\infty$ could theoretically be obtained. However, in the practice of TLC, when the compounds tend not to move from the starting line or to move with the solvent front, the lowest and highest R_F values which can be reliably measured are about 0.03 or 0.97, respectively, corresponding to R_M values of about 1.5 or -1.5.

Steroids:

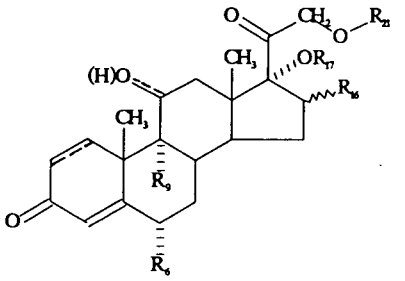

pregnane derivatives

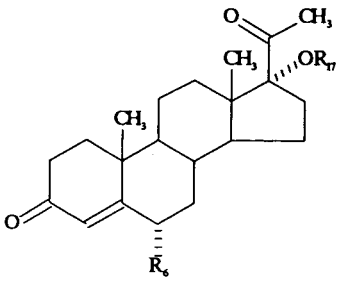

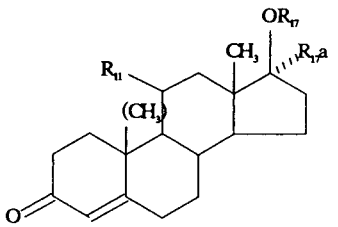

androstane derivatives

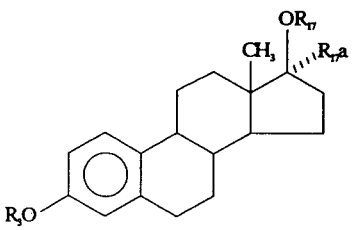

estrane derivatives

Naphthalenes & Quinolines:

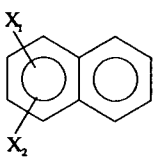

naphthalenes

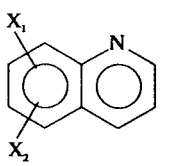

quinolines

Nitroimidazothiazoles:

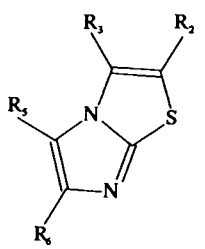

β-carbolines:

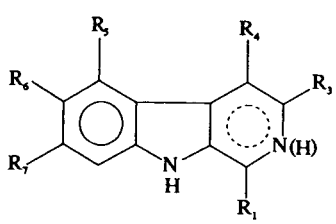

Fig. 1.

Penicillins:

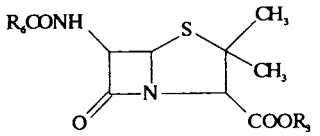

Benzodiazepines:

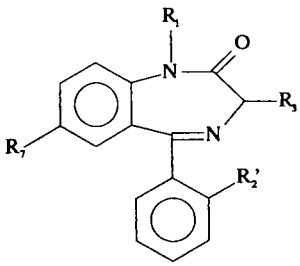

Phenols:

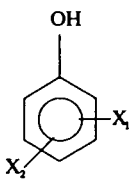

Triazines:

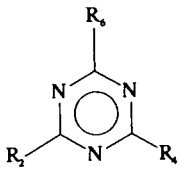

4-nitropyrazoles:

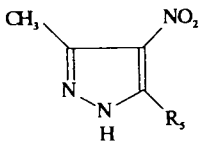

Prostaglandins:

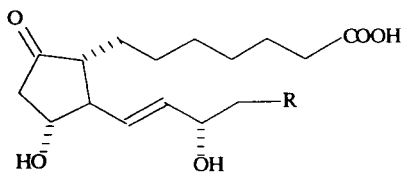

PGE_1 derivatives

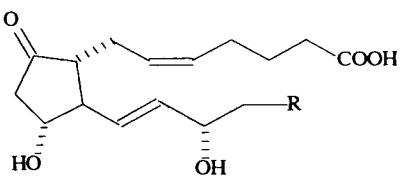

PGE_2 derivatives

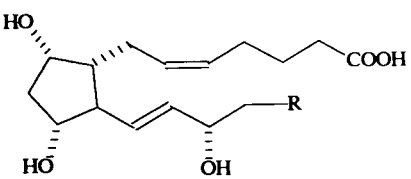

$PGF_{2\alpha}$ derivatives

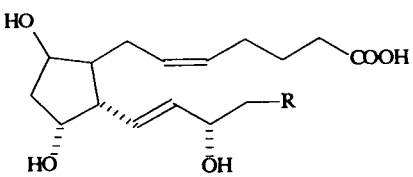

$PGF_{2\beta}$ derivatives

1,4-dihydropyridines:

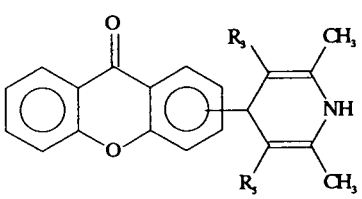

Fig. 1.

(Continued on p. 346)

Cardiac glycosides:

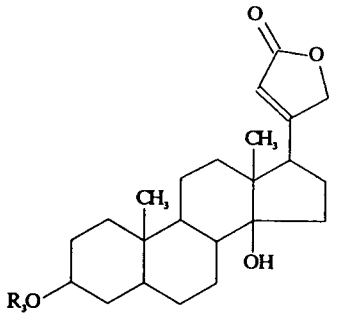

digitoxigenin derivatives

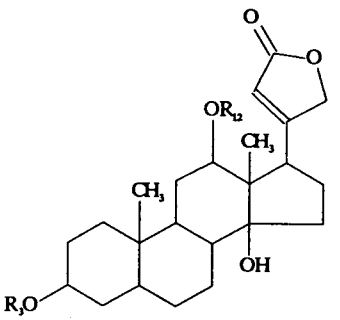

digoxigenin derivatives

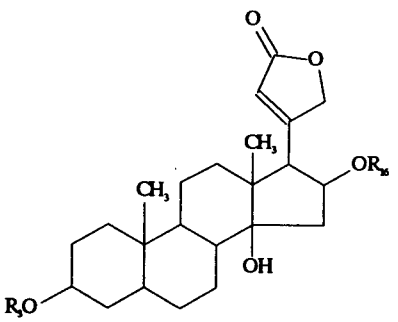

gitoxigenin derivatives

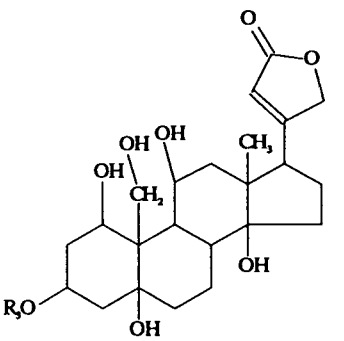

ouabagenin derivatives

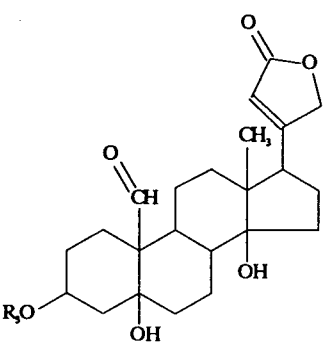

strophanthidin derivatives

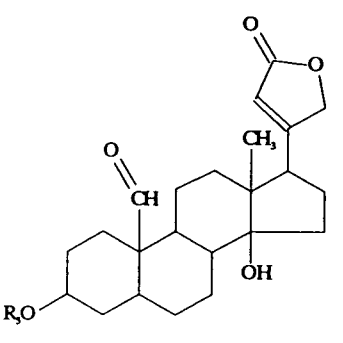

cannogenin derivatives

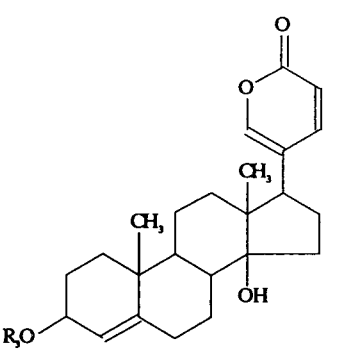

scillarenin derivatives

Fig. 1. (*continued*)

Xanthones:

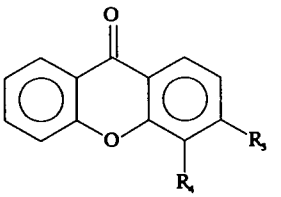

Xanthines & Adenosines:

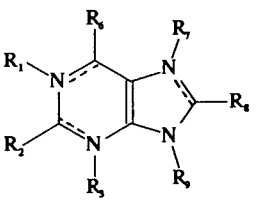

xanthine derivatives

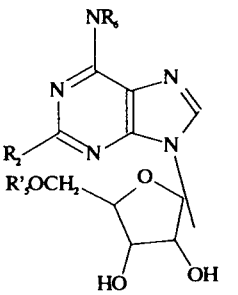

adenosine derivatives

Cephalosporins:

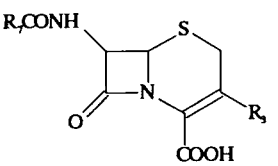

5-nitroimidazoles:

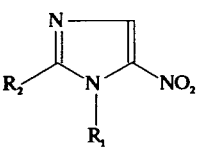

Dermorphins:

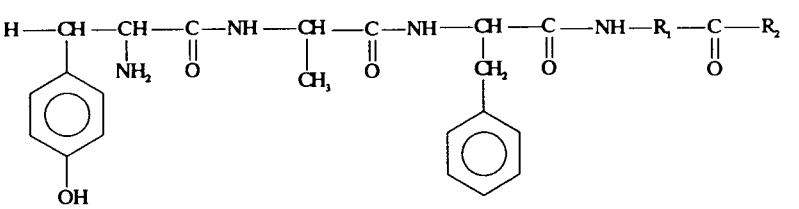

Fig. 1. General formulae for the series of compounds listed in Table I.

In agreement with the first observation of Boyce and Milborrow [2], our chromatographic work has shown that for each compound in all the chemical series taken into consideration there is a range of linear relationship between the R_M values and the organic solvent concentrations in the mobile phase. It is important to note that such a linear relationship has been shown also in reversed-phase HPLC [6,39–42]. In Fig. 2, some examples are reported describing the relationship between the R_M values of selected compounds from the newly investigated series and the composition of the mobile phase in a reversed-phase TLC system. The more lipophilic compounds such as AP 838 (a dihydropyridine derivative) at lower acetone concentrations tend not to move from the starting line (R_M values between 1.2 and 1.3), whereas at higher concentrations they tend to move with the solvent front (R_M values between −1.2 and −1.3). The extrapolation from the linear part of the curve yields the theoretical R_M values at 0% acetone in the mobile phase. This chromatographic behaviour, over the full range of acetone concentrations, was previously described as an S-shaped curve [6]. Werkhoven-Goewie *et al.* [43] showed very similar S-shaped curves describing the relationship between log k' values and the composition of the mobile phase in an HPLC system. On the other hand, the more hydrophilic compounds such as P_3 (a 4-nitropyrazole derivative) show deviations from linearity only at higher acetone concentrations. In fact, even at 0% acetone experimental R_M values can be determined. The first part of the curve can be fitted by a straight line and a theoretical R_M value at 0% can be calculated and compared with the experimental R_M value. A particular case is represented by very hydrophilic compounds, which tend to move with the solvent front even at 0% organic solvent in the mobile phase. For such compounds it is difficult to calculate a TLC equation. In fact, the slope tends to be close to 0. An example of a very hydrophilic compound is 6-aminopenicillanic acid: at pH 1.2 and 0% acetone it shows an R_M value of −0.99 [28]. In Fig. 2 it is shown that any addition of acetone cannot further increase the migration of the compound. The linear part of the curves reported in Fig. 2 is described by the following TLC equations, where % Me_2CO indicates the acetone concentration in the mobile phase:

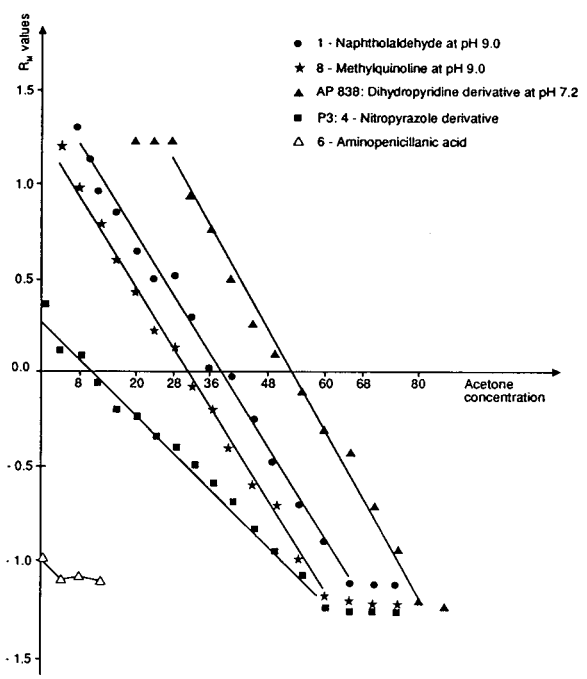

Fig. 2. Relationship between R_M values and acetone concentrations in the mobile phase for some selected compounds.

AP 838 (dihydropyridine derivative):

$$R_M = 2.343(\pm 0.073) - 0.044(\pm 0.001)(\%Me_2CO) \quad (n = 11;\ r = 0.996;\ s = 0.072) \quad (1)$$

1-naphtholaldehyde:

$$R_M = 1.528(\pm 0.038) - 0.040(\pm 0.001)(\%Me_2CO) \quad (n = 14;\ r = 0.996;\ s = 0.064) \quad (2)$$

8-methylquinoline:

$$R_M = 1.246(\pm 0.040) - 0.040(\pm 0.001)(\%Me_2CO) \quad (n = 14;\ r = 0.995;\ s = 0.073) \quad (3)$$

P_3 (4-nitropyrazole derivative):

$$R_M = 0.270(\pm 0.018) - 0.025(\pm 0.001)(\%Me_2CO) \quad (4)$$
$$(n = 15;\ r = 0.997;\ s = 0.037)$$

The intercepts of eqns. 1–4 represent the theoretical R_M values at 0% organic solvent in the mobile phase, *i.e.*, in a standard system, where all the compounds can be compared on the basis of their lipophilicity. In particular, if the assumption is made that reversed-phase TLC is true partition chromatography, the intercepts of the TLC equations can be considered as a measure of the partitioning of compounds between silicone oil (stationary phase) and water or an aqueous buffer (mobile phase at 0% organic solvent). The negative slope of the TLC equation indicates the increase in migration per unit increase in organic solvent concentration, *i.e.*, the rate at which the solubility of the compound increases in the mobile phase.

The chromatographic work carried out over many years in our laboratory provided 734 TLC equations for the chemical classes and under the mobile phase conditions listed in Table I. Most of these equations were published previously. The present analysis of our original chromatographic data resulted in the recalculation of 48 TLC equations, yielding new values for intercepts and/or slopes. In particular, the new TLC equations were 1 out of 22 for the 5-nitroimidazoles, 2 out of 20 for the triazines, 3 out of 47 for the nitroimidazothiazoles, 7 out of 40 for the cardiac glycosides, 2 out of 88 for the steroids, 6 out of 30 for the penicillins and 27 out of 46 for the dermorphins. This means that only 6.5% of the TLC equations had to be recalculated. Moreover, most of these new TLC equations, *i.e.*, 27 out of 48, were calculated for dermorphin-related derivatives. On excluding this class of compounds, the above percentage decreases to 3.0, *i.e.*, only 21 new equations out of 688.

Relationship between experimental and extrapolated R_M values

As the more hydrophilic compounds can migrate in a reliable way even at 0% organic solvent, the equations describing the correlation between their experimental and extrapolated R_M values can be calculated (eqns. 5–18, Table II). In fact, in all the chemical classes listed in Table II there were several hydrophilic compounds, for which it was possible to measure an experimental R_M at 0% organic solvent. The intercepts and slopes of eqns. 5–18 are very close to 0 and 1, respectively, and can support the validity of the extrapolation technique. The only exception is represented by the dermorphin-related derivatives (eqns. 15 and 16). In any case eqns. 5–18 were combined into eqn. 19, which shows that the very good correlation between experimental and extrapolated R_M values does not depend on the structure of compounds and the composition of the mobile phase.

$$R_{M\,\mathrm{exptl}} = 0.031(\pm 0.009) + 1.000(\pm 0.011)R_{M\,\mathrm{extrap}} \quad (19)$$
$$(n = 240;\ r = 0.986;\ s = 0.080;\ F = 8592;\ P < 0.005)$$

TLC equations from different solvent systems

Another interesting point arising from our previous work is the very close overlap of the extrapolated R_M values obtained with different organic solvents in the mobile phase. If the extrapolated R_M values represented the partitioning of the compounds between the silicone oil of the stationary phase and a mobile phase constituted only by water, we would expect the same extrapolated R_M values whether the organic solvent of the mobile phase was acetone, acetonitrile or methanol. This aspect is illustrated by means of five classes of compounds listed in Table III. Eqns. 20–27 (Table III) show very good correlations between the extrapolated R_M values at 0% acetone, acetonitrile or methanol in the mobile phase. Again, only the dermorphin-related derivatives deviate slightly. The slopes and intercepts close to 1 and 0, respectively, show the overlapping of the R_M values extrapolated from different solvent systems. Again, eqn. 20 shows a small difference for the dermorphin-related derivatives. In any case eqns. 20, 21, 24 and 25 were combined into eqn. 28.

TABLE II

CORRELATION BETWEEN EXPERIMENTAL AND EXTRAPOLATED R_M VALUES

Chemical class	TLC system		$R_{M\,exptl} = a + bR_{M\,extrap}$					Eqn. No.	Ref.
	Organic solvent	pH	a	b	n	r	s		
Xanthines and adenosines	Acetone	7.0	0.036	0.972	33	0.997	0.042	5	36
Cardiac glycosides	Acetone	7.2	0.038	1.033	6	0.960	0.065	6	34
Penicillins and cephalosporins	Acetone	1.2	0.036	0.978	27	0.997	0.032	7	28
	Acetone	7.0	0.023	1.021	28	0.996	0.044	8	28
Quinolines and naphthalenes	Acetone	9.0	0.076	0.958	23	0.970	0.062	9	25
	Methanol	9.0	0.066	0.959	23	0.951	0.079	10	25
Triazines	Acetone	7.0	0.010	1.017	5	0.997	0.022	11	31
	Methanol	7.0	0.063	0.940	5	0.985	0.050	12	31
	Acetonitrile	7.0	0.008	0.985	6	0.999	0.015	13	32
5-Nitroimidazoles	Methanol	9.0	−0.002	0.990	22	0.999	0.024	14	37
Dermorphins	Acetone	7.0	0.355	1.026	5	0.986	0.041	15	38
	Methanol	7.0	0.322	0.866	5	0.981	0.048	16	38
4-Nitropyrazoles	Acetone	1.2	0.049	0.996	26	0.991	0.052	17	25
	Acetone	7.0	0.045	0.958	26	0.965	0.099	18	25

$$R_{M\,acetone} = 0.046(\pm 0.047) + 0.926(\pm 0.025)R_{M\,methanol} \quad (28)$$

$$(n = 99;\quad r = 0.967;\quad s = 0.185;\quad F = 1413;\quad P < 0.005)$$

This shows that the linear relationship between R_M values and the mobile phase composition yields extrapolated R_M values that are not dependent on the nature of the organic solvent. In other words, the extrapolated R_M values are referred to a standard system represented only by water and silicone oil.

TABLE III

CORRELATIONS BETWEEN EXTRAPOLATED R_M VALUES FROM DIFFERENT TLC SYSTEMS

Chemical class	Organic solvent		$R_{M\,I} = a + b\,R_{M\,II}$					Eqn. No.	Ref.
	I	II	a	b	n	r	s		
Dermorphins	Acetone	Methanol	−0.252	0.993	23	0.980	0.192	20	38
Prostaglandins	Acetone	Methanol	−0.025	0.958	12	0.967	0.139	21	33
	Acetone	Acetonitrile	−0.197	1.141	12	0.973	0.126	22	25
	Methanol	Acetonitrile	−0.021	1.113	12	0.940	0.187	23	25
Quinolines and naphthalenes	Acetone	Methanol	0.043	0.969	44	0.965	0.178	24	25
Triazines	Acetone	Methanol	0.021	0.961	20	0.981	0.074	25	32
	Acetone	Acetonitrile	−0.013	0.971	20	0.974	0.087	26	32
	Methanol	Acetonitrile	−0.019	0.999	20	0.982	0.075	27	32

Relationship between slopes and intercepts of the TLC equations

As already pointed out, for any chemical agent there is a range of linear relationship between R_M values and organic solvent concentration in the mobile phase, unless it is too hydrophilic. The straight lines describing such linear relationships for a series of twelve prostaglandin derivatives and their TLC equations are reported in Fig. 3 [33]. The plot of Fig. 3b shows that there is a linear relationship between the slopes and the intercepts of the TLC equations, *i.e.*, the extrapolated R_M values. The very good correlation is described by eqn. 37 in Table IV. The correlation is not affected by the lower slope of the TLC equation of compound 9. The plots in Fig. 3a and the negative slope of eqn. 37 mean that with increasing methanol concentration the R_M values of more lipophilic compounds decrease faster than those of less lipophilic derivatives. In other words, lipophilic compounds are more sensitive to variations of the polarity of the mobile phase.

In a similar way, the linear relationships between the slopes and intercepts of the TLC equations for several chemical series were calculated and are reported in Table IV. All the members of the steroid, 5-nitroimidazole, nitroimidazothiazole, phenol, triazine and dermorphin series fitted the respective straight lines, the only exception being prednisolone palmitate. The deviation of this derivative is due to its very high and probably unreliable R_M value (9.15). Therefore, eqn. 29 was calculated without this compound. Although their chromatographic studies have not yet been published, three other series of compounds, 4-nitropyrazoles, 1,4-dihydropyridines and naphthalenes and quinolines, are considered in Table IV. In all three series no deviation was observed from the linear relationships between the intercepts and slopes of the TLC equations. In the case of naphthalenes and quinolines, eqn. 46 was calculated including fifteen naphthols for which the TLC data were available and already published [44].

However, a very interesting aspect is that in several instances not all the members of a chemical series fit the same straight line. The TLC equations reported in Fig. 4a for fifteen β-carbolines show that the chromatographic behaviour of harmaline and harmalol (compounds 12 and 13 in Fig. 4a) is characterized by lower

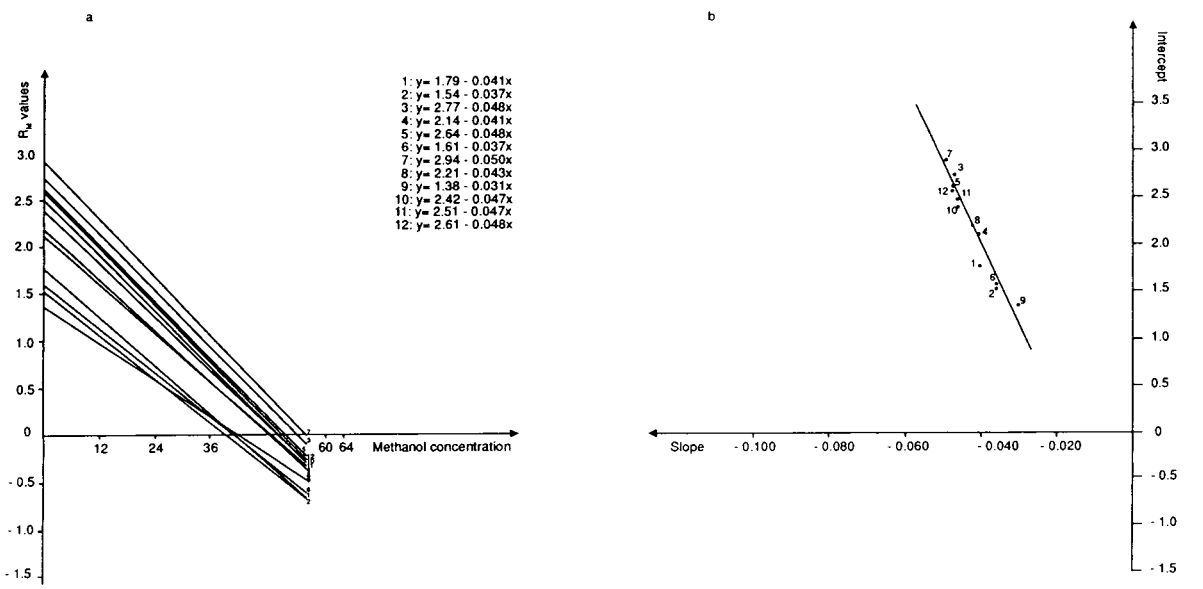

Fig. 3. (a) Relationship between R_M values and methanol concentration in the mobile phase, as described by the TLC equations for twelve prostaglandins. (b) Relationship between slope and intercept of the TLC equations for the prostaglandins in (a) as described by eqn. 37 in Table IV.

TABLE IV

RELATIONSHIP BETWEEN INTERCEPTS AND SLOPES OF TLC EQUATIONS

Chemical class	TLC mobile phase		$R_{M\,extrap} = a + b$ slope					Eqn. No.	Ref.
	Solvent	pH	a	b	n	r	s		
Steroids	Acetone	7.0	−2.294 (±0.076)	−81.625 (±1.203)	88	0.991	0.203	29	24
Nitroimidazo-thiazoles	Acetone	9.0	−1.095 (±0.117)	−78.201 (±3.125)	47	0.966	0.136	30	26
Phenols	Acetone	7.0	−1.166 (±0.137)	−75.383 (±4.357)	28	0.959	0.201	31	30
Triazines	Acetone	7.0	−1.258 (±0.308)	−69.484 (±8.208)	20	0.894	0.173	32	32
	Acetonitrile	7.0	−1.287 (±0.597)	−74.194 (±16.475)	20	0.728	0.265	33	32
	Methanol	7.0	−1.602 (±0.707)	−109.73 (±26.023)	20	0.705	0.279	34	32
Prostaglandins	Acetone	7.0	−2.289 (±0.762)	−61.014 (±10.555)	12	0.877	0.261	35	33
	Acetonitrile	7.0	−2.970 (±1.226)	−73.829 (±18.141)	12	0.790	0.284	36	25
	Methanol	7.0	−1.499 (±0.313)	−86.005 (±7.187)	12	0.967	0.140	37	33
5-Nitroimidazoles	Methanol	7.0	−0.848 (±0.062)	−66.689 (±2.625)	22	0.985	0.120	38	37
Dermorphins	Acetone	7.0	−1.710 (±0.228)	−56.775 (±3.466)	23	0.963	0.263	39	38
	Methanol	7.0	−1.054 (±0.197)	−69.317 (±4.055)	23	0.966	0.249	40	38
4-Nitropyrazoles	Acetone	1.2	−1.593 (±0.137)	−84.834 (±4.397)	32	0.962	0.237	41	25
	Acetone	7.0	−1.645 (±0.122)	−79.483 (±3.494)	32	0.972	0.205	42	25
1,4-Dihydropy-ridines	Acetone	7.0	−1.167 (±0.199)	−69.429 (±3.850)	53	0.930	0.176	43	25
Naphthalenes and quinolines	Acetone	9.0	−1.356 (±0.193)	−62.704 (±4.065)	44	0.922	0.265	44	25
	Methanol	9.0	−1.051 (±0.186)	−87.810 (±6.060)	44	0.913	0.277	45	25
	Acetone	9.0	−1.430 (±0.166)	−64.502 (±3.511)	57	0.928	0.244	46	25

slopes. In fact, these two compounds do not fit the straight line in Fig. 4b and were omitted from the calculation of eqn. 48 (Table V).

The equations in Table V describe the relationship between the slopes and intercepts for two other series of compounds, *i.e.*, cardiac glycosides and benzodiazepines. Ouabain was omitted from eqn. 47 because of its large deviation. In the benzodiazepine series six compounds markedly deviated from the linear relationship: four of them are characterized by very low slopes of their TLC equations and by the presence of a basic chain $CH_2CH_2N(C_2H_5)_2$ in position 1 of the 1,4-diazepine nucleus; two other compounds show higher slopes and the presence of a COOH group. These compounds were omitted from the calculation of eqn. 49.

The analysis of the TLC equations for penicillins and xanthones revealed the presence of a number of subclasses within each series (Table

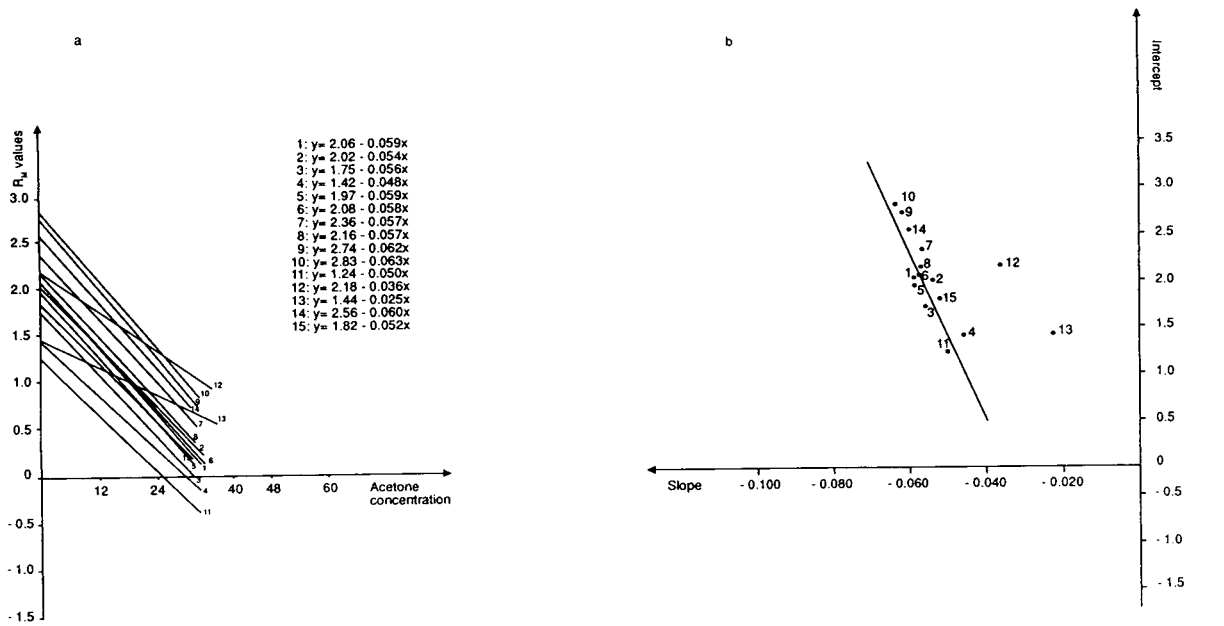

Fig. 4. (a) Relationship between R_M values and organic solvent concentrations, as described by the TLC equations for fifteen β-carbolines. The slopes of the TLC equations of compounds 12 and 13 are clearly lower. (b) Relationship between slope and intercept of the TLC equations for the β-carbolines in (a) as described by eqn. 48 in Table V. Both harmaline (compound 12) and harmalol (compound 13) were omitted from the calculation of the equation.

VI). As regards the penicillins at pH 1.2, eqn. 50 was calculated with ten derivatives bearing a COOH group as the only ionizable one and eqn. 51 with six compounds having both an amino and a carboxyl group. Carbenecillin, because of its large deviation, was omitted from both equations (Fig. 5a). At pH 7.0, eqn. 52 was calculated with all the penicillins except the prodrugs bacampicillin, talampicillin and lenampicillin, where the carboxyl group is esterified (Fig. 5b). Despite its large deviation in Fig. 5b there was no apparent reason for excluding compound 1 from the calculation of eqn. 52.

In the case of xanthone compounds the original series of 41 derivatives had to be split into four subclasses characterized by different substituents in positions 3 and 4 (Table VII). Eqn. 53 was calculated for the 3-alkoxy or 3-NH_2-

TABLE V

RELATIONSHIP BETWEEN INTERCEPTS AND SLOPES OF TLC EQUATIONS

Chemical class	TLC mobile phase		$R_{M\,extrap} = a + b$ slope					Eqn. No.	Ref.
	Solvent	pH	a	b	n	r	s		
Cardiac glycosides	Acetone	7.2	−1.550 (±0.219)	−63.492 (±3.646)	40	0.943	0.303	47	34
β-Carbolines	Acetone	9.0	−3.218 (±0.802)	−93.760 (±14.140)	13	0.894	0.220	48	27
Benzodiazepines	Acetone	7.0	−2.557 (±0.454)	−89.642 (±9.240)	33	0.867	0.231	49	29

TABLE VI

RELATIONSHIPS BETWEEN INTERCEPTS AND SLOPES OF TLC EQUATIONS

Chemical class	TLC mobile phase		$R_{M\,extrap} = a + b$ slope					Eqn.	Ref.
	Solvent	pH	a	b	n	r	s		
Penicillins	Acetone	1.2	−2.143 (±0.299)	−81.782 (±6.380)	10	0.976	0.132	50	28
			−1.949 (±0.274)	−48.528 (±5.249)	6	0.977	0.190	51	28
	Acetone	7.0	−2.540 (±0.422)	−53.744 (±7.092)	14	0.909	0.335	52	28
Xanthones	Methanol	9.0	0.507 (±0.181)	−91.006 (±6.678)	19	0.957	0.129	53	35
			0.594 (±0.026)	−69.490 (±0.810)	4	0.999	0.006	54	35
			−0.185 (±0.565)	−79.518 (±14.861)	7	0.923	0.140	55	35
			−0.831 (±0.139)	−83.796 (±3.938)	11	0.990	0.060	56	35

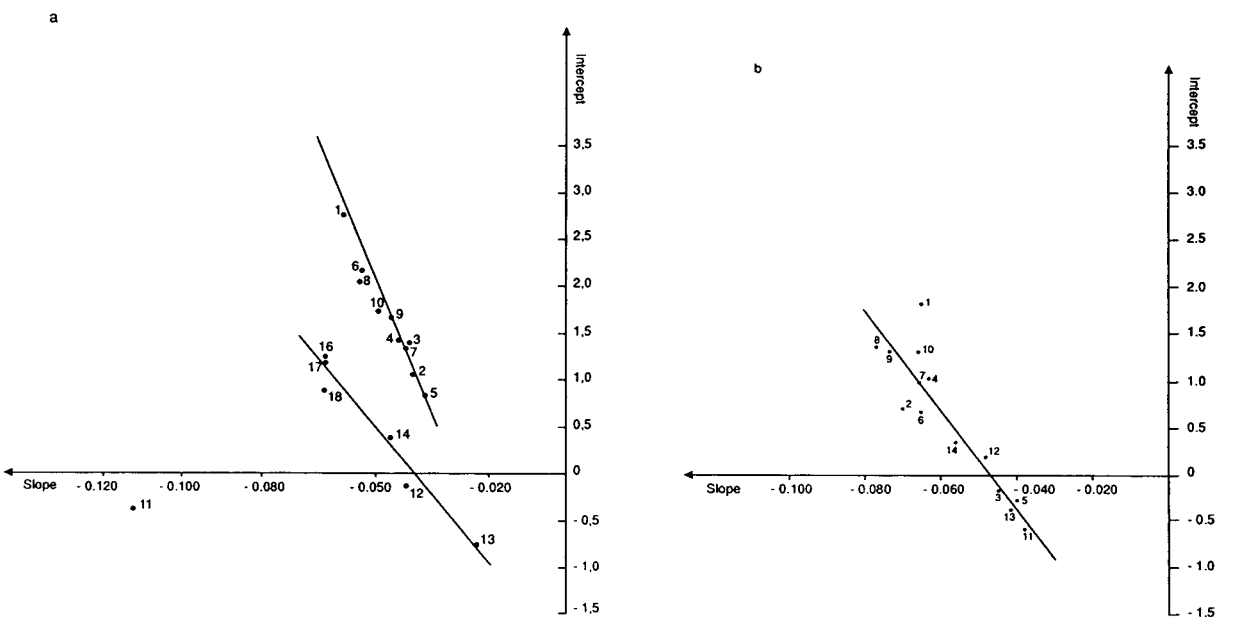

Fig. 5. (a) Relationship between slope and intercept of the TLC equations for penicillins at pH 1.2, as described by eqns. 50 (compounds 1–10) and 51 (compounds 12–14, 16–18) in Table VI. Carbenecillin (compound 11) deviated from both equations. (b) Relationship between slope and intercept of the TLC equations for penicillins at pH 7.0, as described by eqn. 52 in Table VI.

TABLE VII

STRUCTURES OF THE XANTHONE DERIVATIVES FITTING EQNS. 53–56

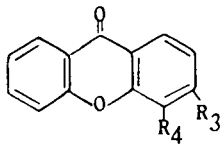

Eqn. 53

No.	R_3	R_4
11	OCH_3	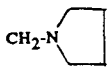
17	OCH_3	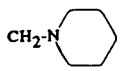
23	OCH_3	CH_2-N(CH_3)$_2$
29	OCH_3	CH_2-N(C_2H_5)$_2$
36	OCH_3	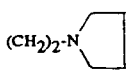
37	OCH_3	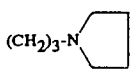
38	OCH_3	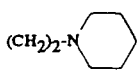
39	OCH_3	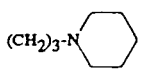
40	OCH_3	(CH_2)$_2$-N(CH_3)$_2$
41	OCH_3	(CH_2)$_3$-N(CH_3)$_2$
42	OCH_3	(CH_2)$_2$-N(C_2H_5)$_2$
43	OCH_3	(CH_2)$_3$-N(C_2H_5)$_2$
15	$OCH(CH_3)_2$	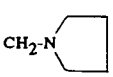
21	$OCH(CH_3)_2$	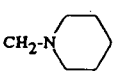
27	$OCH(CH_3)_2$	CH_2-N(CH_3)$_2$

Eqn. 54

No.	R_3	R_4
33	$OCH(CH_3)_2$	CH_2-N(C_2H_5)$_2$
13	NH_2	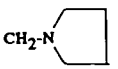
19	NH_2	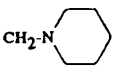
31	NH_2	$CH_2N(C_2H_5)_2$

Eqn. 54

No.	R_3	R_4
10	H	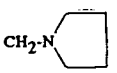
16	H	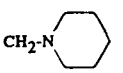
22	H	CH_2-N(CH_3)$_2$
28	H	CH_2-N(C_2H_5)$_2$

Eqn. 55

No.	R_3	R_4
12	Cl	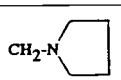
18	Cl	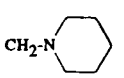
30	Cl	CH_2-N(C_2H_5)$_2$
14	NO_2	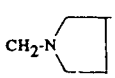
20	NO_2	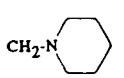

(Continued on p. 356)

TABLE VII (*continued*)

Eqn. 53

No.	R_3	R_4
26	NO_2	CH_2-$N(CH_3)_2$
32	NO_2	CH_2-$N(C_2H_5)_2$

Eqn. 54

No.	R_3	R_4
8	NO_2	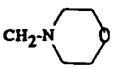
9	$OCH(CH_3)_2$	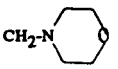
34	OCH_3	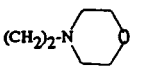
35	OCH_3	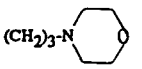
1	H	H
2	OCH_3	H
3	Cl	H

Eqn. 56

No.	R_3	R_4
4	H	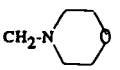
5	OCH_3	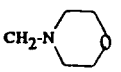
6	Cl	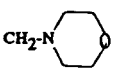
7	NH_2	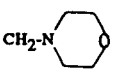

substituted derivatives, eqn. 54 for the 3-H-substituted derivatives and eqn. 55 for the 3-Cl- or 3-NO_2-substituted derivatives. Compounds lacking the 4-aminoalkyl moiety or bearing a 4-morpholinoalkyl moiety were excluded from eqns. 53, 54 and 55. They fitted eqn. 56 (Fig. 6).

Interestingly, the analysis of the chromatographic data on cephalosporins [28] and xanthines and adenosines [36] revealed that these chemical series do not follow the general behaviour so far described. In fact, in the case of cephalosporins there was no correlation between the slopes and intercepts at either pH 1.2 or 7.0 (Fig. 7). For xanthines and adenosines it was not possible to find any structural meaning for some groupings of data (Fig. 8).

Finally, it is important to note that the low correlation coefficient of some of the equations in Tables IV, V and VI might also be due to the fact that the variability of the slopes is lower than that of the intercepts. The lower variability of the slopes yields lower values of the sum of the products of deviations of x and y values (Σxy). Therefore, since $r = \Sigma xy/\sqrt{\Sigma x^2 \Sigma y^2}$, the consequence is a low correlation coefficient.

DISCUSSION AND CONCLUSIONS

The present analysis of our chromatographic work, including some recent unpublished data, points to the reliability of two basic features of the R_M values, which we have been showing in many papers. They can be illustrated by eqns. 19 and 28. The correlation between experimental and extrapolated R_M values strongly supports the validity of the extrapolation technique. The correlation between extrapolated R_M values obtained using different organic solvents is another important support for the reliability of the extrapolated R_M values as an expression of the partitioning between an aqueous mobile phase and the silicone oil of the stationary phase. In fact, the nature of the organic modifier does not affect the extrapolated R_M values. However, this conclusion is based on the eight equations reported in Table III. It might be questionable

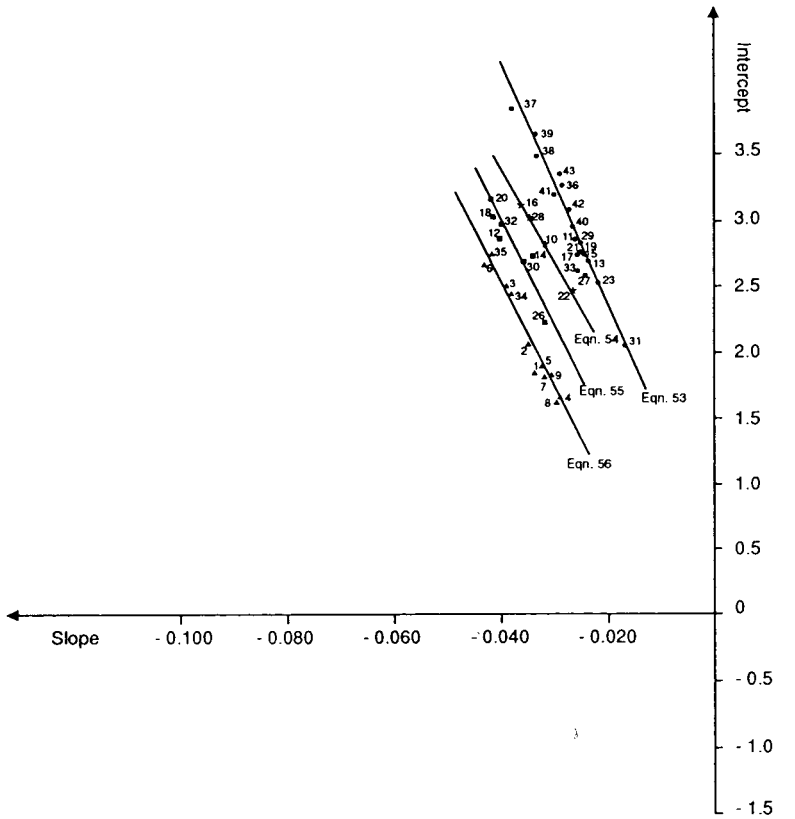

Fig. 6. Relationship between slope and intercept of the TLC equations for xanthone derivatives, as described by eqns. 53, 54, 55 and 56 in Table VII.

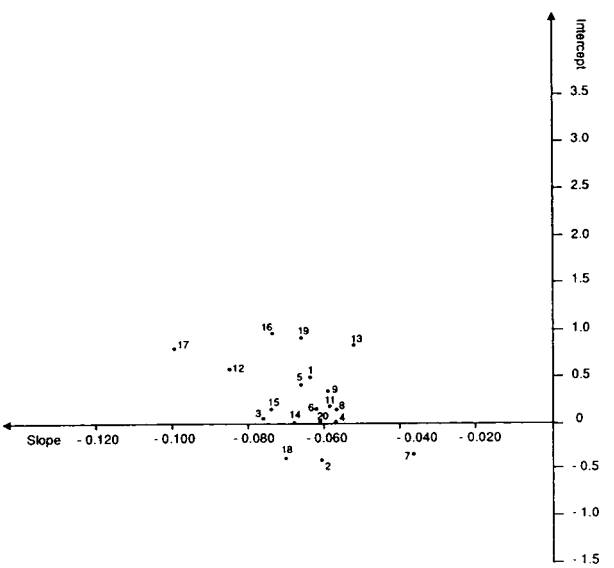

Fig. 7. Plot of slope *vs.* intercept of the TLC equations for cephalosporins at pH 7.0.

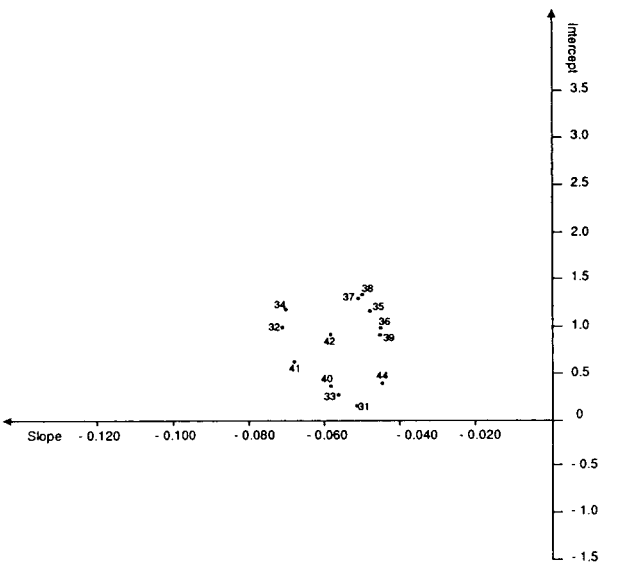

Fig. 8. Plot of slope vs. intercept of the TLC equations for adenosines at pH 7.0.

whether this aspect has general relevance for any chromatographic process. Some HPLC data seem to suggest a different influence of methanol and acetonitrile on the retention of simple organic compounds [45,46].

The most interesting aspect arising from this paper is the finding that the linear relationship between slopes and intercepts of the TLC equations seems to be another basic feature of the chromatographic determination of lipophilicity. In order to understand the relationship between slopes and intercepts of the TLC equations, the physico-chemical meaning of these two parameters must be discussed. As mentioned above, the intercept of the TLC equation can be considered as a measure of the partitioning of the compounds between a polar mobile phase and a non-polar stationary phase, *i.e.*, as the result of the balance between the interactions with the non-polar phase and the interactions with the polar phase.

On the other hand, less attention has been devoted to the physical meaning of the slope of the HPLC or TLC equations. As already pointed out, the slope of the TLC equation indicates the rate at which the solubility of the compound increases in the mobile phase. The increased solubility is due to the decreased polarity of the mobile phase, altering the balance of polar and non-polar interactions between each phase and the solute. According to Horváth *et al.* [40], the increased migration can be related to a decrease in the surface tension of the mobile phase, thus resulting in a better solubility. From a molecular point of view, Murakami [47] has interpreted the slope in terms of the so-called "displacement model" as the number of mobile phase solvent molecules in the solvation sphere of the solute. This is the number of solvent molecules that are released after the formation of the stationary phase–solute complex, and it depends on the area of the apolar surface characterizing any organic compound and on the type and number of polar substituents present in the solute structure [17]. Therefore, Murakami [47] pointed out again the importance of polar and non-polar interactions in determining the relationship between retention and the composition of the mobile phase.

As a consequence of the above considerations both the intercept and slope of the TLC equation seem to be related to the same physico-chemical factors, and therefore they should be interrelated. However, the data in Tables IV, V and VI and those of Valkó [16] and Kuchar *et al.* [20] show that the correlation holds only within series of congeneric compounds. An attempt to explain this aspect could be based on the concept of "hydrophobic surface availability", introduced by Kaibara *et al.* [48]. The retention should depend not just on the hydrophobic surface area but also on that part of it actually available for the interactions with the non-polar stationary phase. The shape of this surface might be the critical factor for differentiating series of congeneric compounds. This interpretation could be in agreement with the definition of a congeneric series proposed by Ariëns [49], i.e. "a three-dimensional homology of the various molecular fragments in the chemical framework of the series". From this point of view all the members of the series listed in Table IV seem to be congeneric. On the other hand, the series reported in Tables V and VI are characterized by the presence of compounds which do not fit the same linear equation. Whereas for the series in Table V this concerns only a few compounds as shown in Fig. 4, for the penicillins and xanthones (Table VI) a number of subclasses can be identified (Figs. 5 and 6). As the number of outliers in the series of penicillins and xanthones is sufficiently high, an equation for each subclass could be calculated.

In particular, congenerity might be broken down by the presence of ionizable groups which could modify the interactions of the compounds with the polar and/or non-polar phase. In fact, this is the case for the benzodiazepine, penicillin and β-carboline series. Benzodiazepines bearing the basic chain $CH_2CH_2N(C_2H_5)_2$ or a COOH group deviated from eqn. 49. At pH 1.2 penicillins bearing only one COOH group and those bearing both one NH_2 and one COOH group fitted eqns. 50 and 51 respectively. Carbenecillin with two COOH groups deviated from both equations. The presence of the second (non-ionized) carboxyl group can probably alter the shape of the hydrophobic surface of carbenecillin

with respect to those characterizing the compounds fitting eqns. 50 and 51. At pH 7.0 a similar mechanism could induce the deviation of ester prodrugs from eqn. 52. Finally, it must be noted that the two β-carbolines excluded from the calculation of eqn. 48 are characterized by the non-aromatic C ring, which implies the presence of a dihydropyridine ring instead of a pyridine ring. This again might be the cause of different polar and/or non-polar interactions.

In order to explain the deviation of ouabain from eqn. 47, the presence of a higher number of OH groups on its genin (ouabagenin) when compared with the other genins of the series (digoxigenin, digitoxigenin, gitoxigenin, k-strophanthidin, cannogenin and scillarenin) (Fig. 1) can be pointed out. In this case a different frame of intra- and intermolecular interactions could change the shape of the hydrophobic surface. The most striking example of the influence of structural differences on the slopes of TLC equations is provided by the xanthone derivatives. The series is characterized in position 3 of the xanthone nucleus by the presence of a number of substituents with different electronic properties and in position 4 by the presence of different aminoalkyl groups or by the lack of any substituent at all (Table VII).

The straight lines in Fig. 6 referring to the subclasses of Table VII show that when the amine in position 4 is dimethylamine, diethylamine, pyrrolidine or piperidine the properties of the substituents in position 3 make a difference among the compounds bearing the same amine (eqns. 53, 54 and 55). On the other hand, if the amine in position 4 is morpholine or if there is no aminoalkyl group in that position, all the compounds are congeneric despite the different substitution in position 3 (eqn. 56). The reason for the grouping of the xanthones into four subclasses could be found in different ionization patterns altering the availability of the hydrophobic surface. In fact, when there is no aminoalkyl group in position 4, the molecules are non-ionizable, whereas the presence of the aminoalkyl moiety in position 4 introduces an ionizable group. The experimental pK_a values of these compounds are not available. However, they should not be far from the pK_a values of the corresponding methylamines [50]: trimethylamine (9.76), methyldiethylamine (10.29), N-methylpyrrolidine (10.46), N-methylpiperidine (10.08) and N-methylmorpholine (7.41). At the pH of our TLC system (9.0), the compounds with a morpholino group should be mostly non-ionized; in fact, they fit the same equation as the 4-unsubstituted compounds. On the other hand, the presence of dimethylamino-, diethylamino-, pyrrolidino- or piperidinoalkyl groups renders the molecules more ionized at pH 9.0, which is not far from their pK_a values.

The extent to which these molecules are ionized can be influenced by the electronic character of the substituents in position 3, and the subclasses fitting eqns. 53, 54 and 55 can be identified on the basis of the electronic properties of these substituents. Eqn. 53 groups the compounds bearing alkoxy and NH_2 substituents, which might increase the pK_a of the amino group via an electron-donating effect, stabilizing the cation. The H substituent does not exert any electronic effect (eqn. 54). The Cl and NO_2 substituents are electron-withdrawing groups, able to lower the basic ionization constant. Consistently, the curve representing eqn. 55 lies close to that representing eqn. 56, that was calculated for the non-ionized compounds. As regards cephalosporins and also xanthines and adenosines, it was not possible to establish any meaningful relationships between slopes and intercepts. One must conclude that the members of these series of compounds are not congeneric from the chromatographic point of view. This does not imply that any series of cephalosporins or xanthines and adenosines would behave in the same way. At this stage of our work we are not able to interpret in structural terms the reasons for this chromatographic non-congenerity.

In conclusion, the relationship between slopes and intercepts of the TLC equations can be considered as a basic aspect of the chromatographic determination of lipophilicity, provided that one is dealing with strictly congeneric compounds. Recently, the slope of TLC or HPLC equations has been proposed as an alternative lipophilic parameter to be used in QSAR studies [20]. However this suggestion deserves some comment. The relationship holds only for a

series of strictly congeneric compounds and it is very difficult to define *a priori* congenerity in terms of chromatographic behaviour. The variability of the slopes is much smaller than that of the corresponding R_M values. In the case of a linear relationship with another variable, this implies a lower correlation and therefore a lower predictive value of the model.

Work is in progress aimed at collecting experimental and/or calculated log P values for all the compounds studied in our laboratory, with a view to an analysis of their relationship with the intercepts or slopes. This study will allow us to establish which of the two chromatographic parameters is best suited as an alternative measure of lipophilicity. A general equation correlating R_M and log P values could also be used as a calibration graph for the prediction of log P values from R_M measurements. Preliminary results have already pointed out the significant correlation existing between R_M and experimental and/or calculated log P [4,5].

REFERENCES

1 A. Leo, C. Hansch and D. Elkins, *Chem. Rev.*, 71 (1971) 525.
2 C.B.C. Boyce and B.V. Milborrow, *Nature*, 208 (1965) 537.
3 G.L. Biagi, A.M. Barbaro, M.C. Guerra, G. Cantelli-Forti and M.E. Fracasso, *J. Med. Chem.*, 17 (1974) 28.
4 G.L. Biagi, M. Recanatini, A.M. Barbaro, M.C. Guerra, A. Sapone, P.A. Borea and M.C. Pietrogrande, in H. Kalász and L.S. Ettre (Editors), *New Approaches in Chromatography '91*, Fekete Sas Könyvkiadó, Budapest, 1993, p. 215.
5 G.L. Biagi, M. Recanatini, A.M. Barbaro, M.C. Guerra, A. Sapone, P.A. Borea and M.C. Pietrogrande, in C. Silipo and A. Vittoria (Editors), *QSAR: Rational Approaches to the Design of Bioactive Compounds*, Elsevier, Amsterdam, 1991, p. 83.
6 M.C. Pietrogrande, C. Bighi, P.A. Borea, A.M. Barbaro, M.C. Guerra and G.L. Biagi, *J. Liq. Chromatogr.*, 8 (1985) 1711.
7 G.L. Biagi, M.C. Pietrogrande, A.M. Barbaro, M.C. Guerra, P.A. Borea and G. Cantelli-Forti, *J. Chromatogr.*, 469 (1989), 121.
8 G.L. Biagi, M.C. Guerra, A.M. Barbaro, S. Barbieri, M. Recanatini and P.A. Borea, *J. Liq. Chromatogr.*, 13 (1990) 913.
9 A. Hulshoff and J.H. Perrin, *J. Chromatogr.*, 129 (1976) 263.
10 M.C. Guerra, A.M. Barbaro, G. Cantelli-Forti, G.L. Biagi and P.A. Borea, *J. Chromatogr.*, 259 (1983) 329.
11 M.C. Guerra, A.M. Barbaro, G. Cantelli-Forti, M.C. Pietrogrande, P.A. Borea and G.L. Biagi, *J. Liq. Chromatogr.*, 7 (1984) 1495.
12 R. Kaliszan, *Quantitative Structure–Chromatographic Retention Relationships*, Wiley, New York, 1987.
13 P.J. Schoenmakers, H.A.H. Billiet and L. de Galan, *J. Chromatogr.*, 175 (1979) 179.
14 P. Jandera, *J. Chromatogr.*, 314 (1984) 13.
15 K. Valkó, *J. Liq. Chromatogr.*, 7 (1984) 1405.
16 K. Valkó, *J. Liq. Chromatogr.*, 10 (1987) 1663.
17 D.J. Minick, J.H. Frenz, M.A. Patrick and D.A. Brent, *J. Med. Chem.*, 31 (1988) 1923.
18 R.B. Taylor, N.A. Ochekpe and J. Wangboonskul, *J. Liq. Chromatogr.*, 12 (1989) 1645.
19 A. Kaibara, C. Hohda, N. Hirata, M. Hirose and T. Nakagawa, *Chromatographia*, 29 (1990) 275.
20 M. Kuchar, E. Kraus and M. Jelinkova, *J. Chromatogr.*, 557 (1991) 399.
21 M. Kuchar and M. Jelinkova, in M. Kuchar (Editor), *QSAR in Design of Bioactive Compounds, Second Telesymposium on Medicinal Chemistry*, J.R. Prous International, Barcelona, 1992, p. 65.
22 T. Cserháti, *J. Liq. Chromatogr.*, 16 (1993) 1805.
23 G.L. Biagi, A.M. Barbaro, M.F. Gamba and M.C. Guerra, *J. Chromatogr.*, 41 (1969) 371.
24 G.L. Biagi, A.M. Barbaro, O. Gandolfi, M.C. Guerra and G. Cantelli-Forti, *J. Med. Chem.*, 18 (1975) 873.
25 G.L. Biagi, unpublished data.
26 M.C. Guerra, A.M. Barbaro, G.L. Biagi, M.C. Pietrogrande, P.A. Borea, A. Andreani and G. Cantelli-Forti, *J. Chromatogr.*, 320 (1985) 281.
27 G.L. Biagi, M.C. Pietrogrande, A.M. Barbaro, M.C. Guerra, P.A. Borea and G. Cantelli-Forti, *J. Chromatogr.*, 469 (1989) 121.
28 G.L. Biagi, A.M. Barbaro, M.C. Guerra, S. Barbieri and M. Recanatini, in M. Kuchar (Editor), *QSAR in Design of Bioactive Compounds, Second Telesymposium on Medicinal Chemistry*, J.R. Prous International, Barcelona, 1992, p. 47.
29 G.L. Biagi, A.M. Barbaro, M.C. Guerra, M. Babbini, M. Gaiardi, M. Bartoletti and P.A. Borea, *J. Med. Chem.*, 23 (1980) 193.
30 G.L. Biagi, O. Gandolfi, M.C. Guerra, A.M. Barbaro and G. Cantelli-Forti, *J. Med. Chem.*, 18 (1975) 868.
31 G.L. Biagi, M.C. Guerra, A.M. Barbaro, M. Recanatini, P.A. Borea and A. Sapone, *Sci. Total Environ.* 109/110 (1991) 33.
32 G.L. Biagi, A.M. Barbaro, A. Sapone and M. Recanatini, *J. Chromatogr.*, 625 (1992) 392.
33 A.M. Barbaro, M.C. Guerra, G.L. Biagi, M.C. Pietrogrande and P.A. Borea, *J. Chromatogr.*, 347 (1985) 209.
34 G.L. Biagi, A.M. Barbaro, M.C. Guerra, P.A. Borea and M. Recanatini, *J. Chromatogr.*, 504 (1990) 163.
35 A.M. Barbaro, M.C. Guerra, G. Cantelli-Forti, G. Aicardi, G.L. Biagi, P. Da Re, P. Valenti and P.A. Borea, *J. Chromatogr.*, 242 (1982) 1.
36 G.L. Biagi, M.C. Guerra, A.M. Barbaro, S. Barbieri, M. Recanatini, P.A. Borea and M.C. Pietrogrande, *J. Chromatogr.*, 498 (1990) 179.

37 M.C. Guerra, A.M. Barbaro, G. Cantelli-Forti, M.T. Foffani and G.L. Biagi, *J. Chromatogr.*, 216 (1978) 93.
38 A.M. Barbaro, M.C. Guerra, G. Cantelli-Forti, P.A. Borea and G.L. Biagi, *J. Chromatogr.*, 287 (1984) 259.
39 H. Hemets, W. Measfeld and H. Richer, *Chromatographia*, 6 (1976) 171.
40 C. Horváth, W. Melander and I. Molnár, *J. Chromatogr.*, 125 (1976) 129.
41 L.R. Snyder, J.W. Dolan and J.R. Gant, *J. Chromatogr.*, 165 (1979) 3.
42 N. Tanaka and E.R. Thornton, *J. Am. Chem. Soc.*, 99 (1977) 7300.
43 C.E. Werkhoven-Goewie, U.A. Th. Brinkman and R.W. Frei, *Anal. Chem.*, 53 (1981) 2072.
44 G.L. Biagi, A.M. Barbaro, M.C. Guerra, G. Hakim, G.C. Solaini and P.A. Borea, *J. Chromatogr.*, 177 (1979) 35.
45 R.M. Smith and C.M. Burr, *J. Chromatogr.*, 475 (1989) 57.
46 R.M. Smith and C.M. Burr, *J. Chromatogr.*, 550 (1991) 335.
47 F. Murakami, *J. Chromatogr.*, 178 (1979) 393.
48 A. Kaibara, M. Hirose and T. Nakagawa, *Chromatographia*, 30 (1990) 99.
49 E.J. Ariëns, *Quant. Struct.–Act. Relat.*, 11 (1992) 190.
50 H.K. Hall, Jr., *J. Am. Chem. Soc.*, 79 (1957) 5441.

ELSEVIER

Journal of Chromatography A, 662 (1994) 363–368

JOURNAL OF CHROMATOGRAPHY A

Evaluation of susceptibility to oxidation of linoleyl derivatives by thin-layer chromatography with flame ionization detection

Gloria Márquez-Ruiz, Maria Carmen Pérez-Camino and Maria Carmen Dobarganes*

Instituto de la Grasa y sus Derivados (CSIC) Avda. Padre García Tejero 4, 41012 Seville, Spain

(First received August 9th, 1993; revised manuscript received November 2nd, 1993)

Abstract

A simple and rapid method for the evaluation of susceptibility to oxidation in microsamples was developed using a thin-layer chromatographic–flame ionization detection (TLC–FID) system. The procedure was applied to linoleic acid, methyl linoleate, trilinolein and sucrose octalinoleate. Samples of 15 μg were spotted on Chromarods, subjected to different temperatures for various times and analysed by TLC–FID. Oxidized products from linoleyl derivatives were determined from the amounts of unoxidized samples, determined in turn by two approaches, *i.e.*, using calibration graphs or adding squalane an an internal standard.

1. Introduction

Although many analytical methods are available for the measurement of lipid oxidation [1,2], it is difficult to determine the extent of oxidation and its evolution owing to the complex nature and variety of lipid oxidation products formed [3]. Moreover, published studies vary widely in their experimental conditions and analytical methodology, hence there are difficulties in drawing general conclusions [4–9]. An indirect analytical approach consists in measuring oxidative stability by means of accelerated methods using elevated temperatures, such as the Rancimat test [10], but a possible drawback with this method is the requirement for 2–3 g of lipid sample. It must also be considered that oxidation occurring in accelerated heating tests involve mechanisms that can be different from those encountered in practical situations, *e.g.*, storage conditions. Therefore, the necessity to develop and standardize accelerated tests under ambient conditions, essentially based on the exposure of oil to atmospheric oxygen at very high surface-to-volume ratio, has been reported [11].

The thin-layer chromatography with flame ionization detection (TLC–FID) has been used for the determination of polar components and oxidation products in edible oils subjected to different oxidation tests [12–16]. However, there is little information relating to its direct application to determine susceptibility to oxidation [17,18]. One of the chief advantages of TLC–FID over the other separation methods is the possibility of simultaneously developing and analysing ten samples so that direct comparison among samples under identical conditions can be made. The rapidity of the analysis and the small amount of sample required are of great convenience when a large number of samples need

* Corresponding author.

0021-9673/94/$07.00
SSDI 0021-9673(93)E1166-W

to be prepared or when only minimum amounts are available. Manipulation of the sample prior to analysis is usually not necessary as multiple solvent systems for development may be tried depending on the compounds to be evaluated. Additionally, reference standards may be incorporated in the sample to evaluate response factors [19].

In this paper, we describe a new possibility for determining susceptibility to oxidation in microsamples using TLC–FID. The method was applied to linoleic acid, methyl linoleate, trilinolein and sucrose octalinoleate.

2. Experimental

2.1. Materials

Linoleic acid (LA) and methyl linoleate (ML) were purchased form Nu-Check-Prep (Elysian, MN, USA). Squalane was purchased from Sigma (St. Louis, MO, USA). Trilinolein (LLL) was obtained by esterification of linoleic acid and glycerol, using *p*-toluenesulphonic acid as a catalyst [20]. Sucrose octalinoleate (SOL) was prepared starting from sucrose and excess of linoleic chloride to form the complete ester [21]. Isolation and purification of trilinolein and sucrose octalinoleate were carried out by means of silica gel column chromatography as described elsewhere [22].

2.2. Sample oxidation

Samples were dissolved in hexane (15 mg/ml) and 1 μl (15 μg) was spotted on Chromarods S-III quartz rods with a coating of silica gel (Iatron Labs., Tokyo, Japan). In another set of experiments, samples were dissolved in hexane containing 10 mg/ml of squalane, used as an internal standard, so that 10 μg of squalane plus 15 μg of sample were applied to each rod. All analyses were performed in triplicate. In order to study surface oxidation at different temperatures, rods were maintained at room temperature or heated in an oven at 60 or 100°C. Samples were analysed at various intervals for up to 10 h at room temperature, 6 h at 60°C and 30 min at 100°C.

2.3. Determinations

After the oxidation phase the Chromarods were developed in light petroleum (b.p. 60–70°C–diethyl ether–acetic acid (90:10:2) for 35 min and scanned in an Iatroscan MK-5 TLC–FID analyser (Iatron Laboratories) equipped with a flame ionization detector. The Iatroscan was operated under the following conditions: flow-rate of hydrogen, 150 ml/min; flow-rate of air, 1500 ml/min; and scanning speed, 0.33 cm/s. Unoxidized substrate was analysed for LA, ML, LLL and SOL using calibration graphs of peak area *versus* amount. Five determinations for each of five concentrations (1, 2.5, 5, 10 and 15 μg/μl) were made. Alternatively, squalane was used as an internal standard. The percentage of total oxidized compound was calculated by subtracting the percentage of unaltered sample from 100. The induction time period was determined by the Rancimat method at 60 and 100°C [10] using 0.5-g samples.

2.4. Statistical analysis

Each reported value represents the mean of three determinations and the standard error of the mean (S.E.M.). Student's *t*-test was applied to determine the significance of differences between means ($P < 0.05$).

3. Results and discussion

Calibration graphs for LA, ML, LLL and SOL using TLC–FID were plotted as amount in micrograms (Q) *versus* peak area (A), according to the following equations ($n = 25$ in each instance): LA, $Q = 0.13 + 0.217 \cdot 10^{-3}\ A$, $r = 0.9974$; ML, $Q = 0.24 + 0.267 \cdot 10^{-3}\ A$, $r = 0.9989$; LLL, $Q = 0.70 + 0.189 \cdot 10^{-3}\ A$, $r = 0.9993$; and SOL, $Q = 0.76 + 0.191 \cdot 10^{-3}\ A$, $r = 0.9997$.

All the compounds showed fairly good linearity in the concentration range employed. The

relative response of ML, LLL and SOL with respect to LA were 0.81, 1.15 and 1.14, respectively. Such variations were expected according to previous results [23] and the specific characteristics of this technique [19]. The coefficient of variation of the area measurement ranged from 0.90% at 10-μg load levels of ML to 4.31% at 1-μg load levels of SOL, which indicated a high reproducibility. Unoxidized compounds remaining after the oxidation phase were determined using these calibration graphs or else by the internal standard method. Squalane was selected as the internal standard particularly for its resistance to alteration under the experimental conditions, provided that it fulfilled the basic requirements for use as an internal standard. In preliminary assays, five samples of 10 μg of squalane were spotted on Chromarods, heated in an oven at 100°C for 5 h and simultaneously analysed with five original samples. No significant differences were found between the treated and original squalane samples. The relative responses of squalane with respect to LA, ML and LLL were 1.13, 1.37 and 0.97, respectively. Total oxidized products, or higher polarity than that of the original lipid, were determined by difference. We used this approach because the polar fraction is a complex mixture of oxidation products and its composition depends on the heat treatment and could therefore change drastically from one sample to another. These differences would be expected to induce changes in the FID response factors and thereby considerable errors may result from direct analysis of the polar fraction. Moreover, volatile compounds originating from the breakdown of peroxides and hydroperoxides may be lost prior to detection.

Fig. 1 presents typical TLC–FID traces for initial samples and those obtained after oxidation at 100°C for 15 min. As can be observed, the selected solvent system permitted for all samples a good separation of the unoxidized compound from the more polar oxidized products. The procedure allowed the evaluation of susceptibility to oxidation in 15-μg samples at various temperatures and time periods, in a short analysis time and with the possibility of revealing the whole lipid pattern of the sample, thus adding to the reliability of the determination. Special care was taken with regard to sample purity and also cleanliness of the rods and evenness of the temperature within the oven, which were essential factors for good reproducibility.

Table 1 gives selected results for total oxidation products from all the compounds deter-

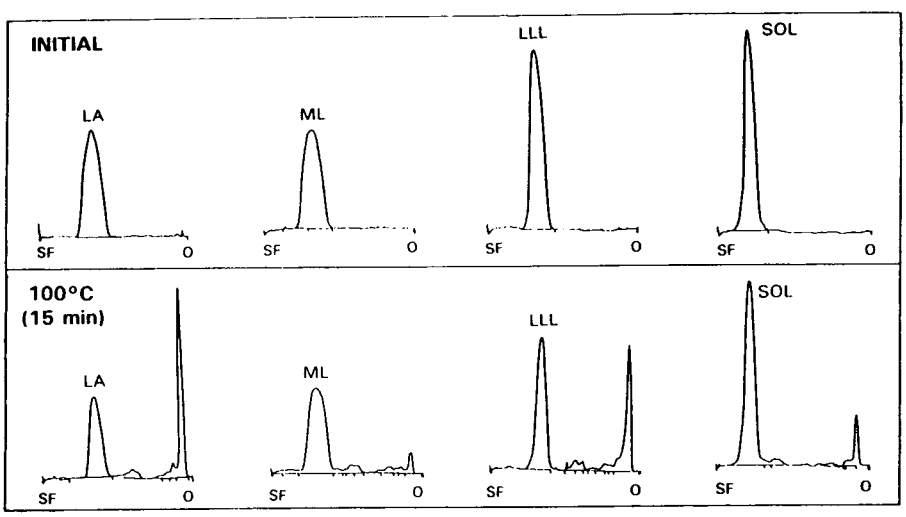

Fig. 1. Iatroscan TLC–FID traces for linoleic acid (LA), methyl linoleate (ML), trilinolein (LLL) and sucrose octalinoleate (SOL) showing the effect of oxidation on Chromarods after 15 min at 100°C. O = Origin; SF = solvent front.

Table 1
Total oxidation products of linoleic acid (LA), methyl linoleate (ML), trilinolein (LLL) and sucrose octalinoleate (SOL) on Chromarods S-III at 25 and 100°C (% of total compounds).

Compound	25°C			100°C		Induction period at 100°C (h)
	3 h	5 h	10 h	15 min	30 min	
LA	n.d.	8.3 ± 2.9^{a}	28.4 ± 3.3^{a}	52.9 ± 3.6^{a}	69.7 ± 6.1^{a}	0.6
ML	n.d.	n.d.	11.9 ± 3.0^{b}	18.1 ± 2.9^{b}	30.5 ± 3.0^{b}	0.9
LLL	n.d.	19.6 ± 3.1^{b}	52.9 ± 3.1^{c}	48.1 ± 3.1^{a}	62.7 ± 3.2^{a}	1.1
SOL	n.d.	5.1 ± 2.9^{a}	16.3 ± 2.8^{b}	8.3 ± 1.8^{c}	21.7 ± 2.8^{b}	1.3

Values are means ± S.E.M. of three determinations. Values in a column with different superscript letters are significantly different ($P < 0.05$). n.d. = Not detectable.

mined following oxidation at room temperature (*ca.* 25°C) and 100°C. Unoxidized substrate was determined using calibration graphs. The last column shows the induction periods at 100°C using the Rancimat apparatus. From the results obtained, comparisons between sample behaviours were possible. The oxidation rate of compounds was dependent on the temperature tested. Thus, the rise in oxidized substrate was fastest and most extensive for LA at 25°C whereas both LA and LLL showed the highest values at 100°C. Several papers have been published on the comparison of the oxidation rates of various types of unsaturated fatty acid esters [24–27]. It has been shown that oxidation of the fatty acid was more rapid than that of the methyl or ethyl ester, probably owing to the participation of the carboxyl groups in the decomposition of peroxides [25,28]. Also, higher oxidation rates have been found for triacylglycerol than for the fatty acid ester, although the kinetics of triacylglycerol autoxidation did not seem to follow the usual rate law [26]. It is important to note that among linoleic esters, LLL and SOL, in contrast to ML, may undergo oxidation in up to three or eight fatty acyls, respectively. Hence greater total oxidized substrates, as determined by this method, could be expected for LLL and SOL than for ME, substantiated by the fact that a considerable proportion of oxidized molecules contain unoxidized fatty acyl groups [29]. This could explain in part that higher oxidized amounts resulted from LLL than for ML. However, SOL showed unexpected lower percentages of oxidized products than LLL at any temperature tested, and generally similar values to those for ML. Further, it should be stressed that similar values of total oxidation products for SOL and ML would still indicate lower levels of oxidized fatty acyls for SOL (eight fatty acyls per molecule) than those for ML (1 fatty acyl per molecule). These data were consistent with the induction period at 100°C, which was longer for SOL than for ML and LLL. The differences between LLL and SOL agreed with our previous results [22], which indicated that the oxidation of sucrose octaesters occurred more slowly than that of the triglyceride with a similar fatty acid composition when starting from pure compounds. In contrast, it has also been reported that the autoxidation rates of sucrose esters were higher than those of triacylglycerols and methyl esters of safflower oil [27]. However, whereas triacylglycerols and methyl esters were purified, sucrose esters were not completely acylated as the average number of acyl groups per molecule was six, which means the presence of compounds with a wide range of polarity.

Table 2 summarizes the results obtained at 60°C when the internal standard method was used for quantification. The last column lists the induction periods as measured with the Rancimat apparatus. SOL was not included as it overlapped with squalane with the elution system used. Clearly, the use of an internal standard was advantageous in that the reproducibility and

Table 2
Total oxidation products of linoleic acid (LA), methyl linoleate (ML) and trilinolein (LLL) on Chromarods S-III at 60°C (% of total compounds)

Compound	1 h	2 h	4 h	6 h	Induction period at 60°C (h)
LA	n.d.	11.0 ± 2.1	84.6 ± 0.8[a]	85.2 ± 0.4[a]	2.5
ML	n.d.	n.d.	9.4 ± 0.7[b]	18.6 ± 1.8[b]	12.2
LLL	n.d.	n.d.	21.1 ± 0.9[c]	20.8 ± 1.6[c]	14.9

Values are means ± S.E.M. of three determinations. Values in a column with different superscript letters are significantly different ($P < 0.05$). n.d. = Not detectable.

accuracy of the determination were not affected by possible variations in the amount of sample applied to the rod. In general, the results showed the same alteration order as that observed at 100°C. LA oxidized more rapidly than LLL and ML and these findings were in good agreement with the induction periods. Differences between the Rancimat and TLC–FID techniques, such as the surface-to-volume ratio, detection system and the possible influence of silanol groups accessible on the surface, did not contribute to modifying the alteration order of the samples, which was found to be consistent with both methods.

Overall, the results obtained in this study with linoleyl derivatives give evidence of the important influence of the compound structure on the oxidation rate. The approach suggested here for evaluating oxidative stability by TLC–FID can be widely applied to compare different lipid samples that are available only in milligram amounts. Another valuable application of the proposed technique could be as a rapid and simple method to determine the potential influence of minor compounds and the protective effect of antioxidants on oil and fat stability. Experiments along these lines are in progress.

4. Acknowledgement

This work was supported by CICYT (project ALI 91-0544).

5. References

[1] J. Kanner and I. Rosenthal, *Pure Appl. Chem.*, 64 (1992) 1959–1964.
[2] J. Löliger, *Rev. Fr. Corps Gras*, 36 (1989) 301–308.
[3] E.N. Frankel, *J. Sci. Food Agric.*, 54 (1991) 495–511.
[4] K. Warner, E.N. Frankel and T.L. Mounts, *J. Am. Oil Chem. Soc.*, 66 (1989) 558–564.
[5] C.L. Tautorus and A.R. McCurdy, *J. Am. Oil Chem. Soc.*, 67 (1990) 525–530.
[6] H.R. Liu and P.J. White, *J. Am. Oil Chem. Soc.*, 69 (1992) 528–532.
[7] H.R. Liu and P.J. White, *J. Am. Oil Chem. Soc.*, 69 (1992) 533–537.
[8] M.C. Dobarganes, G. Márquez-Ruiz and M.C. Pérez-Camino, *J. Agric. Food Chem.*, 41 (1993) 678–681.
[9] J.F. Toro-Vázquez, A.A. Castillo-M. and R. Hernández-C., *J. Am. Oil Chem. Soc.*, 70 (1993) 261–267.
[10] M.W. Läubli and P.A. Bruttel, *J. Am. Oil Chem. Soc.*, 63 (1986) 792–795.
[11] B.J.F. Hudson, in J.C. Allen and R.J. Hamilton (Editors), *Rancidity in Foods*, Elsevier, Amsterdam, 1989, pp. 53–65.
[12] J.K. Kaitaranta, *J. Am. Oil Chem. Soc.*, 58 (1981) 710–713.
[13] J.L. Sébédio, C. Septier and A. Grandgirard, *J. Am. Oil Chem. Soc.*, 63 (1986) 1541–1543.
[14] J.L. Sébédio, P.O. Astorg, C. Septier and A. Grandgirard, *J. Chromatogr.*, 405 (1987) 371–378.
[15] O. Katoh, M. Tanaka, J. Ishii and T. Itoh, *J. Jpn. Oil Chem. Soc.*, 36 (1987) 19–23.
[16] N. Okada and T. Fujii, *J. Jpn. Oil Chem. Soc.*, 41 (1992) 28–32.
[17] J.J. Ríos, M.C. Pérez-Camino, G. Márquez-Ruiz and M.C. Dobarganes, in J. Velísek (Editor), *Proceedings of the Symposium on Chemical Reactions in Foods, Prague, September 1992*, Czechoslovak Chemical Society, Prague, 1992, pp. 238–243.
[18] S.F. O'Keefe, V.A. Wiley and D.A. Knauft, *J. Am. Oil Chem. Soc.*, 70 (1993) 489–492.

[19] M. Ranny, *Thin-Layer Chromatography with Flame Ionization Detection*, Reidel, Dordrecht, 1987, pp. 69–81.
[20] T.D. Hilditch and J.G. Rigg, *J. Chem. Soc.*, (1935) 1774.
[21] F.H. Mattson and R.A. Volpenhein, *J. Lipid Res.*, 3 (1962) 281–296.
[22] J.J. Ríos, M.C. Pérez-Camino, G. Márquez-Ruiz and M.C. Dobarganes, *Food Chem.*, 44 (1992) 357–362.
[23] J.K. Kaitaranta and N. Nicolaides, *J. Chromatogr.*, 205 (1981) 339–347.
[24] R.T. Holman and O.C. Elmer, *J. Am. Oil Chem. Soc.*, 24 (1947) 127–129.
[25] K. Miyashita and T. Takagi, *J. Am. Oil Chem. Soc.*, 63 (1986) 1380–1384.
[26] J.P. Cosgrove, D.F. Church and W.A. Pryor, *Lipids*, 22 (1987) 299–304.
[27] K. Miyashita and T. Takagi, *J. Am. Oil Chem. Soc.*, 65 (1988) 1156–1158.
[28] H. Yoshida, I. Kondo and G. Kajimoto, *J. Am. Oil Chem. Soc.*, 69 (1992) 1136–1140.
[29] G. Márquez-Ruiz, M.C. Pérez-Camino and M.C. Dobarganes, *J. Chromatogr.*, 514 (1990) 37–44.

ELSEVIER

Journal of Chromatography A, 662 (1994) 369–373

JOURNAL OF CHROMATOGRAPHY A

Determination of the isoelectric point of the capillary wall in capillary electrophoresis Application to plastic capillaries

Vojtěch Rohlíček, Zdeněk Deyl*, Ivan Mikšík

Institute of Physiology, Vídeňská 1083, Prague 4, Czech Republic

(First received October 12th, 1993)

Abstract

A refined method for measuring endoosmotic flow in capillaries based on weighing the amount of liquid transferred is described. The method has been applied to the estimation of isoelectric points of two types of plastic capillaries (polytetrafluoroethylene and polytetrafluoroethylene–polyhexafluoropropylene copolymer). Contrary to expectation both plastic capillaries exhibited considerable electroosmotic flow and changes in hydrodynamic flow resistance without applied voltage. The nature of these phenomena is discussed.

1. Introduction

A crucial phenomenon in capillary electrophoresis is electroosmotic flow. This flow originates from the negative charges caused by the presence of silanol groups on the inner surface of the fused-silica capillary. Though widely used mainly because of their commercial availability, fused-silica capillaries exhibit some disadvantages caused mainly by sorption of solutes to the capillary wall. In our attempts to apply capillaries made of other UV-transparent materials the need of estimating their isoelectric point has arisen. In the present communication we describe a simple and precise approach for estimating isoelectric points.

Several methods have been described for measuring the electroosmotic flow in capillaries [1]. By weighing the solution emerging from the capillary on an analytical microbalance the problem of adsorbing a neutral marker on the capillary wall can be circumvented [2,3]. Another method exploits the measurement of the electrophoresis current when a buffer with different ionic strength is introduced [4]. It is also possible to measure directly the ζ potential of the capillary wall as reported by Van de Goor *et al.* [5]. This measurement either uses weighing of the effluent (see also Altria and Simpson [2,3]) or involves measuring of the streaming potential when the solvent is pumped through the column. In this way the ζ potential and electroosmotic flow of polytetrafluoroethylene (PTFE) capillaries was measured.

A number of papers have been published on manipulating the electroosmotic flow [6,7]. In the simplest case the pH and the ionic strength of the electrolyte can be adjusted to give the optimum speed for a given separation. Another possibility is to vary the electroosmotic flow by

* Corresponding author.

0021-9673/94/$07.00
SSDI 0021-9673(93)E1237-T

introducing additives to the background buffer. By using surface active agents or organic solvents electroosmotic flow speed can be changed dramatically or reversed [8,9]. No matter what method of electroosmotic flow adjustment is used, the charge of the capillary wall plays an important role in these considerations.

2. Experimental

2.1. Material and methods

For capillary wall isoelectric point measurement a set of 5 m*M* disodium citrate buffers was used. The rather low buffer concentration was used to keep the current within reasonable limits (less than 80 μA) during the experiment. Buffer components were of analytical-reagent quality and were obtained from Lachema (Brno, Czech Republic). Runs with applied voltage were run at 4.0 kV per 70 cm × 200 μm I.D. capillary. The applicability of the method was demonstrated with PTFE (Norton Performance Plastics, Willich, Germany) and polytetrafluoroethylene–polyhexafluoropropylene (Kablo, Vrchlabi, Czech Republic) capillaries. When purchased the outer diameter of the tested capillaries was 1 mm with an I.D. of 500 μm; before measurement the capillaries were drawn to achieve I.D. of 200 μm. This rather large I.D. was used in order to obtain easily measurable volumes of transferred electrolyte. For stabilization after drawing the capillaries were left to rest for at least one day. Stabilization time was also necessary after filling the capillary with the electrolyte, because even modest filling pressure made the inner diameter expand and this causes additional flow upon shrinking. A stabilization time of 1 h was found sufficient.

2.2. Procedure

Estimation of the isoelectric point of the capillary was based on measuring the electroosmotic flow in a capillary inclined to give a gravity flow around of 8 mg per 5 min. The amounts of the background electrolyte that have passed through the capillary were plotted against pH and the isoelectric point of the capillary was estimated as the intersection of lines obtained with and without applied voltage.

The determination of the isoelectric point of the capillary wall was done by weighing. The experimental set-up is shown in Fig. 1. There were two reasons for not using levelled electrode jars: (1) constant flow allowed for more precise weighing of the liquid that has passed through the capillary and (2) the constant flow through the capillary cooled the system and avoided bubble formation inside the capillary column. The capillary was for most of its part placed into a tube filled with circulating paraffin oil for cooling and temperature stabilization. The cathode jar was placed on a balance tray of a digital balance (Sartorius 2004 MP6; Sartorius, Göttingen, Germany). Because it was demanded that the accuracy of weighing was 0.1 mg at least, any influence on the jar mass had to be eliminated. There were four possible sources of error foreseen, namely (i) transmission of the small changes of the position of the capillary assembly, (ii) friction between the contact and the negative terminal of the high-potential source (HTS), (iii) electrostatic forces inside the balance room and (iv) evaporation of the fluid in the jar.

Fig. 2 shows this part of the arrangement in detail. At the passage of the capillary through the end of the paraffin oil bath the capillary is extended with a highly elastic silicon rubber tube. This tube passes tightly through the upper part of the jar. A thin Pt wire is placed into this tube (the path of the current is short-circuited in

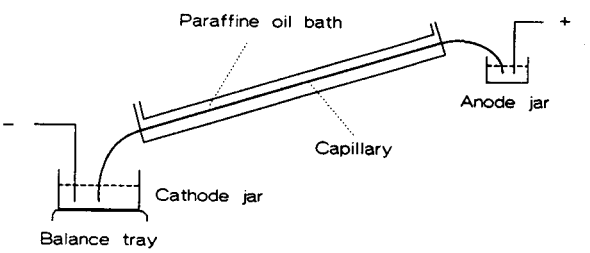

Fig. 1. Schematic representation of the experimental apparatus.

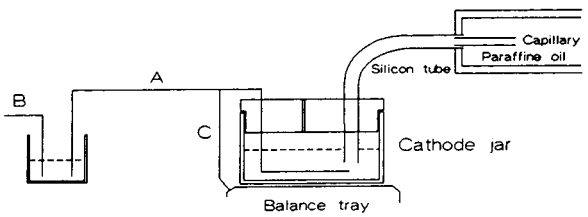

Fig. 2. Detailed representation of the cathode end arrangement. For details see Experimental.

this way) to abolish any electro-endoosmotic forces in it.

The connection to the negative terminal of the HTS was performed by a fluid contact materialized by wire A tightly passing the upper part of the jar. The other end of this wire was immersed in a vessel outside the balance tray filled with a 1% NaCl solution. Wire B connects the fluid in this vessel with the negative terminal of the HTS. An auxiliary wire C connects the metallic balance tray with the fluid contact. Because the metallic case of the balance was also connected with the negative HTS output any electrostatic field inside the balance was eliminated.

A small (0.4 mm) hole was drilled in the upper part of the jar to eliminate the influence of air pressure changes caused by the changing liquid height in the jar as well as possible changes in the atmospheric pressure. The diameter of the jar was 30 mm; in this way transferring of 10 μl of the fluid during one measurement caused a fluid height difference in the jar of only 0.03 mm which can be neglected.

The upper electrode jar was connected to the positive output of the HTS source. Because of its elevated position hydrostatic flow from this jar through the capillary was generated. This arrangement was preferred to the "zero flow" mode (equilibrated jar levels) as in the set-up used no reversed flow due to pH changes could occur. Finally the ratio between the flow with and without applied potential was evaluated and the pH at which this ratio = 1 defined the isoelectric point. The measurements were done over a 5-min period at 4 kV and 0.1 mA. The mean value of 10 pairs of measurements was used for constructing the graph.

3. Results and discussion

As demonstrated in Fig. 3 both the PTFE and polytetrafluoroethylene–polyhexafluoropropylene capillaries exhibited distinct electroosmotic flow with isoelectric points at 3.25 and 3.0, respectively. The reliability of these measurements is evaluated in Table 1. Estimation of electroosmotic flow by the weighing method has been shown to be precise and uncomplicated confirming the previous results of Altria and Simpson [2,3]. There are, however, two phenomena which need some discussion. First, as the capillaries are made of tetrafluoroethylene and tetrafluoropropylene–hexafluoropropylene, respectively, they should be devoid of any chargeable functional groups on their inner surface. Consequently, from the strictly theoretical point of view they should be also devoid of any electroosmotic flow, which, however, is not the case. Investigations at the producers of these capillaries confirmed that no additives (softeners) of any kind that may be responsible for the inner surface charge are used during manufacturing of these products. As also dipole-caused charges are unlikely to occur in these capillaries, it is feasible to assume that charged buffer components may be sorbed on the capillary wall loading it with some (reproducible) charge that causes the electroosmotic flow when the capillary is attached to a high-voltage source. This conclusion is supported by the fact that electroosmotic flow at very low pH (below 2.5) ceases and the data obtained in this range are poorly reproducible. The decrease of the electroosmotic flow at very low pH values with imposed voltage as compared to the flow without voltage could be ascribed to the properties of the electric double layer.

The other phenomenon seen in Fig. 3 is the incline of the line corresponding to the flow at no imposed voltage. It has to be emphasized that practically no differences in buffer specific densities were observed (5 mM buffers were used) and therefore the phenomenon observed cannot be explained on this basis. Theoretically this dependence should be represented by a horizontal line parallel to the x-axis. However, if one

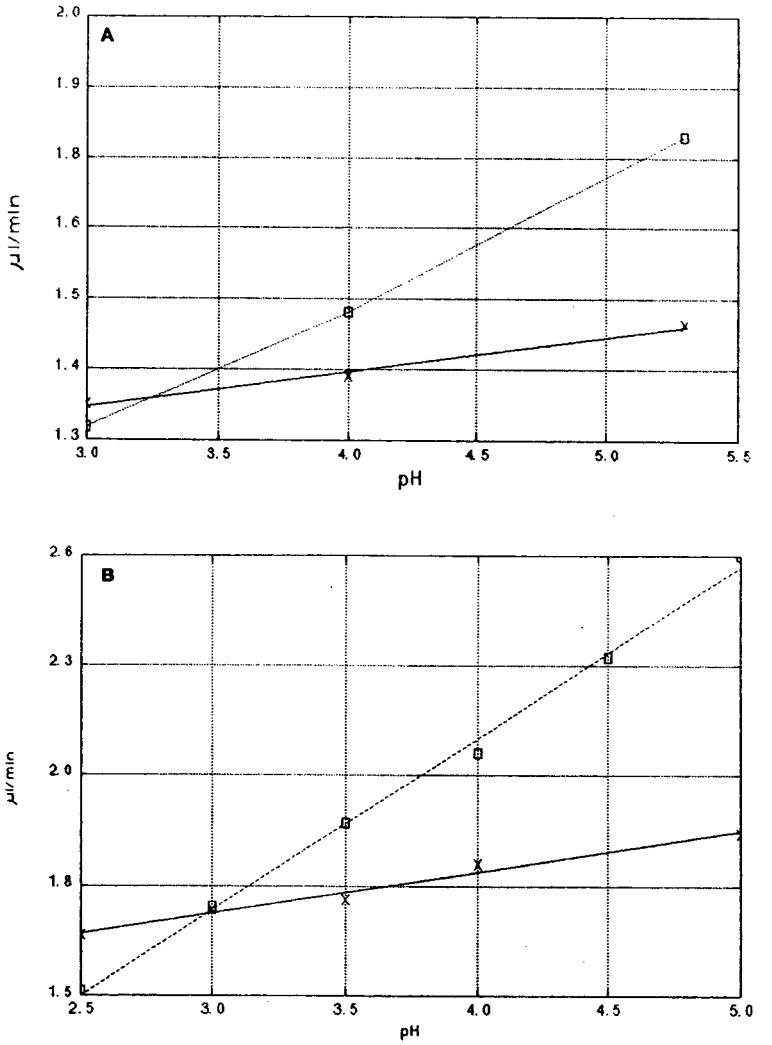

Fig. 3. Electroosmotic (dotted lines) and gravity (solid lines) flow *vs.* pH with (A) the PTFE capillary and (B) the polytetrafluoroethylene–polyhexafluoropropylene copolymer capillary. × = 0 V; □ = 4 kV.

Table 1
Parameters of the regression lines (flow *vs.* pH) in Fig. 3

	PTFE		Polytetrafluoroethylene–polyhexafluoropropylene	
	0 kV	4 kV	0 kV	4 kV
Intercept	1.180273	0.684799	1.392216	0.426285
Slope	0.057819	0.209398	0.102162	0.426857
R^2	0.990419	0.998017	0.977752	0.996776

admits that the buffer components are sorbed on the inner capillary wall, then its properties are likely to change bringing about changed conditions for the hydrodynamic flow. From the nature of the experimental arrangement it is feasible to assume that the forces causing buffer components sorption should be hydrophobic by nature and rather independent on the pH of the running buffer used. Consequently the changes in the amount of the liquid flowing through the capillary should reflect its hydrodynamic flow resistance, for instance if the sorbed entities are more charged at higher pH being acidic by nature, then at higher pH the capillary should be more easily wettable, exhibit lower hydrodynamic resistance and offer a higher flow-rate. In this case, however one would expect that beyond a certain pH where practically all functional groups sorbed to the wall are charged, the line of the pH *versus* flow-rate dependence will bent to become parallel to the x-axis. Such an effect was, however, not observed. On the other hand it is necessary to keep in mind that as with fused-silica capillaries the sorbed charged entities will act in a similar way as the ionized silicic acid groups, *i.e.* they will be neutralized by hydronium ions (hydrated cations) forming a compact layer overlaid (due to the thermal motion) by a loosely held layer termed usually diffuse layer. Combination of these effects may lead to the linear dependences seen in Fig. 3. As a matter of fact the difference of the investigated capillaries to the commonly used fused silica may be that while the charged silanol groups in fused-silica capillaries are covalently bound to the capillary surface, with the plastic-type capillaries the charge observed stems from hydrophobic sorption forces. The flow-rate changes observed at different pH values are also unlikely to be caused by slow changes in capillary dimensions during use; both systematic experiments and random measurements were done with the same result.

Application of capillaries manufactured from other material than fused silica may broaden the possibilities of capillary electrophoresis and may help to overcome some well known problems *e.g.* irreproducible sorption of biopolymers to the capillary wall.

4. Acknowledgement

This work was supported in part by the Czech Ministry of Education, Youth and Sports, grant No. 0711.

5. References

[1] S.F.Y. Li, *Capillary Electrophoresis* (*Journal of Chromatography Library*, Vol. 52), Elsevier, Amsterdam, 1992.
[2] K.D. Altria and C.F. Simpson, *Anal. Proc.*, 23 (1986) 453.
[3] K.D. Altria and C.F. Simpson, *Chromatographia*, 24 (1987) 527.
[4] X. Huang, M.J. Gordon and R.N. Zare, *Anal. Chem.*, 60 (1988) 1837.
[5] A. van de Goor, B. Wanders and F. Everaerts, *J. Chromatogr.*, 470 (1989) 95.
[6] H.H. Lauer and D. McManigill, *Anal. Chem.*, 58 (1986) 166.
[7] S. Fujiwara and S. Honda, *Anal. Chem.*, 58 (1986) 1811.
[8] S. Terabe, K. Otsuka, K. Ichikawa, A. Tsuchiya and T. Ando, *Anal. Chem.*, 56 (1984) 111.
[9] X. Huang, J.A. Lucker, M.J. Gordon and R.N. Zare, *Anal. Chem.*, 61 (1989) 766.

ELSEVIER

Journal of Chromatography A, 662 (1994) 375–381

JOURNAL OF CHROMATOGRAPHY A

Capillary electrophoresis, combined with an on-line micro post-column enzyme assay

Åsa Emmer, Johan Roeraade*

Department of Analytical Chemistry, Royal Institute of Technology, S-100 44 Stockholm, Sweden

(First received September 7th, 1993; revised manuscript received November 8th, 1993)

Abstract

A system for capillary electrophoresis (CE), combined with a micro post-column reactor for on-line enzyme assays is described. Two detectors are employed. The first detector is an on-column UV detector, utilized to monitor the CE separation, while the second detector is monitoring the reaction product which is formed by adding a flow of substrate in the post-column section.

Factors affecting the band broadening in the post-column reactor have been investigated. A short reaction distance as well as a high flow-rate of substrate showed to be optimal.

A CE separation of glucose-6-phosphate dehydrogenase (G-6-PDH) and 6-phosphogluconic dehydrogenase (6-PGDH) was performed, where the enzyme activity could be monitored after reaction with nicotinamide–adenine dinucleotide phosphate/glucose-6-phosphate. The minimal detectable amount of G-6-PDH was shown to be in the order of $5 \cdot 10^{-16}$ mol ($2 \cdot 10^{-7}$ *M*).

1. Introduction

Electro-driven separations, carried out in capillary tubes have a considerable potential for improved separations of biomolecules. Due to the superior heat dissipation characteristics of the miniaturized format, the electrophoresis can be carried out under high field strength, which leads to a rapid and efficient separation [1–4]. Furthermore, the use of on-line detection devices provides far better quantitative data than those obtained with classical staining techniques. An additional important benefit of capillary electrophoresis (CE) is the ease of automation of the procedure. The number of applications of CE for separation of biomolecules like amino acids, peptides, proteins and DNA fragments is therefore growing very rapidly [5,6].

In this context, CE separation of enzymes is of great interest. Apart from the advantages mentioned, an important characteristic of CE is that only nl to pl volumes are handled by the column. Combined with appropriate miniaturized sample holders [7], it is possible to obtain qualitative and quantitative information even from very small amounts of material. This would be very valuable in several fields, such as in pre-natal clinical diagnostics or in studies of single-cell metabolics.

Enzymes are usually quantified and/or identified by measuring their biological activity, since this is the most relevant property in their biochemical context. The standard procedure in such measurements is to measure/monitor the

* Corresponding author.

0021-9673/94/$07.00
SSDI 0021-9673(93)E1187-5

reaction rate with a substrate. Under initial reaction conditions, where an excess of substrate is present, and no interference from the accumulated reaction product occurs, each enzyme displays a specific reaction rate constant. By simply mixing the substrate with the enzyme and a subsequent incubation of the reaction mixture, the amount of enzyme present can be determined.

For enzymes, separated by CE, it is possible to determine their activity after fraction collection as demonstrated *e.g.* by Banke *et al.* [8]. However, this is a rather laborious procedure, and an on-line method would be highly desirable, particularly in routine applications (*e.g.* in a clinical laboratory).

On-line enzyme assays in the form of a post-column reaction have been described for liquid chromatography [9–11], where the substrate is added to the column effluent in a mixing tee and the formed reaction product is measured at a downstream point.

Recently, Bao and Regnier [12] described a system, where the substrate was an integral part of the running buffer. During the electrokinetic transport, a broad band of reaction product is formed, due to differences in electrophoretic mobilities between the enzyme, the reaction product and the substrate. By a temporary interruption of the applied potential (and thereby the electrokinetic flow) a local increase in signal is generated, the strength of which is related to the activity of the enzyme and the interruption period.

In the present work, we report a system for CE–post-column micro-enzyme assays, where two detectors are employed. The first detector is an on-column UV detector, to monitor the separation in the CE column, while the second detector is mounted downstream after mixing the column effluent with substrate, to monitor the generated reaction products.

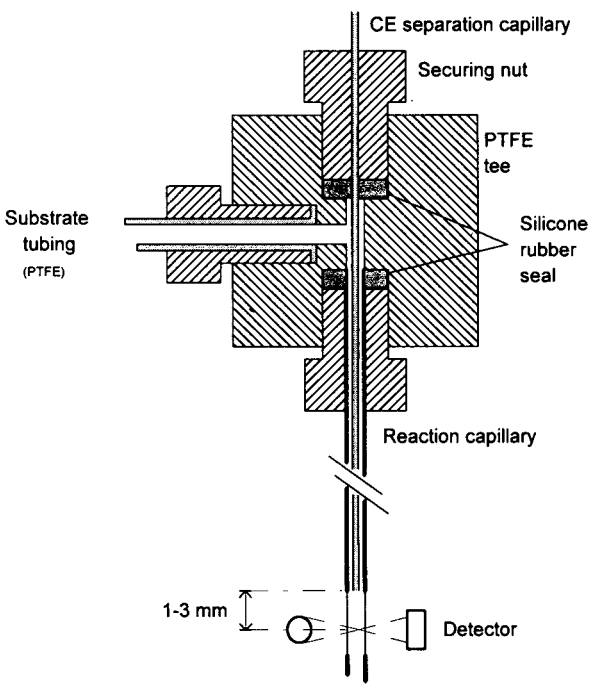

Fig. 1. Schematic of the post-capillary reactor.

2. Experimental

2.1. Post-capillary reactor

Fig. 1 shows a schematic of the reactor. It consists of a PTFE tee (0.7 mm I.D. holes) in which both the separation and reaction capillaries are mounted. The separation capillary (50 μm I.D. × 360 μm O.D.) is inserted into the reaction capillary (0.53 mm I.D., 0.7 mm O.D.) in such a way that the outlet is positioned 1–3 mm above the detection window of the reaction capillary. The substrate stream is introduced into the tee by a PTFE tube (0.7 mm I.D. × 1.6 mm O.D.).

Fig. 2 shows a set up where the position of the reactor in the total capillary zone electrophoresis (CZE) system is shown.

2.2. Instrumentation

The apparatus used consisted of two variable-wavelength UV detectors (Model UVIS 200; Linear Instruments, Reno, NV, USA) each equipped with an on-column capillary cell (Model 9550-0155, Linear Instruments) and further connected to a strip-chart recorder (Linear Instruments). The high-voltage supply, ± 0–30

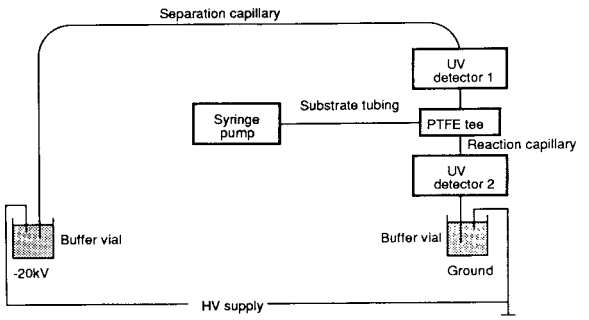

Fig. 2. The CE system including the post-capillary reactor. HV = High voltage.

kV, was constructed from a Spellman CZE 100 (Plainview, NY, USA) unit. The CZE column was placed in a Plexiglass box with a high-voltage safety interlock, which also housed an injection device and arrangements for *in situ* flushing by action of pressurized air (0.5–2.0 bar). Substrate flow was introduced by using a syringe pump (Model 351; Sage Instruments, Orion Research, Boston, MA, USA). Plastic syringes (2–5 ml) (Millipore, Bedford, MA, USA) were used. Actual flow-rates were determined by weighing the dispensed liquid. Sample injections were accomplished by electromigration.

A reversed polarity set up was employed, where the capillary inlet was kept at negative potential, while the detection side of the capillary was grounded.

2.3. Materials and reagents

Fused-silica tubing was obtained from Chrompack (Middelburg, Netherlands). The total length of the separation capillary was 75 cm. The length to detector 1 was 60 cm, the total length of the reaction capillary was 15 cm and the length from the inlet of the reaction capillary to detector 2 was about 7 cm.

The fluorosurfactant (FC134) was obtained from 3M Co. (St. Paul, MN, USA). The water used to prepare solutions was passed through a Milli-Q system (Millipore). Glucose-6-phosphate dehydrogenase (G-6-PDH) (torula yeast), nicotinamide–adenine dinucleotide phosphate (NADP) and glucose-6-phosphate (G-6-P) were purchased from Sigma (St. Louis, MO, USA). 6-Phosphogluconic dehydrogenase (6-PGDH) was a gift from the Department of Biochemistry and Biotechnology, Royal Institute of Technology (Stockholm, Sweden).

Enzyme solutions with a protein concentration of 0.2 mg/ml for G-6-PDH and 0.05 mg/ml for 6-PGDH were freshly prepared before electrophoresis experiments in 0.05 *M* phosphate buffer with a pH of 5. Substrate solution was prepared freshly in 0.05 *M* phosphate buffer, pH 8, with a G-6-P concentration of 1 m*M* and a NADP concentration of 0.2 m*M*.

The running buffer contained 100 μg/ml FC134 in 0.05 *M* phosphate buffer at pH 5. Before use, new capillaries were rinsed for 30 min with 0.4 *M* NaOH, 10 min with water and 20 min with running buffer. Between each run the separation capillary was rinsed for 3 min with running buffer.

3. Results and discussion

One of the most important considerations in designing the enzyme reactor was to maintain the resolution, obtained by the separation capillary. The major factors that contribute to post-column peak broadening are diffusion and dispersion due to the parabolic Taylor flow profile, generated by the pressure-driven flow of substrate. The influence is dependent on the diameter of the reactor capillary, the flow velocity of the substrate and, particularly important, on the distance between the outlet of the CE capillary and the point of detection in the reaction capillary. To avoid an excessive loss of efficiency, this distance had to be kept to a few mm only.

In order to evaluate the band-broadening characteristics of the post capillary reactor without possible influences from the reaction process, mesityloxide was injected in the separation capillary and monitored before and after passing through the reactor. Fig. 3 and Table 1 show the results obtained for different substrate flow-rates and for different distances between the separation capillary and the second detector. As can be

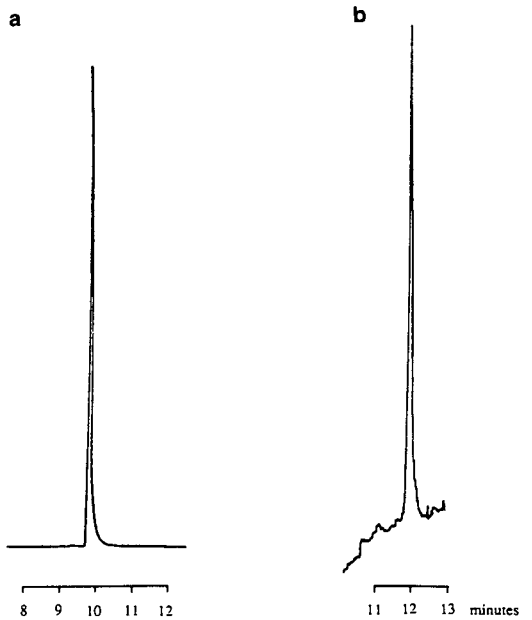

Fig. 3. Electropherogram of mesityloxide. (a) Signal from detector 1, before the post column reactor, (b) signal from detector 2, after the reactor. Concentration: 0.01%, detector wavelength: 254 nm for both detectors 1 and 2, sensitivity range: detector 1, 0.005 AUFS and detector 2, 0.002 AUFS, separation voltage: − 20 kV, syringe pump flow-rate: 43.2 μl/min (no substrate added to the reactor buffer), distance between the separation capillary outlet and detector 2: 1 mm.

seen, the position of the second detector, relative to the CE capillary outlet is very critical. While the loss of efficiency is relatively small at 2 mm distance, it becomes unacceptable at 3 mm distance. Since the 2 mm setup allows a longer reaction time for the enzyme assay than the 1 mm setup, all subsequent experiments were carried out with the 2 mm distance set up. Under these conditions, the influence of the substrate flow-rate on the efficiency is not very pronounced as can be seen from the last part of Table 1.

Table 1
Influence of the distance between the separation capillary outlet and detector 2, and of the ratio of the linear flow-rates in the reactor and the separation capillary (v_{react}/v_{sep}) on the ratio of the number of plates (N_{det2}/N_{det1}) for mesityloxide before (detector 1) and after (detector 2) the post-capillary reactor

Distance between the separation capillary and detector 2 (mm)	v_{react}/v_{sep}	N_{det2}/N_{det1}
1	2.3	1.2
2	2.3	0.80
3	2.3	0.29
2	1.2	0.86
2	2.3	0.80
2	3.3	0.98

When the mesityloxide passed the second detector, a decrease in sensitivity of about one order of magnitude was observed, compared to the signal obtained from the first detector. This is likely to be caused by the dilution of the sample in the reactor flow. The increased total volume results in a hundredfold decrease in sensitivity, while the increase in pathlength only gives rise to a tenfold sensitivity increase. The optics of the employed detector cell are optimized for capillary dimensions of 50–100 μm I.D. and 360 μm O.D., according to the manufacturer (Linear Instruments). Since the reactor capillary has considerably larger cross-sectional dimensions, the light beam will not be focused on the centre of the capillary, which could also contribute to decreased sensitivity.

The enzyme reaction studied in this work is the interaction of G-6-PDH with G-6-P in presence of NADP. The schematic of the reaction is shown below:

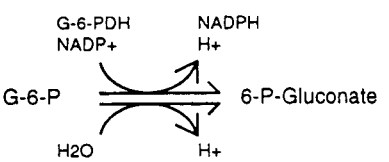

To suppress the wall adsorption of G-6-PDH, a cationic fluorosurfactant was added to the running buffer. As we have shown earlier, the presence of a very small amount of this detergent leads to remarkably improved efficiency and reproducibility [13]. Due to the formation of an admicellar bilayer at the wall, the electroosmotic flow is reversed and positively charged species are repelled from the wall.

G-6-PDH has a p*I* of 6 and therefore a running buffer pH of 5 was used to effect the repellation. Under these conditions the direction of the electrophoresis of the enzymes and the electroendosmotic flow are opposed to each other. This should improve the resolution [2].

According to our earlier findings, the influence of fluorosurfactant buffer additives on the enzymatic activity is very moderate [14]. We attribute this behaviour to the lipophobic character of the fluorocarbonic chains and the fact, that the surfactant is present in only very low concentrations. Fig. 4 shows the electropherograms obtained for G-6-PDH before and after the reaction. As can be seen, the peaks, due to the enzyme in the first detector and the monitored reaction product (NADPH) in the second detector are of similar width.

Band broadening in the post-capillary reactor

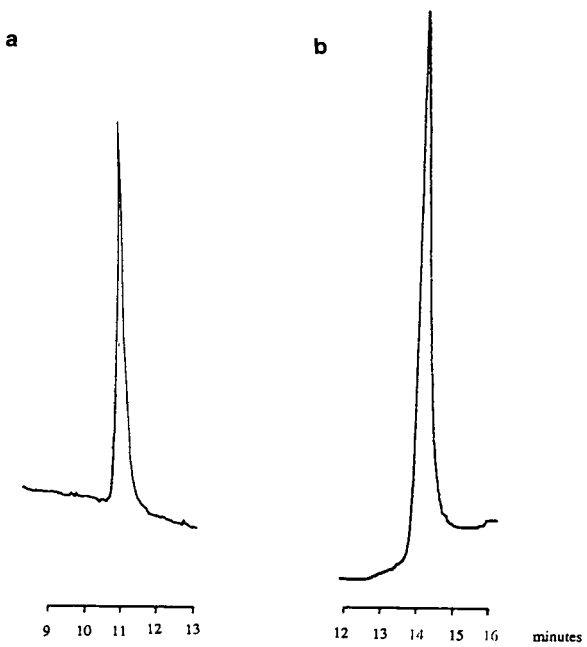

Fig. 4. Electropherograms before and after the reaction of G-6-PDH and NADP/G-6-P. (a) Signal from detector 1, before the reaction, (b) signal from detector 2, after the reaction. Detector wavelength: detector 1, 210 nm; detector 2, 340 nm. Sensitivity range: detector 1, 0.005; detector 2, 0.002 AUFS. Separation voltage: − 20 kV, substrate flow: 9.8 μl/min, distance between the separation capillary outlet and detector 2: 2 mm, enzyme concentration: 0.2 mg/ml.

is promoted by several phenomena. Initially, when leaving the column exit, the solutes are picked up by the surrounding substrate and are transported in the centre part (corresponding to the inner cross-section of the CE column) of the parabolic flow profile of the substrate. At the same time, the enzyme–substrate reaction takes place, while a dispersion of the solutes as well as the reaction products is induced by diffusion in both radial and longitudinal direction. Since the diffusion coefficient is dependent on the molecular mass of the solutes, the dispersion is most pronounced for the reaction products. The diffusion rate can be calculated from the Einstein equation:

$$x = (2Dt)^{1/2} \quad (1)$$

where x is the diffusion distance, D is the diffusion coefficient and t is the mean time for diffusion. Assuming a D of $1 \cdot 10^{-5}$ cm^2/s (which would be a typical value for a low-molecular-mass compound in water), and reaction times before the detection takes place as in our experiments (0.6–2.7 s), the dispersion would be 35–73 μm. Thus, the solutes will not reach the more stagnant regions of the parabolic flow profile near the wall of the reactor, which would have caused a very significant band broadening. Also the axial dispersion caused by diffusion is negligible, since it would only add *ca.* 1% to the variance of the solute band. Of additional importance is that the speed of the surrounding sheath flow of substrate was of the same order as the endosmotic flow [15–17].

A further cause of peak broadening, as identified by Rose and Jorgenson [15] is the radial dispersion, induced by the electric field in the post-column section. In our case, an axial electric spread of the reaction product could also be visualized, since the products obtained are likely to have different electrophoretic mobilities, compared to the enzymes. In the present post-column design, the large difference in diameter between the CE capillary and the reactor is of a significant advantage, since this reduces the electrical potential across the reactor. In fact, the calculated field strength over the reactor employed is only *ca.* 2 V/cm, for a corresponding

value over the separation capillary of 270 V/cm, this under assumption that the solutions have the same specific conductivity. Since the ion strength of the running buffer and the substrate solution were of the same order of magnitude, the electrical dispersion in our post-column reactor should therefore be neglectable.

Fig. 5 shows a response curve for the G-6-PDH experiments, using the described setup.

Under these conditions, the minimal detectable amount of G-6-PDH showed to be in the order of $5 \cdot 10^{-16}$ mol ($2 \cdot 10^{-7}$ M). A longer reaction time would increase the sensitivity, but at the expense of a deteriorated peak resolution. A further improvement could be visualized, by scaling down the ratio between inner diameter of the reactor and the outer diameter of the CE capillary, as has been shown by Rose and Jorgenson in a fluorescence post-column reactor. However, the procedure is more complicated, involving HF etching of the capillary ends. Moreover, the back pressure at the end of the CE capillary will rapidly increase when the inner diameter of the reactor capillary becomes small. This could lead to a backflow of liquid in the column, and cause an extra-column band broadening as well as retention shifts. The back pressure can be calculated from the Poiseuille equation

$$\Delta p = 8FL\eta/\pi r^4 \quad (2)$$

where F is the reagent flow through the reactor, r is the inner diameter of the reactor, Δp is the pressure drop and L and η are the length of the reactor and the viscosity of the reagent solution, respectively. In our reactor, the calculated back pressure is only between 6 and 26 Pa for the different flow-rates used, and therefore neglectable in the present separation system.

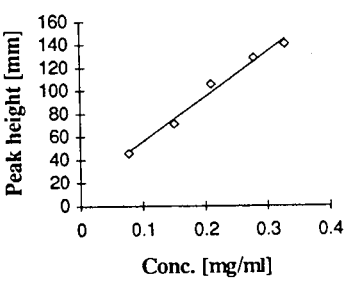

Fig. 5. Response curve for the G-6-PDH/NADP reaction system. Conditions as in Fig. 4.

Another route towards improved sensitivity would be to prolong the reaction time prior to detection. One possibility would be to employ a reaction medium with a higher viscosity, which would allow longer reaction times without increasing the dispersion to an unacceptable level. A limiting factor would be a rapid local depletion of substrate, since a mixing of the phases is supressed. However, for very low sample concentrations, this would be less of a problem.

Our present post-column reactor arrangement provides the freedom to separately optimize the electrophoretic separation conditions and the enzymatic reaction conditions (type of buffer ions, pH, ion strength, additives etc.).

There are for example many cases, where the pI of the enzyme is considerably lower than the pH, where the enzyme has its full activity. Since the best electrophoretic separation selectivity is often around the pH of the isoelectric point, the post-column concept offers an important advantage compared to schemes, where the enzyme reaction is performed within the CE capillary. Moreover, it is easy to change the substrate and optimize its flow-rate.

To illustrate the applicability of CE separations in combination with the micro post-column enzymatic assay, a system including G-6-PDH and 6-PGDH was examined. 6-PGDH has reportedly an activity for the combination with G-6-P/NADP of about a hundredfold lower than G-6-PDH. This corresponds well with our results, shown in Fig. 6, which shows a CE separation of G-6-PDH and 6-PGDH and the subsequent enzyme activity profile.

The possibility to obtain a CE separation pattern together with the corresponding enzymatic activity profile should be of interest in a number of applications. With further improvements in CE separations (*e.g.* improved column technology) it should be possible to quantify different isoenzymes for the purpose of clinical diagnostics. Such work is currently in progress.

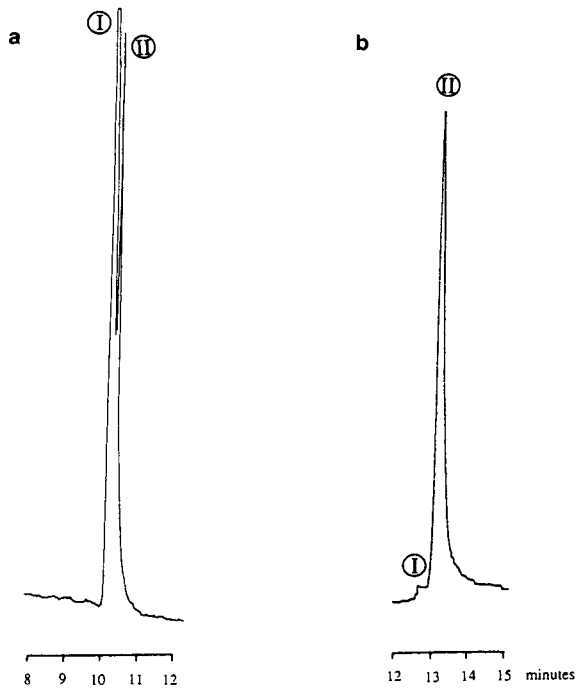

Fig. 6. Electropherograms showing the separation and enzymatic activity profile of G-6-PDH and 6-PGDH. (a) Detector 1, (b) detector 2. I = 6-PGDH, concentration 0.05 mg/ml; II = G-6-PDH, concentration 0.2 mg/ml. Conditions as in Fig. 4.

4. Acknowledgements

This work was financially supported by the Swedish Natural Research Council and the Swedish National Board for Industrial and Technical Development.

5. References

[1] F.E.P. Mikkers, F.M. Everaerts and Th.P.E.M. Verheggen, *J. Chromatogr.*, 169 (1979) 11.
[2] J.W. Jorgenson and K.D. Lukacs, *Anal. Chem.*, 53 (1981) 1298.
[3] S. Hjertén, *J. Chromatogr.*, 347 (1985) 191.
[4] R.J. Nelson, A. Paulus, A.S. Cohen, A. Guttman and B.L. Karger, *J. Chromatogr.*, 480 (1989) 111.
[5] S.F.Y. Li, *Capillary Electrophoresis —Principles, Practice and Applications*, Elsevier, Amsterdam, 1992.
[6] D. Perrett and G. Ross, *Trends Anal. Chem.*, 11 (1992) 156.
[7] M. Jansson, Å. Emmer and J. Roeraade, *J. Chromatogr.*, 626 (1992) 310.
[8] N. Banke, K. Hansen and I. Diers, *J. Chromatogr.*, 559 (1991) 325.
[9] J.A. Fulton, T.D. Schlabach, J.E. Kerl, E.C. Toren Jr. and A.R. Miller, *J. Chromatogr.*, 175 (1979) 269.
[10] J.A. Fulton, T.D. Schlabach, J.E. Kerl and E.C. Toren Jr., *J. Chromatogr.*, 175 (1979) 283.
[11] T.D. Schlabach, A.J. Alpert and F.E. Regnier, *Clin. Chem.*, 24 (1978) 1351.
[12] J. Bao and F.E. Regnier, *J. Chromatogr.*, 608 (1992) 217.
[13] Å. Emmer, M. Jansson and J. Roeraade, *J. Chromatogr.*, 547 (1991) 544.
[14] Å. Emmer, M. Jansson and J. Roeraade, *J. Chromatogr.*, submitted.
[15] D.J. Rose and J.W. Jorgenson, *J. Chromatogr.*, 447 (1988) 117.
[16] B. Nickerson and J.W. Jorgenson, *J. Chromatogr.*, 480 (1989) 157.
[17] Y.F. Cheng, S. Wu, D.Y. Chen and N.J. Dovichi, *Anal. Chem.*, 62 (1990) 496.

ELSEVIER

Journal of Chromatography A, 662 (1994) 383–388

JOURNAL OF CHROMATOGRAPHY A

Measurement of the enzymatic specificity of carboxypeptidase A by capillary zone electrophoresis

M.J. Perron, M. Pagé*

Department of Biochemistry, Faculty of Medicine, Université Laval, Sainte-Foy, Québec, G1K 7P4 Canada

(First received September 23rd, 1993; revised manuscript received October 25th, 1993)

Abstract

The development of a novel method using capillary zone electrophoresis for monitoring enzymatic assays involving carboxypeptidase A and methotrexate-α-peptides is reported. Since the hydrolysis product, methotrexate, and the substrate have the same absorption spectrum, spectrophotometry could not be used to monitor the reaction. Eleven methotrexate amino acid prodrugs were synthesized and tested as substrates for carboxypeptidase A. Since the product has a charge difference with the substrate, the reaction could be monitored easily by capillary zone electrophoresis. This method may be adapted to various enzyme kinetics.

1. Introduction

Capillary electrophoresis techniques are increasing in popularity due to their versatility and their powerful analytical capacity. They are used for the separation and characterization of a large variety of biomolecules. Many techniques involving different separation mechanisms have already been described [1,2] showing their advantages in comparison with other common separation procedures such as HPLC and supercritical fluid chromatography [3]. Capillary zone electrophoresis (CZE) is often used for the separation of small peptides or drug molecules and their metabolites. CZE is characterized by rapid analysis times (5–30 min), small sample volumes (10 nl–10 μl), a sensitivity at the nanogram level and a high resolution [4]. These features combined with a high efficiency and reproducibility lead us to use CZE instead of HPLC for monitoring an enzymatic assay in which carboxypeptidase A (CP-A) hydrolyses methotrexate-α-peptides leading to the release of free methotrexate (MTX).

Since MTX-α-peptides and MTX share comparable absorption spectra and a λmax at 372 nm, the spectrophotometry could not be used for monitoring the reaction. It is possible with CZE to separate the substrate and the product according to the electrophoretic mobility. In this case, the lysis of the C-terminal amino acid changes the mass-to-charge ratio and therefore the electrophoretic mobility of the product with respect to the substrate.

In order to test the method and get the most promising MTX prodrug for CP-A, a range of 11 MTX-α-peptides were selected on the basis of their polarity and structure, and then synthesized. Enzymatic assays were then performed on all of them and the hydrolytic potential of

* Corresponding author.

0021-9673/94/$07.00
SSDI 0021-9673(93)E1159-W

carboxypeptidase A was evaluated for each MTX analogue using CZE.

2. Experimental

2.1 Materials

Chemicals used for buffers were ACS reagent grade material. Bovine pancreatic carboxypeptidase A Type II-DFP (EC 3.4.17.1) and hippuryl-L-phenylalanine were obtained from Sigma (St. Louis, MO, USA). 0.1 *M* phosphate buffer pH 2.5 (cat no. 148-5010), capillary wash solution (cat. no. 148-5022) and the 24 cm × 25 μm coated capillary cartridge (cat. no. 148-3031) were supplied by Bio-Rad (Mississauga, Ontario, Canada). 0.45-μm nylon filters were purchased at Micron Separations (Westborough, MA, USA).

2.2 MTX-α-peptides synthesis

The solid-phase synthesis of MTX-Arg, MTX-Asn, MTX-Cys, MTX-Gln, MTX-His, MTX-Lys, MTX-Met, MTX-Phe, MTX-Pro, MTX-Trp and MTX-Tyr will be described elsewhere. Briefly, they were synthesized on the BioLynx 4175 Peptide Synthesizer (LKB Biochrom, Pharmacia, Baie d'Urfée, QC, Canada) using the Fmoc method.

2.3 Carboxypeptidase A enzymatic assay

Hippuryl-L-phenylalanine

The CP-A activity was measured using the following modifications of the procedure described by Haenseler *et al.* [5]. 1.0 m*M* hippuryl-L-Phe contained in 2.95 ml of 0.1 *M* Tris-HCl buffer pH 7.3–0.2 m*M* $ZnSO_4$ was incubated at 37°C. The enzymatic reaction was initiated by adding 50 μl of CP-A in order to obtain a final reaction volume of 3.0 ml. The increase in absorbency was monitored with a Philips UV/Vis Scanning Spectrophotometer (Model PU 8720) at 254 nm for 15 min. In accordance with the Worthington Enzyme Manual [6], a value of $\Delta\epsilon mM = 13.6$ was used for the reaction and the CP-A concentration was calculated from $\epsilon mM = 64.2$ at 278 nm.

MTX-α-peptides

The same reaction conditions as described above were set for the CP-A assay with the 11 MTX-α-peptides. Fourteen identical reaction mixtures containing 1.0 m*M* MTX-Phe were prepared in separated test tubes in order to stop the enzymatic reaction at 0, 1, 2, 3, 4, 5, 7, 10, 13, 15, 20, 25, and 30 min. No enzyme was added to the 14th tube which contained only the substrate used as a control. When the reaction time had elapsed for each respective vial, a 200-μl aliquot was transferred into 400 μl of boiling water in a microcentrifuge tube for 10 min to stop the reaction and the aliquots were then centrifuged (100 *g*) to discard the enzyme in the pellet. 500-μl aliquots of the 14 supernatants containing the unreacted MTX-Phe and the MTX freed by the reaction were then evaporated to dryness in vacuo with a Savant SpeedVac Model SC200 (Savant Instruments, Farmingdale, NY, USA). The same procedure was repeated for the 10 other MTX derivatives. The value of $\epsilon mM = 33$ for the reaction at 204 nm was determined experimentally.

2.4 Capillary zone electrophoresis

Sample preparation

The 14 MTX-Phe/MTX containing pellets obtained above, each corresponding to a reaction time ranging from 0 to 30 min, were dissolved in 200 μl of 0.1 *M* phosphate buffer pH 2.5 mixed with 100 μl of the same buffer diluted 1:10. Prior to analysis, samples were filtered through a 0.45-μm nylon filter.

Sample analysis

A BioFocus 3000 Automated Capillary Electrophoresis System (Bio-Rad) was used for all CZE experiments. A minimum of 20 μl of each of the 14 samples was put in specially adapted microcentrifuge tubes. The samples were introduced into a 24 cm × 25 μm I.D. coated capillary cartridge by an 8-s electrophoretic injection.

The injection and the analysis were performed

under a 10 kV constant voltage with a current limit of 50 μA. The polarity was set from positive to negative. The compounds were detected at 0.01 AUFS by a built-in UV/Vis detector operating at 204 nm. The running buffer was 0.1 *M* phosphate pH 2.5 for the whole 11 min fully automated runs. Wash cycles were carried out with deionized water, the capillary wash solution and a nitrogen gas purge. Data were obtained using the BioFocus 3000 Spectra and BioFocus 3000 Integrator software provided with the apparatus computer system.

3. Results and discussion

Only data regarding the reaction of CP-A on MTX-Phe are presented in this section. The other MTX-α-peptides were poorly or not at all hydrolyzed by CP-A except for MTX-Tyr and MTX-Gln which showed a weaker activity than MTX-Phe.

The difference in the respective migration of MTX and MTX-Phe is mainly due to their mass-to-charge ratio. Since the polarity is set from + to −, MTX has the tendency to move faster than MTX-Phe which is in turn larger than MTX. Thus, prior to sample analysis, the CZE apparatus was standardized with MTX and MTX-Phe to check their peak positions. MTX had a retention time (RT) of 8.0 min (data not shown) and MTX-Phe was detected after an average of 9.8 min (see Table 1).

Hydrolysis of MTX-Phe by CP-A was easily followed by capillary zone electrophoresis showing the substrate disappearance and the product appearance. As shown in Fig. 1, the progressive increase of MTX was paralleled by the decrease of MTX-Phe. During previous testings, the formation of a small peak (RT 13 min) was also noticed (data not shown), probably corresponding to phenylalanine which is the secondary reaction product. As Kuefner *et al.* have already reported [7], no cleavage of the MTX peptide bond between the glutamyl and the pteroyl moieties by CP-A was observed.

At time = 0 min of the enzymatic assay (see Fig. 1B), the electropherogram showed that the reaction has already started while the substrate MTX-Phe should be the only compound present.

Table 1

Parameters generated by the BioFocus 3000 Integrator

Reaction time (min)	No. of peaks	Retention time (min)		Peak area (%)		Peak height (%)		Absorbance (204 nm)	
		MTX	MTX-Phe	MTX	MTX-Phe	MTX	MTX-Phe	MTX	MTX-Phe
Control (MTX-Phe)	1	–	10.7	–	100	–	100	–	0.0077
0	2	8.39	9.90	16.84	83.16	21.04	78.96	0.0020	0.0076
1	2	8.22	9.77	35.44	64.56	40.64	59.36	0.0039	0.0057
2	2	8.14	9.72	60.48	39.52	65.17	34.83	0.0067	0.0036
3	2	8.12	9.76	81.01	18.99	82.32	17.68	0.0085	0.0018
4	2	8.04	9.70	92.79	7.21	92.93	7.07	0.0089	0.0007
5	2	8.06	9.74	96.54	3.46	96.52	3.48	0.0089	0.0003
7	1	8.04	–	100	–	100	–	0.0098	–
10	1	8.02	–	100	–	100	–	0.0102	–
15	1	8.03	–	100	–	100	–	0.0098	–

Values are related to the peaks corresponding to MTX-Phe and MTX, respectively. The progression of the enzymatic reaction may then be monitored. The separation conditions are described under Experimental.

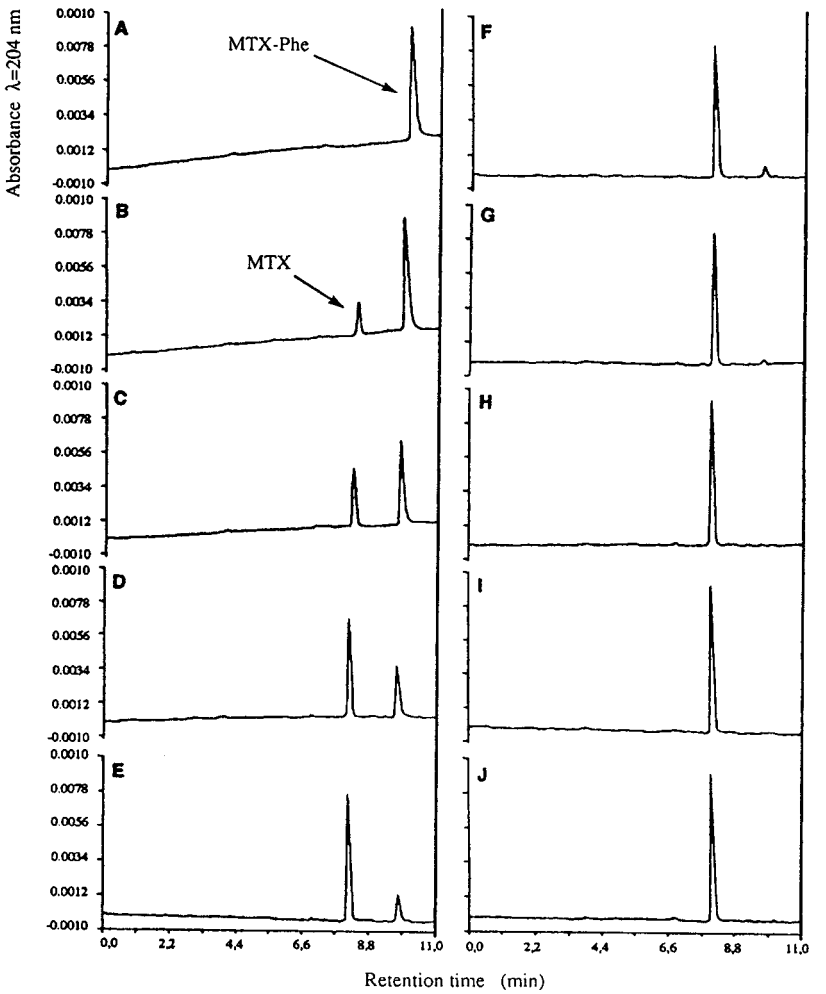

Fig. 1. Electropherograms showing the increase of MTX paralleled by the decrease of MTX-Phe in relation to the progression of the enzymatic hydrolysis. (A) MTX-Phe as a control, and after (B) 0 min, (C) 1 min, (D) 2 min, (E) 3 min, (F) 4 min, (G) 5 min, (H) 7 min, (I) 10 min, (J) 15 min reaction. The separation conditions are described under Experimental.

This was probably due to the method used to stop the enzymatic reaction. Actually, when an aliquot of the reaction mixture was transferred into boiling water, it may have taken a few seconds before the enzyme denaturation occurred.

Many attempts have been made to find a method by which the enzymatic reaction could be stopped instantly. Acids and bases were rejected because of their harmful effects on the compounds and the same is true for any inhibitors such as 1,10-*o*-phenanthroline that could have left undesired residues mixed with MTX which could have made electropherograms difficult to read.

The wavelength selected for monitoring the enzymatic assay by CZE was 204 nm because it is one of the four major peaks in MTX absorption spectrum along with 258, 302 and 372 nm. It is also the most adequate wavelength for measuring the presence of peptides and smaller molecules which are best detected in the range of 190

to 220 nm. The use of CZE is advantageous in this instance because other separation techniques often use solvents that have UV cutoff which prevents the use of these lower wavelengths. Nevertheless, a few assays were carried out at 372 and 302 nm but the peaks appeared to be much smaller for the same amount injected and, combined with a very noisy baseline, an important loss of sensitivity was observed.

As shown in Fig. 2 and as mentioned earlier, CP-A was totally non-responding to MTX-Lys, MTX-His, MTX-Cys and MTX-Arg as substrates and the activity still remained very weak for MTX-Trp, MTX-Pro, MTX-Met and MTX-Asn. Carboxypeptidase A catalyses the hydrolysis of acidic and neutral amino acids from the C-terminal end of a peptide except for proline [8] which is in accordance with the above results. Since lysine, histidine and arginine are basic amino acids and cysteine is an inhibitor of CP-A [6], the non-reactivity of the enzyme towards the corresponding MTX derivatives was not surprising. Also, compounds containing a free carboxyl group or an heterocyclic ring are generally stated as competitive inhibitors [9]. In our study, tryptophan was hydrolysed much more slowly than phenylalanine; in addition, we found that asparagine and glutamine with their amide groups were also poorly hydrolysed by CP-A. Since the structures of tyrosine and phenylalanine are alike, their similar activity was predictable.

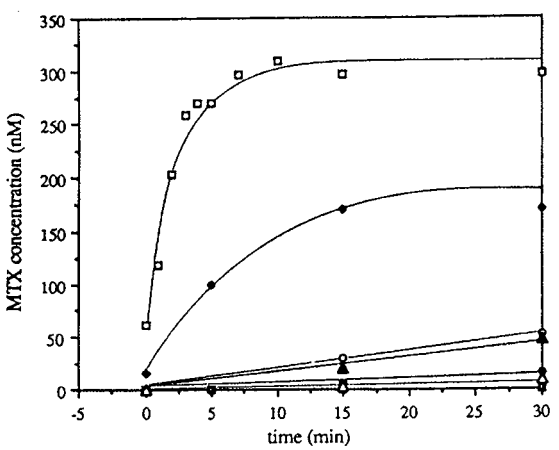

Fig. 2. Enzymatic activity of CP-A on the 11 MTX-α-peptides: MTX-Phe (□), MTX-Tyr (◆), MTX-Gln (○), MTX-Met (▲), MTX-Trp (●), MTX-Asn (△), MTX-Lys, MTX-His, MTX-Cys, MTX-Arg and MTX-Pro (■). (See Experimental for the reaction conditions.)

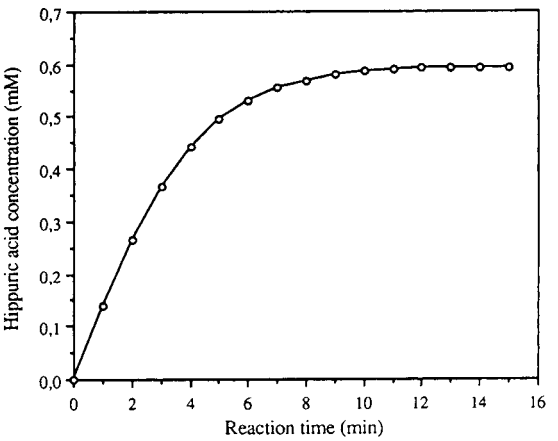

Fig. 3. Enzymatic activity of CP-A on hippuryl-L-phenylalanine. (See Experimental for the reaction conditions.)

As a reference, an enzymatic assay was performed using another CP-A substrate, hippuryl-L-phenylalanine, in conditions used for MTX-Phe (see Fig. 3 and Experimental).

4. Conclusion

In summary, the purpose of this paper was to report a new approach for monitoring enzymatic assays involving MTX-α-peptides hydrolyzed by CP-A. Presently, the synthesis of this type of MTX derivative has an application in the field of cancer research. They may be used as prodrugs which are activated on contact with CP-A thus releasing MTX, an anticancer drug [5,7,10]. These prodrugs are now tested for a more selective and localized chemotherapy [11,12].

The CP-A enzymatic assays monitored by CZE could have an application for the development and the selection of the most suitable MTX prodrugs. Here, MTX-Phe was found to be the best substrate for CP-A out of the eleven tested. The hydrolysis of MTX-Phe by CP-A was com-

parable to the hydrolysis of hippuryl-L-Phe which is a natural substrate for CP-A.

Compared to HPLC and other separation techniques, the CZE method is very rapid, reproducible and requires minimal amounts of material. The progression of the reaction can be visualized easily, combined with a high sensitivity.

References

[1] Z. Deyl and R. Struzinsky, *J. Chromatogr.*, 569 (1991) 63.
[2] S. Fanali and P. Boćek, *Electrophoresis*, 11 (1990) 757.
[3] W. Steuer, I. Grant and F. Erni, *J. Chromatogr.*, 507 (1990) 125.
[4] F. Stover, *Electrophoresis*, 11 (1990) 750.
[5] E. Haenseler, A. Esswein, K.S. Vitols, Y. Montejano, B.M. Mueller, R.A. Reisfeld and F.M. Huennekens, *Biochemistry*, 31 (1992) 891.
[6] C.C. Worthington (Editor), *Worthington Enzyme Manual*, Worthington Biochemical Corporation, Freehold, NJ, 1988, p. 60.
[7] U. Kuefner, U. Lohrmann, Y.D. Montejano, K.S. Vitols and F.M. Huennekens, *Biochemistry*, 28 (1989) 2288.
[8] R.H. Haschemeyer and A.E.V. Haschemeyer, *Proteins: A guide to study by physical and chemical methods*, Wiley and Sons, New York, NY, 1973, pp. 77, 89.
[9] T.E. Barman, *Enzyme Handbook*, Vol. II, Springer-Verlag, New York, NY, 1969, p. 606.
[10] U. Kuefner, A. Esswein, U. Lohrmann, Y. Montejano, K.S. Vitols and F.M. Huennekens, *Biochemistry*, 29 (1990) 10540.
[11] K.D. Bageshawe, C.J. Springer, F. Searle, P. Antonis, S.K. Sharma, R.G. Melton and R.F. Sherwood, *Br. J. Cancer*, 58 (1988) 700.
[12] K.D. Bageshawe, *Br. J. Cancer*, 60 (1989) 275.

ELSEVIER

Journal of Chromatography A, 662 (1994) 389–395

JOURNAL OF CHROMATOGRAPHY A

Electrophoretically mediated microanalysis of calcium

Dale H. Patterson, Bryan J. Harmon, Fred E. Regnier*

Purdue University, Department of Chemistry, West Lafayette, IN 47907-1393, USA

(Received November 9th, 1993)

Abstract

Electrophetically mediated microanalysis (EMMA) was used for the determination of calcium. The faster analyte zone containing the calcium was injected spatially behind a slower zone of *o*-cresolphthalein complexone in a capillary electrophoresis based system. Upon application of the electric field the calcium zone was electrophoretically mixed with the reagent and product was formed. The bulk electroosmotic flow carried the product to the detector where the absorbance of the resulting complex at 575 nm was measured.

Quantitation using an internal standard yielded a linear response with an R.S.D. of 8.1%. An inter-method comparison was performed with the standard bulk method and yielded results that did not significantly differ. The advantages of EMMA with respect to traditional methods were addressed.

1. Introduction

Traditionally capillary electrophoresis has been applied to the separation of species on the basis of differences in electrophoretic mobilities as dictated by the chosen electrophoretic medium. However, as we recently described [1], electrophoretically mediated microanalysis (EMMA) utilizes this phenomenon to bring spatially distinct zones of chemical reagents of different mobilities into physical contact in order to perform a reaction-based chemical analysis. Capillary electrophoretic systems, as employed in EMMA, are capable of performing each of the tasks required in reaction based chemical analysis: (1) the metering of the analyte(s) and analytical reagent(s); (2) the mixing of analyte(s) and analytical reagent(s); (3) a time period in which the quantitative analytical reaction is allowed to occur and (4) the detection of one or more species whose production or depletion is indicative of the quantity or concentration of analyte(s) present.

Electrophoretic mixing offers numerous advantages over the mixing of bulk solutions employed in traditional chemical analysis. As species electrophorese essentially independently of the bulk solution, electrophoretic mixing interpenetrates zones with differential mobilities under the application of an electric field without an additive change in volume and, therefore, without mixing-induced dilution of the zones. Additionally, electrophoretic mixing allows for zones to be merged without the need for turbulent flow and the concurrent loss of efficiency experienced in traditional methods of mixing. Further advantages of the EMMA method include the separative power of capillary electrophoretic systems. This capability allows for the development of assays which do not require the

* Corresponding author.

0021-9673/94/$07.00
SSDI 0021-9673(93)E0003-D

production or depletion of a species with unique detection properties. EMMA's separative capacity also permits multiple analytes to be determined if the analytes or respective analytical reagents or products possess unique electrophoretic properties in the chosen electrophoretic medium [2]. The small dimensions of capillary electrophoretic systems are a major benefit of the EMMA method as they allow for the microanalysis of nanoliter scale volumes of analyte utilizing sub-microliter scale volumes of analytical reagents.

We have recently reported EMMA methods for the determination of enzymes [1–4] and substrates [1,5]. Liu and Dasgupta [6] demonstrated the applicability of this phenomenon to complexation reactions using a flow-injection analysis (FIA) format. This paper describes an EMMA method for the determination of calcium by reaction with *o*-cresolphthalein complexone. Calcium is one of the many analytes routinely determined in the clinical laboratory. The clinical significance of calcium is vast and has been well documented [7]. Calcium ions decrease neuromuscular excitability, are an active agent in blood coagulation and neurotransmitter release, activate many enzymes, and play an important role in inorganic ion transport across cell membranes [8]. It is, therefore, significant to monitor the calcium levels in serum and urine to detect conditions, such as hypercalcemia and hypocalcemia, which could have serious detrimental effects, such as tetany. Many different methods have been used to determine the calcium concentrations in biological fluids, such as redox titrations [9,10], precipitation reactions [11,12], EDTA titrations [13,14], emission flame photometry [15], atomic absorption spectrophotometry [7], and reaction with *o*-cresolphthalein complexone [16,17]. Of these methods the latter has become the choice for most clinical laboratories due to its simplicity and ease of automation. The reaction of *o*-cresolphthalein and calcium forms a purple complex whose absorbance at 575 nm is indicative of the amount of calcium present. However, the monitoring of calcium levels in interstitial fluids has frequently proven to be difficult using traditional methods due to the micro-sample volumes. Due to its minimal sample requirements, EMMA offers potential for the detection of calcium in such sampling environments.

2. Experimental

2.1. Instrumentation

The assays were carried out using an in-house design. Polyimide-coated, fused-silica capillaries (Polymicro Technologies, Phoenix, AZ, USA) of 75 μm I.D., 360 μm O.D., and 35 cm in total length were uses as the columns. The separation length (distance from anodic injection end to detection window) was 20 cm. Detection was achieved with an ISCO (Lincoln, NE, USA) CV^4 capillary electrophoresis absorbance detector at 575 nm. A Spellman (Plainview, NY, USA) Model FHR 30P 60/EI power supply was utilized to apply the electric field across the capillary. The spectrophotometry experiments were performed with a Spectronic 20D (Milton Roy Company, Niagara Falls, NY, USA) operated at 575 nm.

2.2. Chemicals

The *o*-cresolphthalein complexone reagent and buffer solutions were obtained from Sigma (St. Louis, MO, USA). The analytical reagent solution was prepared by mixing the *o*-cresolphthalein complexone reagent and buffer solutions in a 1:1 ratio. The resulting 250 m*M* 2-amino-2-methyl-1,3-propanediol working buffer at a pH of 9.0 contained the *o*-cresolphthalein complexone at a concentration of 0.189 m*M* and 8-hydroxyquinoline at a concentration of 8.61 m*M* and was allowed to sit for no more than 4 h before being replaced. 8-Hydroxyquinoline is utilized to eliminate interference from magnesium. Calcium chloride standards were prepared by serial dilutions form a 20 m*M* standard purchased from Sigma. The bromophenol blue used as an internal standard was obtained from

Aldrich (Milwaukee, WI, USA). All sample solutions were prepared from in-house double-distilled-deionized water and were degassed to remove interferences from air bubbles.

2.3. Electrophoresis procedures

The capillaries were treated with 1 *M* NaOH for 10 min and then rinsed with buffer solution for 10 min prior to use. The assays were effected by filling the capillary and the buffer reservoirs with the analytical reagent solution and injecting a plug of calcium analyte solution or a plug of pre-reacted complex. In the latter case, the reaction was allowed to go to completion by sitting for three minutes prior to the injection. Hydrodynamic injections were made into the anodic end by siphoning for a fixed time (1–2 s) at a fixed height (10–15 cm). Following injection, a constant potential was applied, and the absorbance at 575 nm was monitored. In order to limit the operating current to 40–60 μA, electric field strengths of 85 to 114 V/cm were applied. All assays were performed without temperature control at ambient temperature.

2.4. Spectrophotometry procedures

The spectrophotometric determination of calcium in samples was performed as described in the manual accompanying the Sigma Diagnostic kit [18].

3. Results and discussion

3.1. EMMA methodology

The *o*-cresolphthalein complexone reaction with calcium is a simple reaction that can be utilized to demonstrate EMMA's ability to perform sensitive chemical analysis with a rapid sample throughput while utilizing small amounts of both analyte and analytical reagent. Electrophoretic mixing requires that the reagents involved in an EMMA reaction, calcium and *o*-cresolphthalein in this assay, differ in electrophoretic mobility so that spatially distinct zones of the reagents will migrate at different rates and thereby merge under the influence of an electric field. In the chosen electrophoretic medium, calcium and *o*-cresolphthalein complexone have a differential mobility of $8.2 \cdot 10^{-4}$ cm^2/(Vs) as indicated by the electrophoretic and mobilities listed in Table 1. This differential mobility allows the two species to be rapidly electrophoretically mixed under the influence of an applied potential.

Since the magnitude of the electrophoretic mobility of the negatively charged *o*-cresolphthalein complexone is less than the magnitude of the electroosmotic flow, the *o*-cresolphthalein complexone has a net apparent mobility in the direction of the cathode. Therefore, both the *o*-cresolphthalein complexone and the positively charged calcium will migrate from anode to cathode. However, since the apparent mobility of the calcium is greater than that of the *o*-

Table 1
Electrophoretic mobilities of chemical species at pH 9

Chemical species	Electrophoretic mobility [cm^2/(Vs)]	Apparent electrophoretic mobility [cm^2/(Vs)][a]
Calcium	$4.3 \cdot 10^{-4}$	$9.7 \cdot 10^{-4}$
o-Cresolphthalein complexone	$-3.9 \cdot 10^{-4}$	$1.5 \cdot 10^{-4}$
Calcium complex	$-9.1 \cdot 10^{-5}$	$4.5 \cdot 10^{-4}$
Bromophenol blue	$-2.5 \cdot 10^{-4}$	$2.9 \cdot 10^{-4}$

[a] Apparent electrophoretic mobilities were calculated as the sum of the electrophoretic mobility and the electroosmotic flow [$5.4 \cdot 10^{-4}$ cm^2/(Vs)].

cresolphthalein complexone, the *o*-cresolphthalein complexone must be introduced into the capillary prior to the injection of the calcium at the anode so that the faster migrating zone of calcium can overtake the slower migrating zone of *o*-cresolphthalein complexone.

The EMMA mode chosen was to initially fill the capillary and the buffer reservoirs with a solution containing the *o*-cresolphthalein complexone buffered at pH 9.0. A plug of solution containing the calcium analyte was then hydrodynamically injected at the anodic end of the capillary, and a potential was applied across the capillary. Under the influence of the electric field, the calcium ions quickly exited their injection environment and penetrated the adjacent zone containing the *o*-cresolphthalein complexone. The time required to completely electrophoretically mix an analyte zone in a broader analytical reagent zone t_{mix} can be estimated as

$$t_{mix} = \frac{w_A}{\Delta\mu_{ep,A-R}E} \quad (1)$$

where w_A is the width of the analyte zone, $\Delta\mu_{ep,A-R}$ is the difference in electrophoretic mobilities between the analyte and analytical reagent zones, and E is the electric field strength. Based upon their differential mobility and a typical experimental electric field strength of 100 V/cm, a 0.5-mm calcium plug was fully merged within the adjacent *o*-cresolphthalein complexone region in approximately 600 ms following the application of the potential.

As the reagent zones were electrophoretically mixed, the calcium and *o*-cresolphthalein complexone reacted to form the product, which was transported toward the cathode. Since the product differed in electrophoretic mobility from the analyte [$\Delta\mu_{ep} = 5.2 \cdot 10^{-4}$ cm^2/(Vs)], as the plug of unreacted calcium traversed the zone of *o*-cresolphthalein complexone, the product formed was electrophoresed away from the vicinity of the unreacted analyte at a rate V_{diff} equal to the product of this differential mobility $\Delta\mu_{ep,P-A}$ and the electric field strength:

$$v_{diff} = \Delta\mu_{ep,P-A}E \quad (2)$$

As a result, if the reaction was not immediate, the product peak would have been skewed with the asymmetry attributable to the kinetics of the reaction. Since the analyte had a greater apparent mobility than the detected product, the first product formed was the last to reach the detector position as it must traverse the greatest portion of the separation distance of the capillary with a lower mobility, that of the product. The last product formed migrates with a higher apparent mobility, that of the analyte, for the greatest period of time and was thus the first product to react the detection position.

At the concentrations of calcium and *o*-cresolphthalein complexone utilized in these experiments, the reaction approached completion very rapidly as indicated by the sharp product peaks obtained. To confirm that the mixing of reagents and the reaction are rapid in the EMMA assay, calcium samples were assayed both by the EMMA method and by reacting the calcium and *o*-cresolphthalein complexone prior to injection. A calcium sample was first injected at the anodic end of the capillary. After application of the potential for approximately 2.9 min a previously reacted calcium *o*-cresolphthalein complexone complex was injected. As illustrated in Fig. 1, indistinguishable product peaks for the two in-

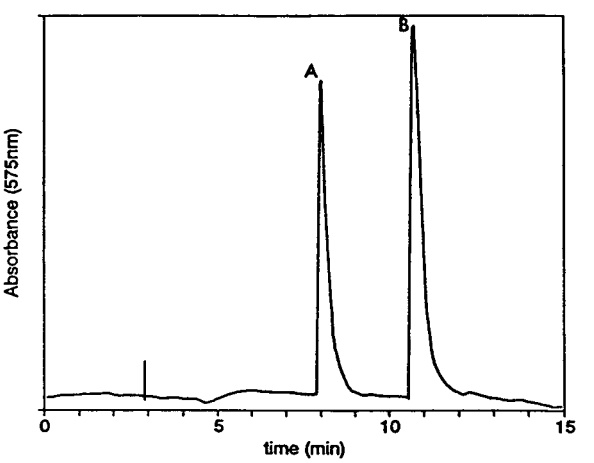

Fig. 1. A determination of a 1 m*M* calcium sample injected at the anode by the EMMA method and a pre-reacted 1 m*M* calcium *o*-cresolphthalein complexone complex injected after the application of potential for 2.9 min; (A) product peak from the EMMA determination and (B) pre-reacted product peak. The applied field strength was 93 V/cm.

jections were obtained in the resulting electropherogram. Identical calculated electrophoretic mobilities indicated that the mixing and reaction processes occurred nearly instantaneously. If the calcium had existed in its more mobile, uncomplexed form for a significant time during the EMMA assay, the migration time of the product would have differed for that formed in the EMMA analysis and that reacted prior to injection. Furthermore, the similarity in peak shapes signifies that any kinetic effects manifested as peak skewness were insignificant relative to the effects of diffusional broadening, thus again indicating that the mixing and reaction processes occurred rapidly. While the immediate nature of the reaction would seemingly allow the use of a narrower plug of analytical reagent, it was decided to use a broad zone of *o*-cresolphthalein complexone so that the analyte and product would remain merged within the analytical reagent zone throughout their migration to the detection position thereby inhibiting dissociation of the product complex.

Since product peak area determines the quantity, rather than concentration, of calcium injected, the poor reproducibility of hydrodynamic injection volumes for capillary electrophoresis required the use of an internal standard as a measure of injection volume for the determination of analyte concentrations by EMMA. The dye bromophenol blue was selected due to its large absorbance at 575 nm as well as its differential mobility [$\Delta\mu_{ep} = 1.59 \cdot 10^{-4}$ $cm^2/(V\ s)$] from the product thereby preventing comigration of the internal standard and product peaks. A typical electropherogram of an EMMA determination of calcium using the internal standard is shown in Fig. 2.

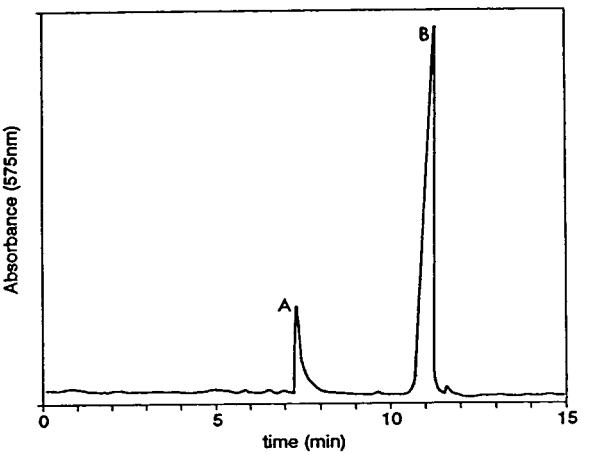

Fig. 2. A typical electropherogram obtained by the EMMA determination of a 0.75 m*M* calcium standard; (A) calcium *o*-cresolphthalein complexone complex (analytical reaction product) and (B) bromophenol blue (internal standard) peaks. The applied field strength was 103 V/cm.

3.2. Linearity and reproducibility of EMMA method

To determine the linearity of the EMMA calcium determination, a calibration curve (Fig. 3) was constructed. The concentration of the internal standard was held constant at 0.75 m*M* while the concentration of the calcium was varied between 0.010 and 1.0 m*M*. Six trials were performed for each of the eight samples. Quantitation was based upon the relative peak areas observed for the complex and the internal standard. The EMMA method proved to be linear over this entire calcium concentration range with a correlation coefficient of 0.9936. The lower limit of detection, based upon a signal-to-noise ratio of 3, was found to be ap-

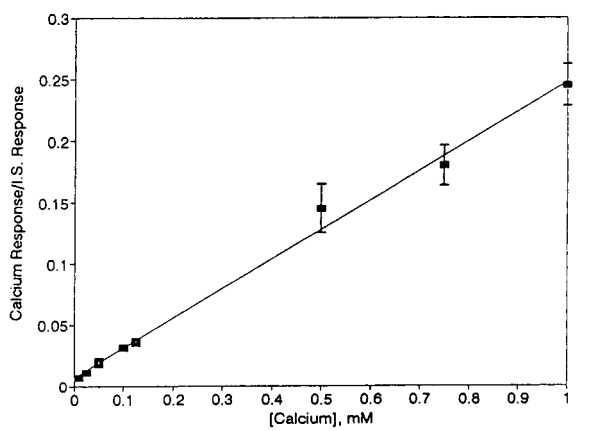

Fig. 3. A calibration curve for the EMMA determination of calcium. Points are the mean of six replicates, and the brackets represent the 95% confidence intervals. The line represents the line regression of 0.01 to 1 m*M* data (R^2 = 0.9936). Conditions stated in text. I.S. = internal standard.

proximately $5 \cdot 10^{-3}$ mM. Assuming an injection volume of about 2 nl, this detection limit corresponded to the determination of $1 \cdot 10^{-14}$ mol of calcium. This lower limit of detection does not approach that observed in the previously published EMMA determination of enzymes [2–5] due to the non-amplifying nature of the complexatory reaction.

Reproducibility ranged from 6.5 to 10.2% relative standard deviations (R.S.D.) with an average value of 8.1% R.S.D. This R.S.D. is larger than that obtained for the spectrophotometric determination of the samples (average of 3.1%) presumably due to error in the determination of peak areas by the cut and weigh methodology.

3.3. Comparison of EMMA to spectrophotometric determination

To assess the validity of the EMMA method of calcium determination, an inter-method correlation with the Sigma Diagnostic spectrophotometric method was performed. Four calcium samples varying between 0.058 and 0.22 mM were assayed by both techniques. Four determinations were made of each sample by each method. Fig. 4 compares the results of the two assays. Least-squares regression yielded y (Sigma) = 0.989x (EMMA) − 0.00140 mM with a correlation coefficient of 0.9992. A paired Student's t calculation showed that the two methods did not yield significantly different values at a 95% confidence level. The two methods agreed well indicating that the EMMA technique is a viable procedure for the determination of calcium.

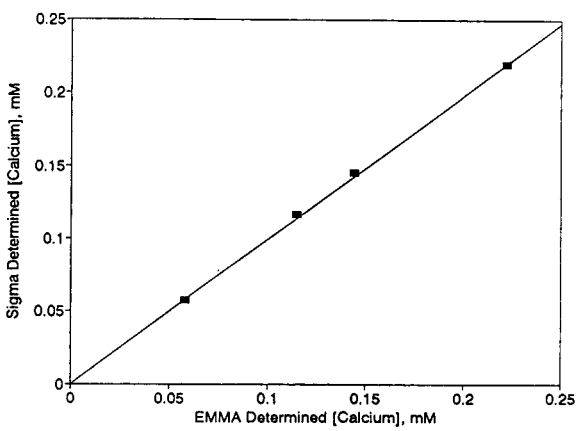

Fig. 4. An inter-method correlation of four calcium determinations by EMMA and Sigma spectrophotometric methods. The line represents the linear regression results (R^2 = 0.9992). Conditions stated in text.

3.4. Advantages of EMMA determination

Although the reproducibility of the Sigma method was superior to the EMMA assay, the EMMA technique holds many advantages over the bulk methodology including its ability to allow the analyte to encounter many times its volume in analytical reagent without concurrent dilution due to electrophoretic mixing. As previously described, any unreacted calcium will continue to traverse the *o*-cresolphthalein complexone region thereby continually encountering unreacted analytical reagent. In the mode described, the volume of analytical reagent encountered relative to the initial volume of analyte, R_{vol} can be estimated as

$$R_{vol} = \frac{\Delta\mu_{ep,A-R} l}{(\mu_{ep,A} + \mu_{eo}) w} \quad (3)$$

where l is the distance from injection to detector, $\mu_{ep,A}$ is the electrophoretic mobility of the analyte, and μ_{eo} is the electroosmotic flow. Based upon the differential mobility of the calcium and *o*-cresolphthalein complexone, as a 0.5 mm wide plug of calcium passed from injection point to the detection window through a typical separation distance of 20 cm, the calcium zone effectively encountered approximately 340 times its own initial volume in *o*-cresolphthalein complexone. This advantage allows for the effective linear range to be extended without the detrimental dilution exhibited by the bulk mixing of increased volumes of solutions.

One major advantage EMMA possesses over standard spectrophotometric methods is its small sample and analytical reagent requirements. As demonstrated by this study, EMMA was capable of analyzing nanoliter scale sample volumes, such as that encountered in the determination of

analytes in interstitial tissues. Furthermore, the volumetric consumption of the reagent/buffer solution was minimal. Based upon the bulk electroosmotic flow-rate, at an experimental electric field strength of 100 V/cm with an inner capillary diameter of 75 μm, the volumetric consumption of the *o*-cresolphthalein complexone/buffer solution V_f was approximately 15 μl/h as calculated by

$$V_f = \pi r^2 \mu_{eo} E \quad (4)$$

where r is the radius of the capillary. Our experimental determinations involved runs of approximately 12 min from injection of analyte to detection of product peak due to the 20 cm separation length utilized. This limitation was imposed by the spatial restrictions of our instrumental design. However, the immediate nature of the mixing and reaction processes exhibited by the EMMA determinations would allow an experimental apparatus with capillaries on the order of a centimeter in separation length to be utilized. With such a design, the analysis could be completed in less than 1 min. Increased sample throughput can also be obtained by running many samples sequentially in the capillary. For the stated experimental apparatus and parameters, an injection would be made every 2.7 min without overlapping of product or internal standard peaks thereby allowing a sample throughput of 22 assays/h. Furthermore, the availability of commercial capillary electrophoresis instruments with autoinjectors would allow the EMMA method to be readily automated.

4. Acknowledgements

Financial support was received from the National Institute of Health (Grant No. GM 25431) and the Purdue Research Foundation. We gratefully acknowledge the generous loan of the capillary electrophoresis CV[4] variable-wavelength absorbance detector from ISCO.

5. References

[1] B.J. Harmon, D.H. Patterson and F.E. Regnier, *Anal. Chem.*, 65 (1993) 2655.
[2] D. Wu and F.E. Regnier, *Anal. Chem.*, 65 (1993) 2029.
[3] J. Bao and F.E. Regnier, *J. Chromatogr.*, 608 (1992) 217.
[4] K.J. Miller, I. Leesong, J. Bao, F.E. Regnier and F.E. Lytle, *Anal. Chem.*, 65 (1993) 3267.
[5] B.J. Harmon, D.H. Patterson and F.E. Regnier, *J. Chromatogr. A*, 657 (1993) 429.
[6] S. Liu and K. Dasgupta, *Anal. Chim. Acta*, 268 (1992) 1.
[7] N.W. Tietz (Editor), *Fundamentals of Clinical Chemistry*, Saunders, Philadelphia, PA, 1982, pp. 901–917.
[8] J.B. Henry and R.A. McPhearson (Editors), *Todd–Sanford–Davidsohn Clinical Diagnosis and Management by Laboratory Method*, Saunders, Philadelphia, PA, 17th ed., 1984, p. 133.
[9] B. Kramer and F.F. Tisdall, *J. Biol. Chem.*, 47 (1921) 475.
[10] E.P. Clark and J.B. Collip, *J. Biol. Chem.*, 63 (1925) 461.
[11] P.V. Ferro and A.B. Ham, *J. Clin. Pathol.*, 28 (1957) 208.
[12] P.V. Ferro and A.B. Ham, *J. Clin. Pathol.*, 28 (1957) 689.
[13] H.D. Appleton, M. West, M. Mandel and A. Sala, *Clin. Chem.*, 5 (1959) 36.
[14] H. Diehl and J.L. Ellingboe, *Anal. Chem.*, 28 (1956) 882.
[15] M. Margoshes and B.L. Vallee, *Methods of Biochemical Analysis*, Vol. 3, Interscience Publishers, New York, 1956, p. 353.
[16] G. Kessler and M. Wolfman, *Clin. Chem.*, 10 (1964) 686.
[17] H.J. Gitelman, *Anal. Biochem.*, 18 (1967) 521.
[18] *Procedure No. 586*, Sigma Diagnostics, St. Louis, MO, 1991.

ELSEVIER

Journal of Chromatography A, 662 (1994) 396–400

JOURNAL OF CHROMATOGRAPHY A

Short Communication

Modification of the *h*-root method for the determination of multicomponent Langmuir coefficients in liquid chromatography

S.C. David Jen, Neville G. Pinto*

Department of Chemical Engineering, University of Cincinnati, Cincinnati, OH 45221-0171, USA

(First received October 18th, 1992; revised manuscript received November 30th, 1993)

Abstract

A refined version of the *h*-root method is presented for the measurement of Langmuir equilibrium coefficients in liquid chromatography. As in the original method, the measurement is based on the column behavior in the frontal mode. However, in the present case only frontal capacity factors are required, as opposed to the original requirement of a complete effluent composition history. It has been shown that this refinement significantly reduces the experimental effort required for the measurement of the equilibrium coefficients.

1. Introduction

The equilibrium adsorption of the solutes from liquids onto solids is of fundamental importance in liquid chromatography. Adsorption behavior is conventionally described in terms of adsorption isotherms. For linear chromatography, solute concentrations in the liquid are low, and interferences between species both in the liquid and on the solid surface are negligible. Thus, adsorption is restricted to the linear region, and a limited amount of adsorption data are necessary for system design and optimization; typically, the Henry's law constant, expressed as the elution capacity factor, obtained from single-component data, is sufficient. In contrast, for non-linear (overload) chromatography, solute concentrations are high and interferences between species can be significant. Thus, characterization of adsorption behavior over a much wider range of the composition space is essential.

The conventional approach to measuring adsorption isotherms in liquid–solid systems is batch equilibrations. Unfortunately, this approach is tedious and time consuming, especially for multicomponent systems. In an attempt to develop quick and accurate methods for measuring isotherms, particularly multicomponent isotherms, a number of chromatographic techniques have been proposed [1–4]. Among these is the *h*-root method (HRM) [4]. HRM is based on the coherence theory of chromatography [5], and is applicable to systems obeying the multicomponent Langmuir isotherm. In its present form the method requires isocratic elution to establish behavior in the dilute solution region, and a single multicomponent frontal experiment to characterize competitive interferences. A practical difficulty concerns the latter experiment. HRM requires the determination of a complete

* Corresponding author.

0021-9673/94/$07.00
SSDI 0021-9673(93)E1278-8

effluent composition history; that is, the column effluent concentration trace for each component must be experimentally obtained. For example, for a four component system, a detailed composition history similar to Fig. 1 has to be generated. This is an exacting analytical requirement. Furthermore, though ideally only one frontal experiment is necessary, the possibility of experimental error necessitates at least one other confirming frontal experiment, further increasing the required experimental effort.

In this communication, a refined form of HRM is presented. This version eliminates the need for a complete frontal composition history, and uses instead the feed composition and frontal capacity factors to determine competitive interactions. The practical implication of this refinement is important. Where HRM originally required a detailed frontal chromatogram such as Fig. 1, for the current approach only the frontal capacity factor for each of the fronts, that is, the detector response of the effluent (Fig. 2), is necessary. Thus, no additional analytical work is necessary. The refined HRM method has also been presented in terms of conventional chromatographic parameters (capacity factors), facilitating its use.

Because this contribution is a refinement of a published method, the basis and assumptions of HRM will not be repeated, and the unfamiliar reader is referred to the original publication [4] for details.

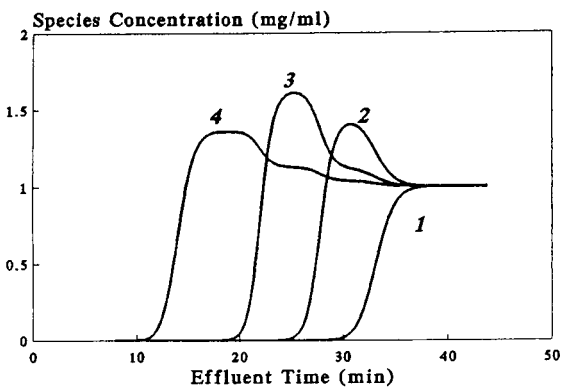

Fig. 1. Typical frontal effluent composition history for a four-component mixture.

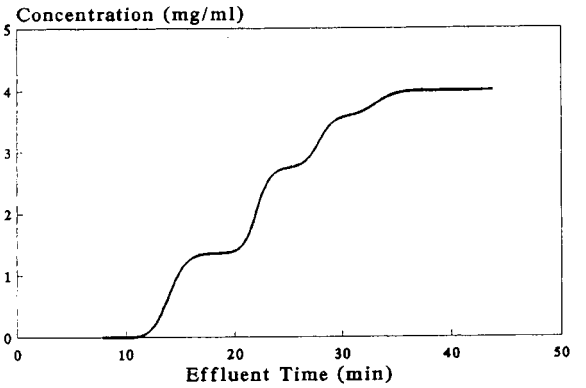

Fig. 2. Typical frontal detector response for a four-component mixture.

2. Theory

HRM is based on the multicomponent Langmuir isotherm, which for an n component system takes the form:

$$Q_i^* = \frac{k_i' c_i}{1 + \sum_{j=1}^{n} b_j c_j} \qquad i = 1, \ldots, n \tag{1}$$

where Q_i^* is the adsorbed concentration based on the column volume. Within the framework of the coherence theory of chromatography [5], the composition space is orthogonalized into the h-space using the transformation:

$$\sum_{i=1}^{n} \frac{b_i c_i}{h \frac{k_i'}{k_1'} - 1} = 1 \tag{2}$$

In the h-space, the adjusted velocity of a composition front with the jth root as the variable root is given by:

$$U_j = h_j \prod_{i=1}^{n} h_i \prod_{i=1}^{n} \alpha_{i1} \tag{3}$$

The relation between true and adjusted velocities is:

$$\frac{L}{T_j} = u_j = \frac{u_0}{1 + \frac{k_{n+1}'}{U_j}} \tag{4}$$

where the $(n+1)$th component is considered a "dummy" species. This is a fictitious species present in both phases. The concentration of this species is defined as the difference between the total concentration of all real species present in each phase and some arbitrary constant [5]. The introduction of a dummy species enables the treatment of an n-component non-stoichiometric system as an equivalent $(n+1)$-component stoichiometric system.

2.1. Frontal chromatography

A schematic representation of the column profile for frontal development of an n-component mixture is shown in Fig. 3. The horizontal lines represent sharp waves, and the compositions of the plateau regions are expressed in terms of h roots. Notice that across each wave only one h root varies. This is an important advantage of the h transformation. Using this characteristic with the known presaturant composition (h'') and the wave velocities (v_i), Eq. 3 can be used to calculated the influence composition (h'). Initially, the column contains no adsorbates and (h'') can be calculated from [4]:

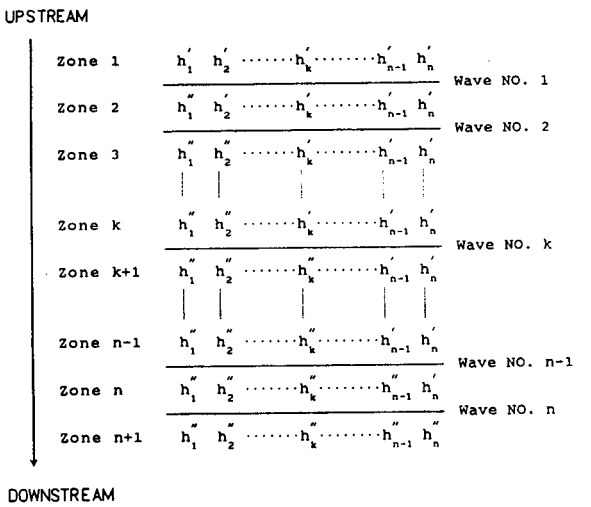

Fig. 3. Schematic representation of column behavior in h-space for frontal chromatography of an n-component mixture. Solid, horizontal lines represent migrating composition waves.

$$h''_j = \frac{k'_1}{k'_j} \quad j = 1, \ldots, n \tag{5}$$

Also, it has been shown [4] that

$$h'_n = \frac{k'_1}{k'_{n+1}} U_n \tag{6}$$

and

$$h'_j = \frac{k'_1}{k'_{j+1}} \frac{U_j}{U_{j+1}} \quad j = 1, \ldots, n-1 \tag{7}$$

Defining the frontal capacity factor, K'_i, as:

$$K'_i = \frac{T_i - T_0}{T_0} \tag{8}$$

the adjusted velocities can be related to chromatographic retention. Substituting Eq. 8 in Eq. 4,

$$U_j = \frac{k'_{n+1}}{K'_j} \tag{9}$$

Substituting Eq. 9 in Eqs. 6 and 7,

$$h'_n = \frac{k'_1}{K'_n} \tag{10}$$

and

$$h'_j = \frac{\dfrac{k'_1}{K'_j}}{\dfrac{k'_{j+1}}{K'_{j+1}}} \quad j = 1, \ldots, n-1 \tag{11}$$

2.2. Methodology of modified h-root method

HRM divides the determination of Langmuir parameters into two parts. Intrinsic affinity coefficients, a_i ($a_i = k'_i/\phi$), are obtained from linear elution chromatography, and competitive interference coefficients, b_i, from non-linear frontal experiments. In the modified approach, the determination of a_i remains unchanged, and are calculated from linear retention data as follows:

$$k'_i = \frac{t_i - t_0}{t_0} = a_i \phi \tag{12}$$

a_i can also be calculated from the frontal capacity factor, since in the linear region $k'_i = K'_i$.

As in the original method, the modified approach also uses non-linear frontal chromatography for the determination of b_i. However, the calculation method, and, hence, the data required are different. For non-linear frontal chromatography, the feed compositions, expressed in the h space, are given by Eqs. 10 and 11. Substituting these in Eq. 2,

$$\sum_{i=1}^{n} \left(\frac{c_i^f}{\frac{k'_i}{K'_n} - 1} b_i \right) = 0 \quad (13)$$

and

$$\sum_{i=1}^{n} \left(\frac{c_i^f}{\frac{K'_{j+1}k'_i}{K'_j k'_{j+1}} - 1} b_i \right) = 0 \quad j = 1, \ldots, n-1 \quad (14)$$

All the terms in Eqs. 13 and 14, except b_i, can be experimentally obtained. The elution capacity factors, k'_i, can be obtained from linear elution data (Eq. 12). Feed concentrations will generally be known, or can be determined. The frontal capacity factors can be calculated from the non-linear frontal chromatogram, by applying Eq. 8 to each of the fronts. Thus, the n equations Eqs. 13 and 14 can be used to determine the n unknowns b_i. It should be noted that with this approach the composition history of the non-linear frontal chromatograms is not required, facilitating the experimental effort significantly.

3. Conclusions

A modified version of HRM has been presented for the calculation of multicomponent Langmuir coefficients. At a minimum, the modified method requires only an elution experiment and a detector trace of the frontal column response. This substantially reduces experimental effort, as compared to the original method, which was based on the availability of a complete frontal composition history.

4. Symbols

a_i Langmuir affinity coefficient (ml/g)
b_i Langmuir competitive interference coefficient (ml/mg)
c_i mobile phase concentration based on fluid volume (mg/ml)
c_i^f feed concentration based on fluid volume (mg/ml)
h_i h-root (dimensionless)
k'_i elution capacity factor at infinite dilution (dimensionless)
K'_i frontal capacity (dimensionless)
L column length (cm)
Q_i^* equilibrium concentration (mg/ml)
t_i retention time for linear, isocratic elution (min)
t_0 column hold-up time (min)
T_i breakthrough time for frontal boundary (min)
T_0 column hold-up time (min)
u_i velocity (cm/min)
u_0 interstitial velocity (cm/min)
U_i adjusted velocity (dimensionless)

Greek symbols
α_{ij} separation factor (dimensionless)
ϕ column phase ratio (g/ml)

Superscripts
$'$ feed
$''$ presaturant

Subscripts
i species i
j species j

5. Acknowledgement

This work was supported by Grant No. CTS-8909742 from the National Science Foundation. This support is gratefully acknowledged.

6. References

[1] J.R. Conder and C.L. Young, *Physicochemical Measurements by Gas Chromatography*, Wiley, New York, 1979, p. 353.

[2] J.M. Jacobson, J.H. Frenz and Cs. Horvath, *Ind. Eng. Chem. Res.*, 26 (1987) 43.
[3] Z. Ma, B.C. Lin, A.M. Katti and C. Guiochon, *J. Phys. Chem.* 94 (1990) 6911.
[4] T.-W. Chen, N.G. Pinto and L. Van Brocklin, *J. Chromatogr.*, 484 (1989) 167.
[5] F. Helfferich and G. Klein, *Multicomponent Chromatography*, Marcel Dekker, New York, 1970.
[6] S.C.D. Jen, *Ph.D. Thesis*, University of Cincinnati, Cincinnati, OH, 1991.
[7] P.R. Levison, S.E. Badger and D.W. Toome, *J. Chromatogr.*, 590 (1992) 49.

ELSEVIER

Journal of Chromatography A, 662 (1994) 401–406

JOURNAL OF CHROMATOGRAPHY A

Short Communication

Normal-phase high-performance liquid chromatographic resolution of 5′-O-protected deoxynucleoside methylphosphonamidites

James F. Cormier*, Jeffry B. Plomley

Department of Chemistry, Trent University, Peterborough, Ontario K9J 7B8, Canada

(First received August 24th, 1993; revised manuscript received November 20th, 1993)

Abstract

High-performance liquid chromatography has been used for the analytical and preparative resolution of some nucleoside methylphosphonamidites. The pure diastereomers were required for a study on the mechanism of the coupling reactions of these compounds.

1. Introduction

The use of linkage-modified oligonucleotide analogues as agents for the antisense control of gene expression has received considerable attention recently [1], and many phosphorus-modified and dephospho internucleotide linkages have been examined. One of the more intensively studied classes of analogues is the oligonucleoside methylphosphonates. These appear to show considerable promise as antisense agents. Unfortunately, substitution of methyl for a non-bridging oxygen creates a new asymmetric centre at phosphorus. Considerable experimental [2] and theoretical [3] evidence indicates that Rp-configured oligomers are much more effective binders than their Sp-configured counterparts. It would therefore be useful to have access to a synthetic route which permits the stereospecific synthesis of these important molecules. Leznikowski *et al.* [2] have developed and we have modified [4] such a route, which is based on the displacement of an alkoxide from a resolved nucleoside methylphosphonate. It requires, however, the use of a nucleoside alkoxide, and as such, is not amenable to automation. In addition, coupling yields are too low for the efficient preparation of oligomers more than perhaps eight units in length. We are interested in the use of the more reactive nucleoside phosphonamidites in a stereospecific synthesis. In particular, we are exploring the use of resolved phosphonamidites and non-nucleophilic catalysts in coupling reactions. This report describes a procedure for the resolution of these phosphonamidites.

2. Experimental

HPLC was performed on a Waters system using a 600E system controller, 484 tunable absorbance detector and 470 scanning fluorescence detector. All solvents were premixed, and

* Corresponding author.

0021-9673/94/$07.00
SSDI 0021-9673(93)E1285-8

Table 1
Analytical resolution of methylphosphonamidites **1a**

B	Flow (ml/min)	t_{R1} (min)	t_{R2} (min)	R_s
Thymidine	2.0	10.5	511.8	51.20
N^4-Benzoylcytosine	8.0	1.40	1.70	1.28
N^6-Benzoyladenine	2.0	5.77	6.61	1.03
N^2-Isobutyrylguanine	8.0	1.65	1.98	1.06

B = nucleoside heterocyclic base, protected at the exocyclic amino group where appropriate. t_{R1} and t_{R2} refer to the retention times of the first- and second-eluting peaks, respectively. 5′-OH protecting group is dimethoxytrityl. See Experimental for further details regarding column and operating conditions.

hexane–dichloromethane mixtures were sparged with helium for 10 min at 100 ml/min, to avoid excessive solvent evaporation. A Waters μPorasil (300 × 3.9 mm, 10 μm particle size, 125 Å pore size) column was used for analytical runs, and preparative chromatography was done on a larger μPorasil (300 × 19 mm 15–20 μm particle size, 125 Å pore size). Detection was achieved by monitoring absorbance at 254 nm for analytical runs, and by monitoring fluorescence at 511 nm (excitation at 254 nm) for preparative runs. The mobile phase velocity for analytical runs is given in Table 1, and was 45 ml/min for preparative runs. For preparative separations, 250 μl of a solution of **1b** (140 mg/ml, in the mobile phase) was injected. Diastereomeric purity was checked by NMR and analytical HPLC. 5′-O-Dimethoxytritylmethylphosphonamidites **1a** were purchased from ABN (Hayward, CA, USA). 5′-O-Monomethoxytritylmethylphosphonamidites were prepared in this laboratory, and used for reasons of economy. ^{31}P NMR chemical shifts are reported relative to 85% phosphoric acid.

3. Discussion

We initially tried a procedure reported by Lebedev *et al.* [5], in which was described such a resolution. In that report, an Alltech 2.25 RSil 10-μm silica gel HPLC column was treated with a solution of triethylamine (1%) in chloroform–ethanol (99:1). Subsequent washing of the column with an ethanol–chloroform (2.5:97.5) solution, followed by the loading of the phosphonamidites and elution with ethanol–chloroform (1:99) reportedly gave resolution, with quantitative recovery, on a preparative scale.

In our initial attempts to reproduce this separation, we achieved excellent resolution on an analytical scale, using a Waters μPorasil analytical column. Unfortunately, this initial success was short-lived, as we noted rapid degradation of column performance after only a few injections. Plate count dropped from *ca.* 6000 to *ca.* 3000, with a corresponding decrease in resolution. The manufacturers of the column indicated that treatment of the stationary phases with triethylamine could lead to such a degradation in column performance. Although partial recovery of column performance was possible by passing a stream of helium through the warm (60°C) column, we were not satisfied. We desired a procedure which would reliably resolve the compounds without risk of degradation of the expensive columns.

We therefore decided to try other methods for this resolution. Preliminary experiments to perform the separation on a reversed-phase column (Waters C-18 μNovapak radial-pak cartridge) failed, although it has been reported that a similar system can be used to resolve a nucleoside 5′-O-dimethoxytritylmethoxyphosphoramidite [6]. Returning to the solvent system reported by Lebedev [5], we observed that, in the absence of triethylamine pretreatment, unresolved diastereomers were recovered in quantitative yield, with very short retention times (<1 min). Stengele and Pfleiderer [7] have reported the resolution of cyanoethylphosphoramidite diastereomers without the use of base pretreatment.

Lowering solvent polarity (1% to 0% ethanol in dichloromethane, at a constant mobile phase velocity of 1.00 ml/min) led to an increase in retention times, but no resolution. Varying mobile phase velocity for a given composition did not improve the situation. This increased retention times, but significant band broadening also occurred.

As a result, solvent composition was altered to improve both resolution of the diastereomers and to prevent column degradation. Using a mobile phase composed of hexane–dichloromethane (60:40), we achieved a small degree of resolution, but with unacceptably long retention times (>30 min). This led to poor recovery of the amidites, apparently due to degradation on the column. Addition of absolute ethanol, and further refinement of the system, led to a solvent composition of hexane–dichloromethane–ethanol (59.7:39.8:0.5). This mobile phase gave excellent resolution with reasonably short retention times (Table 1). Purine phosphonamidites gave noticeably poorer resolution than did their pyrimidine counterparts. This seems largely due to peak tailing and was also noted by Lebedev, in the case of guanosine phosphonamidites. Guanosine methylphosphonamidites are only poorly soluble in this mobile phase.

Preparative HPLC used the stationary and mobile phases described above. For preparative purposes, we used 5′-O-monomethoxytrityl-protected phosphonamidites. Injecting about 35 mg per run, we were able to achieve partial resolution of the diastereomers. Fluorescence detection was used to monitor the eluate. Although baseline resolution was not achieved, we were able to isolate diastereomerically pure material by collecting three fractions: baseline to apex, apex to apex, and apex to baseline. The first and last fractions contained pure material, while the middle peak was composed of unresolved isomers. Evaporation of the solvent gave the pure methyl phosphonamidites as white powders. Yields and other data are given in Table 2. Representative analytical chromatograms and ^{31}P NMR spectra are shown in Figs. 1 and 2. A representative preparative chromatogram is given in Fig. 3. We were unable to isolate significant amounts of diastereomerically pure 2′-deoxyguanosine methylphosphonamidites on a preparative scale. Variation of flow-rate and ethanol concentration failed to give preparative resolution, apparently because of extensive peak tailing.

In conclusion, we have developed a system for the resolution of protected nucleoside methylphosphonamidites which allows for reasonably straightforward isolation of the diastereomers. The present method avoids damage to the stationary phases of the columns, and the desired compounds are recovered as powders, avoiding the need for precipitation as a last step.

4. Acknowledgements

This work was supported by a start-up grant from Trent University to J.F.C. J.B.P. is the recipient of NSERC and OGS Postgraduate Scholarships. We thank Sue Blake of Queen's University for acquiring NMR spectra, and Dean Ostrander for technical assistance.

Table 2
Preparative resolution of methylphosphonamidites **1b**

B	t_R (min)	^{31}P NMR (C^2H_3CN)	Recovery (%)	Total recovery (%)
Thymidine	9.571	20.92	32.0	84
	11.42	120.52	28.6	
N^4-Benzoylcytosine	9.13	123.27	33.7	86
	10.64	121.02	31.8	
N^6-Benzoyladenine	5.89	121.38	28.8	94
	7.64	119.96	28.8	

t_R = retention time, recovery refers to percentage of injected material recovered stereochemically pure, total recovery refers to percentage of injected material recovered, including unresolved diastereomers. Flow-rate was 45 ml/min. 5′-OH protecting group is monomethoxytrityl. See Experimental for further details on column and operating conditions.

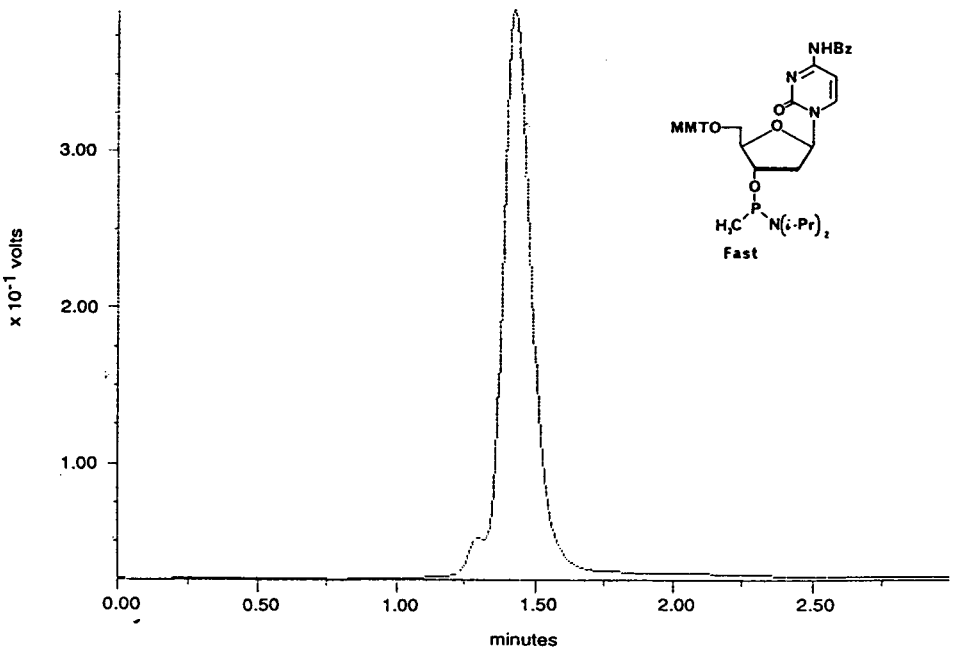

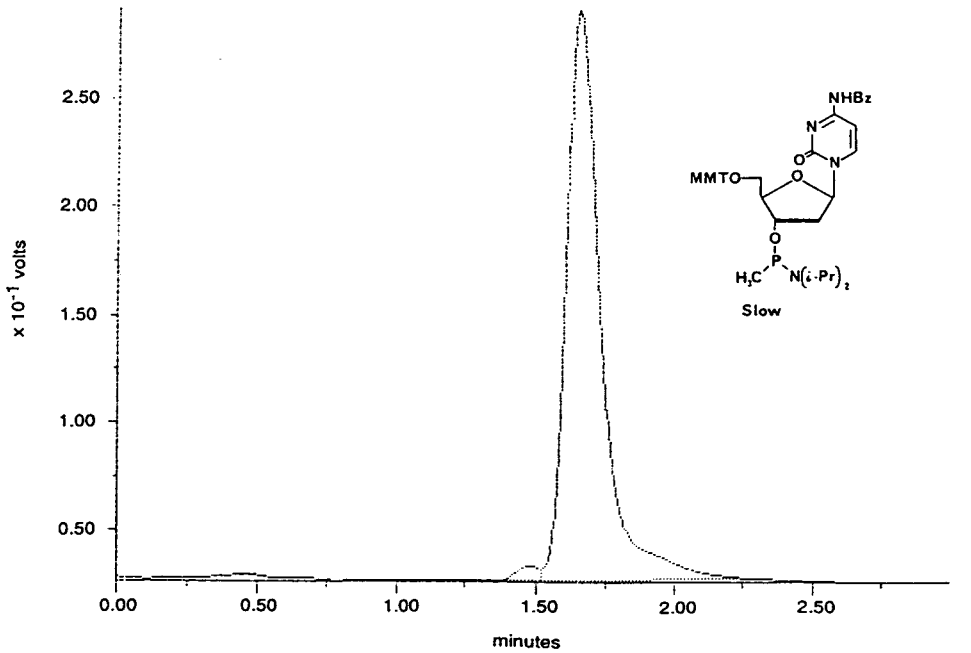

Fig. 1. Analytical chromatograms of resolved phosphonamidites.

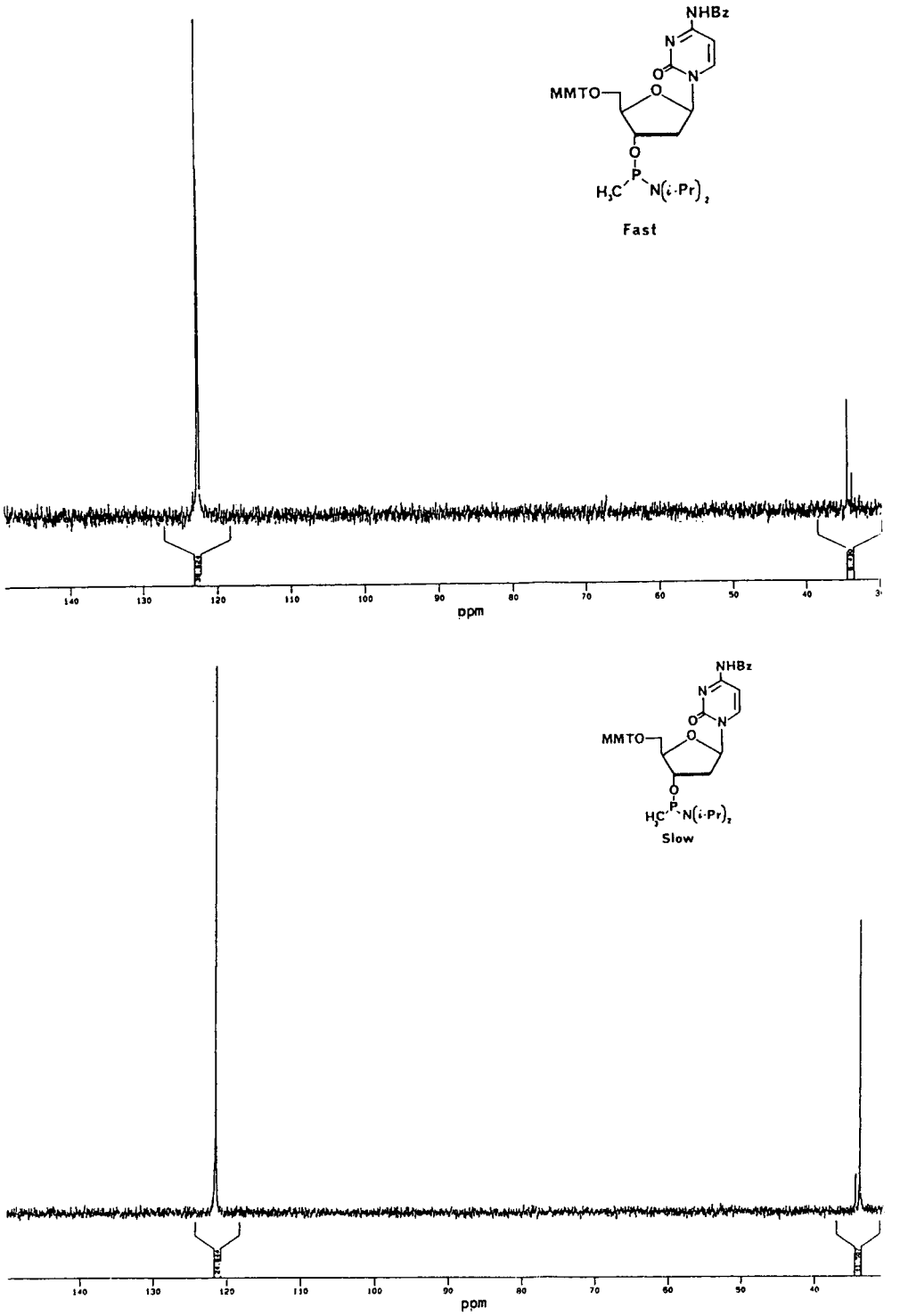

Fig. 2. ^{31}P NMR spectra of resolved phosphonamidites.

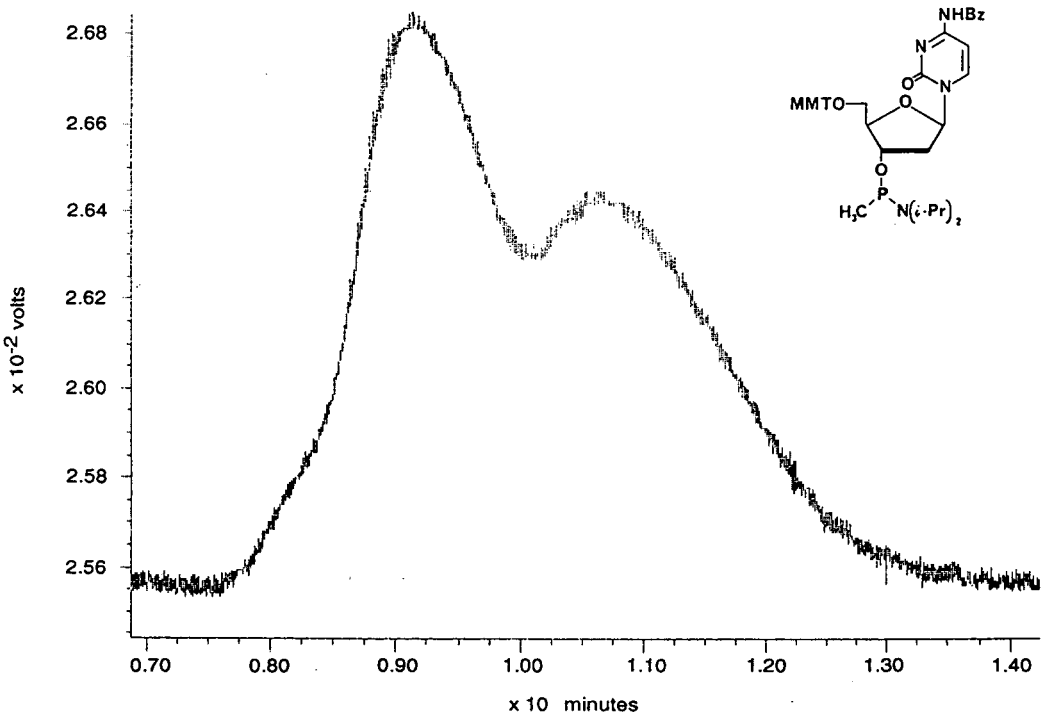

Fig. 3. Preparative chromatogram of N-benzoylcytidine phosphonamidite.

5. References

[1] E. Uhlmann and A. Peyman, *Chem. Rev.*, 90 (1990) 543–584.

[2] Z.J. Leznikowski, M. Jaworska and W.J. Stec, *Nucleic Acids Res.*, 18 (1990) 2109–2115, and references cited therein.

[3] F.H. Hausheer, B.G. Rao, J.D. Saxe and U.C. Singh, *J. Am. Chem. Soc.*, 114 (1992) 3201–3206.

[4] J.F. Cormier and T. Pannunzio, *Tetrahedron Lett.*, 32 (1991) 7161–7164.

[5] A.V. Lebedev, A.I. Riker, J.P. Rife and E. Wickstrom, *Tetrahedron Lett.*, 31 (1990) 3673–3676.

[6] W.J. Stec and G. Zon, *Tetrahedron Lett.*, 25 (1984) 5279–5283.

[7] K.-P. Stengele and W. Pfleiderer, *Nucleosides and Nucleotides*, 9 (1990) 423–427.

ELSEVIER

Journal of Chromatography A, 662 (1994) 407–413

JOURNAL OF CHROMATOGRAPHY A

Short Communication

High-performance liquid chromatography of a mixture of two dodecyltins by sensitive fluorescence tagging with morin

M. Pfeffer*, B. Gelbe, B. Woicke, B. Wykhoff

Research Laboratories, Schering AG, Berlin, Müllerstrasse 178, D-13353 Berlin, Germany

(First received May 4th, 1993; revised manuscript received November 3rd, 1993)

Abstract

A high-performance liquid chromatographic (HPLC) method for the determination of a 6:4 mixture of tris(isooctyloxycarbonylmethylthio)monododecyltin (**I**) and bis(isooctyloxycarbonylmethylthio)didodecyltin (**II**) combined with fluorescence detection following postcolumn morin complexation is presented. The HPLC method is selective for the compounds investigated as no other peaks were observed. The instrumental detection limit was 14 ng for **I** and 9 ng for **II** per 5-μl injection (*i.e.* 2.8 μg/ml of **I** and 1.8 μg/ml of **II** in 2-propanol), the method detection limit was 10 μg/ml of 6:4 mixture in peanut oil and the limit of determination was 0.22 mg/ml. The linearity of the detector signals was verified within the range 50 ng–1.0 μg of 6:4 mixture per injection (*i.e.* 2.5–50 μg/ml in 2-propanol). Within the range 0.22–50 mg/ml, the accuracy was 90–102% of the expected values and the intra-assay precision (relative standard deviation) was <5%. The HPLC results and atomic absorption spectrometric data were concordant.

1. Introduction

Organotins are extensively used as PVC stabilizers, polymerization catalysts and biocides in industry and agriculture. To investigate their toxicological potential, the organotins are administered to test animals via suitable formulations. A mixture of monododecyltin and didodecyltin isooctylthioglycolates has been recommended as a stabilizer for rigid PVC in food packaging and is included in the recommendations of the Plastics Committee of the German Federal Health Office (BGA). As a part of the toxicological characterization of this mixture, studies on embryotoxicity in rats and rabbits were performed. Oral administration was performed using solutions in peanut oil. The preparations need to be checked for the correct concentration and stability of the active ingredients.

UV and fluorescence detectors are commonly applied in high-performance liquid chromatography (HPLC). However, owing to the lack of chromophores the direct determination of organotins by HPLC is difficult. Consequently, HPLC is often combined with element-specific detectors such as atomic-absorption spectrometers [1–5], flame photometers or inductively coupled plasma atomic emission spectrometers [6,7]. However, such equipment is highly sophisticated and expensive. Another approach is achieved by UV and fluorescence labelling with 8-quinolinol [8] and morin [9–15], respectively. The 8-quinolinol complexation was per-

* Corresponding author.

0021-9673/94/$07.00
SSDI 0021-9673(93)E1239-V

formed with an on-column procedure. Pre/on-column [9,10] or postcolumn techniques [11–15] were used to obtain highly fluorescent organotin–morin complexes. Ebdon and Garcia Alonso [15] and Kleiböhmer and Cammann [16] reported that the fluorescence of these complexes could be enhanced by using micellar systems. In this paper, a postcolumn technique with morin for organotin derivatization in a micellar system is presented. The procedure was applied to two novel PVC stabilizers.

2. Experimental

2.1. Materials

Tris(isooctyloxycarbonylmethylthio)monododecyltin (**I**) and bis(isooctyloxycarbonylmethylthio)didodecyltin (**II**) (Fig. 1) were synthesized in the laboratories of Schering (now Witco) (Bergkamen, Germany). A 6:4 (w/w) mixture of **I** and **II** was used for the experiments. Liquid chromatographic grade acetonitrile, 2-propanol and water were obtained from Merck (Darmstadt, Germany). Analytical-reagent grade morin, lithium chloride, Triton X-100 and acetic acid were also purchased from Merck.

2.2. Apparatus

The HPLC equipment consisted of a Model 510 pump (Waters, Eschborn, Germany), set at a flow-rate of 1.2 ml/min and equipped with a membrane pulse filter and a 25 cm × 4.6 mm I.D. stainless-steel column packed with 10-μm silicon carbide by VDS Optilab Chromatographie Technik (Berlin, Germany), an ISS-100 autosampler (Perkin-Elmer, Überlingen, Germany), a reagent-delivery module (Waters), set at a flow-rate of 1.0 ml/min, and a Perkin-Elmer LC-240 fluorescence detector. The detector was connected via an interface to a VAX 8810 mainframe computer (Digital Equipment, Munich, Germany) for data acquisition and evaluation. The chromatograms were evaluated with ACCESS · CHROM 1.6 (Perkin-Elmer).

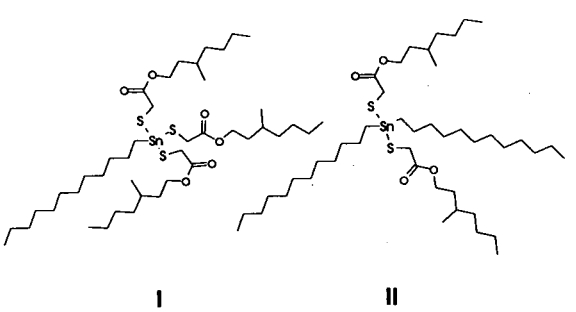

I II

Fig. 1. Structural formulae of compounds **I** and **II**.

2.3. Chromatography and postcolumn derivatization

Chromatographic columns of dimensions 2 cm × 4.6 mm I.D. (analytical column) and 12.5 × 4.6 mm I.D. (precolumn) was packed with Hypersil MOS and SAS Hypersil, respectively, by M & W Chromatographie Technik (Berlin, Germany). The mobile phase was a mixture of 800 ml of acetonitrile, 140 ml of doubly distilled water, 60 ml of acetic acid and 6 g of lithium chloride. The postcolumn reagent proposed by Ebdon and Garcia Alonso [15] was modified and consisted of 15 mg of morin, 600 μl of acetic acid, 7 g of Triton X-100 and ad 500 ml of water containing 37% (v/v) 2-propanol. The mobile phase and postcolumn derivatization reagent were degassed under water-jet vacuum.

2.4. Sample work-up

The peanut oil solutions were diluted with 2-propanol by volume factors from 20 (samples of 0.5 mg/ml) to 2500 (samples of 150 mg/ml). Aliquots of 5–10 μl were injected into the HPLC system.

2.5. Calibration and evaluation

Six calibration samples for an analytical run were prepared by dissolving the 6:4 mixture in 2-propanol. The proportion of the peanut oil in

the calibration samples was the same (0.04–5%, v/v) as that in the real samples diluted for injection. For example, in the analysis of samples containing 5 mg/ml of 6:4 mixture in peanut oil, the portions of the analytes injected were in the range 50–600 ng of 6:4 mixture per 5 μl. Thus the calibration range was from 1.0 to 12.0 mg/ml. With respect to evaluation, peak heights were preferred because peak areas were difficult to determine owing to peak tailing. An unweighted linear regression (model: $y = a + bx$) was used to fit the data. The calculation of the found 6:4 mixture concentration was normally performed by evaluating peak height of **II**, which was converted to the 6:4 mixture concentration in the sample, and if necessary by use of the peak height of **I**. That can be done because the proportion of **I** to **II** is fixed and both for calibration and for the preparation of the samples the same substance batches were used.

2.6. Experimental characterization of the HPLC procedure

The instrumental detection limit was determined at a signal-to-noise ratio ≥ 2 and the linearity by use of 2-propanol standard solutions. The mass loss caused by traces of peanut oil in the injected solutions was investigated by the analysis of real samples combined with calibration standards that contained no peanut oil. The results are reported in terms of recovery. Accuracy and intra-assay precision data were obtained by the analysis of real samples on the basis of **I** and **II**. The inter-assay precision was calculated based on the standard deviation obtained in routine analyses. Finally, the acceptance criteria for the method's limit of determination were a relative standard deviation (R.S.D.) of $\leq 5\%$ and a bias of $\leq 10\%$ of expected concentration obtained following the analysis of a series of real samples with decreasing concentrations. Additionally, selected samples were analysed by atomic absorption spectrometry (AAS) as described below. The total tin concentrations found were compared with the HPLC data.

2.7. Comparative analysis by AAS

Some real samples were analysed by means of AAS as described by Tölg [17] and Welz [18] to confirm the results obtained by HPLC. The samples were dissolved and diluted with acetone–2-propanol (1:1, v/v). Each sample was processed in triplicate. For six-point calibration, an oily tin standard was dissolved and diluted with acetone–2-propanol (1:1, v/v). Within the analytical run the calibration standards were measured before and after the samples. Atomic absorption was measured at 286.3 nm. Linear regression was applied for the calculation of the calibration graph. Within each assay a quality control sample containing dibutyltin bis(2-ethylhexanoate) was analysed.

2.8. Stability tests

The stability of the dodecyltins in peanut oil was monitored over a period of 1 week. The expected concentrations were 0.5, 5.0 and 50 mg/ml of 6:4 mixture. Samples of 100 ml were prepared and stored at room temperature protected from light in a glass container. Immediately after preparation and 6 h, 3 days and 7 days afterwards 3–5 aliquots of 0.5 ml were withdrawn, diluted with 2-propanol and injected into the HPLC system.

3. Results and discussion

3.1. Separation and detection of the organotins

Because of its two lipophilic hydrocarbon chains, **II** is retained much more strongly than **I** on octadecyl reversed phases. An acceptable retention behaviour of the two compounds and a short run time of 10 min were achieved by use of the very small analytical columns filled with octyl reversed-phase material. Longer columns and octadecyl phases yielded flat and strongly retained peaks of **II** that could not be evaluated. Also, strong tailing of the peaks of **I** and **II** was observed and is probably due to the strong interaction of the organotin cations with the

residual hydroxy silanol groups of the stationary phase. These unwanted adsorption effects could be reduced significantly by addition of lithium chloride to the mobile phase as proposed by Lakata *et al.* [8]. However, the autosampler and pump have to be protected from corrosion by purging with water and 2-propanol after the runs. Finally, chromatograms of samples containing ≤0.5 mg/ml of 6:4 mixture often showed negative peaks interfering with the peak of **I**. Consequently, the evaluation of the disturbed peaks was difficult. It could be shown that negative peaks were caused by 2-propanol and disappeared when using small injection volumes and additionally the 12.5-cm precolumn, which improved the diffusion of injected 2-propanol in the mobile phase.

In order to achieve peaks of roughly the same height, the wavelengths were changed during the progress of each run. At the start of each chromatography, the fluorescence detector was set at an excitation wavelength of 400 nm and an emission wavelength of 560 nm. The emission wavelength was chosen to be above the emission maximum of **I** of 500 nm because **I** showed much stronger fluorescence than **II** and the proportion of **I** in the samples was 50% higher than that of **II**. As a result, the fluorescence of **I** was prevented from exceeding the dynamic range of the detector. Before the elution of **II** the detector was reset to the optimum sensitivity (emission maximum 460 nm). A representative chromatogram of the two compounds is shown in Fig. 2.

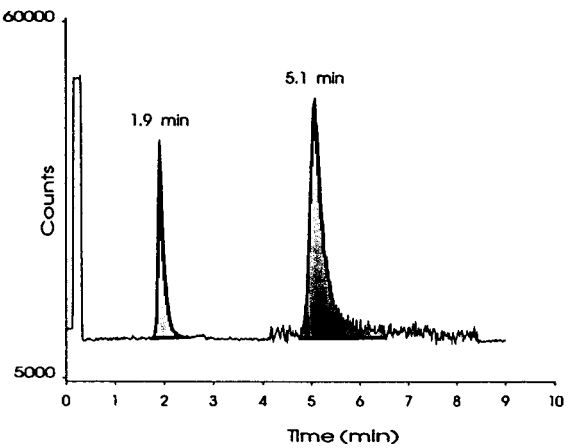

Fig. 2. Chromatogram of a peanut oil sample containing 5.0 mg/ml of 6:4 dodecyltin mixture. Compounds **I** and **II** were eluted at 1.9 and 5.1 min, respectively.

3.2. Characterization of the HPLC method

The system was very selective for the compounds investigated as no other peaks were observed. The instrumental detection limit was 25 ng of 6:4 mixture (corresponding to 14 ng of **I** and 9 ng of **II**) per injection. Including a dilution factor of 20 and an injection volume of 5 μl, the method detection limit was then 10 μg/ml of 6:4 mixture in peanut oil. The sensitivity for **I** could be enhanced further by a factor of at least ten if optimum detections conditions for **I** (emission maximum 500 nm) were applied. Additionally, flow-rates of the postcolumn reagents ≤1.0 ml/min led to higher sensitivity. The limit of detection of **II** could be lowered by increasing the injection volume and perhaps also by application of postcolumn UV irradiation as reported by Stäb *et al.* [13].

The linearity of the peak heights of the dodecyltins was tested within the range of 50 ng–1.0 μg of 6:4 mixture per injection (*i.e.* 2.5–50 μg/ml) and could be verified.

The recovery data are summarized in Table 1. The recovery of **I** was 80 and 75% and that of **II** was 66 and 62% at the levels of 0.22 and 0.51 mg/ml of 6:4 mixture, respectively. At the 5 and 51 mg/ml levels, the recovery of **I** was 92 and 103% and that of **II** was 86 and 97%, respectively. No mass loss of the two compounds was observed only with the sample of 51 mg/ml. The loss was presumably caused by the peanut oil matrix, which contaminated the stationary phases and adsorbed the dodecyltins on the column. To obtain optimum accurate analytical results in spite of this mass loss, the calibration standards therefore ought to be spiked with peanut oil according to the samples involved. In addition, a special sequence for the analyses of samples containing ≤1.0 mg/ml of 6:4 mixture should to be adopted. First, the calibration standards (low, medium and high levels) were chromatographed, then the blank peanut oil

Table 1
Recovery, accuracy and intra-assay precision data

Expected concentration (mg/ml of 6:4 mixture)	Recovery (% of expected values)		Accuracy and intra-assay precision			
			I		II	
	I	II	Accuracy (%)	R.S.D. (%)	Accuracy (%)	R.S.D. (%)
0.22	80	66	98	4	95	5
0.51	75	62	92	3	90	3
4.99	92	86	98	2	98	2
50.66	103	97	102	1	100	2

The accuracy and intra-assay precision of the method are given as mean values and R.S.D.s of analyses performed with five replicates. The accuracy data are given as a percentage of the expected concentration of the prepared samples. Under the heading Recovery the results obtained without mass compensation are tabulated. The mean values of five replicates are given. The results were related to the expected concentrations. The data were calculated on basis of the peak heights of both **I** and **II**.

sample, subsequently a dodecyltin sample in triplicate, the blank peanut oil sample again, followed by the same calibration standards, blank sample, dodecyltin samples, and so on.

To determine the accuracy and intra-assay precision of the method, the four peanut oil solutions mentioned in Table 1 and another four samples containing 0.50–0.55 mg/ml of 6:4 mixture were analysed. At the 0.50–0.55 mg/ml level, the accuracy ranged from 87 to 93% of the expected values when the peak of **I** and from 90 to 105% when the peak of **II** was evaluated. For the other samples the expected concentrations were exactly met. Hence, the two steps proposed above diminished the influence of the mass loss so that sufficient accuracy was obtained.

The results of the total tin determination and the HPLC data are summarized in Table 2. The

Table 2
Comparison of the results obtained by analysis of real samples by HPLC and AAS (mean values of 2–5 determinations)

Expected concentration (mg/mol of 6:4 mixture)	Accuracy (% of expected concentration)		
	AAS (total tin)	HPLC	
		I evaluated	**II** evaluated
0.5	114	123	113
	118	137	113
	104	74	97
	98	84	98
	111	90	102
5.0	104	104	106
	102	102	104
50	104	99	115
	106	97	98

comparison showed that the HPLC data (evaluation of the peak of **II**) agreed very well with the AAS data. Only for one sample did the deviation of the result exceed 10%. Following evaluation of the peak of **I**, the difference between the AAS and HPLC data was up to 30%.

The intra-assay precision (R.S.D.) was in the range 1–4% and 2–5% when the peaks of **I** and **II** were used for evaluation, respectively. With respect to the inter-assay precision, the R.S.D.s obtained from different analytical runs were about 6% at the 0.5 mg/ml of 6:4 mixture level, about 2% at the 5.0 mg/ml level and about 4% at the 15–150 mg/ml level.

The recovery, accuracy, precision and AAS data show that the method always gave optimum results when the concentration of the 6:4 mixture was calculated on the basis of **II**. The lowest concentration tested, 0.22 mg/ml, was defined as limit of determination.

3.3. Application of the method

Within the framework of an analytical service for the validation of toxicological studies, the formulations used are monitored systematically for correct preparation. The stability of the active ingredients has to be tested before the studies begin. If the results are within the range of acceptance (90–110% of the expected concentration), the formulations are considered to be correctly prepared and the preparation process to be valid. The stability of the test substance is deemed to be proved for a defined time period when the decrease in concentration amounts to ≤10% with reference to the initial value. For the 6:4 mixture of dodecyltins the peanut oil formulations that had been routinely analysed so far conformed with the acceptance range and were considered to have been prepared correctly.

With respect to stability at the 5 and 50 mg/ml of 6:4 mixture levels, the analyses resulted in negligible changes in the concentrations of **I** and **II** during 1 week, as shown in Fig. 3. However, at the lowest concentration level of 0.5 mg/ml the concentration of **I** decreased from 84% to 14% within 1 week; the level of **II** remained

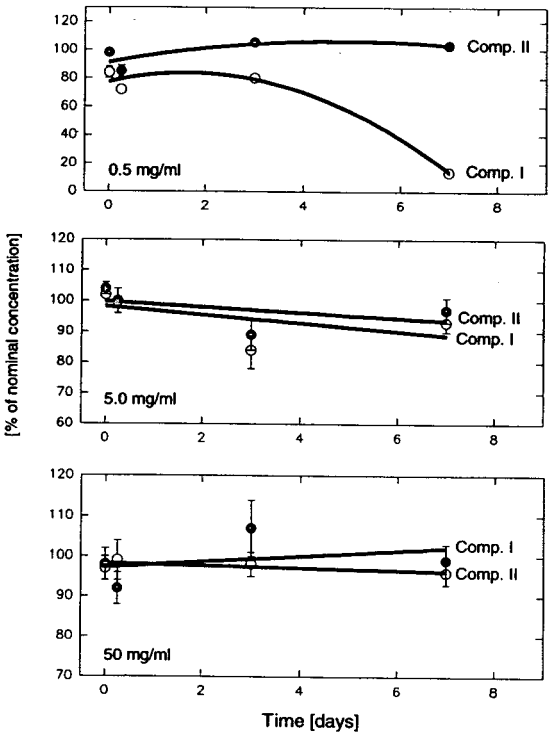

Fig. 3. Stability of the two docecyltins at different concentration levels. The graphs show the analytical results of the stability test. At the 5 and 50 mg/ml of 6:4 mixture levels, five aliquots per time point were processed for HPLC. The sample processing was performed in triplicate at the lowest concentration level (0.5 mg/ml of 6:4 mixture). In the top graph, the error bars disappear behind the symbols indicating the mean values because the standard deviation of the results is very low.

almost constant, 98% being found at the beginning and 103% at the end of the study. At the 0.5 mg/ml level, the 6:4 mixture of dodecyltins was considered to be stable for only a maximum of 3 days because of the decrease in **I** after that time. This means that formulations with concentrations of >5 mg/ml can be used for administration during 1 week and samples containing 0.5–5 mg/ml for a maximum of 3 days. Hence formulations have to be prepared twice per week for use in studies with daily administration.

Finally, the conclusion can be drawn that the described method is suitable for the analysis of peanut oil samples containing ≥0.22 mg/ml of

6:4 dodecyltin mixture. Good sensitivity, excellent selectivity and sufficient accuracy and precision are features of the procedure. The analytical results were reliable and both the correct preparation of formulations and the stability of the active ingredients could be monitored successfully.

4. References

[1] F.E. Brinckman, W.R. Blair, K.L. Jewett and W.P. Iverson, *J. Chromatogr. Sci.*, 15 (1977) 493.
[2] D.T. Burns, F. Glockling and M. Harriot, *Analyst*, 106 (1981) 921.
[3] L. Ebdon, S. Hill and P. Jones, *Analyst*, 110 (1985) 515.
[4] I.S. Krull and K.W. Panaro, *Appl. Spectrosc.*, 39 (1985) 960.
[5] K.L. Jewett and F.E. Brinckman, *J. Chromatogr. Sci.*, 19 (1981) 583.
[6] L. Ebdon, R.W. Ward and D.A. Leathhard, *Anal. Proc.*, 19 (1982) 921.
[7] D. Bushdee, I.S. Krull, R.N. Savage and S.B. Smith, *J. Liq. Chromatogr.*, 5 (1982) 463.
[8] W.G. Lakata, E.P. Lankmayr and K. Mueller, *Fresenius' Z. Anal. Chem.*, 319 (1984) 563.
[9] W. Langseth, *Talanta*, 31 (1984) 975.
[10] W. Langseth, *J. Chromatogr.*, 315 (1985) 351.
[11] M. Pfeffer, B. Gelbe, P. Hampe, B. Steinberg, E. Walenciak-Reddel, B. Woicke and B. Wykhoff, *Fresenius' J. Anal. Chem.*, 342 (1992) 839.
[12] W. Kleiböhmer and K. Cammann, *Fresenius' J. Anal. Chem.*, 335 (1989) 780.
[13] J.A. Stäb, M.J.M. Rozing, B. van Hattun, W.P. Cofino and U.A.Th. Brinkman, *J. Chromatogr.*, 609 (1992) 195.
[14] T.H. Yu and Y. Arakawa, *J. Chromatogr.*, 258 (1983) 189.
[15] L. Ebdon and J.I. Garcia Alonso, *Analyst*, 112 (1987) 1551.
[16] W. Kleiböhmer and K. Cammann, *Fresenius' Z. Anal. Chem.*, 335 (1989) 775.
[17] G. Tölg, *Talanta*, 19 (1972) 1489.
[18] B. Welz, *Atomic Absorption Spectrometry*, Verlag Chemie, Weinheim, 1975.

ELSEVIER

Journal of Chromatography A, 662 (1994) 414–419

JOURNAL OF CHROMATOGRAPHY A

Short Communication

Competitive adsorption of α-lactalbumin and bovine serum albumin to a sulfopropyl ion-exchange membrane

Wendy F. Weinbrenner[a], Mark R. Etzel*[,b]

[a]Department of Chemical Engineering, 1415 Johnson Drive, University of Wisconsin, Madison, WI 53706-1619, USA
[b]Department of Food Science, 1605 Linden Drive, University of Wisconsin, Madison, WI 53706-1519, USA

(First received September 22nd, 1993; revised manuscript received November 23rd, 1993)

Abstract

Breakthrough curves were measured for pure solutions of α-lactalbumin (ALA) and bovine serum albumin (BSA) individually, and for a binary mixture of the proteins, using a sulfopropyl ion-exchange membrane. The breakthrough curves were qualitatively consistent with local-equilibrium theory predictions. Competitive adsorption caused displacement of bound BSA monomer by the more strongly binding BSA dimer, illustrating that even apparently single-protein systems may display multicomponent competitive behavior. In the two-protein experiment, ALA was competitively displaced by the more strongly binding BSA monomer and dimer, indicating that the binding strength was in the order: BSA dimer > BSA monomer > ALA.

1. Introduction

Conventional ion-exchange protein separation protocols utilize a packed column containing porous beads onto which the ligand is immobilized. Increasing the rate at which equilibrium between the protein solution and ion-exchange adsorbent is approached is of great practical importance because it maximizes the throughput of the process. In packed columns, the separation rate is typically limited by slow intra-bead diffusion for large beads, or low axial velocities and high column pressure drops for small beads. The rate at which the protein binds to the ion-exchange site is usually fast enough not to limit the overall rate. Only under ideal conditions do packed columns operate at local equilibrium and are separations based solely on differences in the equilibrium sorption isotherms [1–3].

Ion-exchange membranes are a promising new bioseparation technology designed to overcome the limitations of conventional packed columns. In ion-exchange membranes, pressure drop limitations are negligible because the membranes are thin, whereas intra-bead diffusional limitations are negligible because the feed solution flows by convection through the fine pores (pore size ≈ 1 μm) of the membrane. Consequently, properly designed and operated ion-exchange membranes may eliminate the mass-transfer and flow limitations associated with packed columns, and may approach local-equilibrium behavior.

Competitive ion-exchange sorption has been analyzed extensively, both theoretically and ex-

* Corresponding author.

0021-9673/94/$07.00
SSDI 0021-9673(93)E1260-7

perimentally, for packed columns [4–8], but not for ion-exchange membranes. But, packed columns cannot be used to cleanly test the assumptions of local-equilibrium theory for protein adsorption because of complications arising from slow and restricted intra-bead diffusion.

In this work, predictions from local-equilibrium theory will be compared qualitatively to experimental data from single-protein and binary-protein ion-exchange membrane separations, and used to determine the extent to which ion-exchange membranes approach local-equilibrium behavior.

2. Experimental

2.1. Materials

Bovine serum albumin (BSA) (A 0281) and α-lactalbumin (ALA) (L 6010) were obtained from Sigma (St. Louis, MO, USA) and used without further purification. The sulfopropyl (SP) MemSep 1010 ion-exchange membrane chromatography cartridge (CISP 15H 01) was supplied by Millipore (Bedford, MA, USA). It contained a stack of 72 regenerated cellulose membranes, with a 1.2 μm pore size [9,10]. The stack was 1 cm high, 4.9 ml in volume, and the porosity was 85%. The ion-exchange capacity was 2.3 meq per cartridge [10]. Thin polypropylene gasket rings were inserted by Millipore between every three or four membranes in the stack to avoid lateral flow towards the walls of the housing. The membrane stack was then compressed by Millipore to seal the gaskets, and to eliminate gaps between the individual membranes. Millipore placed a non-woven polypropylene disc filter on top of the first membrane in the stack to evenly distribute the flow [10].

The loading/washing buffer was 0.1 *M* NaOAc, adjusted to pH 3.0 with HCl, the elution buffer was 0.375 *M* Tris, pH 8.8, and both buffers contained 0.05% NaN_3. All solutions were vacuum filtered and degassed before use.

2.2. Methods

Standard procedures

The cartridge was cleaned and regenerated prior to each use by pumping in sequence 25 ml each of 0.1 *M* NaOH, loading buffer, and 0.1 *M* HCl through the membrane. It was then washed and equilibrated to pH 3.0 by pumping 50 ml of loading buffer through the membrane. A UV detector (Model 111 with a 10 μl volume, 2 mm pathlength flow cell, Gilson, Middleton, WI, USA) measured the absorbance of the stream exiting the membrane. A fraction collector (Retriever II, Isco, Lincoln, NE, USA) collected 1–2 ml fractions. All experiments were performed at 4.0 ml/min.

Measurement of system dispersion

Dispersion was determined from the breakthrough curve for 1.0 mg/ml BSA in elution buffer. The cartridge was washed with 50 ml of elution buffer, then 35 ml of the protein solution was loaded, followed by washing with elution buffer.

Breakthrough curve measurement

An aliquot of 150 ml of the two-protein solution, containing 1.0 mg/ml each of BSA and ALA in loading buffer, and 360 ml of each single-protein solution, containing 1.0 mg/ml of either BSA or ALA in loading buffer, was loaded. Loading buffer was then pumped through the system to wash unadsorbed protein from the membrane system. The adsorbed protein was eluted from the membrane until the absorbance returned to baseline.

Determination of protein concentration

Excluding the ALA single-protein experiment, fractions were analyzed by HPLC (Model 2350 pump and Model V^4 detector, Isco, Lincoln, NE, USA) at a wavelength of 280 nm. A 50-μl injection loop was used with a mobile phase buffer consisting of 0.2 *M* Na_2HPO_4 pH 7.0 at 2.0 ml/min through a gel filtration column (ZORBAX GF-250, E.I. du Pont de Nemours, Wilmington, DE, USA). Peaks were integrated

by a computer-based system, calibrated using pure samples of each protein in solutions of known concentration.

In experiments involving only one protein, a ratio of the UV detector voltage due to the feed solution, without the membrane in the system, to the concentration of the feed solution was used to convert all voltages to concentration. The concentration of the feed solution was calculated from the absorbance at 280 nm. The extinction coefficient of ALA was 1.78 ml mg^{-1} cm^{-1}, and of BSA was 0.6 ml mg^{-1} cm^{-1} at pH 3.0 and 20°C.

3. Results

3.1. System dispersion

In the dispersion experiment, BSA emerged in the effluent after 5.2 ml were loaded. This is the system dead volume, which includes the membrane void volume of 4.2 ml. Next, an additional 2.8 ml was loaded during which the effluent concentration rose to the feed concentration. If there were no dispersion in the system, the effluent concentration would have instantly risen to the feed concentration. An aliquot of 4.4 ml was required during washing for the effluent concentration to return to zero.

3.2. BSA breakthrough curve

Fig. 1 contains the breakthrough curve for 1.0 mg/ml BSA in loading buffer. The effluent concentration rose quickly after an effluent volume of 70 ml. Later, the breakthrough curve was very broad and asymmetric. After an effluent volume of 350 ml, the effluent concentration of BSA rose to only 96% of the feed solution concentration. Based on the area above the breakthrough curve, 102 mg of BSA were removed from the feed solution.

The compositions of the effluent fractions were determined by gel filtration HPLC and are plotted in Fig. 2. The feed solutions were essentially binary solute solutions because approximately 20% of the BSA existed as a dimer, and 80% existed as a monomer. After an effluent volume of 70 ml, BSA monomer only emerged from the membrane. Then, the BSA monomer concentration in the effluent rose to 9% above the feed solution concentration of BSA monomer. After an effluent volume of 140 ml, BSA dimer emerged in the effluent, and the BSA monomer concentration in the effluent decreased to the concentration of BSA monomer in the feed solution, and remained there. As loading continued, the BSA dimer concentration in the effluent continued to rise slowly, but did not

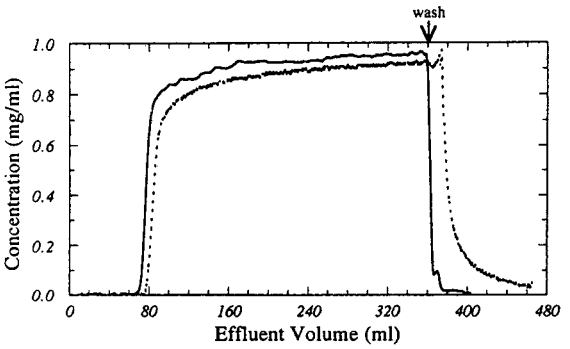

Fig. 1. Single-protein breakthrough curves from the UV detector for ALA (dashed line) and BSA (solid line). The feed solution contained 1 mg/ml of either ALA or BSA in 0.1 *M* NaOAc pH 3 buffer. The flow-rate was 4 ml/min, and 360 ml of each protein solution were loaded onto the membrane.

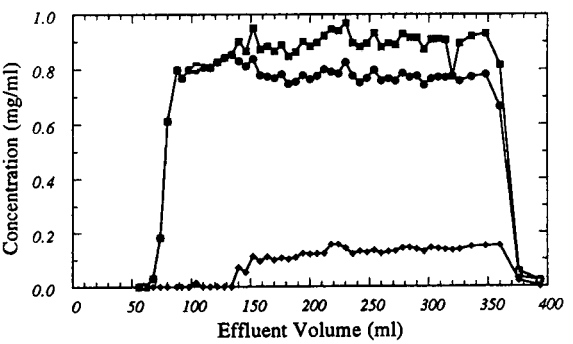

Fig. 2. BSA breakthrough curves for monomer (○), dimer (◆) and total (□). The total curve is the sum of the monomer and dimer curves. Fractions were collected from the BSA experiment of Fig. 1 and analyzed by HPLC.

reach the concentration of BSA dimer in the feed solution.

3.3. ALA breakthrough curve

Fig. 1 contains the breakthrough curve for a pure solution of ALA in loading buffer. The effluent concentration rose quickly after an effluent volume of 75 ml. Later, the breakthrough curve was very broad and asymmetric. After an effluent volume of 350 ml, the effluent concentration rose to only 92% of the feed concentration. Based on the area above the breakthrough curve, 94 mg of ALA were removed from the feed solution.

3.4. Two-protein breakthrough curve

Fig. 3 contains the breakthrough curve for a feed solution containing 1.0 mg/ml each of BSA and ALA in loading buffer. ALA emerged in the effluent after an effluent volume of 42 ml. For an effluent volume from 42 to 52 ml, the effluent contained pure ALA. The ALA concentration in the effluent peaked at 145% of the feed concentration of ALA at an effluent volume of 52 ml. After this point, BSA monomer emerged in the effluent, and the ALA concentration decreased to that in the feed solution. At an effluent volume of 120 ml, the BSA monomer concentration in the effluent peaked at 107% of the feed concentration of BSA monomer. Then it quickly decreased to an asymptote equal to the feed concentration of BSA monomer. At this point, BSA dimer emerged in the effluent. However, the feed solution concentration of BSA dimer was not reached. By subtracting the amount of protein in the effluent from that which was loaded, it was estimated that the membrane bound 38 mg of ALA, 43 mg of BSA monomer, and 24 mg of BSA dimer.

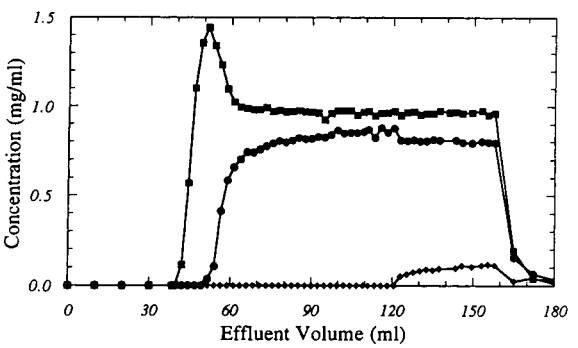

Fig. 3. Breakthrough curves for a mixture of BSA monomer (○), BSA dimer (◆) and ALA (□). The feed solution contained 1 mg/ml each of ALA and BSA in 0.1 *M* NaOAc pH 3 buffer. The flow-rate was 4 ml/min, and 150 ml of each protein solution were loaded onto the membrane. Fractions were analyzed by HPLC.

4. Discussion

The experimental results from this work will be qualitatively compared to the predictions of local-equilibrium theory, in which separation dynamics are described by purely thermodynamic factors [8,11–14]. In local-equilibrium theory, the mobile phase and the stationary phase are assumed to be in equilibrium at any point. For a single step increase in influent composition for a multiprotein feed solution containing *i* solutes, the predicted breakthrough curves contain *i* composition plateaus [11–13,15]. Initially, all the proteins are completely removed from the feed solution, and the effluent is free of protein. Then, the first plateau emerges in the effluent and contains only the lowest-affinity protein at a concentration usually greater than the feed concentration. Subsequent plateaus emerge in the effluent and contain the previous proteins plus the next lowest-affinity protein. Each transition between plateaus is sharp and vertical. The last plateau emerges in the effluent after saturation of the membrane, and has the same composition as the feed solution.

4.1. Multicomponent adsorption behavior in single-protein systems

If local-equilibrium theory for single solutes is applicable, then a single sharp transition to the feed concentration should occur in the breakthrough curve. However, during loading of a pure solution of BSA, as plotted in Fig. 2, BSA monomer and dimer appeared to compete for

adsorption sites, with BSA dimer displacing the more weakly bound BSA monomer. This displacement probably caused the peak in the BSA monomer concentration. Then, after an effluent volume of 140 ml, BSA dimer emerged in the effluent and BSA monomer displacement gradually ceased. Without displacement, the BSA monomer concentration in the effluent returned to the feed concentration.

The coincidence of BSA dimer emergence in the effluent, and simultaneously the BSA monomer concentration in the effluent returning to the feed concentration is characteristic of multicomponent local-equilibrium behavior. Evidently, even apparently single-protein systems may display multicomponent behavior.

The slow approach to the inlet concentration in the BSA breakthrough curve has been reported for sulfopropyl gel-bead packed columns at pH 5.0 [5]. It was attributed to slow dimer formation between adsorbed and free BSA. The slow formation of dimers on the surface should result in removal of monomer from solution, leading to a slow approach of the monomer concentration to that in the inlet. This did not occur in Fig. 2. Instead, there was a slow approach of the dimer concentration to that in the inlet. This probably was caused by the slow continued removal of BSA dimer from solution. BSA dimers do not form in solution in the absence of Cu(II) at pH 3.0 [16], which may explain the difference between these results and those for the packed column at pH 5.0.

4.2. Multicomponent adsorption and competition in two-protein systems

In the two-protein breakthrough curve of Fig. 3, all proteins were removed from the feed solution for the first 42 ml of effluent volume. Then bound ALA, the weakest binding protein, was displaced from the membrane by BSA monomer and dimer. This caused the ALA concentration in the effluent to peak at 145% of the feed concentration of ALA. Simultaneous to the peak in the ALA concentration, BSA monomer emerged in the effluent. The BSA monomer concentration peaked when BSA dimer emerged in the effluent. The peak in the BSA monomer concentration in the effluent probably resulted from displacement of bound BSA monomer from the membrane by the more strongly binding BSA dimer. These results are in good agreement with multicomponent local-equilibrium theory. Based on the order of emergence in the effluent, the binding strength to the SP ion-exchange membrane was in the order: BSA dimer > BSA monomer > ALA.

In summary, based on the results of this work, ion-exchange membranes qualitatively display local-equilibrium behavior. Thus, ion-exchange membranes overcome many of the limitations of conventional packed columns. Because of the relative absence of non-equilibrium effects, ion-exchange membranes are a useful tool for examining competitive protein sorption behavior. Based on the data, even apparently single-proteins systems may display multicomponent competitive behavior.

5. Acknowledgements

Funding for this work was provided by the Wisconsin Center for Dairy Research, and the Wisconsin Milk Marketing Board. Shing-Yi Suen supplied important technical advice while reviewing the manuscript.

6. References

[1] C.K. Lee, Q. Yu, S.U. Kim and N.-H.L. Wang, *J. Chromatogr.*, 484 (1989) 29–59.
[2] F.D. Antia and C. Horváth, in C.A. Costa and J.S. Cabral (Editors), *Chromatographic and Membrane Processes in Biotechnology*, Kluwer, Boston, 1991, pp. 115–136.
[3] C.A. Costa, in C.A. Costa and J.S. Cabral (Editors), *Chromatographic and Membrane Processes in Biotechnology*, Kluwer, Boston, 1991, pp. 3–24.
[4] G.L. Skidmore and H.A. Chase, *J. Chromatogr.*, 505 (1990) 329–347.
[5] G.L. Skidmore, B.J. Horstmann and H.A. Chase, *J. Chromatogr.*, 498 (1990) 113–128.
[6] A. Velayudhan and C. Horváth, *J. Chromatogr.*, 443 (1988) 13–29.

[7] R.D. Whitley, R. Wachter, F. Liu and N.-H.L. Wang, *J. Chromatogr.*, 465 (1989) 137–156.
[8] Q. Yu and N.-H.L. Wang, *Sep. Purif. Methods*, 15 (1986) 127–158.
[9] M.S. Le and J.A. Sanderson, *US Pat.*, 4 895 806 (1990).
[10] *SP MemSep ion exchange membrane chromatography cartridge: operating instructions, Cat. No. MSGF 147*, Millipore, Bedford, MA, 1991.
[11] E. Glückauf, *Proc. R. Soc. London A*, 186 (1946) 35–57.
[12] F. Helfferich and G. Klein, *Multicomponent Chromatography. Theory of Interference*, Marcel Dekker, New York, 1970.
[13] H.-K. Rhee, R. Aris and N.R. Amundson, *Philos. Trans. R. Soc. London A*, 267 (1970) 419–455.
[14] D.D. Frey, *Chem. Eng. Sci.*, 45 (1990) 131–142.
[15] S.-Y. Suen, M. Caracotsios and M.R. Etzel, *Chem. Eng. Sci.*, 48 (1993) 1801–1812.
[16] J.F. Foster, in V.M. Rosenoer, M. Oratz and M.A. Rothschild (Editors), *Albumin Structure, Function and Uses*, Pergamon Press, Oxford, 1977, p. 59.

ELSEVIER

Journal of Chromatography A, 662 (1994) 420–423

JOURNAL OF CHROMATOGRAPHY A

Short Communication

Monitoring the conversion of cycloheptanone to methyl 7-oxoheptanoate by gas chromatography☆

R.D. Wakharkar*, S.S. Biswas, H.B. Borate, D.E. Ponde

National Chemical Laboratory, Poona 411 008, India

(First received January 22nd, 1993; revised manuscript received November 15th, 1993)

Abstract

Methyl 7-oxoheptanoate is an important intermediate required for the synthesis of prostaglandins by three-component coupling methodology. It can be efficiently prepared in two steps from cycloheptanone via the formation of 1-methoxy-1-cycloheptene and its ozonolysis. An efficient and reproducible method for the baseline separation of the components in the reaction mixtures in the above steps by gas chromatography is reported.

1. Introduction

During the course of our studies on prostaglandin synthesis we required methyl 7-oxoheptanoate (**1**) [1,2], and we decided to prepare it by ozonolysis [1] of 1-methoxy-1-cycloheptene (**2**), which in turn can be prepared from cycloheptanone (**3**) and trimethyl orthoformate (**4**) (Fig. 1). Wohl [3] reported a one-step procedure for the synthesis of cyclic enol ethers via intermediate acetals, in which the acetal content could not be judged by GC analysis. No suitable methods [4–6] were available to monitor these reactions by GC and, to our knowledge, there is no report giving conditions for separating a mixture of cycloheptanone (**3**), trimethyl orthoformate (**4**), 1,1-dimethoxycycloheptane (**5**) and 1-methoxy-1-cycloheptene (**2**) simultaneously. In this work, we achieved a baseline separation and developed GC conditions for the quantitative analysis of the reaction mixtures so that these reactions could be optimized for the maximum yield of **1**.

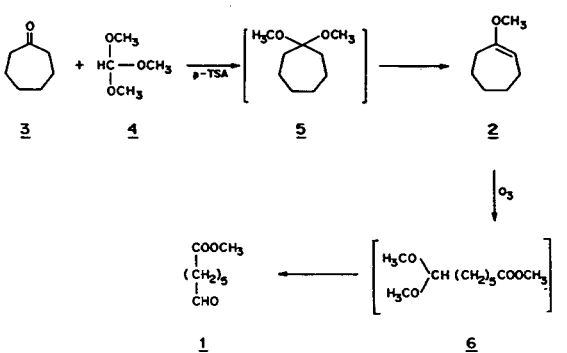

Fig. 1. Conversion of cycloheptanone (**3**) into methyl 7-oxoheptanoate (**1**) via the intermediates **5** and **2**.

* Corresponding author.

☆ NCL Communication No. 5712.

0021-9673/94/$07.00

SSDI 0021-9673(93)E1225-O

2. Experimental

2.1. Materials and solvents

Cycloheptanone (**3**) and trimethyl orthoformate (**4**) were purchased from Merck (Darmstadt, Germany). *p*-Toluenesulphonic acid (Fluka) was used as received. Other compounds, *viz.*, methyl 7-oxoheptanoate (**1**), 1-methoxy-1-cycloheptene (**2**) and 1,1-dimethoxycycloheptane (**5**), were prepared (see Section 2.2) in our laboratory, isolated in pure form by distillation and characterized by IR, NMR and mass spectrometry. The purified materials were analysed by GC and GC–MS to confirm their retention times.

2.2. Methods

Cycloheptanone was subjected to Wohl's conditions [3] for the preparation of **2**, *i.e.*, a mixture of trimethyl orthoformate, cycloheptanone and *p*-toluenesulphonic acid was stirred at room temperature for 24 h and then heated to remove the methanol liberated. We found that the reaction mixture could be directly heated under reflux (120°C) for 8 h to achieve complete conversion. The progress of this reaction was monitored by GC analysis as described. Further, the **2** thus obtained (after distillation) was subjected to ozonolysis [1] in methanol at −78°C to give **1**. The methanolic solution was analysed directly by GC.

2.3. Apparatus and conditions

A Hewlett-Packard Model 5880 gas chromatograph equipped with dual flame ionization detectors and coupled to a level 4 integrator was used with a stainless-steel column (6 ft. × 1/8 in. O.D.) packed with Chromosorb W HP (80–100 mesh) coated with 10% diethylene glycol succinate (DEGS).

The column was operated at 60°C with the injection port at 40°C above the oven temperature and a detector temperature of 250°C for the separation of methyl formate, methanol and trimethyl orthoformate. However, baseline separation and monitoring of the progress of the reactions were achieved using the same column operated at a detector temperature of 250°C, an oven temperature either isothermal at 90°C or programmed from 90 to 150°C at 20°C/min and an injection port temperature 40°C above the oven temperature. Nitrogen was used as the carrier gas at a flow-rate of 30 ml/min; the hydrogen flow-rate was 30 ml/min and the air flow-rate 350 ml/min.

2.4. Preparation of standard solutions

For quantitative analysis, mixtures of compounds **2** and **3** of different compositions ranging from 1:9 to 10:0 (**2**:**3**) were prepared in dichloromethane, *e.g.*, 10 mg of **2** and 90 mg of **3** were dissolved in 10 ml of dichloromethane. With an injection volume of 2 μl, GC analysis of all the solutions was carried out; calibration graphs for **2** and **3** were plotted separately and were found to be linear. Aliquots of the reaction mixture to be monitored were analysed by GC directly at different intervals.

3. Results and discussion

The separation of a mixture of trimethyl orthoformate (**4**), cycloheptanone (**3**), 1,1-dimethoxycycloheptane (**5**) and 1-methoxy-1-cycloheptene (**2**) was initially tried on 5% OV-101 at 100°C, but **2** and **5** eluted at nearly the same retention time. A baseline separation was successfully achieved using 10% DEGS at 90°C, as shown in Fig. 2. The order of elution was **4** ($t_R = 0.97$), **2** ($t_R = 2.05$), **5** ($t_R = 4.42$) and **3** ($t_R = 7.20$ min). The total time required for the separation of all the components was less than 8 min.

In order to follow the presence of methyl formate and methanol formed during the preparation of **5** and **2**, indicating the progress of the reaction, the reaction mixture was analysed at 60°C on the same column and the order of elution was methyl formate ($t_R = 0.67$), methanol ($t_R = 0.96$) and **4** ($t_R = 2.19$ min). The pro-

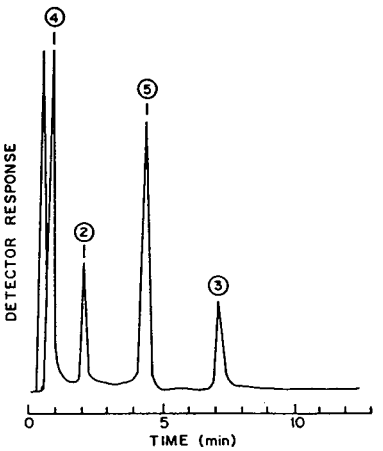

Fig. 2. Gas chromatogram showing separation of the reaction mixture during the conversion of **3** into **2**, obtained using a 10% DEGS column at 90°C. Peaks: 4 = trimethyl orthoformate (**4**) (t_R = 0.97 min); 2 = 1-methoxy-1-cycloheptene (**2**) (t_R = 2.05 min); 5 = 1,1-dimethoxycycloheptane (**5**) (t_R = 4.42 min); 3 = cycloheptanone (**3**) (t_R = 7.20 min).

Table 1

Progress of the reaction monitored by gas chromatography

Reaction conditions	Concentration (%)		
	3	**2**	**5**
Stirred at room temperature for 24 h	12.43	37.64	40.56
Room temperature for 24 h then 120°C for 6 h	–	92	5
120°C for 4 h	1.36	18.00	72.37
120°C for 8 h	–	94.07	2.87

gress of the conversion of **3** into **2** using different reaction conditions was monitored by GC as described and the results are given in Table 1.

In order to determine the accuracy of the method (external standard method), calibration graphs were plotted of area counts on the ordinate *versus* mass in mg on the abscissa. When 2 μl of solution of known concentration were injected under similar conditions, we found that the mass deduced from this graph matched the actual mass. The graphs thus obtained for **2** and **3** were found to be linear with slopes of 1.2 and 1.0, respectively. The results obtained after injecting unknown synthetic mixtures (aliquots from the reaction mixture) are given in Table 2. Statistical evaluation of the method showed that the reproducibility of quantitative measurements is fairly good, as indicated by the standard deviation, ranging from 0.432 to 0.886%.

Compound **2** was subjected to ozonolysis using the reported conditions [1] and the reaction was monitored by GC. The column temperature was programmed from 90 to 150°C at 20°C/min. The chromatogram in Fig. 3 shows the separation between **3**, **6** and **1**, the retention times being 7.20, 12.26 and 13.81 min, respectively (during the reaction a small amount of **2** is converted into the more stable keto form, cycloheptanone). It was assumed that the peak at t_R = 12.26 min was due to the intermediate methyl 7,7-dimethoxyheptanoate, which disappeared after acid hydrolysis with increase in the amount of **1** present (t_R = 13.81 min).

Table 2

Results obtained from calibration graph for different batches

Sample	Concentration of **2** present (mg/ml)	Concentration of **2** found from calibration graph (mg/ml)	Conversion (%)	Standard deviation (%)[a]
A	62	60	96.77	0.886
B	53	51	96.22	0.432
C	55	53	96.36	0.714

[a] Peak area for six determinations.

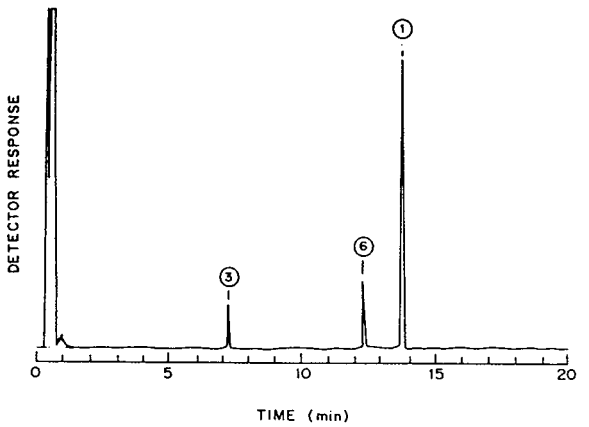

Fig. 3. Gas chromatogram showing the separation of the products after ozonolysis of **2** to **1**. Column, 10% DEGS; temperature, programmed from 90°C (7.5 min) to 150°C at 20°C/min. Peaks: 3 = cycloheptanone (**3**) (t_R = 7.20 min); 6 = methyl 7,7-dimethoxyheptanoate (**6**) (t_R = 12.26 min); **1** = methyl 7-oxoheptanoate (**1**) (t_R = 13.81 min).

4. Conclusions

A clear separation of **2** and **3** was achieved by selecting suitable column and temperature conditions for GC. This was especially useful as the usual TLC technique was not satisfactory. Further conversion of **2** into **1** could also be monitored directly in the reaction mixture.

5. References

[1] M. Suzuki, T. Kawagishi, A. Yanagisawa, T. Suzuki, N. Okamura and R. Noyori, *Bull. Chem. Soc. Jpn.*, 61 (1988) 1299.
[2] L. Van Hijfte and M. Kelb, *Tetrahedron*, 48 (1992) 6393.
[3] R.A. Wohl, *Synthesis*, (1974) 38.
[4] M. Verzele, M. Acke and M. Anteunis, *J. Chem. Soc.*, (1963) 5598.
[5] K. Schank and W. Pack, *Chem. Ber.*, 102 (1969) 1892.
[6] H.O. House, L.J. Czula, M. Gall and H.D. Olmstead, *J. Org. Chem.*, 34 (1969) 2324.

ELSEVIER

Journal of Chromatography A, 662 (1994) 424–433

JOURNAL OF CHROMATOGRAPHY A

Short Communication

Solid-phase trapping of polychlorinated biphenyls in supercritical fluid extraction

Søren Bøwadt*,[a], Berit Johansson[a], Fabio Pelusio[a], Bo R. Larsen[a], Costanza Rovida[b],

[a] *Environment Institute, EC Joint Research Center, TP 290, I-21020 Ispra (VA), Italy*

[b] *Hewlett-Packard, Analytical Group, Via G di Vittoria 9, I-20063 Cernusco S/N (Mi), Italy*

(Received August 9th, 1993)

Abstract

A method for the interference-free analysis determination of polychlorinated biphenyl (PCB) congeners in sewage sludge in less than 2 h with quantification limits down to 10–20 ppb (w/w) is presented. Evaluations were made of four different trapping materials for the supercritical fluid extraction of PCBs from sewage sludge. The influence of modifiers at different concentrations and temperatures was studied for different trapping materials with respect to their trapping efficiency with spiked samples.

1. Introduction

The improper use and disposal of commercial materials containing polychlorinated biphenyls (PCBs) has resulted in the contamination of the environment with these compounds. The monitoring of PCBs in environmental, technical and biological samples is incorporated in the legislation of all developed countries. The determination of PCBs at trace levels requires efficient extraction methods and extensive clean-up procedures to remove interferences contributed by the matrix.

Recent studies have demonstrated that the use of supercritical fluids in analytical extraction provides a powerful alternative to traditional liquid extraction methods (reviewed by King [1] and Hawthorne [2]). Apart from the concern that PCBs must be extractable from their matrix, the system being used to trap the PCBs after the supercritical fluid extraction (SFE) must perform efficiently. Until recently, the most popular trapping technique was liquid collection. Most SFE experiments have been carried out at high concentration levels (ppm), mainly with artificially fortified samples, which allowed the direct analysis of the extract without clean-up [1–4]. Real samples contaminated at trace levels require a high degree of extract concentration before analysis. Although SFE can be carried out with some selectivity, real samples produce extracts with residues of matrix components that inevitably end up in the concentrated extracts after liquid collection unless clean-up is performed.

More recently, SFE extracts have been collected on sorbents such as silica gel or bonded-phase packings and then eluted with liquid solvents for subsequent analysis [5–10]. The packing material provides two trapping mecha-

* Corresponding author.

0021-9673/94/$07.00
SSDI 0021-9673(93)E1216-M

nisms (cryogenic trapping caused by the cooling of the expanding supercritical fluid and absorption) and a clean-up mechanism (liquid chromatography in the elution phase). Solid-phase trapping is more complex than liquid collection and requires a high degree of optimization of the experimental conditions (choice of trapping material, supercritical fluid modifier, trapping temperature and elution solvent). However, it potentially allows the simultaneous extraction, clean-up and concentration of the extract.

The aim of this study was the evaluation of the selective extraction of PCBs from sewage sludge. The impact of added modifiers was investigated with respect to the efficiency of trapping PCBs on different trapping materials.

2. Experimental

2.1. Chemicals

PCBs and certified sewage sludge (CRM 392) were obtained from the Community Bureau of Reference (BCR) (Brussels, Belgium). PCBs (IUPAC Nos. 28, 52, 101, 105, 118, 128, 138, 149, 153, 156, 170 and 180), received as neat crystals, were mixed in a spiking solution at concentrations from 5.0 to 17.2 ng/μl. The solvents used were all of pesticide grade (Merck, Darmstadt, Germany). The CO_2- and methanol (MeOH)-modified extraction fluids were all obtained as SFE/SFC grade from SIAD (Milan, Italy). The ethanol (EtOH)-modified extractions were performed by adding absolute ethanol directly to the extraction cells.

2.2. Supercritical fluid extraction

A Hewlett-Packard Model 7680A supercritical fluid extractor was used for all the work presented.

For spike extractions, 50 μl of the spiking solution were added to 10 g of anhydrous Na_2SO_4, giving concentrations of the single PCB congeners from 25 to 86 ppb. Extractions were performed with a number of different modifier concentrations (CO_2, CO_2 + 2% MeOH, CO_2 + 5% MeOH and CO_2 + 2% EtOH) and trap temperatures (20, 65 and 78°C) at a density of 0.75 g/ml and a flow-rate of 1 ml/min liquid CO_2 for 30 min at 60°C. The nozzle temperature was kept at 45°C. The traps were filled with *ca.* 1 ml of trapping material, *i.e.*, 100-μm stainless-steel beads, 30-μm octadecyl-functionalized silica gel (ODS, Hypersil), silica gel 60 (230–400 US mesh) or Florisil (60–100 US mesh, 0.16–0.25 mm). They were eluted with 2 × 1.5 ml of *n*-heptane and 50 μl of internal standard solution (PCBs 35 and 169 at 21.6 and 4.3 ng/μl, respectively) were added and the final volume adjusted to 1.8 ml with *n*-heptane, giving internal standard concentrations of *ca.* 600 pg/μl for PCB 35 and *ca.* 120 pg/μl for PCB 169.

Sewage sludge extractions were made as follows: 1-g portions of sewage sludge were mixed with 9 g of anhydrous Na_2SO_4 and packed into 7-ml extraction cells. Extractions were performed as for the spiked samples using pure CO_2 and a trap temperature of 20°C. The traps were eluted with 2 × 1.5 ml of *n*-heptane, then 1 × 1.5 ml of methanol, followed by 2 × 1.5 ml of *n*-heptane. After extraction, the final volume was adjusted to 1.8 ml with *n*-heptane.

2.3. Dual-column gas chromatography

The extracts were analysed using a pressure-controlled Hewlett-Packard (HP) Model 5890 II gas chromatograph equipped with two ^{63}Ni electron-capture detectors and an HP Model 7673A autosampler. Aliquots (1 μl) of the extracts were injected on-column into two parallel-coupled columns, a 60 m × 0.25 mm I.D. 50% diphenyl–dimethylsiloxane DB-17 (0.25 μm) column (J&W Scientific) and a series combination of a 25 m × 0.25 mm I.D. 5% diphenyl–dimethylsiloxane SIL-8 column (0.25 μm) (Chrompack) and a 25 m × 0.22 mm I.D. 1,7-dicarba-*closo*-dodecarborane dimethylpolysiloxane HT-5 (0.10 μm) column (Scientific Glass Engineering). The columns were installed in the GC oven together with a 2 m × 0.53 mm I.D. fused-silica retention gap using a quick-seal glass T. The GC column oven programme was as follows: initial temperature 90°C, held for 2 min,

then increased at 20°C/min to 170°C, held for 7.5 min, then increased at 3°C/min to 280°C, which was held for 10 min. The hydrogen flow-rate was 43.5 cm/s, held constant by the pressure-controlled inlet throughout the whole temperature programme. This choice of columns and GC conditions has been shown to give optimum separations of PCB congeners [11,12].

2.4. Soxhlet extraction

Aliquots of 1 g of certified sewage sludge were mixed with 9 g of anhydrous Na_2SO_4 and extracted with *n*-hexane–acetone (1:1) for 18 h. The extracts were loaded on a 15 cm × 6 mm I.D. column with activated silica impregnated with 40% (w/w) concentrated sulphuric acid and eluted with 50 ml of *n*-hexane. The extracts were evaporated to dryness and the residues were dissolved in 1.8 ml of iso-octane.

3. Results and discussion

3.1. Performance of the different trap sorbents with various modifier concentrations and trapping temperatures

The importance of the trapping temperature in relation to the modifier concentration has been studied recently by Mulcahey and co-workers [5,7]. Using a broad range of chemical compounds representing various degrees of volatility and polarity, they came to the conclusion that with pure CO_2 as the supercritical fluid, the trapping efficiency is almost unaffected by the trapping temperature. However, with increasing concentrations of methanol as modifier in the supercritical fluid CO_2, the trapping needs to be optimized for a sufficient trapping efficiency. For PCBs, little work has been published on the trapping efficiency as a function of the trapping conditions [5,8,10]. It was therefore decided to investigate the performance of different trap sorbents with various modifier concentrations and trap temperatures. To focus on the trapping mechanism, this study was undertaken with spiked Na_2SO_4, which does not pose any difficulties in the extraction of PCBs [10]. The trapping was carried out below or at the boiling point of the modifier. The results are given for the different trap sorbents in Tables 1–4.

It is evident that with pure CO_2 as the supercritical fluid all trapping materials provide quantitative trapping efficiencies.

When methanol or ethanol is added at a level of 2%, only Florisil and ODS give *ca.* 100% recoveries at the two trapping temperatures for all twelve PCB congeners. Silica has problems with the lower chlorinated PCBs. Stainless-steel works unsatisfactorily below the boiling point of the modifier for all twelve PCB congeners and has problems with lower chlorinated PCBs when the trapping is carried out at the boiling point of the modifier.

When the modifier concentration is increased to 5%, none of the trap sorbents produce satisfactory results at temperatures below the boiling point of the modifier. The mean recoveries are in the range 18–34% and for lower chlorinated PCBs as low as 2%. At this combination of high modifier concentration and low trapping temperature, liquid methanol is formed in the trap during the expansion of the supercritical CO_2, which mechanically rinses (elutes) the trapped PCBs into the waste bottle [5,7]. Residues of liquid methanol are even seen in the final extract after elution with *n*-heptane. The formation of liquid methanol is avoided when the trapping temperature is raised to the boiling point of the modifier. However, this may lead to the loss of the lower chlorinated PCBs, which are more volatile, as is clearly seen for silica and stainless steel. Only ODS and florisil produce quantitative trapping efficiencies at a 5% modifier concentration. Whether this is attributable to chemical interactions between the Florisil and ODS sorbents and the PCBs or to the mechanical properties of the sorbent surface remains unclear.

3.2. Performance of the different trap sorbents in SFE of sewage sludge

For the realistic evaluation of the solid-phase trapping of PCBs in SFE, a complicated matrix, contaminated at trace levels, was chosen. BCR

Table 1
SFE recovery of spiked samples on an ODS trap

PCB	CO_2 (20°C)		CO_2 + 2% MeOH				CO_2 + 5% MeOH				CO_2 + 2% EtOH			
			20°C		65°C		20°C		65°C		20°C		78°C	
	Recovery (%)	S.D. (%)	Recovery (%)	S.D. (%)	Recovery (%)	S.D. (%)	Recovery (%)	S.D. (%)	Recovery (%)	S.D. (%)	Recovery (%)	S.D. (%)	Recovery (%)	S.D. (%)
28	103	3	81	2	100	1	10	4	94	1	96	5	94	2
52	101	1	86	4	102	2	15	5	99	1	91	4	99	3
101	100	1	91	4	100	1	19	5	100	2	94	3	100	4
105	100	1	94	4	103	1	16	5	100	1	95	1	96	3
118	99	1	93	4	100	1	19	5	99	1	97	1	97	2
128	98	1	92	5	100	1	18	5	100	1	89	6	99	2
138	100	1	91	5	101	1	19	5	101	2	94	2	100	3
149	100	1	92	5	101	2	20	5	100	1	91	5	100	3
153	99	1	92	5	100	1	22	5	100	1	96	2	101	4
156	99	1	94	5	102	1	20	5	99	1	101	2	99	4
170	98	1	93	5	100	1	21	5	99	1	96	2	100	3
180	98	1	92	6	101	1	22	4	100	1	101	1	101	4
Mean	100	1	91	5	101	1	18	5	99	1	95	3	99	3

S.D. = standard deviation ($n = 4$).

Table 2
SFE recovery of spiked samples on a Florisil trap

PCB	CO_2 (20°C)[a]		CO_2 + 2% MeOH				CO_2 + 5% MeOH				CO_2 + 2% EtOH			
			20°C[a]		65°C[a]		20°C[a]		65°C		20°C		78°C	
	Recovery (%)	S.D. (%)	Recovery (%)	S.D. (%)	Recovery (%)	S.D. (%)	Recovery (%)	S.D. (%)	Recovery (%)	S.D. (%)	Recovery (%)	S.D. (%)	Recovery (%)	S.D. (%)
28	98	3	108	3	115	4	31	13	106	2	100	30	93	5
52	96	5	103	3	111	3	34	13	102	1	100	25	96	4
101	96	6	101	3	109	3	35	12	101	3	95	14	97	3
105	97	4	104	3	112	4	33	12	104	3	94	9	94	3
118	97	5	100	3	107	3	34	12	101	4	93	9	96	4
128	96	5	107	4	116	4	34	13	100	5	92	8	92	4
138	96	5	100	3	108	4	34	11	101	3	93	6	98	4
149	96	6	101	3	107	3	35	12	101	4	94	8	97	3
153	97	5	100	3	107	3	36	11	101	3	93	8	98	4
156	97	4	99	3	108	4	34	11	101	3	92	7	96	4
170	96	6	102	3	111	4	36	11	101	5	92	7	98	5
180	97	5	100	3	108	4	35	11	100	4	92	7	97	3
Mean	97	5	102	3	110	4	34	12	102	3	94	12	96	4

S.D. = standard deviation ($n = 4$).
[a] Calculated without the use of internal standard.

Table 3
SFE recovery of spiked samples on a silica trap

PCB	CO_2 (20°C)		CO_2 + 2% MeOH				CO_2 + 5% MeOH				CO_2 + 2% EtOH			
			20°C		65°C		20°C		65°C		20°C		78°C	
	Recovery (%)	S.D. (%)	Recovery (%)	S.D. (%)	Recovery (%)	S.D. (%)	Recovery (%)	S.D. (%)	Recovery (%)	S.D. (%)	Recovery (%)	S.D. (%)	Recovery (%)	S.D. (%)
28	104	1	83	6	76	3	7	5	21	9	73	8	77	1
52	103	1	82	5	83	3	9	7	35	6	82	5	91	2
101	101	1	93	3	92	2	14	9	63	3	90	2	97	1
105	101	1	100	1	98	1	14	9	64	6	92	5	93	3
118	102	1	100	1	96	1	18	11	67	5	91	3	94	1
128	101	1	96	1	95	1	14	9	68	6	93	3	100	1
138	101	2	96	2	93	2	18	11	70	5	94	3	101	1
149	101	1	93	3	91	2	16	10	72	6	94	1	103	1
153	101	1	97	1	93	1	24	13	72	4	94	1	102	1
156	101	2	102	2	98	1	25	13	71	4	96	5	98	1
170	101	1	99	1	94	1	27	12	72	5	95	2	103	1
180	102	1	100	2	94	1	32	14	74	3	97	3	103	1
Mean	102	1	95	2	92	2	18	10	62	5	91	3	97	1

S.D. = standard deviation ($n = 4$).

Table 4
SFE recovery of spiked samples on stainless steel trap

PCB	CO_2 (20°C)		CO_2 + 2% MeOH				CO_2 + 5% MeOH				CO_2 + 2% EtOH			
			20°C		65°C		20°C		65°C		20°C		78°C	
	Recovery (%)	S.D. (%)	Recovery (%)	S.D. (%)	Recovery (%)	S.D. (%)	Recovery (%)	S.D. (%)	Recovery (%)	S.D. (%)	Recovery (%)	S.D. (%)	Recovery (%)	S.D. (%)
28	101	4	35	8	28	4	2	3	7	2	68	25	38	8
52	99	2	40	7	60	5	7	4	29	6	77	23	66	12
101	97	3	40	7	92	1	20	14	80	18	77	23	82	14
105	94	5	38	8	98	2	24	17	91	9	70	24	79	14
118	95	4	40	8	98	3	26	18	92	12	74	24	81	15
128	95	4	38	8	93	3	26	18	95	8	75	24	87	14
138	94	4	38	8	91	2	27	18	94	8	76	23	87	15
149	96	3	40	7	90	1	28	18	92	10	78	21	88	14
153	95	3	40	7	92	2	28	18	94	9	77	22	87	14
156	96	4	40	8	98	1	27	17	97	8	74	25	88	16
170	94	3	39	7	92	2	30	16	97	7	78	23	91	13
180	94	3	39	8	93	1	29	17	96	6	77	23	91	14
Mean	96	4	39	8	85	2	23	15	80	9	75	23	80	14

S.D. = standard deviation ($n = 4$).

certified sewage sludge (CRM 392) has previously been demonstrated to pose problems in the extraction phase [14]. This material contains PCBs at ppb levels (Table 5) and a broad range of interfering compounds such as lipids, surfactants and mineral oil.

David *et al.* [15] have recently demonstrated the potential of SFE (under mild conditions) for the simultaneous extraction and clean-up of PCBs in sewage sludge using ODS traps. In order to extend the scope of this anlysis, extractions were performed on all four sorbents used above. Chromatograms (SIL-8–HT-5) for eluates after SFE of sewage sludge with trapping on (A) silica and (B) Florisil are compared with (C) the cleaned-up Soxhlet extract in Fig. 1. All possible interfering compounds are marked with asterisks. It is evident that Florisil produces eluates (extracts) with less interference from matrix components in the sludge than silica. The stainless-steel traps produced eluates comparable to silica (data not shown), and it can be concluded that these two trapping materials are unsuitable for the direct analysis of sewage sludge SFE eluates. Compared with the cleaned-up Soxhlet extract, the Florisil eluate still contains some non-PCB components. However, any potential interference is separated by dual-column GC from the target PCBs. The ODS eluates were comparable to those with Florisil (data not shown).

In Table 5, the SFE recovery of endogenous PCBs from sewage sludge is compared with that given by Soxhlet extraction. The results were obtained by comparing peak heights on SIL-8–HT-5 and controlled by comparing peak heights on DB-17. The recoveries by Soxhlet extraction were normalized to 100%. It appears from Table 5 that SFE produces PCB recoveries as high as Soxhlet extraction. No significant difference is observed between the mean results and the mean standard deviation is of the order of 3–5%. No

Table 5
SFE Recovery of PCBs from sewage sludge compared with Soxhlet extraction

PCB	Florisil[a]		ODS[a]		Soxhlet[b]		Certified value[c]	
	Recovery (%)	S.D. (%)	Recovery (%)	S.D. (%)	Recovery (%)	S.D. (%)	Concentration (ng/g)	S.D. (ng/g)
28	120	26	100	4	100	5	100	20
52	112	12	105	2	100	4	78	16
101	98	3	100	3	100	3	134	21
105	100	4	101	4	100	3	–	–
118	97	2	100	4	100	4	97	21
128	101	2	106	2	100	5	–	–
138	100	2	104	3	100	4	[d]	–
149	100	2	102	1	100	3	–	–
153	99	1	103	3	100	5	288	36
156	100	3	103	3	100	2	–	–
170	106	2	108	2	100	5	–	–
174	101	3	103	2	100	3	–	–
180	101	1	104	4	100	4	313	49
194	112	5	109	3	100	4	–	–
199	105	3	107	3	100	3	–	–
Mean	103	5	104	3	100	4		

Samples extracted for 18 h in hexane–acetone (1:1). All mean values in Soxhlet set to 100%.
[a] Mean values of 3 replicates.
[b] Standard deviation of mean values of 3 replicates.
[c] Values not indicated are in the range 10–300 ng/g.
[d] Certified value for PCB 138 withdrawn because of a *ca.* 30% interference from PCB 163 [13].

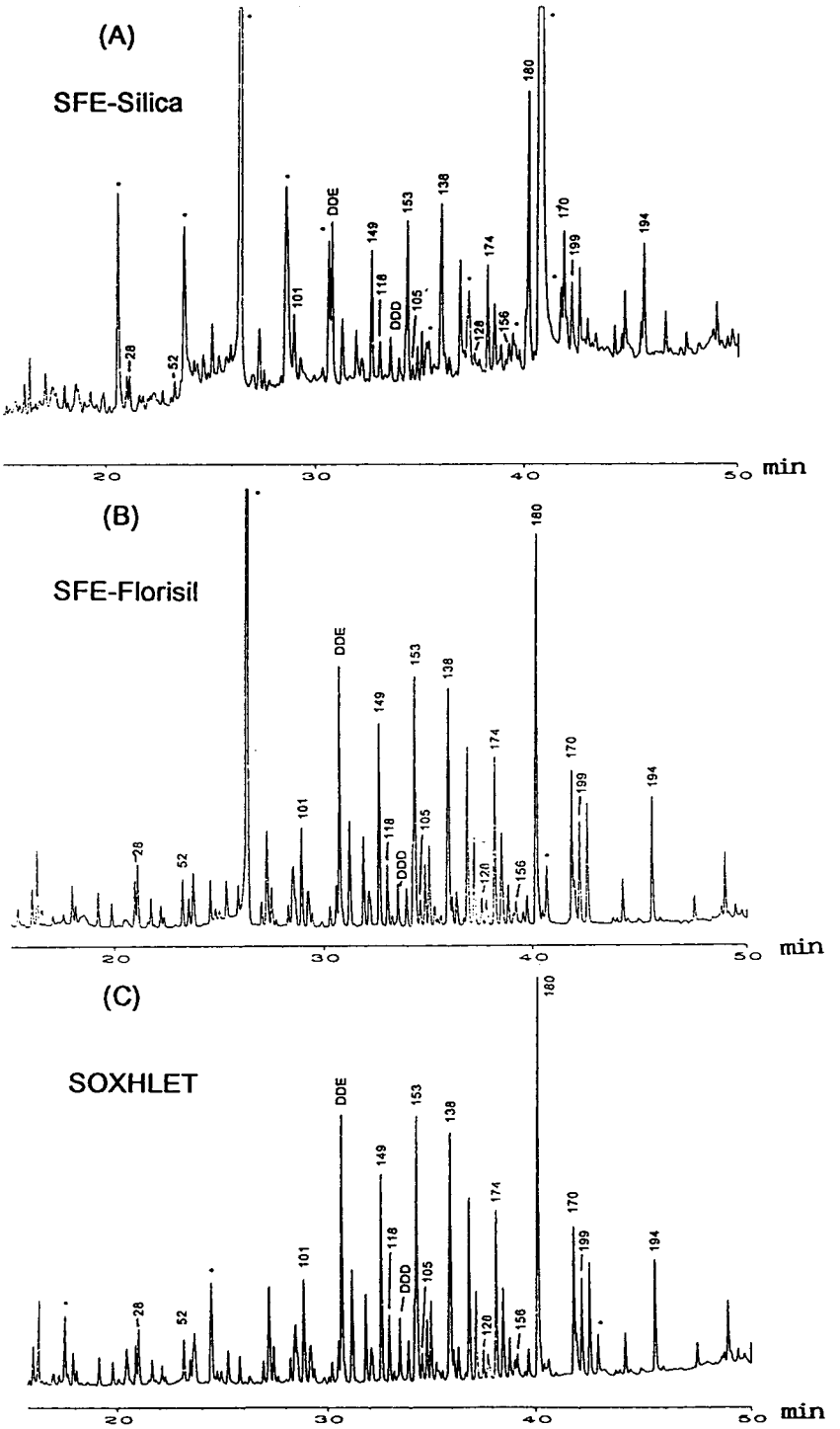

Fig. 1. GC–ECD (SIL-8–HT-5) of (A) raw extract from SFE with silica, (B) raw extract from SFE with Florisil and (C) cleaned-up extract from Soxhlet extraction.

difference is observed for mean recoveries between the two trapping materials Florisil and ODS in SFE. Only PCBs 28 and 52 gave slightly higher results for Florisil (112–120%). This was due to a single high result, probably caused by a dirty GC injection port. If this result is disregarded, the recovery of PCBs 28 and 52 on Florisil is decreased to 100–105%.

Continued extraction of the sewage sludge for longer periods (1 h) or sequential extraction with 2–5% methanol as modifier did not alter the results. In fact, only interfering matrix compounds were found in the later fractions after sequential extraction (data not shown).

4. Conclusions

By choosing the appropriate extraction conditions, trap material, trap temperature and eluent, it is possible on a routine basis to perform interference-free congener-specific analysis of PCBs in sewage sludge by off-line SFE and GC with electron-capture detection (ECD). The total analysis time (from the beginning of the extraction to the end of the GC–ECD run) can be shortened to less than 2 h without any manual sample work-up between extraction and GC analysis.

For the SFE of PCBs in sewage sludge using *n*-heptane as trap eluent, it is only possible to use either Florisil or ODS (of the four sorbents tested) if a clean PCB extract is necessary. Concerning the SFE of PCBs with the help of modified CO_2 (MeOH and EtOH), less than 2% of modified should be used, preferably at a trap temperature above the boiling point of the modifier. Of the four sorbents tested, stainless steel can only be used in special cases (pure CO_2 or extraction of high-boiling PCBs with <2% of modifier). Only Florisil and ODS were able to perform satisfactorily using 5% of methanol as modifier, and then only with a trap temperature at the boiling point of methanol (65°C). Given the purity of the PCB extracts from a real sewage sludge sample, Florisil and ODS must be the sorbents of choice among the four tested, at these permit the reproducible use of modifiers. If the cost of the sorbents is taken into consideration, Florisil is the better choice, as its price is less than 10% of that of ODS.

5. Acknowledgements

The authors are grateful to Hewlett-Packard Italiana (Milan, Italy) for making the HP 7680A SFE extractor available. The technical assistance of Mr. M.S. Rahman is gratefully acknowledged.

6. References

[1] J.W. King, *J. Chromatogr. Sci.*, 17 (1989) 355.
[2] S.B. Hawthorne, *Anal. Chem.*, 62 (1990) 633A.
[3] J.L. Snyder, R.L. Grob, M.E. McNally and T.S. Oostdyk, *Anal. Chem.*, 64 (1992) 1940.
[4] J.J. Langenfeld, M.D. Burford, S.B. Hawthorne and D.J. Miller, *J. Chromatogr.*, 594 (1992) 297.
[5] L.J. Mulcahey, J.L. Hedrick and L.T. Taylor, *Anal. Chem.*, 63 (1991) 2225.
[6] M.H. Liu, S. Kapila, A.F. Yanders, T.E. Clevenger and A.A. Elseewi, *Chemosphere*, 23 (1991) 1085.
[7] L.J. Mulcahey and L.T. Taylor, *Anal. Chem.*, 64 (1992) 2352.
[8] M.M. Schantz and S.N. Chesler, *J. Chromatogr.*, 363 (1986) 397.,
[9] A.L. Howard and L.T. Taylor, *J. High Resolut. Chromatogr.*, 16 (1993) 39.
[10] S. Bøwadt, F. Pelusio, L. Montanarella and B.R. Larsen, *J. Trace Microprobe Tech. Lett.*, 11 (1993) 117.
[11] M.S. Rahman, S. Bøwadt and B.R. Larsen, Presented at the *International Symposium on Capillary Chromatography, Riva del Garda, May 24–28, 1993.*
[12] S. Bøwadt, H. Skejø-Andresen, L. Montanarella and B. Larsen, *Int. J. Environ. Anal. Chem.*, in press.
[13] B.R. Larsen and J. Riego, *Int. J. Environ. Anal. Chem.*, 40 (1990) 59.
[14] G.M.T. Tuinstra, *Determination of Selected Chlorobiphenyl Congeners in a Standard Mixture, a Cleaned Sludge Extract, a BCR Reference Material of Sludge and a BCR Candidate Reference Material of Mussel Tissue*, RIKILT, Wageningen, 1986.
[15] F. David, M. Verschuere and P. Sandra, *Fresenius' J. Anal. Chem.*, 344 (1992) 479.

ELSEVIER

Journal of Chromatography A, 662 (1994) 434–436

JOURNAL OF CHROMATOGRAPHY A

Short Communication

pH-Independent determination of aluminium as a cationic complex using capillary electrophoresis

K. Bächmann *, Th. Ehmann, I. Haumann

Fachbereich Chemie der Technischen Hochschule Darmstadt, Hochschulstrasse 10, D-64289 Darmstadt, Germany

(First received June 30th, 1993; revised manuscript received November 2nd, 1993)

Abstract

The determination of aluminium as complex with desferrioxamine in presence of alkali and alkaline earth ions using indirect UV detection is shown. Desferrioxamine added to the analyte allows the pH-independent cationic determination of aluminium between pH 2 and 10 although the original aluminium is anionic.

1. Introduction

Aluminium has recently been recognised as a causative agent for dialysis encephalopathy and renal osteodystrophy [1,2]. This has led to the development of various analytical methods for the determination of aluminium such as graphite furnace atomic absorption spectroscopy (AAS) [3–7] or high-performance liquid chromatography (HPLC) [8]. In a recent work [9] aluminium was measured as a fluoro complex by using capillary electrophoresis (CE). In CE the detection is limited to a narrow pH range because the ionic form of aluminium strongly varies with the pH of the sample as shown in Fig. 1. Consequently the pH value of the sample has to be known. That means a greater volume of sample is needed to measure the pH so that the advantage of small samples is lost. In addition the introduction of an acidified sample is restricted on hydrostatic injection.

In aluminium-intoxicated haemodialysis desferrioxamine (DFO; 1-amino-6,17-dihydroxy-7,10,18,21-tetraoxo-27-(N-acetylhydroxyamino)-6,11,17,22-tetraazaheptaeicosane; Fig. 2) is used in chelation therapy [2,10]. Under the assumption that human serum can be seen as an aqueous system DFO was examined as a chelating agent in CE. According to Schwarzenbach and

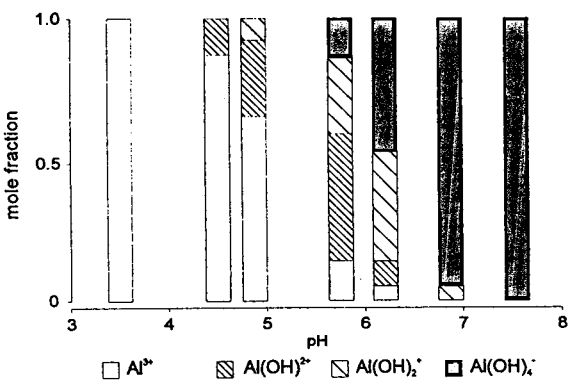

Fig. 1. Molecular forms of soluble aluminium hydroxide at different pH values. Redrawn from ref. 10.

* Corresponding author.

0021-9673/94/$07.00
SSDI 0021-9673(93)E0005-F

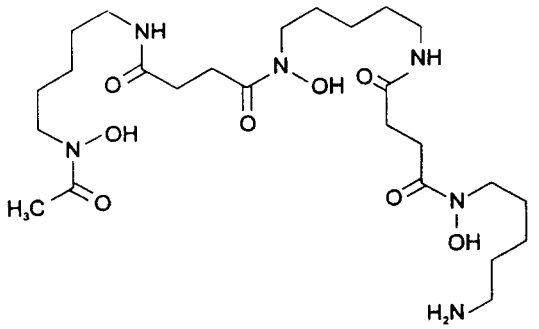

Fig. 2. Structural formula of desferrioxamine.

Schwarzenbach [11] DFO has four acidic protons, three from the hydroxamic acid group and one from the protonated terminal amino group —short formula $[H_4\text{–DFO}]^+$. It shows the following reaction

$$H_4\text{–DFO}^+ + Fe^{3+} \rightarrow 3H^+ + Fe[H\text{–DFO}]^+$$

The complex $Fe[H\text{–DFO}]^+$ is aprotic between pH 2 and 10. The analogous complex is assumed for aluminium.

2. Experimental

The capillary zone electrophoresis system has been described elsewhere [12] with the exception of the UV detector (Dionex, Sunnyvale, CA, USA). All solutions, electrolytes and standards were prepared using water purified with a Milli-Q system (Millipore, Eschborn, Germany). DFO was obtained from Ciba-Geigy (Wehr, Germany). All other reagents were of analytical-reagent grade from Merck (Darmstadt, Germany). Stock solutions (10 mmol/l) of each cation were used to prepare the sample solutions. Samples containing DFO were made by adding a stock solution (20 mmol/l DFO) after adjusting the pH with sodium hydroxide solution or hydrochloric acid and diluted to 1 mmol/l DFO. The capillary was rinsed for 5 min with 0.1 mol/l sodium hydroxide solution, water and electrolyte at the start of each day and for 2 min with electrolyte between all electrophoretic separations.

3. Results and discussion

4-Methylaminophenol sulphate (metol) was chosen as background electrolyte for the indirect UV detection of alkali and alkaline earth metal ions. Using this electrolyte aluminium can be determined as cationic Al^{3+} below pH 4. At higher pH values aluminium changes its ionic form and cannot be observed in an electrophoretic cation separation (Fig. 1). Although citric acid, hydroxyisobutyric acid and tartaric acid are useful complexing agents aluminium complexes of these agents could not be detected under the given CE conditions. The addition of DFO to the analyte allows the pH-independent cationic determination of aluminium between pH 2 and 10. DFO is an unsuitable additive for the electrolyte because it absorbs in the chosen range of UV and interacts with the fused-silica capillary wall. Because of the complex between aluminium and DFO has a higher absorbance than the background electrolyte $Al[H\text{–DFO}]^+$ was detected as a positive peak in simultaneous determination with other ions. DFO builds very stable complexes with Fe^{3+} but under the described experimental conditions a 100 μmol/l Fe^{3+} standard solution shows no peak as free ion as well as complex bound with DFO. Fluoride —also a well complexing agent for aluminium— was added in several concentrations between 10 μmol/l and 1 mmol/l before the addition of DFO. The formation of the Al–DFO complex was not disturbed.

The ionic mobility of the background electrolyte coion lies between those of the high-mobile alkali and alkaline earth and the low-mobile DFO–aluminium complex so that the peak symmetry is sufficient for all ions analysed in this study.

A representative collection of electropherograms (Fig. 3) shows the behaviour of peaks at different values of sample pH. In all measurements the pH value of the electrolyte was 5. The sample solution has a pH value of 4. In order to obtain a pH lower than in the standard solution hydrochloric acid was used. Furthermore a sodium hydroxide solution was added to raise the pH value. Therefore the peak area of sodium in Fig.

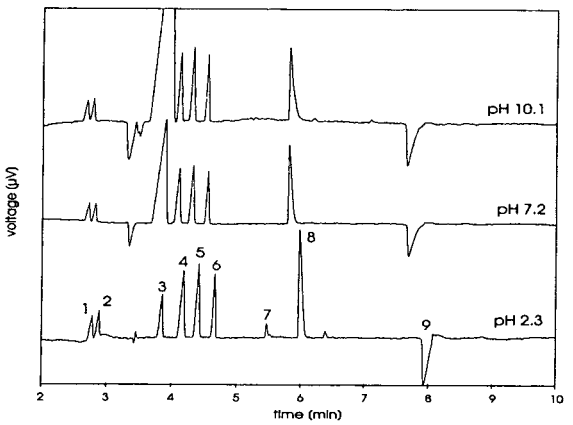

Fig. 3. Electropherograms of alkali, alkaline earth metal and aluminium ions at different sample pH values. Electrolyte 4 m*M* metol; fused-silica capillary 60 cm × 75 µm I.D.; voltage 30 kV; hydrostatic sample introduction (10 cm, 30 s). Peaks: 1 = caesium; 2 = potassium; 3 = sodium; 4 = calcium; 5 = magnesium; 6 = lithium; 7 = aluminium (Al^{3+}); 8 = cerium; 9 = aluminium ($Al[H–DFO]^+$); (each 100 µmol/l).

3 increases with increasing pH. At pH 2 a peak additional to the $Al[H–DFO]^+$ signal can be detected at the migration time of Al^{3+} in a system without DFO. At the increase of pH only the aluminium complex was detected. Reported complexation between DFO and calcium or magnesium [13] were not observed under CE conditions. The peak area of the aluminium complex shows pH independence in a range of pH 2 and 10 as shown in Fig. 4. Each data point

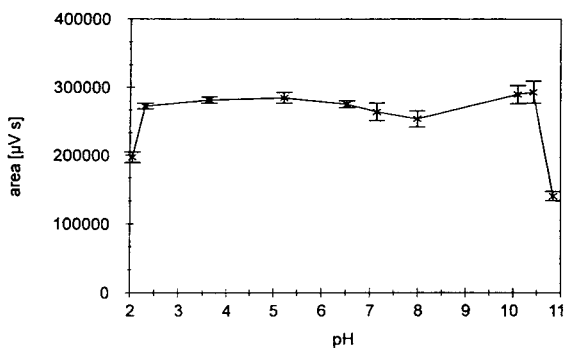

Fig. 4. Plot of the peak area of the desferrioxamine–aluminium complex (corresponding to 100 µmol/l Al^{3+}) *vs.* different values of sample pH.

in Fig. 4 is the mean value of five measurements with hydrostatic injection (10 cm, 30 s) of a 100 µmol/l Al standard solution. The relative standard deviation lies ranges between 0.02 and 0.05%. The precision of migration time amounts to 97.9%. The sample could be injected hydrostatically and electrokinetically. The peak areas show a linear dependence on concentration with coefficients of correlation of $r^2 = 0.994$ for electrokinetic injection (from 1 to 50 µmol/l) and $r^2 = 0.998$ for hydrostatic injection (from 25 to 500 µmol/l).

The measurement of aluminium with other complexing agents, as well as with DFO, limits of detection and determination in human serum will be reported in a following, more detailed publication.

4. References

[1] M.R. Wills and J. Savory, *Lancet*, ii (1983) 29.
[2] W.K. Stewart, in R. Massey and D. Taylor (Editors), *Aluminium in Food and the Environment*, Royal Society of Chemistry, London, 1988, pp. 6–19.
[3] F.R. Alderman and H.J. Gitelman, *Clin. Chem.*, 26 (1980) 258.
[4] F.Y. Leung and A.R. Henderson, *Clin. Chem.*, 28 (1982) 2139.
[5] S. Brown, R. Bertholf, M.R. Wills and J. Savory, *Clin. Chem.*, 30 (1984) 1216.
[6] P.E. Gardiner, M. Stoeppler and H.W. Nurnberg, *Analyst*, 110 (1985) 611.
[7] C.D. Hewitt, K. Winborne, D. Margrey, J.R.P. Nicholson, M.G. Savory, J. Savory and M.R. Wills, *Clin. Chem.*, 36 (1990) 1466.
[8] E. Kaneko, H. Hoshino, T. Yotsuyanagi, N. Gunji, M. Sato, T. Kikuta and M. Yuasa, *Anal. Chem.*, 63 (1991) 2219.
[9] N. Wu, W.J. Horvath, P. Sun and C.W. Huie, *J. Chromatogr.*, 635 (1993) 307.
[10] R.L. Bertholf, J. Savory, M.R. Wills, *Trace Elem. Med.*, 3 (1986) 157.
[11] G. Schwarzenbach and K. Schwarzenbach, *Helv. Chim. Acta*, 46 (1963) 1390.
[12] K. Bächmann, J. Boden and I. Haumann, *J. Chromatogr.*, 626 (1992) 259.
[13] G. Anderegg, F. l'Eplattenier and G. Schwarzenbach, *Helv. Chim. Acta*, 46 (1963) 1400.

Journal of Chromatography, 662 (1994) 437
Elsevier Science Publishers B.V., Amsterdam

CHROM. 25 735

Book Review

Capillary electrophoresis technology (*Chromatographic Science Series*, Vol. 64), by N.A. Guzman, Marcel Dekker, New York, 1993, 880 pp., price US$165.00, ISBN 0-8247-9042-1.

What is especially impressive about this book is that it contains chapters by many of the leaders in this field. The book both teaches the fundamentals and reviews recent advances. Thus the book is comprehensive, covering instrumentation, conditions and applications. Each of the following topics, for example, is given a chapter: micellar electrokinetic chromatography, buffers, organic solvents, coated capillaries (there are five chapters on this topic), external electric fields (to control electrosmotic flow), mass spectrometry, micro-preparation, laser detection, chiral separation, drugs, body fluids and cyclodextrins. Since all the chapters were written independently there is some overlap and repetition. This shortcoming is offset by the extra learning that comes from hearing a given story from different perspectives. Unfortunately the usefulness of the book is compromised by an incomplete subject index. Many topics in the text, or some of their page locations, are not cited in the index.

Boston, MA (USA) Roger W. Giese

Author Index

Erratum

J. Chromatogr. A, Vol. 658, pp. 149–171

On page 153, eqn. 20 should read

$$\left| \int_{t_R}^{t_{R,0}+t_R} C \, dt \right| = \frac{n}{F_v} \qquad (20)$$

J. Chromatogr. A, Vol. 658, pp. 292–313

On page 293, left column, the last line should read:
"supercritical fluids. However, deeper investiga- ".

On page 294, Table I, first column, under "Supercritical fluid":
a white line should be inserted between "T_c, P_c" and "T_c, $4P_c$".

Vol. 662, No. 2

Journal of Chromatography A

NEWS SECTION

ANNOUNCEMENTS

ANATECH 94, 4th INTERNATIONAL SYMPOSIUM ON ANALYTICAL TECHNIQUES FOR INDUSTRIAL PROCESS CONTROL, MANDELIEU LA NAPOULE, FRANCE, 10–13 APRIL, 1994

The capability of a plant to produce efficiently and effectively finished products which meet guaranteed specifications depends on a complex sequence of activities. Each step of the process can have an impact on the success of the operation. It is therefore important that the appropriate tools for managing product quality be available on an integrated basis, with the emphasis on increasing safety, productivity and complying with stringent environment constraints.

Complementing the techniques currently in use in process analytical chemistry, numerous techniques for *in-situ* real-time analysis are emerging in the academic and industrial worlds and enable full advantage to be taken of advanced control.

This symposium is aimed at an interdisciplinary audience of analytical chemists, process and process control engineers with an academic background and will focus on the latest developments in process analytical chemistry.

Authors are requested to submit two copies of abstracts in English.

Papers presented at the conference will be reviewed for publication in a special edition of *Process Control and Quality*.

The official language of the conference will be English.

An exhibition will be arranged in conjunction with the conference. For further details, contact: ANATECH 94 Secretariat, Elsevier Advanced Technology, Mayfield House, 256 Banbury Road, Oxford OX2 7DH, UK. Tel.: (+44 865) 512-242; Fax: (+4 865) 310-981

HPLC '94, 18th INTERNATIONAL SYMPOSIUM ON COLUMN LIQUID CHROMATOGRAPHY, MINNEAPOLIS, MN, USA, 8–13 MAY, 1994

The program will attempt to maintain parallel sessions on fundamental and theoretical aspects of chromatography; applications and automation of chromatography and ancillary techniques; and focus topics such as specific detector technology.

Areas of particular focus for HPLC'94 will include:

- preparative chromatography;
- new advances/characterization in packing materials;
- advances in robotics, automation, and sample preparation;
- advances in separations of biomolecules;

- new detection technologies;
- physicochemical measurements using chromatography; and
- mobile phase modifiers for capillary zone electrophoresis.

All presentations will be displayed as posters to ensure interactions between speakers and attendees. In addition to traditional plenary, symposia, and discussion sessions, HPLC'94 will offer workshops prior to the official opening of the meeting. Topics under development include HPLC methods development, chiral separations, capillary zone electrophoresis, preparative chromatography, and HPLC–CZE–MS.

Papers accepted for lectures or posters at the symposium will be peer-reviewed and published as a special issue of *Journal of Chromatography*. Manuscripts must be delivered to the editor at the symposium.

All registrants will receive a copy of this issue as part of their registration fee.

Please direct any inquiries about HPLC'94 to the Symposium/Exhibit Manager: Mrs. Janet Cunningham, HPLC'94, c/o Barr Enterprises, P.O. Box 279, Walkersville, MD 21793, USA. Tel.: (+1 301) 898-3772; Fax: (+1 301) 898-5596

5th EUROPEAN MEETING ON BIO-CHROMATOGRAPHY AND BIO-ENGINEERING, NANCY, FRANCE, 17–19 MAY, 1994

This meeting, organized by the European Society for Bio-Chromatography (ESBS) will give the opportunity for scientists to exchange information and experience and to discuss new prospects for research. The scientific program will include plenary lectures, short communications and poster sessions focused on the following topics:

- Bio-chromatography: new supports; interactions (hydrophobic, ionic, affinity ...); proteins at the interfaces; purifications.
- Applications: production of molecules with biological, medical or therapeutic interest; extraction from natural media; purification of recombinant proteins.
- Evaluation of chromatography processes and products: regulation aspects; inactivation procedures (viruses or other agents); validation.
- Miscellaneous.

The 5th Meeting of the ESBC will also include, on 18 May, a Satellite Meeting which aims to reflect the most recent progress in the field of *in-vivo* plasma treatment using chromatographic techniques.

For further information contact: ESBC 94, LCPM-ENSIC, BP 451, 54001 Nancy Cedex, France. Tel.: (+33-83) 175 221; Fax: (+33-83) 379 977.

7th INTERNATIONAL SYMPOSIUM ON POLYMER ANALYSIS AND CHARACTERIZATION (ISPAC-7), LES DIABLERETS, SWITZERLAND, 23–25 MAY, 1994

ISPAC-7 will consist of poster sessions, invited lectures, and round-table discussions and information exchange on recent advances in polymer charcterization approaches, techniques, and applications.

ISPAC-7 will focus on molecular characterization in relationship to properties of polymeric systems. Topics will include: aqueous polymeric systems (water-soluble polymers, interacting systems, and physical and chemical gels) and heterogeneous polymeric materials (blends, composites, and multilayered materials). In addition, an introductory course on polyelectrolytes and the characterization of water-soluble polymers will be held on Sunday, May 22, preceding the Symposium.

Further information and regiatration forms may be obtained from ISPAC Registration, 815 Don Gaspar Drive, Sante Fe, NM 87501, USA. Tel.: (+1-505) 989 4735; Fax: (+1-505) 989 1073, or from Dr M. Rinaudo, CERMAV-CNRS, B.P. 53X, 38041 Grenoble Cedex, France. Tel.: (+33-76) 541 145; Fax: (+33-76) 547 203.

3rd SYMPOSIUM ON MOLECULAR CHIRALITY, KYOTO, JAPAN, 24–27 MAY, 1994

Attention will be directed to recent developments in molecular chirality. All fundamental aspects and new applications, including the following will be dealt with:

- generation of molecular chirality;
- chiral discrimination and chiral separation;
- crystal, surface and interfacial chirality;
- functions of chiral compounds in chemistry;
- dynamic aspects of chiral compounds in bio-sys-

tems;
- drug metabolism, pharmaco-kinetics and toxico-kinetics;
- industrial applications of molecular chirality.

Invited plenary and keynote lectures will be presented by internationally recognized scientists. Contributed papers will be presented as oral communications and posters.

A Book of Abstracts of all scientific contributions will be distributed at the meeting. Submitted papers wil be considered for publication in the proceedings, a special issue of the *Journal of Chromatography*.

Travel expenses will be partly provided for participants who submit their papers to the proceedings, on request. The Symposium languages will be English and Japanese.

For further details contact: Prof. Terumichi Nakagawa, Symposium on Molecular Chirality (SMC), Faculty of Pharmaceutical Sciences, Kyoto University, Yoshida-Shimoadachi-cho, Sakyo-ku, 606 Japan. Fax: (+81 48) 471-0310 (Professor Hara).

3rd WORLD CONGRESS ON BIOSENSORS, NEW ORLEANS, LA, USA, 1–3 JUNE, 1994

The World Congress on Biosensors serves those interested in research, development, application and commercialisation of biosensors. Scientists from many disciplines can address the use of biosensors in, for example, clinical diagnostics, environmental monitoring, health and safety compliance, the food industry and defence.

Biosensors '94 is a three-day event consisting of plenary sessions on the following:
- commercial development and application of biosensors (highlighting the issues and elucidating recent successes in this inherently applied subject);
- enzyme-based sensors;
- affinity sensors (including receptor-based systems).

Plenary sessions will be followed by selected original papers presented in three parallel oral sessions and a poster display.

Previously unpublished contributions are invited either within the scope of the plenary topics or under the title: Whole cell-based sensors & general aspects of biosensors.

As a new addition to the Congress, there will be a display of commercial equipment.

Authors of accepted abstracts can submit full papers for refereed special editions of the international journal *Biosensors & Bioelectronics*.

For further information contact: Kay Russell, Elsevier Advanced Technology, Mayfield House, 256 Banbury Road, Oxford OX2 7DH, UK. Tel.: (+44 865) 512242; Fax: (+44 865) 310981.

2nd INTERNATIONAL SYMPOSIUM ON HORMONE AND VETERINARY DRUG RESIDUE ANALYSIS, BRUGGE, BELGIUM, 1–3 JUNE, 1994

This symposium will cover the following topics:
- sample pretreatment, extraction and clean-up procedures (SPE, SFE, IAC, gel permeation, etc.) in drug residue analysis;
- analysis of hormone and veterinary drug residues: chromatographic techniques (high-performance liquid chromatography, capillary gas chromatography, thin-layer chromatography, etc.) and their detection by spectroscopic (UV, IR, MS, luminescence, etc.), electrochemical and other methods (FID, ECD, etc.);
- immunoaffinity techniques and immunoassays (RIA, CLIA, ELISA, FIA, dipstick technology, etc.);
- other techniques applied to hormone and veterinary drug residue analysis in biosamples of human and animal origin;
- metabolism, pharmacokinetics and toxicology of these compounds;
- quality control and reference materials;
- stability of residues in food of animal origin;
- legal aspects and control mechanisms regarding residues of veterinary drugs in food;
- problems concerning consumption of meat originating from hormone treated animals with regard to doping analysis.

All papers should be presented in English. The deadline for receipt of abstract is 1 March, 1994.

For further information, contact: Professor C. van Peteghem, Symposium Chairman, Faculty of Pharmaceutical Sciences, University of Ghent, Harelbekestraat 72, B-9000 Ghent, Belgium. Tel.: (+32-9) 2218951, ext. 235; Fax: (+32-9) 2205243.

VIth INTERNATIONAL SYMPOSIUM ON LUMINESCENCE SPECTROMETRY IN BIOMEDICAL ANALYSIS – DETECTION TECHNIQUES AND APPLICATIONS IN CHROMATOGRAPHY AND CAPILLARY ELECTROPHORESIS, BRUGGE, BELGIUM, 5–7 JUNE, 1994

This symposium envisages to report on the current status and future developments in the field of luminescence techniques used in drug quality control, clinical, chemical, biochemical, pharmaceutical, toxicological, food, environmental analyses and in related areas.

Specific topics include: drug and bioanalysis via fluorescence, NIR-fluorescence, laser fluorescence, delayed fluorescence, phosphorescence and bioluminescence and chemiluminescence; chemiluminescence and fluorescence immunoassays; thermochemiluminescence; luminescence detection techniques in chromatography and in CE; chemical derivatization methods; development of fluorigenic reagents; fluorescent particle imaging; development of luminescent systems for macromolecules in biological samples; the use of expert systems in the analysis of luminescence data generated by HPLC; fiber optical sensors in biomedical sciences; biomedical applications of luminescence in micellar and cyclodextrin media; the development of high-resolution luminescence methods; use of fluorescence and chemiluminescence labels and substrates; lanthanide luminescence spectroscopy; the fluorigenic estimation of enzyme activities; the use of 3D fluorescence spectra; the application of computer-aided fluorescence for drugs and metabolites.

Original research papers can be submitted by registered participants to be presented in a general poster session.

A technical exhibition will be held throughout the meeting.

As before, the proceedings will be published by *Analytica Chimica Acta*, while the abstracts will be separately published.

For further information, contact: Professsor Dr. Willy R.G. Baeyens, Symposium Chairman, University of Ghent, Pharmaceutical Institute, Department of Pharmaceutical Analysis, Laboratory of Drug Quality Control, Harelbekestraat 72, B-9000 Ghent, Belgium. Tel.: (+32-9) 2218951; Fax: (+32-9) 2214175.

6th INTERNATIONAL CONFERENCE ON FLOW ANALYSIS, TOLEDO, SPAIN, 8–11 JUNE, 1994

The Conference will basically be concerned with the following flow analysis topics: general aspects, FI-chemometrics, detection systems, separation techniques (on-line sample treatment), sensors and continuous flow techniques, applications (environmental, food, clinical, industrial analysis), and process control (Biotechnology). Two special sessions devoted to "Flow Analysis Nomenclature" and "Foundation of an International Society for Flow Analysis" will be arranged.

The scientific program will consist of invited lectures and oral and poster presentations. There will also be an exhibition of commercially available instrumentation for flow analysis.

The deadline for submission of abstracts is 1 March, 1994.

As with the earlier conferences the papers will be published in a special issue of *Analytica Chimica Acta*.

For further information contact: M. Valcarcel/M.D. Luque de Castro (Flow Analysis VI). Departamento de Química Analítica, Facultad de Ciencias, E-14004 Córdoba, Spain. Tel.: (+34-57) 218616; Fax: (+34-57) 218606.

1994 PREP SYMPOSIUM & EXHIBIT, INTERNATIONAL SYMPOSIUM ON PREPARATIVE CHROMATOGRAPHY, WASHINGTON, DC, USA, 12–15 JUNE, 1994

At the PREP series of symposia, organized and chaired by Professor Georges Guiochon, new advances and applications in the areas of preparative chromatography and related techniques are presented.

The program of invited and contributed lectures, poster presentations, discussion sessions, workshops, and exhibit will interest scientists, engineers, managers and others involved in the practice of using state-of-the-art chromatography processes for economic production.

Papers accepted as lectures or posters will be peer reviewed and published in a special issue of the *Journal of Chromatography*. Manuscripts must be de-

livered to the journal representative at the symposium.

Submissions are invited describing original research or results in the following areas of preparative chromatography, suggestions for additional topics to be covered are welcome.

- applications to drugs and specialty chemicals;
- applications to recombinant and natural proteins to peptides, other biopolymers, etc.;
- applications to chiral separations;
- instrumentation;
- stationary phases;
- optimization of experimental conditions;
- economics of preparative chromatography;
- theory of non-linear chromatography, overloaded elution and displacement chromatography;
- kinetics of mass transfer at high concentrations.

For further details, contact: Mrs Janet Cunningham, PREP Symposium/Exhibit Manager, c/o Barr Enterprises, 10120 Kelly Road, P.O. Box 279, Walkersville, MD 21793, USA. Tel.: (+1 301) 898-3722; Fax: (+1 301) 898-5596.

4th INTERNATIONAL SYMPOSIUM ON FIELD-FLOW FRACTIONATION, LUND, SWEDEN, 13–15 JUNE, 1994

The symposium will provide a forum for exchange of information on the most recent developments in theory an practice of FFF. This separation methodology is applicable to macromolecules, polymers, colloids and micron sized particulates of synthetic, biological, or natural origin. In addition to performing highly size selective separations, the FFF techniques provide the means for characterizing samples with respect to molecular or particle size and size distributions, density, surface, chemical composition and other properties. Applications address solutions, suspensions and emulsions in many areas of scientific and industrial importance, including polymer chemistry, colloid chemistry, biochemistry, biotechnology, pharmaceutics, and environmental studies.

The program will contain invited and contributed papers, oral as well as poster presentations, and discussion sessions. Maximum 100 participants.

For further details, contact: Dr. Agneta Sjögren, The Swedish Chemical Society, Wallingatan 24, 3 tr, S-111 24 Stockholm, Sweden. Fax: (+46-8) 106678.

WORKSHOP ON BIOSENSORS AND BIOLOGICAL TECHNIQUES IN ENVIRONMENTAL ANALYSIS, PARIS, FRANCE, 12–14 SEPTEMBER, 1994

Rapid advances have been observed in the use of biosensors, immunochemical methods and other biological techniques as new tools for environmental analysis. The workshop will be an opportunity for scientists dedicated to analytical environmental chemistry and often working in different areas to discuss together some special topics of common interest, such as:

- immunological techniques (immunoassays, use of immunosorbents for the sample pretreatment – preconcentration and clean-up –, and coupling with chromatographic techniques, immunosensors, antibody production...);
- enzymatic techniques (enzymatic sensors, enzymatic reactors, inhibition...);
- PCR technology, DNA probes;
- biosensors based on plant, animal and human tissue (whole cells, cell organelles...);
- microbial systems;
- bioanalytical detection techniques (receptor based biosensors, use of membrane proteins...);
- other biosensors;
- validation of results.

For further information contact: Professor M-C. Hennion, Ecole Supérieure de Physique et de Chimie Industrielles de la ville de Paris, Laboratoire de Chimie Analytique, 10 rue Vauquelin, 75005 Paris, France.

INTERNATIONAL ION CHROMATOGRAPHY SYMPOSIUM 1994, TURIN, ITALY, 19–22 SEPTEMBER, 1994

The scientific program will consist of the following session topics:

- separation selectivity,
- developments in separation methodology,
- advances in detection,
- special sample treatment procedures,
- novel applications,
- carbohydrate separations,
- process monitoring and control,
- separation of metal ions,

- pharmaceutical applications,
- environmental applications,
- ion analysis in the electrical generating industry, and
- standard methods and data processing.

The proceedings of the symposium will be published in a special issue of the *Journal of Chromatography*.

For furhter information, contact: Janet R. Strimaitis, Century International Inc., P.O. Box 493, 25 Lee Road, Medfield, MA 02052, USA. Tel.: (+1 508) 359-877; Fax: (+1 508) 359-8778.

5th INTERNATIONAL SYMPOSIUM ON CHIRAL DISCRIMINATION, STOCKHOLM, SWEDEN, 26–28 SEPTEMBER, 1994

This symposium is essentially interdisciplinary in character, comprising aspects of chiral discrimination from many scientific disciplines such as chemistry, biochemistry, pharmacology, biology, pharmacy, medicine and analytical chemistry. The aim of the symposium is to highlight the principal features of chiral discrimination of importance in biology, medicine, pharmacy and environmental research. The program will focus on novel aspects of chiral synthesis, new techniques for chiral separations, recent perceptions regarding stereochemistry and biological activity, as well as on any other item of importance for chiral discrimination. International regulatory issues for the development and control of optically active drugs and other biologically active compounds will also be considered.

The oral session will comprise of lectures by invited speakers and submitted lectures on topics of current interest for chiral discrimination. Most papers will be presented as posters, and these sessions will form the central core of the symposium.

New instrumentation, materials, chemicals and literature related to all aspects of chiral discrimination will be on display during the symposium. All interested exhibitors are invited to contact the organizers for further information.

For further details contact: Swedish Academy of Pharmaceutical Sciences, 5th International Symposium on Chiral Discrimination, PO Box 1136, S-111 81 Stockholm, Sweden. Tel.: (+46-8) 245-085; Fax: (+46-8) 205-511.

16th INTERNATIONAL SYMPOSIUM ON CAPILLARY CHROMATOGRAPHY, RIVA DEL GARDA, ITALY, 26–30 SEPTEMBER, 1994

The scientific program will feature the latest developments in

Micro separation techniques

capillary gas chromatography, capillary GC–MS, GC–FTIR and GC–AES, micro-HPLC, supercritrical fluid chromatography, capillary zone electrophoresis, micellar electrokinetic chromatography

New methods and applications in

environmental analysis, pharmaceutical analysis, petroleum and petrochemicals, food and beverages, biochemical separations, organic chemicals, drug testing, flavors and fragrances, proteins and peptides, trace analysis, sample preparation techniques, supercritical fluid extraction, new columns and instrumentation.

The programm will consist of: *review papers* by leading scientists in the field on the latest developments; *invited papers* by young scientists; contributed papers presented in *poster sessions*; plenary and parallel *discussion sessions*; and *workshop seminars* to present the latest developments in commercial instrumentation.

Authors intending to submit papers for the symposium should send a 300-word abstract before March 1, 1994 to the address given below.

For further details contact: Professor Dr. P. Sandra, I.O.P.M.S., Kennedypark 20, B-8500 Kortrijk, Belgium. Tel.: (+32 56) 204-960; Fax: (+32 56) 204-859.

3rd INTERNATIONAL SYMPOSIUM ON SUPERCRITICAL FLUIDS, STRASBOURG, FRANCE, 17–19 OCTOBER, 1994

The programme will comprise plenary lectures (45 min), oral communications (20 min) and poster sessions.

The symposium aims to reflect the most recent progresses in the area of supercritical fluid technology:

- thermodynamics and particularly high pressure equilibria,
- physico-chemical properties,

- processes and technology: extraction, chromatography, reaction, atomization ...,
- applications: food, chemical, pharmaceutical and bio-industry, fossil fuels, new materials...

The Proceedings will be published in advance of the conference and will be delivered to participants on registration.

For further details, contact: I.S.A.S.F., Mle Brionne, ENSIC, B.P. 451, F-54001 Nancy Cedex, France. Tel.: (+33 83) 350 811; Fax: (+33 83) 175 003.

11th MONTREUX SYMPOSIUM ON LIQUID CHROMATOGRAPHY–MASSS SPECTROMETRY (LC–MS; SFC–MS; CE–MS; MS–MS), MONTREUX, SWITZERLAND, 9–11 NOVEMBER, 1994

The symposium on LC–MS, SFC–MS, CE–MS, and MS–MS, dedicated to the late Roland W. Frei, will deal with all areas of this topic including technical developments with on-line aspects, theoretical considerations and applications of the techniques in environmental, clinical and pharmaceutical analysis and other fields.

Subtopics will be introduced by plenary lectures and invited research lectures followed by brief research presentations and posters.

A substantial part of the workshop will be devoted to new strategies in separation science (LC, CE) and sample pretreatment focussed on MS detection.

The symposium will be preceded by a 2-day short course on LC–MS, SFC–MS and CE–MS.

An exhibition will take place during the symposium/short course.

Those interested in giving a research lecture or a poster presentation should send an abstract (preferably in Wordperfect on a floppy disk) of no more than 200 words to the chairman: Professor J. van der Greef, Center for Bio-Pharmaceutical Sciences, P.O. Box 9502, 2300 RA Leiden, The Netherlands. Tel.: (+31-3404)44400, Fax: (+31-3404)57224.

For further details contact: M. Frei-Häusler, Postfach 46, CH-4123 Allschwil 2, Switzerland. Tel.: (+41-61) 4812789; Fax: (+41-61) 4820805.

CALENDAR OF FORTHCOMING EVENTS

10–13 April, 1994
Mandelieu La Napoule, France
ANATECH 94: 4th International Symposium on Analytical Techniques for Industrial Process Control. *Contact:* ANATECH 94 Secretariat, Elsevier Advanced Technology, Mayfield House, 256 Banbury Road, Oxford OX2 7DH, UK. Tel.: (+44-865)512-242; Fax: (+44-865) 310-981.

□ **19–22 April, 1994**
Munich, Germany
Analytica 94: 14th International Trade Fair for Biochemical and Instrumental Analysis, Diagnostics and Laboratory Technology with International Conference. *Contact:* Münchener Messe- und Ausstellungsgesellschaft mbH, Messegelände, D-80325 München, Germany. Tel.: (+49-89) 5107-0; Fax: (+49-89) 5107-506.

8–13 May, 1994
Minneapolis, MN, USA
HPLC '94: 18th International Symposium on Column Liquid Chromatography. *Contact:* Mrs. Janet Cunningham, Barr Enterprises, P.O. Box 279, Walkersville, MD 21793, USA. Tel.: (+1-301) 898-3772; Fax: (+1-301) 898-5596.

16–19 May, 1994
Ottawa, Canada
24th International Symposium of the International Association of Environmental Analytical Chemistry. *Contact:* Dr. M. Malaiyandi, CAEC, Chemistry Department, Carleton University, 1255 Colonel By Drive, Ottawa, Canada, K1S 5B6. Fax: (+1-613) 788-3749; or Dr. J.F. Lawrence, Food Research Division, Banting Research Centre, Health Protection Branch, Ottawa, Ontario, Canada, K1A 0L2. Fax: (+1-613) 941-4775.

17–19 May, 1994
Nancy, France
5th Meeting of the European Society for Bio-Chromatography. *Contact:* ESBC 94, LCPM-ENSIC, BP 451, F-54001 Nancy Cedex, France. Tel.: (+33-83) 175-221; Fax: (+33-83) 379-977.

□ 18 May, 1994
Nancy, France
Satellite Meeting: Chromatography and *In-Vivo* Plasma Treatment. *Contact:* ESBC 94, LCPM-ENSIC, BP 451, F-54001 Nancy Cedex, France. Tel.: (+33-83) 175-221; Fax: (+33-83) 379-977.

□ 22–26 May, 1994
Venice, Italy
ESEAC'94: 5th European Conference on ElectroAnalysis. *Contact:* ESEAC'94/S. Daniele, Department of Physical Chemistry, University of Venice, Calle Larga S. Marta 2137, I-30123 Venice, Italy. Tel (+39-41) 5298503; Fax: (+39-41) 5298594.

23–25 May, 1994
Les Diablerets, Switzerland
7th Int. Symp. on Polymer Analysis and Characterization. *Contact:* ISPAC Registration, 815 Don Gaspar, Santa FE, NM 87501, USA. Tel.: (+1-505) 989-4735; Fax: (+1-505) 989-1073; or Dr. M. Rinaudo, CERMAV-CNRS, B.P. 53X, F-38041 Grenoble, France. Tel.: (+33) 765-41145; Fax: (+33) 765-47203.

24–27 May, 1994
Kyoto, Japan
3rd Symposium on Molecular Chirality. *Contact:* Prof. T. Nakagawa, Symposium on Molecular Chirality (SMC), Faculty of Pharmaceutical Sciences, Kyoto University, Yoshida-Shimoadachi-cho, Sayo-ku, 606 Japan. Fax: (+81-48) 41-0310.

□ 30 May–1 June, 1994
Bergen, Norway
SSIR-94: 1st Scandinavian Symposium on Infrared and Raman Spectroscopy. *Contact:* Dr. A.A. Christy, Department of Chemistry, University of Bergen, N-5007 Bergen, Norway. Tel.: (+47-55) 213363; Fax: (+47-55) 329058; or Laila Kyrkjebo, Department of Chemistry, University of Bergen. Tel.: (47-55) 213342.

□ 31 May–3 June, 1994
Brugge, Belgium
2nd International Symposium on Hormone and Veterinary Drug Residue Analysis. *Contact:* Prof. C. Van Peteghem, Symposium Chairman, Faculty of Pharmaceutical Sciences, University of Ghent, Harelbekestraat 72, B-9000 Ghent, Belgium. Tel.: (+31-9) 2218951, ext. 235; Fax: (+32-9) 2205243.

5–7 June, 1994
Brugge, Belgium
VIth International Symposium on Luminescence Spectrometry in Biomedical Analysis - Detection Techniques and Applications in Chromatography and Capillary Electrophoresis. *Contact:* Professor Dr. W.R.G. Bayens, Symposium Chairman, Laboratory of Drug Quality Control, Pharmaceutical Institute, Department of Pharmaceutical Analysis, University of Ghent, Harelbekestraat 72, B-9000 Ghent, Belgium. Tel.: (+32-9) 2218951; Fax: (+32-9) 2214175.

□ 6–10 June, 1994
Kent, OH, USA
Course on Fundamentals of Chromatography. *Contact:* Dr Carl J. Knauss, Chemistry Department, Kent State University, Kent, OH 44242, USA. Tel.: (+1-216) 672 2327.

12–15 June, 1994
Washington, DC, USA
1994 PREP Symposium & Exhibit, International Symposium on Preparative Chromatography. *Contact:* Mrs. Janet Cunningham, PREP Symposium/Exhibit Manager, c/o Barr Enterprises, 10120 Kelly Road, P. O. Box 279, Walkersville, MD 21793, USA. Tel.: (+1-301) 898-3722; Fax: (+1-301) 898-5596.

□ 13–15 June, 1994
Lund, Sweden
4th International Symposium on Field-Flow Fractionation. *Contact:* Dr. A. Sjögren, Swedish Chemical Society, Wallingatan 24, 3 tr, S-111 24 Stockholm, Sweden. Fax: (+46-8) 106678.

19–24 June, 1994
Bournemouth, UK
20th International Symposium on Chromatography. *Contact:* Executive Secretary, The Chromatographic Society, Nottingham Polytechnic, Burton Street, Nottingham, NG1 4BU, UK. Tel.: (+44-602) 500-596; Fax: (+44-602) 500-614.

□ 19–24 June, 1994
Loughborough, UK
Radioisotope Techniques Short Course. *Contact:* Dr. P. Warwick, Department of Chemistry, Loughborough University of Technology, Loughborough, Leicestershire LE11 3TU, UK. Tel.: (+44-509) 222 585 or 222 545; Fax: (+44-509) 233 163.

□ 23–28 Aug., 1994
Sapporo, Japan
International Trace Analysis Symposium '94 (ITAS '94). Trace Analysis, Separation, and Speci-

ation for Environmental, Biological and Advanced Material Samples. *Contact:* Professor Hiroto Watanabe, Laboratory of Analytical Chemistry, Faculty of Engineering, Hokkaido University, Sapporo 060, Japan. Tel.: (+81-11) 716 2111 (ext. 6743); Fax: (+81-11) 726 4454.

□12–15 Sept., 1994
Reading, UK
3rd Int. Conf. on Separations for Biotechnology. *Contact:* SCI Conference Office, 14/15 Belgrave Square, London SW1X 8PS, UK. Tel.: (+44-71) 235-3681; Fax: (+44-71) 823-1698.

19–22 Sept., 1994
Turin, Italy
International Ion Chromatography Symposium 1994. *Contact:* Century International, Inc., P.O. Box 493, Medfield, MA 02052, USA. Tel.: (+1-508) 359-8777; Fax: (+1-508) 359-8778.

□21–23 Sept., 1994
Bournemouth, UK
7th International Symposium on Radiochemical Analysis. *Contact:* Dr. P. Warwick, Department of Chemistry, Loughborough University of Technology, Loughborough, Leicestershire LE11 3TU, UK. Tel.: (+44-509) 222585 or 222545; Fax: (+44-509) 233163.

□21–23 Sept., 1994
Stockholm, Sweden
5th International Symposium on Pharmaceutical and Biomedical Analysis. *Contact:* Swedish Academy of Pharmaceutical Sciences, P.O. Box 1136, S-111 81 Stockholm, Sweden. Tel.: (+46-8) 245085; Fax: (+46-8) 205511.

□22–25 Sept., 1994
Leiden, Netherlands
International Symposium on Mechanisms in Nephrotoxicity. *Contact:* Symposium Secretariat, Mrs. F.J. Velthorst, LACDR, P.O. Box 9502, 2300 RA Leiden, Netherlands. Tel.: (+31-71) 274 341; Fax: (+31-71) 274 277.

□25–30 Sept., 1994
Bristol, UK
1994 European Workshop in Chemometrics. *Contact:* Janice Green, School of Chemistry, University of Bristol, Cantock's Close, Bristol BS8 1TS, U.K. Tel.: (+44-272) 303 030 ext. 4421 or 303 672; Fax: (+44-272) 251 295.

□26–28 Sept., 1994
Stockholm, Sweden
5th International Symposium on Chiral Discrimination. *Contact:* Swedish Academy of Pharmaceutical Sciences, P.O. Box 1136, S-111 81 Stockholm, Sweden. Tel.: (+46-8) 245 085; Fax: (+46-8) 205 511.

□3–7 Oct., 1994
St. Petersburg, Russia
International Symposium Chromatography and Mass Spectrometry in Environmental Analysis (ISCMS'94). *Contact:* Dr. A.A. Rodin, State Institute of Applied Chemistry, Dobrolubov Ave., 14, 197198 St. Petersburg, Russia. Tel.: (+7-812) 238 9786; Fax: (+7-812) 233 8989; Telex: 121345 PTB SIGMA.

□5–7 Oct., 1994
Budapest, Hungary
9th International Symposium on Capillary Electrophoresis. *Contact:* Dr. F. Kilár, Central Research Laboratory, University of Pécs, Medical School, Szigeti út 12., H-7643 Pécs, Hungary. Tel.: (+36-72) 324 122 (ext. 2086); Fax: (+36-72) 315 864 or (+36-72) 326 244; E-mail: H712KIL@-ELLA.HU.

□23–25 Oct., 1994
Leiden, Netherlands
International Course on Pharmacokinetic–Pharmacodynamics Modeling, Principles and Applications. *Contact:* Symposium Secretariat, Mrs. F.J. Velthorst, LACDR, P.O. Box 9502, 2300 RA Leiden, Netherlands. Tel.: (+31-71) 274 341; Fax: (+31-71) 274 277.

□25–28 Oct., 1994
Leiden, Netherlands
3rd School on Medicinal Chemistry. *Contact:* Symposium Secretariat, Mrs. F.J. Velthorst, LACDR, P.O. Box 9502, 2300 RA Leiden, Netherlands. Tel.: (+31-71) 274 341; Fax: (+31-71) 274 277.

9–11 Nov., 1994
Montreux, Switzerland
11th Montreux Symposium on Liquid Chromatography–Mass Spectrometry (LC–MS; SFC–MS; CE–MS; MS–MS). *Contact:* Mrs. M. Frei-Häusler, IAEAC Secretariat, Postfach 46, CH-4123 Allschwil 2, Switzerland. Tel.: (+41-61) 4812789; Fax: (+41-61) 4820805.

□8–13 Dec., 1994
Stellenbosch, South Africa
2nd National Symposium on Analytical Science. Analytical Science: Towards the Welfare of People and the Environment. *Contact:* Conference Secretariat (Ms Johlette de Jager), Analytica

'94, Medical Research Council, P.O. Box 19070, Tygerberg 7505, South Africa. Tel.: (+27-21) 938 0433; Fax: (+27-21) 938 0395; E-mail: JDEJAGER@EAGLE.MRC.AC.ZA.

□ **6–10 March, 1995**
PITTCON '95. Pittsburgh Conference on Analytical Chemistry and Applied Spectroscopy. *Contact:* Pittsburgh Conference, Suite 332, 200 Penn Center Blvd., Pittsburgh, PA 15235-9962, USA

□ **8–10 May, 1995**
Lund, Sweden
7th Symposium on Handling of Environmental and Biological Samples in Chromatography. *Contact:* Mrs. M. Frei-Häusler, IAEAC Secretariat, Postfach 46, CH-4123 Allschwil 2, Switzerland. Tel.: (+41-61) 4812789; Fax: (+41-61) 4820805.

□ **28 May–2 June, 1995**
Innsbruck, Austria
HPLC '95, 19th International Symposium on Column Liquid Chromatography. *Contact:* HPLC '95 Secretariat, Tyrol Congress, Rennweg 3, A-6020 Innsbruck, Austria. Fax: (+43-512) 59367.

□ **5–8 June, 1995**
Kent Ridge, Singapore
5th Symposium on our Environment and 1st Asia-Pacific Workshop on Pesticides. *Contact:* The Secretariat, 5th Symposium on Our Environment, c/o Department of Chemistry, National University of Singapore, Kent Ridge, Republic of Singare 0511. Fax: (+65) 779 1691.

□ **27 Aug.–1 Sept., 1995**
Budapest, Hungary
10th International Conference on Fourier Transform Spectroscopy. *Contact:* Mrs. K. Láng or Mr. A. Varga, Conference Office, Roland Eötvös Physical Society, P.O. Box 433, H-1371 Budapest Hungary.

□ **27 Aug.–1 Sept., 1995**
Leipzig, Germany
CSI XXIX, Colloquium Spectroscopium Internationale XXIX. Contact: Gesellschaft Deutscher Chemiker, Abt. Tagungen, P.O. Box 90 04 40, D-60444 Frankfurt/Main, Germany.

□ **6–8 Sept., 1995**
Paris, France
5th Workshop on Chemistry and Fate of Modern Pesticides. Contact: Prof. M.-C. Henion, ESPCI, Lab. Chimi Analytique, 10 Rue Vauquelin, 75005 Paris, France.

□ **12–15 Sept., 1995**
Leuven, Belgium
5th International Symposium on Drug Analysis. *Contact:* Professor J. Hoogmartens, Drug Analysis '95 - Leuven, Institute of Pharmaceutical Sciences, Van Evenstraat 4, B-3000 Leuven, Belgium. Tel.: (+32-16) 283 440; Fax: (+32-16) 283 448.

□ Indicates new or amended entry.

PUBLICATION SCHEDULE FOR THE 1994 SUBSCRIPTION

Journal of Chromatography A and *Journal of Chromatography B: Biomedical Applications*

MONTH	O 1993	N 1993	D 1993	J	F	M	A	
Journal of Chromatography A	652/1 652/2 653/1	653/2 654/1 654/2 655/1	655/2 656/1 + 2 657/1 657/2	658/1 658/2 659/1 659/2	660/1 + 2 661/1 + 2 662/1 662/2	663/1 663/2 664/1	664/2 665/1 665/2 666/1 + 2 667/1	The publication schedule for further issues will be published later.
Bibliography Section						681/1		
Journal of Chromatography B: Biomedical Applications				652/1	652/2 653/1	653/2 654/1	654/2 655/1	

INFORMATION FOR AUTHORS

(Detailed *Instructions to Authors* were published in *J. Chromatogr. A*, Vol. 657, pp. 463–469. A free reprint can be obtained by application to the publisher, Elsevier Science B.V., P.O. Box 330, 1000 AH Amsterdam, Netherlands.)

Types of Contributions. The following types of papers are published: Regular research papers (full-length papers), Review articles, Short Communications and Discussions. Short Communications are usually descriptions of short investigations, or they can report minor technical improvements of previously published procedures; they reflect the same quality of research as full-length papers, but should preferably not exceed five printed pages. Discussions (one or two pages) should explain, amplify, correct or otherwise comment substantively upon an article recently published in the journal. For Review articles, see inside front cover under Submission of Papers.

Submission. Every paper must be accompanied by a letter from the senior author, stating that he/she is submitting the paper for publication in the *Journal of Chromatography A* or *B*.

Manuscripts. Manuscripts should be typed in **double spacing** on consecutively numbered pages of uniform size. The manuscript should be preceded by a sheet of manuscript paper carrying the title of the paper and the name and full postal address of the person to whom the proofs are to be sent. As a rule, papers should be divided into sections, headed by a caption (*e.g.*, Abstract, Introduction, Experimental, Results, Discussion, etc.). All illustrations, photographs, tables, etc., should be on separate sheets.

Abstract. All articles should have an abstract of 50–100 words which clearly and briefly indicates what is new, different and significant. No references should be given.

Introduction. Every paper must have a concise introduction mentioning what has been done before on the topic described, and stating clearly what is new in the paper now submitted.

Experimental conditions should preferably be given on a *separate* sheet, headed "Conditions". These conditions will, if appropriate, be printed in a block, directly following the heading "Experimental".

Illustrations. The figures should be submitted in a form suitable for reproduction, drawn in Indian ink on drawing or tracing paper. Each illustration should have a caption, all the *captions* being typed (with double spacing) together on a *separate sheet*. If structures are given in the text, the original drawings should be provided. Coloured illustrations are reproduced at the author's expense, the cost being determined by the number of pages and by the number of colours needed. The written permission of the author and publisher must be obtained for the use of any figure already published. Its source must be indicated in the legend.

References. References should be numbered in the order in which they are cited in the text, and listed in numerical sequence on a separate sheet at the end of the article. Please check a recent issue for the layout of the reference list. Abbreviations for the titles of journals should follow the system used by *Chemical Abstracts*. Articles not yet published should be given as "in press" (journal should be specified), "submitted for publication" (journal should be specified), "in preparation" or "personal communication".

Vols. 1–651 of the *Journal of Chromatography*; *Journal of Chromatography, Biomedical Applications* and *Journal of Chromatography, Symposium Volumes* should be cited as *J. Chromatogr.* From Vol. 652 on, *Journal of Chromatography A* (incl. Symposium Volumes) should be cited as *J. Chromatogr. A* and *Journal of Chromatography B: Biomedical Applications* as *J. Chromatogr. B*.

Dispatch. Before sending the manuscript to the Editor please check that the envelope contains four copies of the paper complete with references, captions and figures. One of the sets of figures must be the originals suitable for direct reproduction. Please also ensure that permission to publish has been obtained from your institute.

Proofs. One set of proofs will be sent to the author to be carefully checked for printer's errors. Corrections must be restricted to instances in which the proof is at variance with the manuscript.

Reprints. Fifty reprints will be supplied free of charge. Additional reprints can be ordered by the authors. An order form containing price quotations will be sent to the authors together with the proofs of their article.